STRUCTURE-PROPERTY BEHAVIOR OF HYBRID MATERIALS INCORPORATING OLIGOMERIC SPECIES WITH INORGANIC SILICATES BY A SOL-GEL PROCESS

by

Hao-Hsin Huang

Dissertation submitted to the Faculty of the
Virginia Polytechnic Institute and State University
in partial fulfillment of the requirements for the degree of

DOCTOR OF PHILOSOPHY

in

Chemical Engineering

APPROVED:

G. L. Wilkes, Chairman

J. E. McGrath   D. G. Baird

M. E. Davis   W. G. Glasser

February, 1988

Blacksburg, Virginia

STRUCTURE-PROPERTY BEHAVIOR OF HYBRID MATERIALS INCORPORATING OLIGOMERIC SPECIES WITH INORGANIC SILICATES BY A SOL-GEL PROCESS

by

Hao-Hsin Huang

Committee Chairman: Garth L. Wilkes
Chemical Engineering

(ABSTRACT)

A sol-gel process has been utilized to develop novel hybrid materials incorporating organic and inorganic species. The objectives of this project were to study the feasibility of this new bridging route and, if successful, study the structure-property relationships of these new materials. In this thesis, tetraorthosilicate was used to combine with one of three types of oligomers, which included silanol terminated polydimethylsiloxane (PDMS), triethoxysilane endcapped polytetramethyleneoxide (PTMO), and PTMO with multiple triethoxysilane functional groups. The general reaction scheme was to first generate silanols from both components through the hydrolysis reaction, and then form the network structure by a co-condensation reaction with the silanol groups. The preparation of these hybrid materials was successful. Most of these hybrid materials were obtained without significant cracking problems with a initial TEOS loading up to 80 wt%, and the final products were always transparent.

For the PDMS containing systems, the tensile strength was always lower than 8 MPa. and the elongation at break was in the range of 5-25%. Dynamic mechanical results showed a bimodal $\tan\delta$ behavior, which was attributed to two different physico-chemical environments of the oligomers: one was PDMS rich phase and one represented more dispersed PDMS oligomers. The dispersion of the oligomers increased

with acid and silicate content of the system, and this postulation of better PDMS dispersion was strongly supported by the SAXS results which showed a systematic decrease in the mean square electron density fluctuation.

The mechanical properties of PTMO containing materials were considerably enhanced compared to the PDMS hybrid systems. Depending on the composition and oligomeric molecular weight, the tensile strength could reach 33 MPa. Also, the range of the elongation at break increased up to ca. 100%. The tanδ spectra showed a single, broad maximum at temperatures much higher than the T_g of pure PTMO oligomers, which indicated the absence of a pure oligomer phase. A broad maximum in the SAXS profile was observed in most cases, implying the existence of a correlation distance in these PTMO containing materials. To rationalize all the experimental observations, a schematic model was suggested which contains highly condensed TEOS clusters and mixed regions of partially condensed TEOS and PTMO. This model was further supported by swelling data and by agreement between the SAXS correlation length and the estimated PTMO end-to-end distance.

The systems prepared with PTMO possessing multiple triethoxysilane groups showed the most promising results in terms of mechanical properties. The tensile strength ranged from ca. 30 to 55 MPa., and the ambient modulus was nearly 10^8 Pa. Also, a yield point was observed in some cases and was postulated to be an indication of partial continuity of the silicate phase.

ACKNOWLEDGMENTS

TABLE OF CONTENTS

CHAPTER ONE

INTRODUCTION

Organic chemistry has been the backbone of the ever advancing science of macromolecules for more than half a century. From the discovery of the structure of natural rubber, cellulose, and peptides, to the synthesis of polyolefins, polyamides, polyesters, and the versatile polyurethanes, the chemistry has principally been surrounding the major component --- the element of carbon. However, as these polymeric materials became more commonly used to make commercial products, some limitations (e.g. chemical and weather resistance, wearability, thermal stability) have also been noticed and improvements are thus necessitated. Since inorganic compounds are usually more durable in these respects, a combination of organic and inorganic components has thus become a reasonable solution. In addition, the abundance of the inorganic compounds has made this route even more attractive. Two of the many examples of this combination of organic and inorganic components are the synthesis of polysiloxanes and polyphosphazenes; the thermal and chemical stability of these materials have clearly marked the significance of this "bridging" approach. However, most of the combinations of this type have concentrated on the monomeric level, while the examples of bridging different types of oligomeric components are considerably less. One important reason for this is the lack of appropriate chemistry for producing useful materials. However, with the recent development of the sol-gel process, the feasibility of such a combination has been increased.

Although the history of the sol-gel process commenced about fifty years ago, the significant advancement has been made in the last two decades due to the success of

preparing multicomponent glasses that can not be made conventionally [1]. The basic chemistry of the sol-gel process can be illustrated by the following reactions:

$$M(OR)_n + nH_2O \longrightarrow M(OH)_n + nROH$$

$$M(OH)_n \longrightarrow MO_{n/2} + \frac{n}{2}H_2O$$
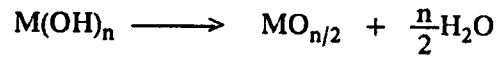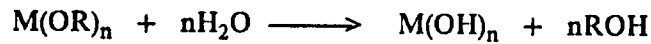
where M is a metal such as Si, Ti, or Al, and R is a organic group such as methyl, ethyl, etc. To further elaborate the reaction scheme, one can see that the first step is the hydrolysis reaction of the metal alkoxide and the second step is, according to the definition by Flory [2], a polycondensation reaction. This process is usually catalyzed by either acid or base and the final structure of the inorganic glasses depend greatly on which type of catalyst used. For making multicomponent glasses, more than one type of metal alkoxide can be employed together and, with some modification of the reaction procedure, an amorphous, homogeneous product can be obtained with almost any composition. This important advantage of producing multicomponent glasses has increased the potential of the sol-gel process tremendously and, as a result, the publications concerning this process have grown exponentially in the last two decades. Another important point about this sol-gel process is that it illustrates that the inorganic glass can be catagorized as a type of polymer network (formed by the polycondensation reaction). This process also forms a concrete connection between the disciplines of macromolecules and ceramics.

Now, by examining the reaction scheme and considering the polymerization nature of the sol-gel process, it seems possible to incorporate organic compounds with inorganic metal alkoxides if cocondensation of the two species can take place and if the problem of incompatibility can be minimized. One obvious approach would be to endcap the

organic compound with certain functional species that either has the MOH group or can be reacted to generate this group. If the incorporation is successful, then the final product made should accordingly show some characteristics of the organic species and also some of the inorganic component. One of the most important advantages of this sol-gel approach in producing hybrid materials is its versatility. The inorganic metal alkoxide used can be chosen from a variety of compounds that are available commercially, while the organic component can be selected from a wide range of oligomers --- glassy or rubbery --- as long as they possess proper functional groups. In addition, a mixture of several compounds in one reaction is also possible assuming that compatibility is not a problem. Therefore, the success of this generalized sol-gel process will mean the initiation of a new way of tailor making materials for specific applications.

As mentioned earlier, this type of combination at the oligomeric level has scarcely been studied. Although there are some investigations being carried out on organically modified silicates (ORMOSIL) [3-7], they mostly concentrate on the final properties of the materials and report nothing on the structure. This apparent gap is somewhat surprising and, thus, some effort to understand the structure-property relationship of these new systems should be conducted.

In this project, three types of elastomeric oligomers have been employed to incorporate with either tetraethoxysilane (TEOS) or tetramethoxysilane (TMOS). The first one is poly(dimethyl siloxane) (PDMS); it was either silanol terminated or endcapped with triethoxysilane through an urea linkage. This choice is mainly due to the similarity of the molecular structures between TEOS and PDMS and also the thermal stability of the oligomer. The second one is poly(tetramethylene oxide) (PTMO), which was endcapped with triethoxysilane through an urethane linkage. The endcapping procedure is believed

to enhance the incorporation due to the high functionality of the resulting oligomers. Finally, higher molecular weight PTMO species with different numbers of pendent functional group along the backbone are employed. The success of this incorporation should expand the choice of usable organic species into polymeric compounds. In addition to the types of oligomers used, acid content, water content, molecular weight of the oligomer, weight ratio of the two components, and the reaction medium have also been varied to study the effect on the final structure and mechanical properties.

The structural information of the hybrid systems under investigation is obtained principally by use of the small angle X-ray scattering technique (SAXS). In addition, wide angle X-ray scattering (WAXS), scanning electron microscopy (SEM), Raman spectroscopy, and solid state NMR have also been utilized for providing further information about the structure. Mechanical properties and dynamic mechanical behavior of these hybrid materials have been concentrated on in this project. Finally, some thermal analysis and swelling experiments have also been carried out to confirm some of the results.

As a summary, the knowledge about the hybrid systems mentioned above is very limited at the present time. Only a few of the combinations have been studied and fewer structure-property relationships have been reported for these new materials. Therefore, the priority should be set on testing additional types of organic and inorganic components and to note the most important variables that will influence the structure and properties of these new systems. In this work, the combination of elastomeric oligomers with silicates is emphasized and to understand the relationship between the structure and mechanical properties is the main goal. However, two other studies, concerning the incorporation of glassy functionalized oligomers with silicates and

elastomeric oligomers with titanium containing silicates, are also currently under investigation in this same laboratory by the author's colleaques. From the fact that the number of publications on the sol-gel process has increased exponentially in the last several years, it is believed that these hybrid systems and the generalized sol-gel process utilized to prepare these materials should raise more interest in the near future.

CHAPTER TWO

LITERATURE REVIEW

The main goal of this study is to probe the possibility of incorporating organic elastomeric oligomers with inorganic silicates by a sol-gel process and, if successful, to study the structure-property relationships of these new hybrid materials. Therefore, an understanding of the basic sol-gel chemistry is crucial to prepare useful materials and to determine the important variables for investigation. This is by no means an easy task when considering the active development of the sol-gel process in the last two decades. However, since silicate is the only inorganic component used in this study, the literature survey will concentrate on silicon sol-gel chemistry only and the investigations about multicomponent sol-gel systems will not be reported. One point should be noted is that the chemistry of the pure sol-gel process can only serve as a reference for the present work. Changes in the reacting system are expected as the organic oligomer is added in terms of the network-forming procedure, homogeneity, bulk structure etc. Hence, new variables, such as the solubility parameter of the oligomer, the composition ratio between organic and inorganic components, and the oligomeric molecular weight, will have to be taken into account. Also necessary in this survey is a review of the related studies on these hybrid systems. Due to the novel features of this research area, relevant work is very limited and, as mentioned earlier, almost no structural information has ever been reported. Nevertheless, the few studies that exist in the literature concerning the preparation of new hybrid systems are reviewed so that potential applications of these novel materials can be recognized.

The first part of this chapter is a general review of the basic chemistry of the pure silicon sol-gel process. A glimpse of the history of the sol-gel process and its advantages and disadvantages are provided. Several important variables that affect the structure and final properties are pointed out along with the rationale behind such results. The second part is an extensive survey on the organically modified silicates (ORMOSIL). These systems are really the first, and almost the only, reported materials that utilize the idea of incorporation of organic and inorganic compounds by the sol-gel process. Although structural information is seldom mentioned in these studies, some potential and interesting applications have been reported and this really lays a firm foundation regarding the practical aspects of these hybrid materials. The last part of this chapter reviews a special system studied by J. E. Mark and coworkers; which is concered with silica filled poly(dimethyl siloxane) rubber. Due to the similarity of this system with the TEOS-PDMS systems that prepared in this work, these publications are reported in detail for both relevancy and comparison.

2.1 PURE SILICON SOL-GEL SYSTEMS

Sol-gel history commenced about fifty years ago [8]. Two German scientists, Geffcken and Berger, prepared a single oxide coating by a dipping method and, subsequently, patented it in 1939. The properties of this coating were similar to that of the oxide glasses made by fusion; however, the thickness was limited by the cracking problem. In the next thirty years, the progress in the sol-gel process was relatively slow. This was mainly due to the high cost of the raw material used (metal alkoxides) and the difficulty encountered in making monolithic objects. In 1969, an oxide glass containing aluminum and magnesium was successfully prepared. This important accomplishment has really made a tremendous upturn in the sol-gel development and the progress and growing of

interest has been very active ever since [1]. The scientists then knew that, in principle, almost any element on the periodical table can be combined into an oxide glass through appropriate sol-gel process. However, the problem of cracking in making large objects still exists. In the last decade, several studies have been carried out trying to develop a procedure to make monolithic glasses [9-13]. Although success has been reported, long period of time and strict conditions were required. This, from the economical point of view, has greatly limited the practical applications of this process. Nevertheless, due to the following inherent advantages of the sol-gel approach [14-16], some high-tech applications are still foreseeable:

1. Low sintering temperature --- For the conventional fusion method of making glasses, the metal oxide is melted under very high temperatures (usually higher than 1400°C) and then shapened and quenched. In the sol-gel method, the gel is usually formed under ambient conditions and then sinters under relatively low temperatures (around 900°C). This difference in the processing temperature results in a significant saving of energy.

2. High purity --- Due to the high fusion temperature of the conventional method, contamination from the container (or furnace) is usually inevitable. However, this problem can now be eliminated since the glass network is always formed under ambient conditions. This point is especially critical for high-tech applications where high purity is required.

3. Free of crystallinity --- In the fusion method, some of the metallic elements (e.g. Na) will often crystallize during the quenching procedure due to the high rate of crystallization. Whereas in the sol-gel method, the glass network is already formed before the sintering procedure. Therefore, the crystallizable component will not be able to form a regular structure (lattice) because of the high restrictions imposed by

the network. This important advantage has made the sol-gel process a indispensable choice in producing multicomponent glasses.

4. High homogeneity --- Phase separation has been a problem in some multicomponent glasses when prepared using the fusion method. Some components tend to coalesce in the quenching procedure. This problem can also be significantly reduced by the sol-gel approach since high homogeneity is always achieved in the solution stage. However, modification has to be made in the reaction procedure to account for the different condensation rate of the metal hydroxides so that no preferential precipitation will take place.

With regard to the disadvantages of the sol-gel process, in addition to the cracking problem mentioned previously, cost of the metal alkoxides and the shrinkage observed in the drying procedures are also crucial limiting factors. However, with the advancement of technology, these drawbacks are expected to be overcome in the foreseeable future [14-16].

Generally speaking, the whole process of making a glass through the sol-gel route can be divided into three stages: solution(sol), gel, and glass. The sol-gel transition includes the formation of the network (polycondensation reaction), the gelation, and the elimination of the residual reaction medium (drying). The gel-glass transition includes the combustion of the residual organic groups, the collapse of the voids, and the densification of the glass. The molecular topology developed in the solution has a direct influence on the gelation process and the final structure of the gel and, consequently, on the properties of the sintered glass. Although the sintering procedure will also affect the final properties, it is the reaction variables involved in the solution that determines the structure of the materials. Besides, the sintering process will have less significance

as some organic modifications are considered. Therefore, this part of review will concentrate on the sol-gel transition.

Before discussing the chemistry of this sol-gel process, it seems proper to show the general reaction scheme again (silicon will be used here for simplicity):

HYDROLYSIS

$$Si(OR)_4 \ + \ 4H_2O \ \longrightarrow \ Si(OH)_4 \ + \ 4ROH$$

POLYCONDENSATION

$$Si(OH)_4 \ \longrightarrow \ SiO_2 \ + \ 2H_2O$$
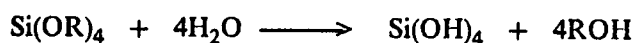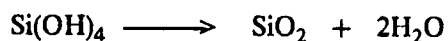
These reactions are usually catalyzed by acid or base so that the time scale of obtaining a gel is reasonable. This simplified reaction scheme shows that the polycondensation starts after the hydrolysis is complete. However, this implication is not correct in most cases. The formation of the Si-O-Si linkage will usually occur during the course of hydrolysis. The relative rate of condensation with respect to the hydrolysis will not only have a decisive influence on the network-forming process, but also directly affect the completeness of the hydrolysis. This complication has made the sol-gel process one of the most difficult systems to understand and to control.

Although a considerable amount of work has been done on the sol-gel process, the exact mechanism and how the reaction variables would influence the molecular topology are still not without ambiguity. Generally speaking, variables that have particularly significant effect are the amount and type of catalyst as well as the amount of water. An early study on the effect of catalyst was done by Aelion et al [17]. In this study, the

rate of the hydrolysis and condensation were determined by monitoring the concentration of alcohol and water. The metal alkoxide employed was TEOS, and the reaction was catalyzed by either acid (HCl) or base (NaOH, NH$_4$OH, and pyridine). For the system with high acid content, it was observed that the hydrolysis was fast and complete while the condensation increased from 86 to 100 % completion with decreasing acid content. At low acid content, the condensation remained complete while hydrolysis became increasingly slow and incomplete, dropping to an extent of 15% for a "neutral" solution. Apparently, the acid would not only change the reaction rate but also affect the equilibrium state. This is partially due to the steric hindrance and the physical environment of the hydrolyzable groups in the solution. As this review continues, this point will become clear. As for the base catalyzed systems, condensation was always fast and complete. However, phase separation or precipitation was observed depending on the type of solvent used.

With these observations, the authors suggested two different hydrolysis models for acid and base catalyzed systems, respectively. Under acidic environment, it was suggested that a complex was formed by the acid proton and a water molecule. This intermediate compound would then attack the metal alkoxide to initiate the hydrolysis reaction. Subsequently, ethanol and water would be released and complete the reaction cycle. For the base catalyzed system, however, the hydroxyl ion would attack the alkoxide directly and release an ethoxy ion. This ethoxy ion would then combine with a water molecule and form ethanol and a hydroxyl ion. These two models formed a foundation for most of the future work studying the mechanism of the sol-gel process. Another important point demonstrated by this work was that the reaction medium used also had a significant influence on the final structure of the sol-gel glasses. This effect has been further studied by other workers and will be discussed later in this section.

A further and more detailed study in modeling the chemical mechanism of the sol-gel process has been carried out by Keefer [18]. In this report, the two mechanisms mentioned previously were further elaborated upon and a model for the condensation reaction was also suggested. Furthermore, an attempt was made to explain the effect of the type of catalyst on the final structure of the sol-gel glasses.

For the acid catalyzed system, an electrophilic mechanism similar to what Aelion suggested was postulated (Fig. 2.1). In this model, the proton has been suggested to be incorporated with the water molecule to form an intermediate ionic species that subsequently attacks the metal alkoxide. Since the attacking species in this case possesses a positive charge, the hydrolysis would be favored if the electron density around the silicon atom is high. Therefore, the first ethoxy group of the metal alkoxide would be the easiest one to be replaced by the hydroxide group. As the number of ethoxy groups on the silicon atom decreases, the tendency of the replacement would decrease as well. The result would be that complete hydrolysis of all four sites of the metal alkoxide would be less likely and, thus, further condensation would lead to the growth of linear "polymer-like" species and a weakly crosslinked system. As the drying and shrinkage of the system proceeded, the gel would become dense due to the driving force of lower surface energy [11,19,20].

For the based catalyzed system, a nucleophilic mechanism should be followed. This is illustrated in Fig. 2.2. A negatively charged hydroxyl group would attack the back side of a metal alkoxide molecule. As a result of the repulsive effect between electrons, such a nucleophilic attack would be favored if the electron density around the silicon atom is low. Therefore, the first ethoxy group of TEOS should be the most difficult one to replace since four ethoxy groups are bonded to the silicon atom. As the number of

ethoxy groups bonded to the silicon decreases, the nucleophilic attack becomes easier. Consequently, this type of mechanism would favor the formation of orthosilicic acid (i.e. $Si(OH)_4$).

With regard to the condensation reaction, a mechanism has been suggested by Iler and it is schematically shown in Fig. 2.3 [21]. In this case, a deprotonated silicic acid is formed and, then, it will attack another silicic acid molecule. After the Si-O-Si linkage is produced, a hydroxide ion is released. Therefore, the most favorable condensation would take place between the most acidic and the most basic species. Now, the acidity of a silanol proton depends on other substituents on the silicon: a replacement of a OH group by a SiO- decreases the electron density around the silicon and thus increases the acidity of the protons on remaining OH groups. Hence, the monomer (orthosilicic acid) would be the least acidic species. Concluding from the above statements, the highly condensed silicate units would continue to react with the monomer (silicic acid) and would grow into very compact clusters. Such a nucleophilic mechanism has been reported to have a minimum rate at pH = 2, and an electrophilic mechanism may become important for systems with pH < 2 [18,21].

As a result of the mechanisms suggested above, the particles formed in a base catalyzed system should be rather compact and dense. However, due to the significant sizes of these particles and their compact structure, the interstitial space between particles would be rather large as these particles coalesce. As a result, the overall density of the base catalyzed gel is usually quite low (ca. 0.9 g/cc). However, the actual density of the matrix (excluding the voids between particles) is always rather high (ca. 1.8 g/cc). Another important point to mention about Figure 2.2 is the molecular inversion after releasing the ethoxy group. This implication and the compact structure of the particle were argued

to be the main reason for the suppression of the reverse hydrolysis reaction (reesterification).

Another crucial difference between the acid and the base catalyzed systems is the extent of reesterification. As mentioned previously, this reverse hydrolysis would be mostly suppressed due to the molecular inversion and steric hindrance imposed by the compact network. For the acidic system, a small amount of residual alcohol could drive the reaction significantly to the left-hand side and generate a considerable amount of unreacted ethoxy groups. This argument has been utilized to account for the fact that, although complete hydrolysis has been observed in the solution stage, some ethoxy groups still exist in the dried gel [18].

One important point to note is that all the mechanisms suggested above can promote the possibility of certain structures but not necessarily determine the actual process of network formation. Other factors such as amount of water will have to be considered. For example, a large amount of water can still lead to a compact, highly crosslinked system even though acid is used as the catalyst. This is because that the excess water will drive the reaction largely to the right-hand side of the hydrolysis reaction according to LeChatelier's principle.

To briefly summarize the mechanisms suggested above, it seems that in a basic solution (pH > 7) compact clusters will always be formed. This is due to the fact that both the hydrolysis and the condensation mechanisms favor a highly cross-linked system. In addition, a ripening theory has been suggested for this type of system [18]. It is stated that in the basic solution the monomer can usually try several sites before being combined into the growing cluster, leading to a denser packing pattern. In the highly acidic solution (pH < 2), polymer-like particles will be produced in the beginning stage

of the reaction and finally shrink into a dense gel. However, the cross-linking density of these systems should be lower than the base catalyzed systems. For the solution with pH between 2 and 7, there should be a transition region that generates intermediate structures. Schaefer et al.[22] utilized these suggested mechanisms and developed a plot for the dependence of the reaction rates (both hydrolysis and condensation) on the solution pH value (Fig. 2.4). Although the relative nature for these two curves may change depending on the metal alkoxide used, the general trend should be correct. With the understanding of the mechanisms suggested by previous workers, one can then choose the appropriate reaction conditions to produce materials with specific structure and properties [11,18,19,23].

As an example, to prepare optical fibers by the sol-gel process, the acid catalyzed system is always used [15,24,25]. This is mainly due to the polymer-like particles formed in this acidic system, which is suitable for fiber spinning. Also important is that, under the same concentration, acid catalyzed systems usually gel faster than base catalyzed systems. The time factor becomes especially crucial as commercial production of these materials is considered. On the other hand, if porosity is the deciding factor, such as making ceramic membranes or porous supports, then the base catalyzed system may well be the obvious choice. One thing to bear in mind is that these guidelines for choosing the proper catalyst to use is only valid if other variables, such as water content and reaction temperature, have also been taken into account.

All the reaction mechanisms suggested in the previous discussions represent the attempt made by chemists to explain the sol-gel reactions. These postulations can be linked with the experimentally measurable properties, such as density and porosity, rather well. However, the actual growing process of the particles is still not without ambiguity. It

seems that there is a need of an experimental technique that can directly or indirectly monitor the growth of the particles. Fortunately, with the recent development of the fractal theory and the earlier well developed small angle X-ray scattering analysis, this need can now be fulfilled.

Fractal theory is a physical concept that has been developed to describe a pattern resulted from a random growth process in nature. These sprawling patterns, or fractals, have the same characteristic of scale-invariance or dilation symmetry. This means that as the pattern is magnified, it reveals repetitive levels of details so that similar structure exists in all scales [22,26,27]. Examples of such patterns include the motion of air bubbles in oil, water seeping through the soil, and shape of the coastlines. Although this fractal concept has been recognized for many years, it was not utilized in the material science until the development of several important growth models [22,27]. With all these suggested models and, most importantly, the usage of a digital computer, the entire process of the growth of a fractal can now be simulated and understood.

Although the dilation symmetry is a common feature, the compactness is still different between various fractals. Therefore, it seems useful to have a quantity that can represent this difference. In the conventional Euclidian space, a dimension has been defined for different geometries. A straight line has a dimension of 1, a plane is 2, and the Euclidian space is 3. In analogy, a fractal dimension has also been defined to describe how dense a fractal can fill the space. However, instead of integers, this fractal dimension can also be fractional. For example, the more nearly a "flat" fractal object fills a plane, the closer its dimension approaches 2. With this definition, one can now approximate the shape of a fractal by simply knowing its fractal dimension.

The growth or aggregation of a silicate colloid has been suggested to be a fractal forming process. In addition, the fractal dimension of the resulting structure can be related to the scattering curves of these materials [26,27]. A typical scattering profile of a random porous material is illustrated in Fig. 2.5. Four regimes have been shown; each corresponds to the structure on a different scale. In the limiting regime, the fluctuation at very long wavelengths is probed. In the Guinier regime, the mean pore size can be determined. In the Bragg regime, the structure in the atomic level can be understood. Finally, the Porod regime provides information about the fractal structure. In this regime, a power-law behavior is always observed for fractal materials. It has been suggested that the slope of the profile in this regime can be related to the fractal dimension of the scatterers. For a silicate aggregate with a slope larger than -3, the scattering is caused by the compactness of the aggregation and the fractal dimension is thus equal to the absolute value of the slope. This is called a mass fractal due to the fact that the molecular weight M can be expressed by the common notation of $M \propto R^D$, where R is the radius and D is the fractal dimension. For aggregates with Porod slope between -3 and -4, a surface fractal is suggested. This means that the particle is rather compact but with a fractally rough surface. For such systems, the slope in the Porod regime is equal to Ds-6, where Ds is the fractal dimension of the surface and its value ranges from 2 (smooth surfaces) to 3 (rough surfaces). A list of the particle structures and their corresponding Porod slope from SAXS is given in Fig. 2.6.

With this background, the study of silicate systems by the combination of fractal theory and SAXS technique can now be illustrated. Some examples of SAXS profiles from different silicate systems are shown in Fig. 2.7. A two-step reaction has been used to prepare solutions that generate SAXS profiles a and b. The first step is to add a small amount of water and acid so that the hydrolysis would be slow and incomplete. Then

some acid (in case a) or base (in case b) with a large amount of water is added after a certain period of time. Both slopes are close to 2 which indicates that the particles are slightly branched or more chain-like particles. However, the small difference indicates that the system with acid in both steps has a more open structure. Curve c is the SAXS profile of a solution prepared by a one-step reaction using base as the catalyst; a slope of 3.3 is obtained. This clearly indicates that the particles are rather compact but possess a rough surface. With this knowledge of the fractal dimension, several growth models are tested so that a best fit can be obtained. The result is that the silicate sol-gel system can be best represented by either a reaction limited monomer-cluster growth model (for the basic system) or a reaction limited cluster-cluster growth model (for the acidic system). The former will result in particles with very compact structure but rather rough surfaces (also known as Eden clusters). Whereas the latter will result in chain-like particles which possess rather open structure.

Another good example is by examining profile d in Fig. 2.7, which is the SAXS result for a single-stage-acid-catalyzed system. A crossover in the profile indicates that a cluster-monomer growth takes place in the beginning, then it is followed by a cluster-cluster growth process. This is interpreted to imply that the hydrolysis is complete before any significant condensation occurs and, therefore, the early stage of growth proceeds by the cluster-monomer route. After the monomer is exhausted a cluster-cluster growth would have to take place and, consequently, creates a polymer-like structure. This success of using the SAXS technique and the fractal theory has indeed assisted in the understanding of the sol-gel process and its dependence on the reaction conditions.

To summarize, two different approaches have been taken to understand the network-forming process of the sol-gel reactions. Chemists make an effort to rationalize the problem by suggesting different mechanisms-- the acidic system with an electrophilic reaction and the basic system with a nucleophilic one. On the other hand, physicists have approached the problem with fractal theory and suggested a Eden cluster model and a reaction limited cluster aggregation model for the acidic and basic systems, respectively. The interesting point is that both groups of researchers reached the same general conclusions which were consistent with the experimental results.

Besides all the mechanisms and models discussed above, the effect of neutralization in the base catalyzed systems should also be noted [17,18]. As shown in the reaction scheme, the silicon alkoxides will undergo hydrolysis first and generate silicic acid before the polycondensation can take place between these species. Due to the inherent acidity of these silicic acid, it tends to neutralize the basic catalyst used in the reaction. The effect of this neutralization process is that the pH value of the solution will be changed and the available hydroxide ion for initiating the reaction will decrease. Therefore, if the concentration of the basic catalyst is not high enough in the beginning, this neutralization process can change the reaction mechanism and, consequently, the structure considerably. However, this situation can be avoided by using a large amount of catalyst.

In addition to the type of catalyst used, the amount of water added is another important variable to be considered in the sol-gel process. As mentioned previously, although the growth process of the sol-gel network is predominantly dependent upon the catalyst used for the reaction, the water content can also influence the structure. One of the example to illustrate this point is by comparing SAXS profiles (a) and (d) in Fig. 2.7. Acid is the

catalyst in both cases. In case (a), a polymer-like structure is observed by SAXS throughout the whole experimental period. This is due to the fact that only a small amount of water (less than 100% stoichiometric amount) is added in the beginning, hence, hydrolysis is not complete and only linear or lightly branched molecules would be formed. This is consistent with the mechanism suggested for the acidic systems. On the other hand, although the acid is the catalyst, a more compact structure is observed in the beginning stage of case (d). This can be attributed to the large excess of water present in the system from the beginning, which strongly promotes the hydrolysis reaction and results in some small ring-like structures. This type of interaction between these two variables-- catalyst and water -- has also been pointed out by other investigators [12,18,24].

Generally speaking, the effect of water content on the growth process and, consequently the final structure, can be understood through the following considerations:

1. Water content will affect the hydrolysis rate. Recalling the simplified reaction scheme mentioned earlier, water is one of the reactants of the hydrolysis reaction. Therefore, for the cases that water is not in large excess, the rate of hydrolysis should increase with the water content. In the systems that use acid as the catalyst [17], it has been shown that the hydrolysis can be viewed as a second order reaction. That is, the rate of reaction is proportional to the concentrations of water and metal alkoxide. This can be further understood by recalling the mechanism shown in Fig. 2.1, in which the proton was suggested to form a complex with a water molecule. This complex would then attack the alkoxide and release alcohol and a proton. According to this, the amount of water in the system should directly affect the rate of hydrolysis. However, for the basic system, it has been reported that the rate of

hydrolysis is independent of the water presented [17]. This somewhat surprising result can be rationalized by the mechanism shown in Fig. 2.2, in which the hydroxide ion would directly attack the backside of the metal alkoxide and release an alkoxide ion. Since water is not a component of this mechanism, the amount of water should not influence the hydrolysis rate. One thing to note is that these result would be valid only in the range of the experimental conditions used in that specific study. Extrapolation of this conclusion to other conditions would be questionable.

2. Water may change the equilibrium state. Although the reaction scheme implies no reverse reaction for both the hydrolysis and condensation, it is not correct in most cases, especially for acidic cases in which the reesterification may be significant. Therefore, the sol-gel process should be viewed as an equilibrium reaction. According to LeChatelier's principle, water should promote the hydrolysis and impede the condensation. In addition, it has been suggested that the water would form an azeotrope with alcohol and be removed first in the drying procedure leaving very little alcohol for the reesterification [18]. Therefore, the overall effect of adding more water would be to shift the hydrolysis reaction toward greater completion. However, a small amount of alkoxide group should always exist due to the entrapment by the network [18,29].

3. Water may dilute the system. The above two effects would be more significant as the amount of water is close to the exact stoichiometry of the hydrolysis reaction. However, as a large excess amount of water is added, the dilution effect may become important. In a dilute solution, since the concentration of the metal alkoxide is low, the probability of a hydrolysed site to undergo condensation with another reactive site would be largely reduced. Thus, the rate of condensation should decrease considerably. As the reaction proceeds, small molecules would be formed in the beginning. Then, the probability of a reactive site on a small molecule to form a

linkage with another reactive site from the same molecule should be relatively high compared to a concentrated solution. The result is that ring-like structures would be considerably promoted. Consequently, the resulting gels would be less compact and have low matrix density [30].

Strawbridge et al.[30] have carried out an extensive study on the effect of the H_2O/TEOS ratio, r, on the structure of gels derived from acid catalyzed system. The silicate used was tetraethoxysilane (TEOS); the ratio r ranging from 2 to 50; and the molar ratio of HCl/TEOS was 0.1 for most cases. For systems with r = 2, the hydrolysis was not complete, and a considerable amount of ethoxy groups still existed in the gel. These systems showed a low matrix density and would fracture at high temperatures. According to the polymerization process suggested before, a system with low water content would mainly consist of linear and lightly branched molecules. Although "entanglements" tends to make the gel denser, the static hindrance caused by the residual ethoxy groups would compensate this effect and result in a low density structure. For a even lower water content (r = 1), a fibrous structure was observed on fractured surfaces of the gels by SEM [31]. This feature may be favorable when fiber-making is desired. As r increased to 4 and 10, the amount of unreacted ethoxy group would decrease and the final structure of the gel would therefore be denser than the previous case. However, polymer-like particles were still the dominant structural component of these systems. The SEM micrographs for these intermediate water content systems showed a layered structure which supported the growth model. For gels obtained from solution with a large excess of water (i.e. r > 20), particulate structures were observed by SEM and the bulk density decreased. This decrease in density was a result of the large interstitial space between large particles.

In addition to the electron microscopy, small angle X-ray scattering technique (SAXS) has been employed to study the gel structure. A two-phase system— pores and polymeric structure— has been postulated for the intermediate and high water content systems. The SAXS results were analyzed using Porod plots. A positive deviation from zero slope in the tail region was observed for both cases, and the magnitude decreased with increasing water content. According to Porod's law, a positive deviation is caused by an imperfection of the matrix [32]. For the system with intermediate water content, the matrix consists of not only polymers but also some small pores. This imperfection of the matrix results in the large positive deviation from Porod's law. For the high water content system, the matrix would be more homogeneous (i.e. free of pores) due to the growth procedure. This results in a decrease in the deviation from Porod's law. These results are consistent with the growth models suggested by fractal theory.

For pure silicate sol-gel systems, the type of catalyst used and the amount of water added are the two most important variables in determining the final structure and properties. It is not only the individual effect, but also the interaction between these two variables are crucial. However, some other variables, such as the type of metal alkoxide used, the reaction temperature, and the type of solvent employed, would also affect the rate of reaction and the final structures.

Although the alkoxide of several metallic elements such as aluminum, titanium, boron, and sodium have been used in the sol-gel process [9,33-41], the one that has been most extensively studied is silicon. The main reason is that silicon alkoxides have the slowest rate of reaction among all the metal alkoxides commercially available [9,39]. This feature greatly enables one to study the kinetics and the growth procedure of this sol-gel system. In addition, one can also have more control on the network-forming process

(e.g., by using different type of catalysts and amount of water) and, therefore, the final structure and properties of the resultant gels. For a fixed type of metal element, the reactivity of the metal alkoxide increases with decreasing molecular weight of the organic group. For example, the reactivities of the three commonly used silicon alkoxides are in the following order:

$$Si(OCH_3)_4 \; > \; Si(OC_2H_5)_4 \; > \; Si(OC_3H_7)_4$$

Therefore, the hydrolysis rate should be affected and so should the final structure. However, the situation is further complicated by the following type of condensation reaction since it will also be affected by the type of silicate used:

$$(RO)_3Si(OR) + (HO)Si(OR)_3 \longrightarrow (RO)_3Si-O-Si(OR)_3 + ROH$$
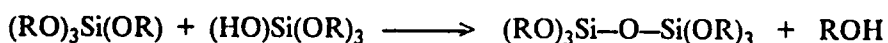
Generally speaking, all the mechanisms and growth models suggested above should still be valid as the type of metal alkoxide is changed. However, a new set of reaction conditions will need to be found if similar structure and properties of the resulting solids are desired.

For a multicomponent sol-gel reaction, the reactivity of each component is crucial in making a useful product. If a one-step reaction is used for components with very different reactivities (e.g., $Ti(OEt)_4$ and $Si(OEt)_4$), preferential condensation would take place and phase separation or precipitation would most likely be observed [7,39]. Therefore, a multistep technique is usually employed. The alkoxide with the slowest reaction rate (usually silicate) is often reacted with an insufficient amount of water first, then the component with the higher reactivity is added to obtain a homogeneous system. The order and timing of this addition will thus become another important variable to consider in such systems.

The sol-gel process has usually been carried out under ambient conditions and, therefore, a gelation time longer than one week is not uncommon. To decrease the gelation time, it is reasonable to increase the reaction rate by raising the reaction temperature. Aelion et al.[17] studied the hydrolysis rate under several temperatures and found out the rate constant increased 10 times as temperature increased from 20°C to 45°C. As for the temperature effect on the condensation reaction, it has not been studied except by measuring the change of gelation time for different temperatures [11,42]. The result showed that the gelation time decreased drastically as the reaction temperature increased. However, this effect was not systematically studied. A recent study on the temperature effect on the final properties such as density and porosity has been carried out by Colby et al.[42]. Although the porosity seemed to decrease with increasing temperature, no conclusive remarks were provided due to the lack of structural characterization.

The final variable which needs to be studied is that of the solvent(s) used for the sol-gel reaction. As mentioned earlier, the metal alkoxides and water are not miscible. Hence, some kind of medium, most often alcohol, is employed to make a homogeneous solution. After the gelation takes place, the solvent can be removed by either vacuum stripping or careful thermal treatment. This step is very crucial in obtaining monolithic glasses since the large drying stresses generated often causes the materials to crack. To try to solve this problem, one can basically approach it through two ways: either to physically control the evaporation rate of the solvent or to use a solvent that has a lower vapor pressure. For the former, success has been achieved in several studies to make monolithic glasses [9,10,20,41,43]. However, it often requires a relatively long time and strict thermal treatment. A supercritical drying procedure has also been developed by some workers as a means to remove the solvent [44,45], and the results seems

encouraging. Generally speaking, these methods of physically controlling the evaporation rate of the solvent(s) should not influence the reaction mechanisms. However, if one chooses to use the second approach (i.e., using different solvent than alcohol), then the chemistry will have to considered.

Wallace and Hench [46] have developed a new method of preventing the cracking problem by adding what they called a "drying control chemical additive" (DCCA). Formamide was the first DCCA reported to be successful in reducing the cracking problem, and it facilitated making dried, monolithic gels of size up to 100 cm³. The DCCA also reduced the gelation, aging, and drying times. Two subsequent studies [47,48] have been carried out to investigate the influence of DCCA on the chemistry of a sol-gel system, and how it affects the final structure of the gel. Orcel and Hench utilized ^{29}Si NMR to study the hydrolysis and early stages of the condensation. The system with DCCA showed a decrease in the hydrolysis rate, which was attributed to the formation of hydrogen bonds between formamide and water. Also shown in the study was an increase in the condensation rate with DCCA, and this has been attributed to the deprotonization of the silanol by the formamide. As to the decrease of the gelation time, it was believed to be caused by the higher rate of condensation.

Artaki et al.[49] also studied the effect of several solvents on the sol-gel process. They separated solvents into three groups: (1) polar protic (methanol, formamide); (2) dipolar aprotic (acetonitrile, dimethyl formamide); and (3) non-polar aprotic (dioxane). Type 1 would form hydrogen bonds and thus decrease the condensation rate, resulting in branched molecules. Type 3 would not interact with any of the components and, therefore, would promote the condensation, resulting in particulate structures. Density measurements showed a maximum for the gel generated by using type 3 solvent, and

TEM micrographs showed this gel had large granular structures. McGrath et al.[50] have used proton NMR to study the rate of hydrolysis of a silicate sol-gel system; two different solvents -- ethanol and DMF -- were used. The result indicated that the system with DMF had a higher hydrolysis rate than that with ethanol. This was attributed mainly to the fact that ethanol is a product of the hydrolysis reaction and, therefore, would promote the reverse hydrolysis reaction if a large amount of ethanol was used.

To summarize this review section on the pure silicate sol-gel process, it is reasonable to say that this new approach of making glasses is still in the developing stage. Chemical mechanisms and physical models have been suggested to account for the relationship between reaction variables and final structure and the results are rather consistent. The type of catalyst used and the amount of water added are believed to be two most important variables in terms of determining the final structure, however, some other variables (e.g., solvents) also affect the product considerably. Due to this complexity, a gel with desirable properties can be prepared but not without very precise experimental conditions. In addition, only the sol-gel transition has been emphasized in this section, the gel-glass transition (i.e., the sintering procedure) is also important. However, due to the interest of this project, this gel-glass transition has not been studied. With regard to the multi-component systems, the situation will be further complicated because of the different reactivities between components. Nevertheless, the basic principles mentioned in this section should still be valid as long as no preferential condensation takes place. In the next section, the existing studies about the organically modified sol-gel glasses will be reviewed.

2.2 ORGANICALLY MODIFIED SOL-GEL GLASSES

The conventional method of making glasses usually requires extremely high processing temperatures to melt the metal oxides before shaping and quenching; this procedure excludes the possibility of combining organic species into inorganic glasses since no organics can sustain such high temperatures. However, with the development of the sol-gel process, this combination can now be achieved. Nevertheless, one important point should be noted before examining the existing work is that, although the incorporation of organic species into a silicate gel is possible through the sol-gel process, the final product has to be used without sintering. This is due to the high sintering temperatures used (around 900°C), though it is relatively low comparing to the fusion method. One exception is to utilize sol-gel process to prepare precursor materials of ceramics. In this case, high temperature treatment will be not only allowable, but required.

Although the sol-gel process has been studied extensively in the last twenty-five years, most of the effort has been devoted to prepare multicomponent inorganic glasses. The idea of utilizing the sol-gel method to incorporate organics and inorganics was not recognized until the last few years. While relatively few studies have been carried out to study the possible incorporation of organic compounds into inorganic glass networks, the results are very encouraging. The inorganic components employed are mainly silicates; the organic species are usually substituents of alkoxides groups on the silicon atom. Not only has production of such systems been successful, but new applications have already been realized for some of these novel systems [3,4,7].

For convenience, the organically modified sol-gel systems can be generally divided into two categories:

1. The organic groups are bonded to the metallic atom of the glass component (e.g. silicon). These substituents are usually of low molecular weight, such as methyl, or they possess some special functional groups that can undergo specific reaction (examples given below). In some cases, bulky groups (e.g., benzyl groups) may be used so that the cross-linking density of the systems may be decreased. Since these substituents will not hydrolyze to generate silanol groups, they can not undergo condensation and, hence, will not be linked into the network. Therefore, the higher the concentration of such substituents, the more open the final network structure will be. Finally, if the functionalized organics are of low molecular weight, potential phase separation problems can thus be avoided.

2. The organic compounds have functional groups that can either generate silanols or form a linkage through other reactions (such as vinyl groups). Polymers or oligomers possess ethoxysilane groups are examples of this type of species. The molecular weight of such organic compounds is often higher than the first category. However, these compounds would be able to link with the inorganics and become part of the network structure. One special case is that the organic compound can form a network by itself; this would result in an interpenetrating network system (IPN). Due to the nature of higher molecular weight, materials made with this category of compound might be heterogeneous and phase separation may occur--possibly a desirable outcome with regard to influencing the final properties.

The structural difference between these two types of systems should be distinct since the former is expected to show a continuous glass phase with dispersed organic species, while the latter may show cocontinuous phases or even a dispersed inorganic phase depending on the composition of the systems. The firing behavior should also be different due to the destruction of the weaker network linkages in the latter case as the

organic compounds degrade under high temperatures. In any event, the final properties such as strength, porosity, and scratch resistance of these organically modified systems should differ considerably from the pure glasses. Several important studies in this area are addressed below.

The most successful aspect so far for the pure sol-gel process is to produce thin coatings. This is because the drying process can proceed easily without producing large stresses and, hence, crack free materials can be obtained. Therefore, it is reasonable for researchers to try to prepare some special coatings through the incorporation of some organic groups into the sol-gel systems [3,7]. For example, amino groups have been widely used in the field of biochemistry as coupling groups for the immobilization of enzymes. Therefore, a reactive surface for this immobilization process can be prepared by a coating containing amino groups, and the organically modified sol-gel process will be a convenient approach to prepare this type of reactive surfaces.

A general reaction scheme, suggested by Schmidt [3], for producing special coatings is shown below:

$$m\ R_2Si(OC_2H_5)_2 + n\ Si(OC_2H_5)_4 + p\ YR'Si(OC_2H_5)_3$$

$$\text{(A)} \qquad\qquad \text{(B)} \qquad\qquad \text{(C)}$$

$$\xrightarrow[\text{H}_2\text{O}]{\text{H}^+}\ -\left[\begin{array}{c}R\\|\\-Si-O-\\|\\R\end{array}\right]_m -\left[\begin{array}{c}O\\|\\-Si-\\|\\O\end{array}\right]_n -\left[\begin{array}{c}R'Y\\|\\-O-\ Si\ -\\|\\O\end{array}\right]_p -$$
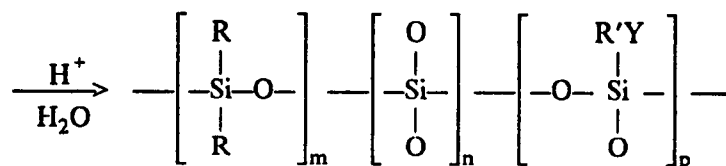
$$\text{(D)}$$

where R is CH_3 or C_6H_5, R' is alkylene, and Y is the functional group desired for specific purpose. In the case of immobilizing enzymes, Y is a amino containing organic

group such as $(CH_2)_3NH_2$. As shown in the reaction scheme, three types of compounds are required for this procedure: compound A is a difunctional silicate used for obtaining a homogeneous solution; compound B is a tetrafunctional silicate which promotes the formation of a 3-dimensional network so that a insoluble coating can result; compound C is a trifunctional silicate which possesses a special organic substituent that can undergo the reaction. At the beginning of the process, a small amount (less than the exact stoichiometry) of water is added to initiate the hydrolysis and condensation reactions. Due to the presence of the difunctional compound (A), the product will be lightly crosslinked and soluble to an appropriate solvent. After being applied onto the inner wall of a glass tube, this prepolymer is treated with a excess amount of hot water to accelerate the hydrolysis and condensation reactions and a layer of insoluble coating can be obtained. This final product (D) would have the desired functional group (Y) on the surface. As the enzyme containing solution, for example, contacts with this reactive surface, the immobilization process would proceed. Another example of this type of functional coating is for the immobilization of triiodine thyronine antibodies [3], which is a powerful tool in medical diagnosis. For this type of application, the functional group Y can be either CHO or CH_2OH. Therefore, it seems that as long as certain specific chemical reaction can take place between the functional group Y and the environment, almost any type of special coating can be produced by this method.

To further generalize this idea of special coatings, one can also achieve some specific purposes by utilizing the physical characteristics of certain organic compounds. For example, the humidity would usually affect the adsorption process of a special coating and reduce the efficiency of this functional surface. This situation can be greatly improved by the incorporation of some hydrophobic groups into the system. It has been shown that by introducing propyl groups into a aminosilane containing coating material,

the water adsorption decreases almost 50% [7]. However, this hydrophobicity may not be desired in some cases. For example, one of the important criteria in selecting material for making contact lenses has been the wettability of the substance. In this case, some hydrophilic functional groups, such as alcohol, should be incorporated into the system so that eye irritation can be avoided [4]. Another potential application for this type of material is in making sensors. By the incorporation of proper organic groups, the coating material can interact with or adsorb certain gaseous components. This interaction or adsorption may cause changes in the electronic state, such as the capacitance, of the material and can be monitored directly by a microelectronic device [7]. Experimental results have shown that the system made with SiO_2 and $(C_2H_5)_2N(CH_2)_3SiO_{3/2}$ exhibits reversible change of capacitance with the adsorption of SO_2 [7]. With this principle, some special sensors can be developed.

However, one crucial property that is related to all the adsorption applications is the surface area of these porous materials. As suggested by the studies on the pure sol-gel systems, the low temperature gels derived from the reactions are always porous. The porosity is dependent on the reaction variables such as system pH values, water addition, etc. For an organically modified sol-gel system, the porosity depends on the structure of the organic compound and the composition of the system as well. This is mainly due to the finite volume of the organic substituent. As one of the hydrolyzable sites of the metal alkoxide is changed into a unhydrolyzable group (e.g., methyl), it not only reduces the ability of this molecule to form chemical linkages with other molecules, but also occupies considerable space so that the surrounding molecules will not be able to cross-link due to the repulsive forces. The result will be to decrease the cross-linking density of the system and to promote the formation of polymer-like structure. This type of structure often causes the porosity to decrease. The higher the concentration of these

organic groups, or the more bulky these groups are, the more significant will be its influence on the porosity. For a system with an aromatic substituent, it has been shown that a slight increase of its concentration will considerably reduce the cross-linking density and the surface area of the final product [7]. This factor will become especially important as materials with high porosity is desired, such as in filtration and membrane processes.

Besides the preparation of reactive coatings, the organically modified sol-gel process has also been utilized to produce coatings that could improve the scratch resistance of the substrates [3]. Some of the organic polymers, such as PMMA and polycarbonate, are known to have poor scratch resistance. Therefore, the development of a coating material for these type of substrate is essential if a hard surface is desired. Although the inorganic glass coatings can provide high hardness, they always require a high sintering temperature to obtain dense bodies. Since no organic polymers can sustain such a high temperature environment, the idea of using a layer of pure sol-gel glass will not be suitable for the coating on a plastic substrate. Hence. the organically modified sol-gel glass coatings become obvious alternatives. As reported by previous studies [3,4,7], the usage of an epoxy modified glass coating has considerably improved the scratch resistance of PMMA. The general reaction procedure for this type of material is shown in the following scheme:
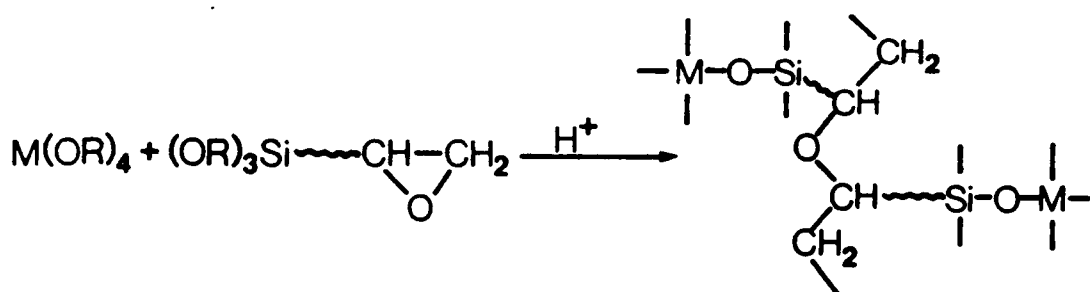
where M is a metal element, and the resulting coating can be cured at 100-120°C within minutes. Four different types of metals-Si, Zr, Al, and Ti- have been tested for the scratching behavior, and the results show that Al and Ti are the most effective ones in this respect. Although the reason for such an improvement is not clear, the result from IR spectroscopy indicates that the scratch resistance increases with decreasing OH content of the material, which implies a higher degree of condensation. This observation is also consistent with the effectiveness of using Ti and Al since both of these elements are known to promote the condensation reaction to further completion. However, the titanium containing system shows a poor UV stability and it has been attributed to its photocatalytic activity.

Most of the materials discussed so far have been in the first category—— the organic groups are substituents on the metal element and do not form a linkage with other components. Before discussing the other category, one interesting point being reported by Schmidt et al. [5,51] should be noted. According to their experimental results and some earlier work, the hydrolysis rate of metal alkoxides would be affected by the presence of unhydrolyzable substituents. Depending on the type of catalyst used (acid or base), the influence would be different. In an acidic solution, the hydrolysis rate increases with increasing number of organic substituent. In other words, the hydrolysis rate of the dimethyldiethoxysilane would be higher than that of the methyltriethoxysilane. Conversely, in a basic solution, more substituent groups result in a slower hydrolysis rate. This observation is crucial to the growth mechanism and, thus, the final structure of the materials. At this point, two questions should be asked:

1. How does this result compare with the reaction mechanisms suggested from the pure sol-gel systems?

2. How does this effect change as the molecular weight of the organic species becomes higher?

To answer the first question, one has to recall the mechanisms suggested by Keefer [18], which are shown in Fig. 2.1 & 2.2. According to this model, the acid catalyzed system would go through an electrophilic mechanism. Therefore, the rate of hydrolysis in an acidic solution would be favored by higher electron density around the silicon atom. For the based catalyzed system, a nucleophilic mechanism has been suggested. Hence, lower electron density surrounding the silicon atom would result in a higher rate of hydrolysis. Now, if one of the alkoxide group is substituted by a methyl group, the electron density around the silicon atom should increase due to the lower electron withdrawing ability of the carbon with respect to the oxygen. Therefore, it should accelerate the hydrolysis reaction. As more alkoxide groups are substituted, the acceleration should become even more significant. Whereas in the based catalyzed system, the hydrolysis rate should decelerate due to a higher electron density around the silicon atom. This means that the mechanisms suggested by Keefer coincide well with the experimental results shown by the organically modified systems, which answers the first question. The answer for the second question is not yet clear. As the molecular weight of the organic group becomes very large (e.g., an oligomer or polymer), the steric hindrance effect may be so high that the hydrolysis rate may be decelerated. In any event, it requires more experimental results before any conclusion can be drawn.

For the pure inorganic glass systems, one of the disadvantages of the sol-gel process is the large stresses developed in the drying process that results in the cracking of the final materials. This cracking problem has significantly limited the application of the sol-gel process in terms of producing bulky materials. The only successful aspect of this new

process is the preparation of very thin coatings. Although carefully controlled drying procedures [10,13,20,41,43] or supercritical methods [44,45] have been developed to reduce the cracking problem, they always require tedious efforts to obtain monolithic materials. Therefore, to make the sol-gel process more realistic from the commercial point of view, some kinds of modifications that can increase the toughness of glasses should be developed. This purpose can be achieved by utilizing the idea of organically modified glasses. Due to the finite volume of the organic groups, the cross-linking density should decrease and polymer-like structure would be promoted. Consequently, the system can sustain higher deformation stress produced in the drying procedure. In addition, one would expect that the modified glasses be even tougher if the organic component can form linkages through other reactions. This improvement in toughness has been reported for the system that used methylmethacrylate as the substituent [47]. This new means of reducing the cracking problem has considerably promoted the potential of the sol-gel process.

The most successful and interesting example of a monolith made by the organically modified sol-gel process has been the development of a new material for contact lenses [4]. A 3-step reaction procedure has been employed to produce this type of new material. First, epoxysilane and methacryloxysilane are mixed with ethanol and HCl under reflux. This step generates linear silane based species while most of the epoxy groups are preserved. Then, a small amount of $Ti(OR)_4$ is added with water to drive the condensation reaction further and, meanwhile, to generate hydrophilic hydroxyl groups by opening the epoxy rings. Finally, monomeric methacrylate and peroxide are added to form a 3-dimensional network. This system is then treated under 150°C to further cure the network structure. The overall reaction is schematically illustrated in Fig. 2.8. To

further elaborate the purpose of each reactant in this reaction, several points should be noted:

1. Tetraalkylorthosilicate has been chosen over other types of metal alkoxides as the dominant inorganic component of this system. This is partially due to that, with the same alkyl group, the silicate has the slowest rate of hydrolysis among all metal alkoxides. As a result, more control over the reaction would be possible. The other important reason is that the silicate glass has a higher permeability to oxygen than any other glasses. This has been an essential consideration in terms of the health of human eyes.

2. In spite of its high permeability to oxygen, the silicate network is highly hydrophobic. This would result in dryness of the eyes and, eventually, cause irritation and disease. Therefore, a modification of incorporating hydrophilic groups into the system is necessary. As mentioned earlier in the section of utilizing the sol-gel process to produce special coatings, the hydroxyl group has been used in improving the hydrophilicity of the materials. However, if the hydroxyl groups are presented in the beginning, a reaction between this hydroxide and the alkoxide from the silane would take place. Consequently, the initial purpose of increasing the hydrophilicity by adding hydroxides would not be achieved. Hence, a latent hydroxide compound would have to be used. An epoxy ring, which could react with water and generate a hydroxyl group, is thus employed. Nevertheless, it is still necessary to keep the water content low in the beginning so that the premature hydrolysis of the epoxy ring can be minimized.

3. The usage of $Ti(OR)_4$ is to accelerate the condensation reaction; this effect of acceleration has been reported in other studies [7]. In addition, the titanium containing glasses often show a denser matrix and result in stiffer materials.

4. The purpose of using the methacrylate substituted silicate and methacrylate monomers is to form a second type of network linkage. This type of linkage would increase the toughness of the final materials and result in more useful products.

From this example, the practical usefulness of the organically modified sol-gel systems can be recognized. More importantly, it demonstrates that multiple purposes can be achieved by appropriately choosing the components. Although the reaction procedure has to be modified somewhat to obtain a homogeneous system and an useful product, the basic principles of sol-gel process can still be used as a guideline. This example also shows that the incorporation of a second type of network linkage (PMMA) is possible, and its influence on the final properties is significant. However, due to the nature of this project, the properties were the only concern. As a result, no structural information was reported.

Recently, a new type of organically modified glass has been developed by incorporating poly(ethylene glycol) (PEO) into a silicate glass network [52]. The product was doped into a solution of a lithium salt. Since the PEO can form a complex with the lithium salt, the conductivity of such lithium-doped material would thus be high and can be used as solid electrolytes. The procedure of making this material is to react TMOS with PEO in the presence of water and acid, then thermally treats the gel at 150°C to obtain a monolith. Although the material has been reported to be transparent, the molecular weight of the PEO has not been specified and the mechanical properties have not been reported. Since the molar ratio of TMOS:PEO is 1:2, the final structure should predominantly be the polymeric component (similar to the filled PDMS systems reported by Mark and coworkers.) Hence, it would be more appropriate to view this material as a novel hybrid system instead of an organically modified glass. Nevertheless, the

production of a highly conductive material does offer another potential application for this organically modified sol-gel process.

In addition to the PEO example shown above, another recent work has been carried out to incorporate oligomeric/polymeric species into a sol-gel network. Parkhurst et al.[53] prepared a hybrid system using a mixture of SiO_2/TiO_2 as the inorganic component and silanol terminated PDMS as the organic species. In these titanium containing TEOS-PDMS systems, two different molecular weights of PDMS—— 1700 & 36000—— were used. TEOS was the inorganic component; either titaniumethoxide or titanium-n-butoxide was the source of the Ti component. Various ratios between the TEOS, titanium alkoxide, and PDMS were used to study the effect on the properties of resulting materials. Differential scanning calorimetry (DSC) was utilized to measure the glass transition temperature and the melting point of the crystalline region if existed. Several conclusive remarks were reported:

1. The addition of the organic component greatly improved the room temperature densification process, and crack-free materials were obtained due to the relaxation and flow characteristics imparted by the polymeric component.

2. The procedure of reaction was crucial to the final properties of the materials. A white, opaque, but crack-free gel was obtained if titanium alkoxide was added in the beginning of the reaction, but the solution was still clear. On the other hand, if TEOS and PDMS were reacted with 50% stoichiometric amount of water first before adding the titanium alkoxide, the final product was transparent. As mentioned previously, this was due to the high reactivity of the Ti alkoxides, which resulted in preferential condensation of the Ti component and thus induced phase separation.

3. As a weight ratio of PDMS/Si(OR)$_4$/Ti(OR)$_4$ = 1/1/1 was used, clear and crack-free materials always resulted regardless the PDMS molecular weight. As the ratio changed to 4/1/1, the resulting materials were also crack-free but opaque for the system with PDMS (MW = 36000). This is somewhat expected since higher PDMS molecular weight tends to promote phase separation, especially since PDMS is extremely hydrophobic and water is present in the sol-gel process.

4. An increase of Ti content (from 1/1/1 to 1/1/4) resulted in cracking of the dried gels, but the samples were still clear. Similar result was observed as the PDMS content decreased (from 1/1/1 to 0.4/1/1).

5. A melting point was observed in some of the samples made with PDMS (MW = 36000), indicating the PDMS would crystallize under low temperatures. However, no crystallinity was observed in the samples made with PDMS of lower molecular weight (MW = 1700). This has been attributed to the successful incorporation of PDMS into the glassy system, which imposed considerable limitation on the motion of PDMS chains to suppress crystallization.

6. From the DSC results, all the samples made with PDMS (MW = 1700) showed two distinct glass transition regions: one was close to the T_g of pure PDMS oligomers, and the other one was shifted to much high temperatures (usually around 0°C). This behavior has been attributed to (i) the endlinking of the oligomers into the network and (ii) the interaction of PDMS chains with glassy species. From this result, it was suggested that a polymer-rich phase and a more dispersed PDMS phase existed in the system. However, no other technique was used to further study this phenomenon.

This study demonstrates the possibility of combining PDMS into a SiO$_2$/TiO$_2$ glass system. Especially for the low molecular weight PDMS, the resulting materials are

always clear indicating no large scale phase separation. With this success, it is reasonable to believe that other organic compounds can also be used to react with the silicates if appropriate functional groups are provided. Although the functional groups are at the ends of the oligomeric/polymeric chains in this case, they can also be at any position along the backbone of the organic species. This indeed opens a new area of research on the production of hybrid materials.

All the previous studies discussed so far choose the silicates as the major inorganic component. From the basic principles of sol-gel reaction, it seems that the employment of other metal elements should also be feasible. Recently, a new type of hybrid system which incorporated vinyl acetate/vinyl alcohol copolymers with aluminum isopropoxides by a sol-gel process has been reported [54]. The objective of that project is to increase the ductility of the sol-gel aluminum glasses. Although the actual mechanism of the incorporation is vague, clear samples are reported to be obtainable. The organic content of these systems ranges from 10 to 20% by weight (based on the aluminum isopropoxide only); the molecular weights of these copolymers are 3000, 95000, and 126000 g/mole. The mechanical properties have been measured and also the thermal stability and transparency of the final products. The highest strain at break is 125%, which is rather impressive in terms of sol-gel glasses; however, the ultimate strength is always lower than 10 MPa. Like most of the previous studies, no structural information was reported.

From the survey of the existing literature on the organically modified sol-gel systems, one notices that most of the organic groups are substituents on the metallic center (e.g., Si). These organic compounds usually have low molecular weight and, in most cases, do not serve as network formers. The cracking problem, which limits the application of sol-gel process, can be avoided by the addition of organic components, and low

temperature densification becomes possible. Consequently, monolithic materials can be produced. Nevertheless, only limited data on the mechanical properties have been reported and, to the author's knowledge, no structural studies have been carried out on any of these novel systems. Such a lack of information, though somewhat surprising and disappointing, strongly provokes the necessity of a study to understand the structure-property relationship of these new hybrid systems.

2.3 TEOS FILLED POLY(DIMETHYL SILOXANE)

The combination of organic and inorganic compounds has been explored in some areas; one of these has been in the development of silica filled PDMS rubbers. Due to the significant differences in objectives and procedures, this system is not considered to be related to the present work. However, in a series of new studies by Mark et al.[55,63], an *in-situ* technique which generated sol-gel silicate fillers has been reported. The procedure of this new approach is rather similar to the present hybrid systems. Therefore, a detailed review of this series of studies should be worthwhile. However, the substantial difference in the objectives between these two systems should still make each stand in its own right.

The general procedure of reinforcing PDMS rubber with *in-situ* precipitated silica is as follows. First, a PDMS network was formed with exact stoichiometric amounts of functionalized PDMS and cross-linking agent. Depending on the functional end groups of the PDMS (vinyl or silanol), the cross-linking agent was either $Si[OSi(CH_3)_2H]_4$ or TEOS. The network thus formed would be a so called "model network", which had a M_c close to M_n of the initial PDMS oligomers. After extraction to remove the sol fraction, this PDMS elastomer was swollen in TEOS until it reached the maximum

swelling ratio. Then the swollen network was immersed into a catalytic solution—— acid, base, or salt—— to initiate the sol-gel reaction for purpose of obtaining precipitated silica particles. Mechanical tests were carried out on these materials, and the result showed great improvement over the unfilled PDMS crosslinked networks. Several important points should be noted about this procedure:

1. A network structure was formed by adding stoichiometric amount of cross-linking agent into the PDMS, and the resulting "model network" implied that the chain extension by self condensation of PDMS was mostly suppressed. The TEOS served as a cross-linking agent in this case and, thus, no aggregation of TEOS was expected in the network-forming step.

2. As mentioned above, the goal of this work on *in-situ* filling of PDMS system was to improve the properties of the PDMS rubbers. Therefore, relative high molecular weight of PDMS has been used (ranged from 8000 to 21600).

3. After the swelling process, the swollen PDMS was immersed into a catalytic solution—— either acidic, basic or a saturated solution of salt—— to undergo the curing reaction of TEOS. A large variety—— up to 39 —— of catalysts were investigated, and the usage of solutions of salts (e.g., sodium chloride, zinc acetate, etc.) always showed greatest improvement on the mechanical properties [57]. In addition, the systems with acidic catalysts were usually very brittle while the basic systems were relatively strong. This is somewhat in line with the growth model suggested for the sol-gel systems mentioned in the first part of this review. Since the acid catalyst tends to produce linear species, the filling effect would not be as good as the based catalysed systems, which tends to produce particulate structure of silica. Regarding the great improvement by the solutions of salts, the reason is not yet clear.

4. Since the samples were immersed into a catalytic solution to undergo TEOS curing in the filled PDMS systems, large excess of water would present for the hydrolysis and condensation reactions of TEOS. According to the sol-gel model for the silica systems, this would favor the formation of particulate-like structure of condensed TEOS, which serves as the filler.

Besides the mechanical experiments, transmission electron microscopy (TEM) has been utilized in this filled PDMS system to characterize the dispersion and structure of the silica fillers [59,60]. The resulting micrographs showed that, for a base or salt catalysed system, the silica generally formed particles with the size of ca. 200 Å and dispersed well in the PDMS matrix. However, for the acid catalysed system (acetic acid with a pH of 2.7), no distinct particle was observed. This was attributed to the formation of linear or less compact structure by the condensed TEOS species, which is consistent with the model suggested by the studies on the pure sol-gel silica systems. Another interesting result reported is the aging effect in a base catalysed system: the filler particles became better defined and dispersed after being soaked in the catalytic solution for 2 months. This implied that some rearrangement of the particles may have taken place. Such an effect has also been suggested by some studies on the pure sol-gel silica systems [18]. However, this only occurs in the base catalysed systems.

Although this *in-situ* filling technique generated impressive results, the procedure was still somewhat tedious. Therefore, in a latter study [61] a simultaneous curing and filling procedure was developed. In this new procedure, instead of employing a swelling procedure after the PDMS network was formed, an excess amount of TEOS was added into the network-forming reaction. The basic assumption was that part of the TEOS would serve as a crosslinking agent as previously mentioned, the excess TEOS molecules

would polymerize and form the silica fillers for the rubbery matrix. The amount of TEOS used in this process was usually less than 20 wt%; an excess amount of water was always employed to ensure the formation of silica particles. The catalyst used was a solution of dibutyltin diacetate and stannous 2-ethyl hexanoate, which was a salt proven to be effective in previous studies [55,57]. This catalyst should favor the formation of particulate-like TEOS based species and, at the same time, suppress the presence of linear molecules. Consequently, the condensed TEOS would mostly form dispersed particles which is exactly the desired structure for fillers. Although this technique of simultaneous curing and filling of PDMS was reported to be successful in terms of improving the mechanical properties of the PDMS rubbers, the structure was not as well defined as the original *in-situ* filling method. As concluded by Mark et al.[61], the exact reaction mechanism should be much more complicated than the previous system due to the presence of excess TEOS. Although TEM micrographs of this new technique was reported to be similar to the previous ones, no data was shown in the publication.

To summarize this section of the review, the *in-situ* filling technique developed by Mark et al. is rather impressive in terms of improving the mechanical properties of PDMS rubbers. The TEM micrographs show good dispersion of the silica particles in the PDMS matrix except for the acidic system, and such result is consistent with the model suggested by the studies on the pure sol-gel silica glasses. Although this process appears to be similar to this study, differences of several crucial parameters between these two systems should be noted, including relative amount of the components, type of catalyst used, amount of water added, and the procedure of the reaction. As a result, the final structures are expected to be distinctly different.
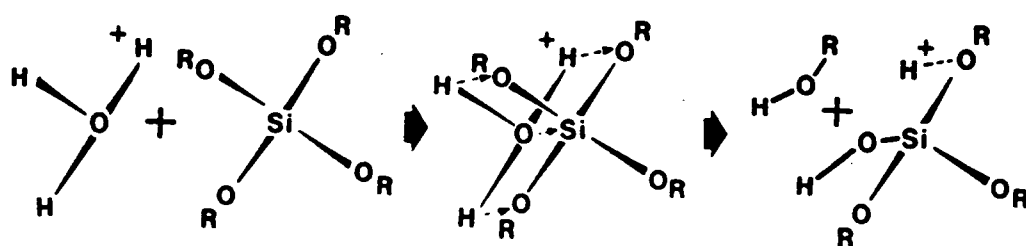
Fig. 2.1 An electrophilic reaction mechanism for the hydrolysis with an acidic catalyst, R = H, C_2H_5, or $Si(OR)_3$ [18].
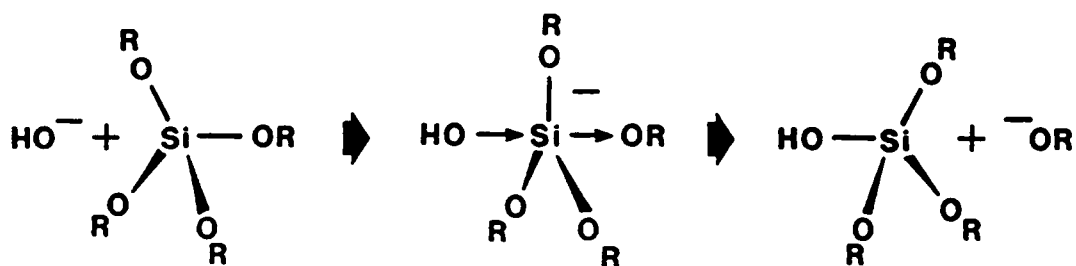
Fig. 2.2 A nucleophilic reaction mechanism for the hydrolysis with a basic catalyst, R = H, C_2H_5, or $Si(OR)_3$ [18].
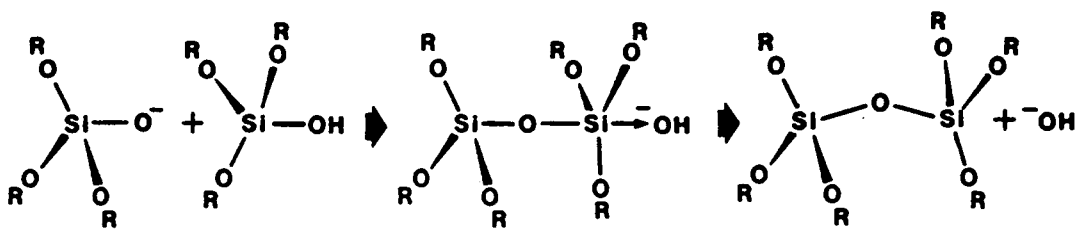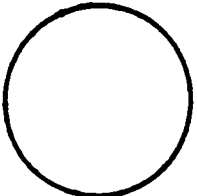
Fig. 2.3 A nucleophilic reaction mechanism for the condensation, R = H, C₂H₅, or Si(OR)₃ [18].
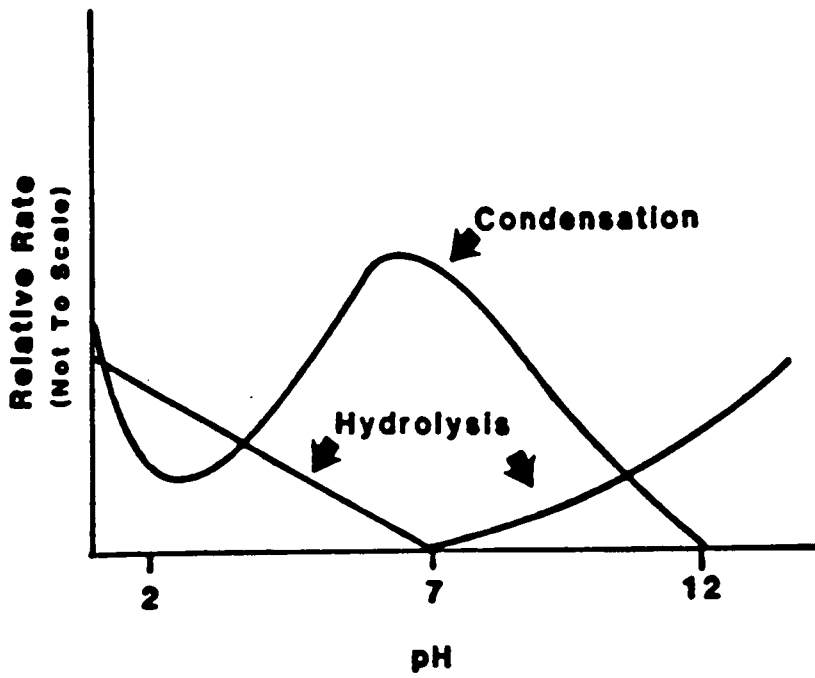
Fig. 2.4 A simplified scheme of the relative rates of hydrolysis and condensation at different pH environment [22]
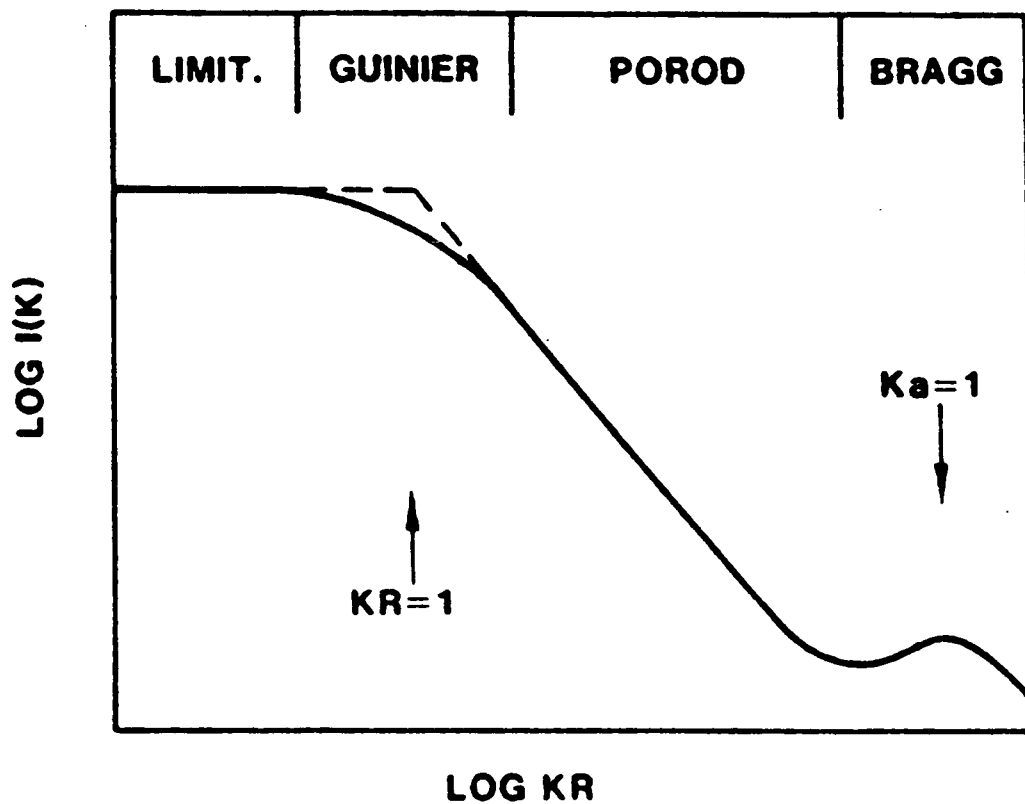
Fig. 2.5 A typical SAXS profile of a random porous material. K is the Fourier spatial frequency defined as $4\pi\sin(\theta/2)/\lambda$, R is the average size of the particles, and a is the chemical length of the monomeric unit [26].

Molecular Structure	Fractal Dimension (from SAXS)
	1.74
	2.00
	2.06
	3.24
	4.00

Fig. 2.6   Molecular structures and corresponding fractal dimensions.
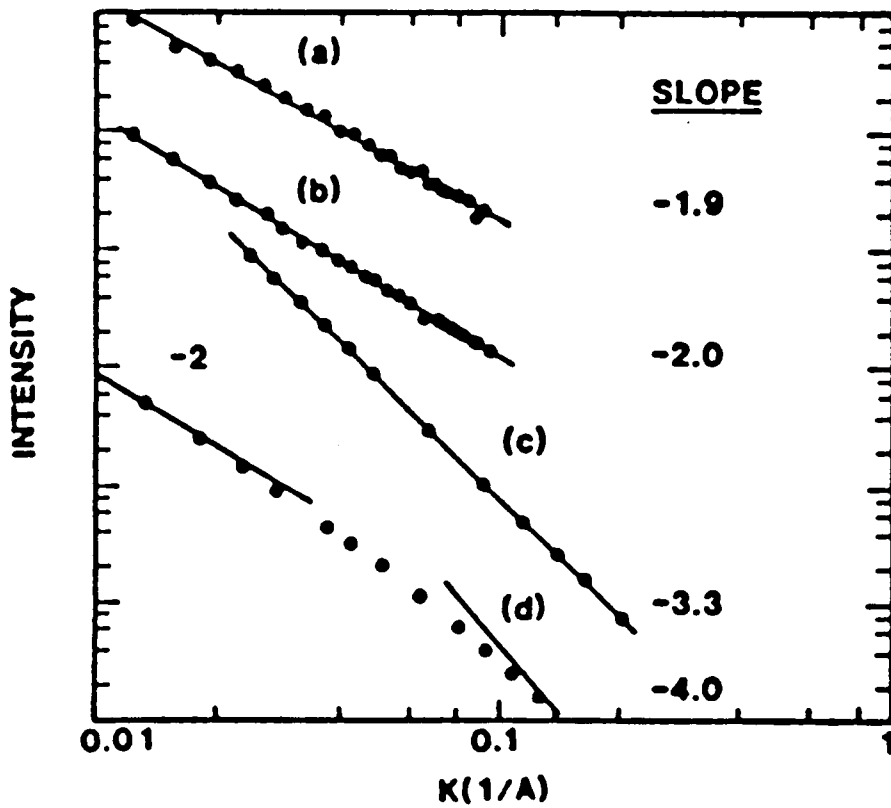
Fig. 2.7 SAXS surves for silicates made with different procedures: (a) a two-stage reaction with an acid catalysed stage followed by an acid catalysed stage (b) a two-stage reaction with an acid catalysed stage followed by a base catalysed stage (c) one-step base catalysed reaction (d) one-step acid catalysed reaction [27].
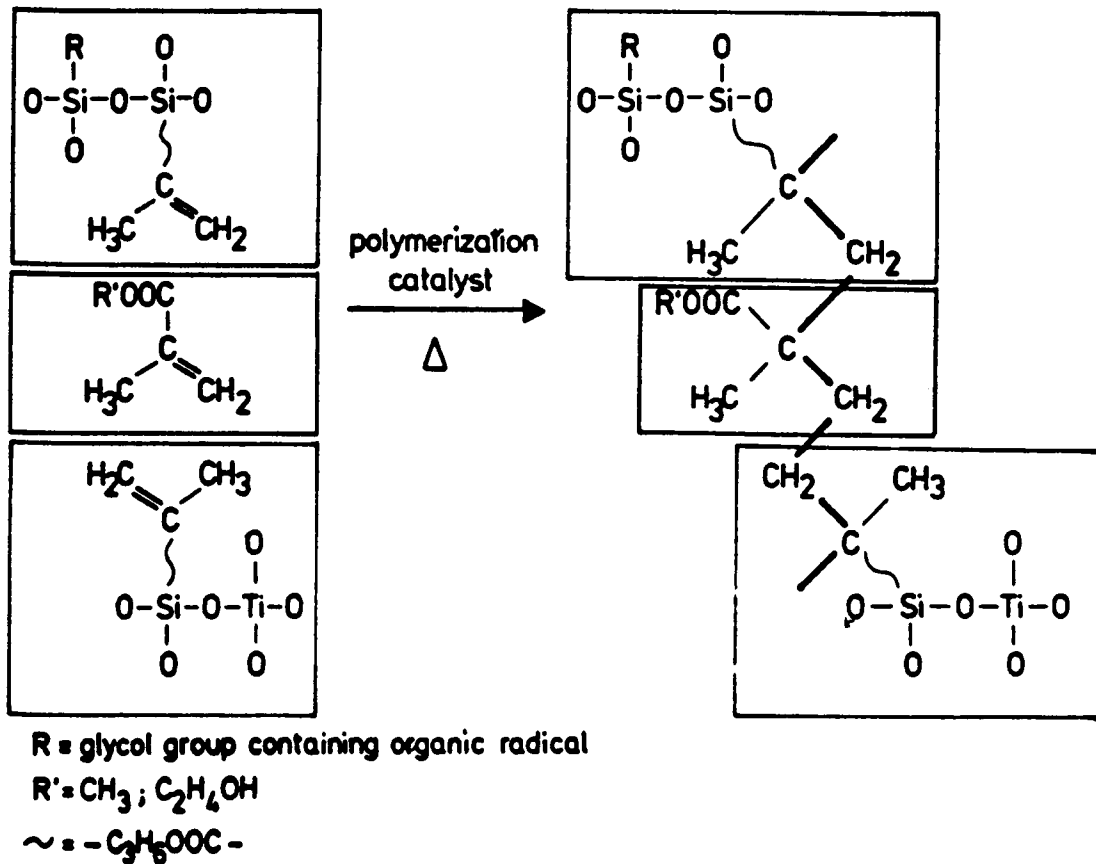
Fig. 2.8   General reaction scheme of preparing PMMA modified SiO_2-TiO_2 system [4].

CHAPTER THREE

EXPERIMENTAL PROCEDURE AND TECHNIQUES

The sol-gel process is utilized in this project as a potential new approach to incorporate organic oligomers with inorganic metal alkoxides. Although more than one type of component can be used, systems consisting of a single compound of the organic and the inorganics are the principal focus. Silicon alkoxides are the inorganic components being chosen due to their somewhat controllable reaction rate; elastomeric oligomers are the organic components used to prepare these unique hybrid materials. After a sufficient period of drying time, experiments are conducted to study the structure and the mechanical properties of the resulting gels. It is the author's intention to understand the effects of several important variables on the structure-property relationship of these hybrid systems.

3.1 MATERIALS

Tetraethoxysilane (TEOS) of 99% purity was obtained from the Fluka Company and Petrarch systems; this is the inorganic component to prepare most of the hybrid materials. However, tetramethoxysilane (TMOS) of 99% purity (from the Fluka company) was used in some cases. The chemical compositions of these two compounds are shown in Fig. 3.1.

Silanol terminated poly(dimethyl siloxane) (PDMS) was obtained from the Petrarch systems; two different number average molecular weights -- 550 and 1700 g/mole -- were used. The composition of this PDMS oligomer is also shown in Fig. 3.1. In addition, two types of triethoxysilane endcapped poly(dimethyl siloxane) (APDMS) were supplied

by the 3M company; the number average molecular weights before the endcapping were 1000 and 2400 g/mole, respectively. The endcapping reaction of these PDMS oligomers, which possess higher functionality than the silanol terminated PDMS, is shown in Fig. 3.2.

Triethoxysilane endcapped poly(tetramethylene oxide) (PTMO) was generously supplied by the 3M company; the endcapping reaction of these oligomers are shown in Fig. 3.3. Four different number average molecular weights of PTMO --650, 1000, 2000, and 2900 before the endcapping -- were used for preparing the hybrid materials. In addition, the 3M company also supplied another type of PTMO which possessed different numbers of triethoxysilane groups along the backbone of the chain. The number average molecular weight of this type of PTMO was 5800 g/mole; the average number of the triethoxysilane groups (including the endgroups) of these compounds ranged from 2 to 5. All the components required to prepare these PTMO(5800) are listed in Fig. 3.4. The preparation procedure of these materials was as following:

> To a one liter flask were added proper amounts of poly(tetramethylene oxide) (DuPont "Terathane 1000"), 1,4-butanediol, trimethylolpropane, and dry tetrahydrofuran. This mixture was stirred under nitrogen to dissolve all components whereupon isophorone diisocyanate and dibutyltin dilaturate were added. The mixture was heated at reflux for 4 hours at which time an IR spectrum of the material showed no isocyanate remained. Proper amount of isocyanatopropyl triethoxysilane was then added and the mixture was held at 60°C for 10 hours. An IR spectrum of this material showed no isocyanate remained.

PTMO(1000) is the soft segment of these PTMO(5800) materials; butanediol is used as the chain extender. Trimethylolpropane is employed to generate the pendent functional groups on the oligomeric chains; the number of pendent groups per chain can be controlled by adjusting the amount of this trifunctional material. It has been assumed
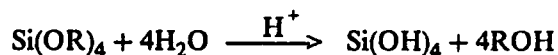
that the first two hydroxyl groups from this trimethylol are as reactive as the hydroxyl groups from PTMO and butanediol, while the last one is less likely to react with the isophorone diisocyanate so that it can be preserved for the latter endcapping reaction. Another important point to note is that the position of these triethoxysilane groups along the chain can not be controlled and, furthermore, the number of reactive groups per chain can only be viewed as an average over the whole system.

Tetrahydrofuran (THF) and isopropanol were obtained from the Fisher Scientific Inc.; these two compounds were the cosolvents of almost all the reactions. Hydrochloric acid (HCl of 10N) was also obtained from the Fisher Scientific Inc.; it was chosen to be the catalyst for the sol-gel reactions. All of the chemicals, including the silicates, oligomers, solvents, and catalyst, were used without further purification.

3.2 REACTION SCHEMES

A simplified reaction scheme of the hybrid systems prepared using the silane and the silanol terminated PDMS is suggested below:

HYDROLYSIS

$$Si(OR)_4 + 4H_2O \xrightarrow{H^+} Si(OH)_4 + 4ROH$$

POLYCONDENSATION (not stoichiometrically balanced)

$$Si(OH)_4 + HO\text{---}(\underset{CH_3}{\overset{CH_3}{Si}}\text{---}O)_x\text{---}\underset{CH_3}{\overset{CH_3}{Si}}\text{---}OH \xrightarrow{H^+} \underset{O}{\overset{O}{\text{---}Si}}\text{---}O\text{---}(\underset{CH_3}{\overset{CH_3}{Si}}\text{---}O)_y\text{---}\underset{CH_3}{\overset{CH_3}{Si}}\text{---}O\text{---}\underset{O}{\overset{O}{Si}}\text{---} + H_2O$$
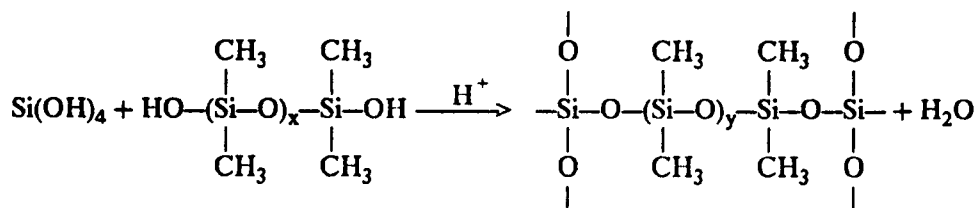
where R is either a methyl or an ethyl group; x and y are the degree of polymerization of the oligomers. Due to the possibility of chain extension and scission of the PDMS, x and y may not be the same. If a chain extension of the PDMS takes place, y would be larger than x. Conversely, x would be larger than y if a chain scission occurs. Both of these reactions are possible due to the high reaction temperature and the strong acidic environment. However, no matter which reaction takes place, the endgroups of the resulting species should always be hydroxyl groups. Hence, the reaction scheme should still be valid. Nevertheless, these reactions-- chain extension and scission-- have considerably complicated the sol-gel reactions. Although a complete hydrolysis is shown in the reaction scheme, this is likely not accurate. As discussed in the previous chapter, the hydrolysis and condensation reactions often take place simultaneously in a sol-gel process. Since the PDMS is silanol terminated, the rate of the hydrolysis of the silicates is of strong importance due to the possible self condensation of the PDMS oligomers.

For the hybrid systems made with silicates and triethoxysilane endcapped oligomers, the suggested reaction scheme is somewhat different. A simplified scheme representing this process is shown below:

HYDROLYSIS

$$Si(OR)_4 + 4H_2O \xrightarrow{H^+} Si(OH)_4 + 4ROH$$

$$(RO)_3Si-(PTMO)-Si(OR)_3 + 6H_2O \xrightarrow{H^+} (HO)_3Si-(PTMO)-Si(OH)_3 + 6ROH$$

POLYCONDENSATION (not stoichiometrically balanced)

$$Si(OH)_4 + (HO)_3Si-(PTMO)-Si(OH)_3 \xrightarrow{H^+} \begin{array}{cccc} | & | & | & | \\ O & O & O & O \\ | & | & | & | \\ -Si-O-Si-(PTMO)-Si-O-Si- \\ | & | & | & | \\ O & O & O & O \\ | & | & | & | \end{array} + H_2O$$
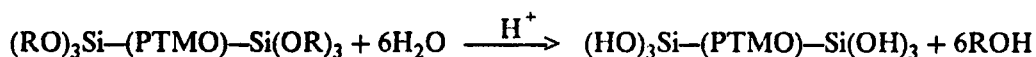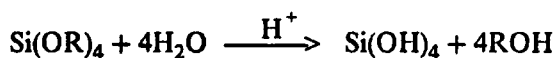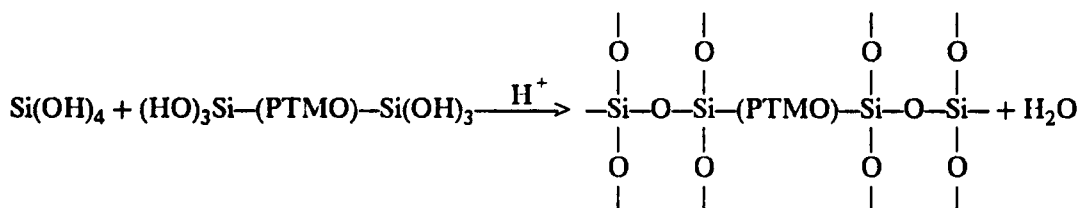
Although the PTMO is used as the example here, this reaction scheme is also valid for the endcapped PDMS. Basically, this scheme is similar to that shown before. However, in this case, the endcapped oligomers would have to undergo hydrolysis to generate the silanol groups. This should greatly reduce the probability of self extension of the oligomeric chains when considering the high molar ratio of silicate to oligomer. Also important is the increase in the functionality of the oligomers -- from 2 in PDMS to 6 in these endcapped species. This higher functionality should assure the incorporation of the oligomers with the inorganic species; dangling ends would thus be rather unlikely. As shown in Figs. 3.2 & 3.3, the endcapping is achieved by either an urea or an urethane linkage. The stability of this linkage with respect to the hydrolysis might become an additional complication to the sol-gel process. Nevertheless, this kind of endcapping approach does offer another alternative of utilizing the organically modified sol-gel reaction. With the success of this approach, some other types of linkages besides urethane (e.g., amide) may also be tried to increase the versatility of this sol-gel process.

For the PTMO with multiple triethoxysilane groups (PTMO(5800)), the reaction scheme would be similar to that of the endcapped PTMO except that the ethoxy group does not have to be in the end of a oligomeric chain. It is expected that the oligomers would most likely be connected into the network in more than two points (i.e., the ends). This should result in a higher restriction on the mobility of the oligomeric chains. Also, the silicate network is expected to show higher continuity than the two previous cases.

3.3 EXAMPLE PROCEDURES

Due to the difference in the structure of the oligomers, slight modification of the reaction procedure is made in each case.

3.3.1 A TEOS-PDMS SYSTEM

An appropriate amount of distilled water and hydrochloric acid was first added to a 100 ml round-bottom flask with 8 ml of isopropanol and 2 ml of THF; the solution was mixed thoroughly until a clear solution was obtained. Then, 10 ml of TEOS and 10.9 ml of PDMS (for a 48 wt% TEOS hybrid system) were poured simultaneously into the solution. Immediately after the addition of TEOS and PDMS, the flask was placed into a water bath at 80°C and the reaction took place under reflux with fast agitation for 20 minutes. The resulting solution, which was usually clear, was then removed from the water bath and poured into several Teflon coated petri dishes and covered with Parafilm to allow the systems to gel. Several small holes were made on the Parafilm to allow the evaporation of the volatiles. After 24 hours under ambient conditions, the sampled gelled and the Parafilm was removed. After that, the samples were dried under ambient conditions for at least another 48 hours before carrying out any characterization.

As reported in several previous studies, the reaction rate of the pure sol-gel process is usually slow at ambient temperature. Hence, using a higher reaction temperature would cause the reaction to go faster and shorten the gelation time. In addition, since the siloxane oligomers are extremely hydrophobic due to the large difference in the solubility parameters, an increase of the reaction temperature would also promote homogeneity of the system. As a result, all the reactions of this type of incorporation are carried out under 80°C. The volume ratio between the isopropanol and THF is fixed at 4:1; this ratio has been shown in some preliminary experiments to result in better homogeneity of the solution. Since the resulting gels would adhere to the surface of a glass petri dish, a layer of Teflon coating on the dish is used. Due to large drying stresses in the drying process, Parafilm is utilized to control the evaporating rate of the solvent to prevent the gels from cracking.

3.3.2 A TEOS-PTMO SYSTEM

Eight milliliters of isopropanol and 2 ml of THF were first added to a 100 ml flask, then 10 grams of TEOS and an appropriate amount of PTMO (depending on the desired compostion) were added and mixed thoroughly at ambient temperature until the solution appeared to be homogeneous. In the meantime, a mixture of HCl and deionized water were prepared according to the stoichiometric calculation. This mixture was then added to the base solution which contained TEOS and PTMO. The resulting system was rapidly mixed for approximately 30 seconds, and the clear solution was then cast into several Teflon coated petri dishes and covered with perforated Parafilm. After 48 hours, the Parafilm was removed and the gel was dried under ambient conditions for another week prior to testing.

In this reaction procedure, the reactants are mixed first to assure high homogeneity of the system. The water and the catalyst (HCl) are added later to promote the reaction. Since the PTMO oligomers are rather viscous, this change of the order of addition is expected to improve the homogeneity of the system. Due to the high functionality of the endcapped PTMO, the gelation time is usually within a few minutes. Therefore, the reaction temperature is lowered to ambient condition so that the system would not gel inside the reactor. Teflon coated petri dishes are still used for this system; however, the usage of polystyrene petri dish has also been successful since the sample can usually be removed from the surface without cracking. This interesting result not only avoids the need of preparing Teflon coatings, but also reduces the lateral shrinkage considerably. Most importantly, due to much smoother surfaces of the polystyrene than the Teflon coatings, the samples produced are extremely transparent and the surface scattering effect is hardly observed. Due to the aging effect of this system (details will be discussed in later chapters), the drying time is longer compared to the PDMS system. One thing to mention is that a small amount of heat is often generated by the reaction. However, since this exotherm occurs in every case, it should not affect the validity of the interpretation in later chapters.

3.3.3 A TEOS-PTMO(5800) SYSTEM

The reaction procedure for these systems is similar to that of the TEOS-PTMO systems.

However, since the oligomers are already dissolved in THF, only isopropanol is added

to the solution. The volume ratio of the isopropanol to the THF is fixed at 1:1. The

gelation time of this system is somewhat longer than that of the TEOS-PTMO system;

this is believed to be caused by the larger amount of solvents used. This increase in the

amount of solvents also excludes the possibility of using plastic petri dishes since THF

interacts with polystyrene and results in difficulty in removing films and turbidity of the

samples.

3.4 NOMENCLATURE

The nomenclature that was developed for this project can be illustrated by the example

shown below:

<p align="center">TEOS(50)---PTMO(2000)---50---0.04---RT</p>

The five items in this expression represents the primary variables that will be studied in

this thesis; they are further explained as follows:

- TEOS(50)--- This indicates the type of silicate used for the sol-gel reaction and its

  weight percent out of the total weight of the silicate and the oligomer.

- PTMO(2000)--- This indicates the type of oligomer used and its molecular weight.

  In the case of PTMO(5800), there is an additional number after the molecular

  weight indicating the average number of triethoxysilane groups on each oligomeric

  chain.

- 50--- This represents the percentage of stoichiometric amount of water added to the sol-gel reaction. A value of 100 indicates the amount of water is in exact stoichiometry of the hydrolysis reaction (i.e., molar ratio of H_2O:ethoxy $= 1$:1.)

- 0.04--- This represents the molar ratio of HCl to silicate.

- RT--- This indicates the reaction temperature used for the sol-gel process. RT means ambient temperature.

In addition to the variables mentioned in the nomenclature, the effect of type of reaction medium has also been studied for the TEOS-PTMO system.

3.5 EXPERIMENTAL TECHNIQUES

In addition to developing a new approach for incorporating organics with inorganics into solid materials, another objective of this work has been to study the structure-property relationships of these hybrid systems. Therefore, after successfully preparing the samples, structural characterization and property measurements are carried out on all the materials. The techniques utilized to accomplish this are listed in the following sections.

3.5.1 STRUCTURAL CHARACTERIZATION

Small angle X-ray scattering (SAXS) --- A Siemens Kratky camera system with a copper target X-ray tube was utilized for this experiment. The wavelength of the $CuK\alpha$ X-ray generated was 1.54 Å; a Nickel filter was used to minimized the intensity of the $CuK\beta$ X-ray. The entrance slit width was 100 microns for all experiments. A General Electric model XRD-6 X-ray generator was utilized; the operating voltage was 40 kv and the current was 20 mA. A position sensitive detector system (PSD) from the M. Braun Inc. was used in conjunction with the Kratky camera. A gas mixture of 10% methane and

90% Argon was utilized as the purge gas for the detector; the gas pressure was 11 bar. A voltage of 3.6 kv was applied to the PSD for all measurements.

A standard lupolen sample (polyethylene) was employed to measure the X-ray intensity of the primary beam; a lead stearate sample with a discrete small angle d-spacing of 49.5 Å was used to calibrate the detector on a daily base. For every sample, the scattering intensity was measured at both the scattering position and the parasitic position. The latter was subtracted from the former to obtain the sample scattering profile. A SAXS analysis program written using the ASYST software package (Macmillan software company) was utilized to process all the experimental results. In addition, a FORTRAN program written by Vonk and coworkers was utilized to calculate the invariant and the mean square electron density fluctuation.

In addition to the detector method, a film method was also utilized to study the X-ray scattered at small angles. A Warhus camera with a sample-to-film distance of 33.5 cm was employed for this purpose.

Wide angle X-ray scattering (WAXS) --- A Philips table-top model 1520 X-ray generator with a copper target X-ray tube and a Ni filter were utilized; the operating conditions were fixed at 40 kv and 20 mA. A Warhus camera system was used to obtain the scattering patterns of all samples. The sample-to-film distance was fixed at 7.6 cm for all WAXS studies; the camera system was kept under vacuum during the experiment.

Scanning Electron Microscopy (SEM) --- A ISI Inc. Super-III scanning electron microscope was utilized to study the structure of the fractured surfaces. All the samples were fractured under a liquid nitrogen environment; the fractured surfaces were then

coated with gold using a sputter coater from Structure Probe Inc. (SPI) to prevent electron saturation (charging) during the experiments.

Limited Raman spectroscopy results were utilized to provide further information on the structure and, most importantly, the degree of reaction of the system. A facility in the Department of Physics was employed for this purpose.

3.5.2 MEASUREMENTS OF PROPERTIES

Mechanical properties --- An Instron model 1122 was utilized to measure the elongation at break, Young's modulus, and the ultimate strength of all the hybrid samples. Dogbone samples of 10mm in length and 2.74 mm in width were used; the crosshead speed was fixed at 2 mm/min.. All the measurements were carried out under ambient conditions.

Dynamic mechanical spectroscopy --- A DDV-IIC Rheovibron dynamic viscoelastometer was employed for this purpose. For most of the TEOS-PDMS hybrid materials, the experiments were carried out by manually adjusting the tension of the samples. The oscillatory frequency was fixed at 110 Hz. The temperature range of investigation was between -150 °C and 300 °C; the heating rate was 1-2°C/min.. For the hybrid systems containing PTMO oligomers, an automated system developed by the Imass company has been added onto the existing Rheovibron. Measurements at three different frequencies -- 1.1, 11, and 110 Hz -- were automatically taken by a multiprogrammer; however, data at 11 Hz was chosen for discussion due to its stability and smoothness. The measurement temperature ranged from -150°C to 150°C; the heating rate was controlled at 1-2°C/min.. The modulus value was calibrated by using a Lexan sample (polycarbonate) under ambient conditions. A pre-purified, dry nitrogen gas was used as

the purge gas for all measurements; liquid nitrogen was used to cool down the system to the desired starting temperatures of the experiments.

Thermal analysis --- A differential scanning calorimetry (DSC) model II from the Perkin-Elmer company was utilized to measure the increase of the specific heat at the glass transition temperature. The temperature range of investigation was from -150°C to 0°C; the heating rate was fixed at 20°C/min.. The calibration for sub-ambient operation was achieved by using a cyclohexane sample, which had a melting temperature at -87°C. A helium gas was used as the purge gas; liquid nitrogen was used as the coolant.

In addition to calorimetry, a thermal gravimetric analyzer (TGA) from the Perkin-Elmer company was utilized to study the weight loss with respect to the temperature. The temperature range of experiments was from the room temperature to 900°C; the heating rate was fixed at 10°C/min..

3.6 SAXS ANALYSIS

As mentioned earlier, small angle X-ray scattering (SAXS) was the main technique in this project for probing the structure of these novel hybrid materials. Although X-ray scattering method has been utilized extensively in the research field, the hazard of radiation has made this technique somewhat mysterious. In order to establish some background for the reader, general principles of SAXS will be given in this section. Furthermore, the analysis utilized in this thesis for data interpretation is also explained in detail. However, it was not the author's intention to give a review on the SAXS analysis. For readers who are interested in better understanding of this SAXS technique

and its application on the polymer system, several publications are recommended [64-71].

3.6.1 PRINCIPLES OF X-RAY SCATTERING

When X-ray (or any other electromagnetic waves) passes through an object, the inherent electric field will cause the electrons in the material to oscillate. This oscillation of the electrons will evolve energy in the form of secondary X-rays (see Fig. 3.5). Although this secondary X-ray will have the same characteristic wavelength and frequency as the primary beam, its direction may be quite apart from the incident X-ray. This phenomenon is known as the Thomson scattering. Since each electron is a source of secondary X-ray, interference between scattering beams will take place. Depending on the distance between the scattering sources (i.e., the electrons), constructive or destructive interference may result (see Fig. 3.6). Since the intensity observed is the product of the amplitude and its complex conjugate, great difference will result by different types of interference. In other words, the observed scattering intensity at different angles will depend on the relative positions of the electrons or, more generally, the structure of the scattering object. In fact, it has been established that the X-ray scattering profile is a fourier transform of the electron density distribution of the material under investigation [69]. As a result, structural information can be obtained from the analysis of the X-ray scattering profile.

Although electrons were viewed as the scattering sources, this concept can also be generalized to larger structures. For example, one can increase the scale so that an atom -- a collection of electrons --is viewed as the scattering source. In this case, the characteristic distance between atoms can be studied by the scattering technique. To

generalize this concept even further, the scattering source can be molecules or a collection of molecules (e.g., domains). Accordingly, structural information concerning these scatterers can be obtained.

In principle, structural information at any scale can be obtained from a scattering profile. However, depending on the size of the scatterer, different part of this scattering profile will have to be emphasized. Since the scattering angle is inversely related to the size of the structure under investigation, the larger the structrue is, the lower the scattering angle range will be. Generally speaking, small angle X-ray scattering (SAXS) provides strucutral information within the range of 2-100 nm. Since most of the domain size in block or segmented copolymers falls within this range, SAXS has therefore been used as an useful technique in studying the structure of these systems [64-68].

3.6.2 BRAGG'S SPACING

The use of SAXS analysis in this thesis can be best illustrated by the simplified scheme shown in Fig. 3.7. The upper row in this figure is the electron density profiles of the polymeric system under investigation. ρ_1 and ρ_2 are the electron densities of the two components, respectively, $\bar{\rho}$ is the average electron density of the system, and d is the distance between two regions with the same value of electron density. In the bottom row, the corresponding SAXS profiles of these systems are shown. The scattering vector s is defined as

$$s = \frac{2\sin\theta}{\lambda}$$

where θ is half of the radial scattering angle, and λ is the wavelength of X-ray.

Figure 3.7(a) shows a system with a fixed correlation distance, d, between two regions which have the same electron density ρ_1. Due to the high "periodicity" of such system, a strong scattering intensity will be observed at an angle corresponding to this correlation distance. This will result in a maximum in the scattering profile. Assuming the system is isotropic and the domains are spherical, the value of this correlation distance d can then be estimated by Bragg's law

$$n\lambda = 2d \sin \theta$$

where n is the order of the scattering maximum. Although higher order maxima may appear on the SAXS profile, it is only for systems with extremely high periodicity. In addition, the intensity of the maximum always decreases as the order becomes higher. For all the samples which showed the existence of a correlation distance in this thesis, only one maximum was observed. Therefore, n is taken to be unity in estimating the correlation distance. To relate this Bragg's spacing with the scattering vector s used in this thesis, one can substitute $s = 2\sin\theta/\lambda$ into this equation and obtain

$$d = \frac{1}{s} = \frac{\lambda}{2\sin\theta}$$

where s is the value of the scattering vector at which the maximum is observed. To obtain a best estimation of the correlation distance by Bragg's law, scattering profiles from pin-hole camera should be used. That is, the data under analysis is desmeared. For this study, a Kratky slit camera was used and, therefore, the resulting profiles were smeared data. The smearing effect always causes the position of the maximum to shift toward lower angles. As a result, the correlation distance calculated by Bragg's law will always be an overestimation. In addition, the system under investigation may deviate

from the assumption of spherical domains, which will also introduce some extent of error to the estimation. Nevertheless, the Bragg's spacing should still be useful as a first estimation of the correlation distance.

3.6.3 INVARIANT ANALYSIS

In addition to the type of electron density profile shown in Fig. 3.7(a), it is also possible that the distance between two regions of the same electron density is not regular, which means that there is no or very low periodicity in the scattering sample. This situation will result in a monotonic SAXS profile as those shown in Fig. 3.7 (b) and (c). The former has a higher electron density contrast and, therefore, results in a higher scattering intensity than the latter. This electron density contrast is usually referred as the "scattering power" of the sample [70], and it is quantitatively represented by the mean square electron density fluctuation

$$\overline{(\Delta\rho)^2} = \overline{(\rho - \bar{\rho})^2}$$

where $\bar{\rho}$ is the average electron density of the scattering sample. For a homogeneous system, the electron density fluctuation is zero and the scattering power is low. The resulting SAXS intensity should be negligible. On the other hand, for a highly phase separated, two-component system, the electron density fluctuation is high and, hence, the SAXS intensity should also be high. Therefore, this value of mean square electron density fluctuation can be used as an index of the homogeneity of the system under investigation.

To obtain the value of mean square electron density fluctuation, $\overline{(\Delta\rho)^2}$, invariant analysis will have to be carried out on the SAXS profile. For a smeared SAXS profile, the invariant, Q, is defined as

$$Q = \int_0^\infty sI(s)ds$$

where I(s) is the smeared SAXS intensity as a function of the scatterin vector s. After obtaining the value of invariant, the mean square electron density fluctuation can be calculated by

$$\overline{(\Delta\rho)^2} = \frac{2\pi a^2 Q}{i_e N^2 d}$$

where the mean square electron density fluctuation is in the square of mole electrons per cubic centimeter and

   a = specimen-to-detector distance in centimeter

   d = specimen thickness in centimeter

   N = Avogadro's number

   $i_e = 7.9 \times 10^{-26}$, the Thomson scattering constant of a free electron

For a particular instrument and scattering specimen, all the parameters shown above are constant. Therefore, the electron density fluctuation, or the scattering power, is proportional to the invariant Q. Therefore, if a SAXS profile shows high intensity throughout the scattering angle range, the invariant will be great and the homogeneity of this specimen is low. However, comparison of scattering power between different

samples can not always be easily indicated by the overall intensity due to the factor of s in the integration. Furthermore, if desmeared data is used, a factor of s^2 should be used instead of s for the calculation of invariant Q.

One point should be noted about this invariant analysis is that, in order to calculate Q from a single SAXS profile, the assumption of isotropic structure will have be made. In some cases (e.g., lamellar), this may not be valid. Then, rotation of the sample may be needed to obtain meaningful structural information.

- tetraethoxysilane (TEOS)
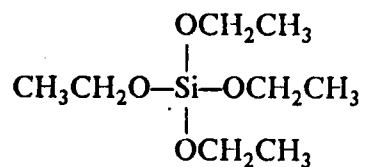
$$
\begin{array}{c}
OCH_2CH_3 \\
| \\
CH_3CH_2O-Si-OCH_2CH_3 \\
| \\
OCH_2CH_3
\end{array}
$$

- tetramethoxysilane (TMOS)

$$
\begin{array}{c}
OCH_3 \\
| \\
CH_3O-Si-OCH_3 \\
| \\
OCH_3
\end{array}
$$

- silanol terminated poly(dimethyl siloxane) (PDMS)

$$
\begin{array}{cc}
CH_3 & CH_3 \\
| & | \\
HO-(Si-O)_n-Si-OH \\
| & | \\
CH_3 & CH_3
\end{array}
$$
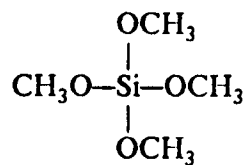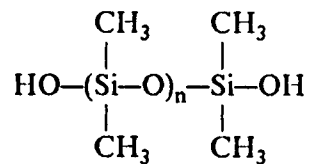
Fig. 3.1   Compositions of the silicates and the silanol terminated PDMS used in the reactions.

amino-propyl terminated poly(dimethyl siloxane)

$$
\begin{array}{cc}
CH_3 & CH_3 \\
| & | \\
H_2N\text{—}(CH_2)_3\text{—}(Si\text{—}O)_n\text{—}Si\text{—}(CH_2)_3\text{—}NH_2 \\
| & | \\
CH_3 & CH_3
\end{array}
$$

+

3-isocyanato-propyl-triethoxysilane

$$
\begin{array}{c}
OC_2H_5 \\
| \\
2 \quad C_2H_5O\text{—}Si\text{—}(CH_2)_3\text{—}N = C = O \\
| \\
OC_2H_5
\end{array}
$$

$$
\begin{array}{c}
OC_2H_5 \; HOH \quad CH_3 \quad CH_3 \quad HOH \quad OC_2H_5 \\
| \quad | \, \| \, | \quad | \quad | \quad | \, \| \, | \quad | \\
C_2H_5O\text{—}Si(CH_2)_3NCN(CH_2)_3\text{——}(Si\text{—}O)_n\text{—}Si\text{—}(CH_2)_3NCN(CH_2)_3Si\text{—}OC_2H_5 \\
| \quad\quad\quad\quad\quad\quad | \quad | \quad\quad\quad\quad\quad | \\
OC_2H_5 \quad\quad\quad\quad CH_3 \quad CH_3 \quad\quad\quad OC_2H_5
\end{array}
$$
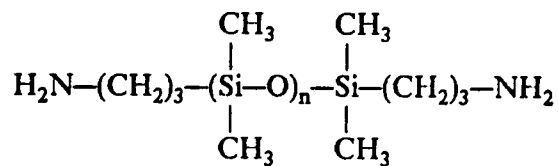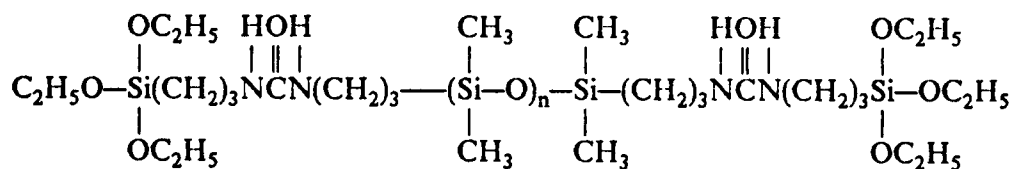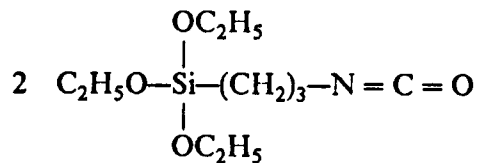
Fig. 3.2   The reaction scheme to prepare triethoxysilane endcapped PDMS.

poly(tetramethylene oxide)

$$HO-(-CH_2-CH_2-CH_2-CH_2-O-)_n-H$$

+

3-isocyanato-propyl-triethoxysilane

$$2 \quad C_2H_5O-\underset{\underset{OC_2H_5}{|}}{\overset{\overset{OC_2H_5}{|}}{Si}}-(CH_2)_3-N=C=O$$

$$C_2H_5O-\underset{\underset{OC_2H_5}{|}}{\overset{\overset{OC_2H_5}{|}}{Si}}-(CH_2)_3-\underset{\overset{H}{|}}{N}-\overset{\overset{O}{\|}}{C}-O-(CH_2CH_2CH_2CH_2O)_n-\overset{\overset{O}{\|}}{C}-\underset{\overset{H}{|}}{N}-(CH_2)_3-\underset{\underset{OC_2H_5}{|}}{\overset{\overset{OC_2H_5}{|}}{Si}}-OC_2H_5$$
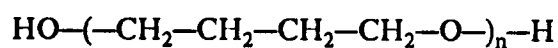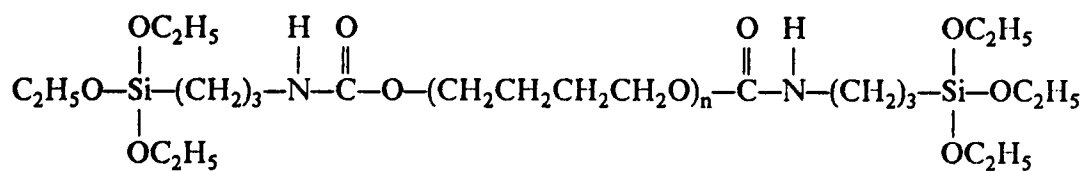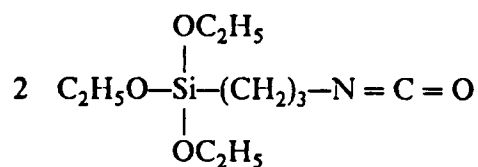
Fig. 3.3   The reaction scheme to prepare triethoxysilane endcapped PTMO.

- poly(tetramethylene oxide)

$$HO-(-CH_2-CH_2-CH_2-CH_2-O-)_n-H$$

- isophorone-diisocyanate

$$
\begin{array}{c}
NCO \\
\\
OCN-H_2C \quad\quad CH_3 \\
CH_3 \quad CH_3
\end{array}
$$

- butanediol

$$HO-(CH_2)_4-OH$$
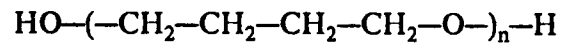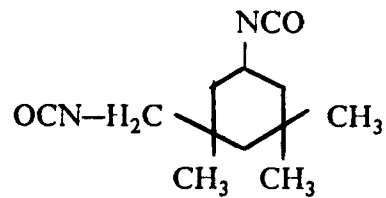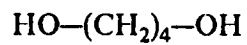
- trimethylol propane (to produce pendent OH)

$$
\begin{array}{c}
CH_2OH \\
| \\
CH_3-CH_2-C-CH_2OH \\
| \\
CH_2OH
\end{array}
$$
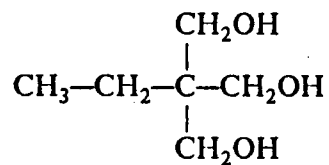
Fig. 3.4   The components for preparing PTMO with multiple hydroxyl groups.
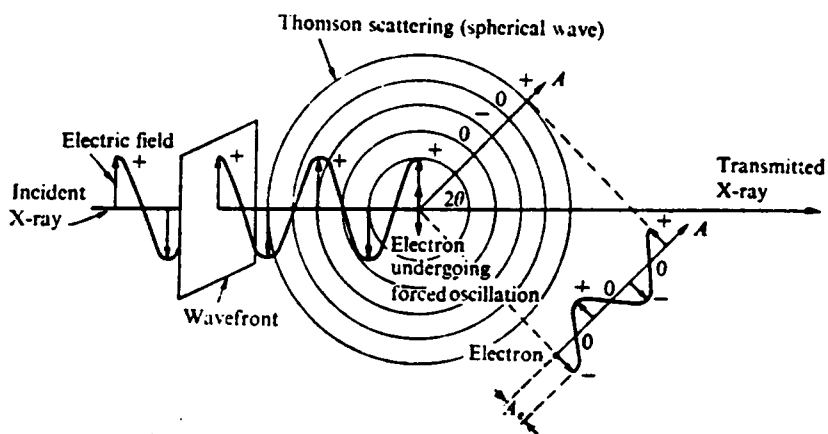
Fig. 3.5 Generation of spherical secondary X-ray by the Thomson scattering effect [69].
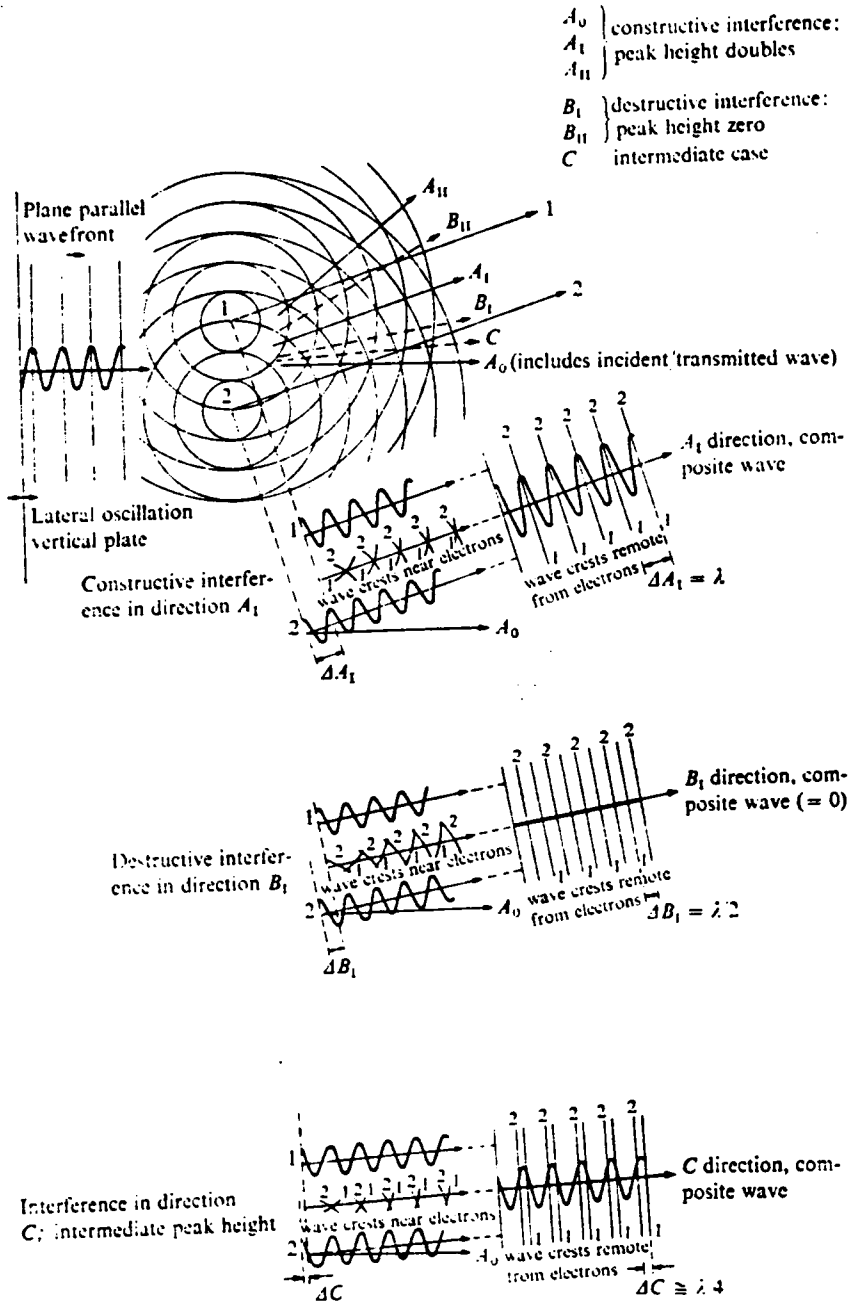
Fig. 3.6 Scattering and Interference from two scattering centers [69].
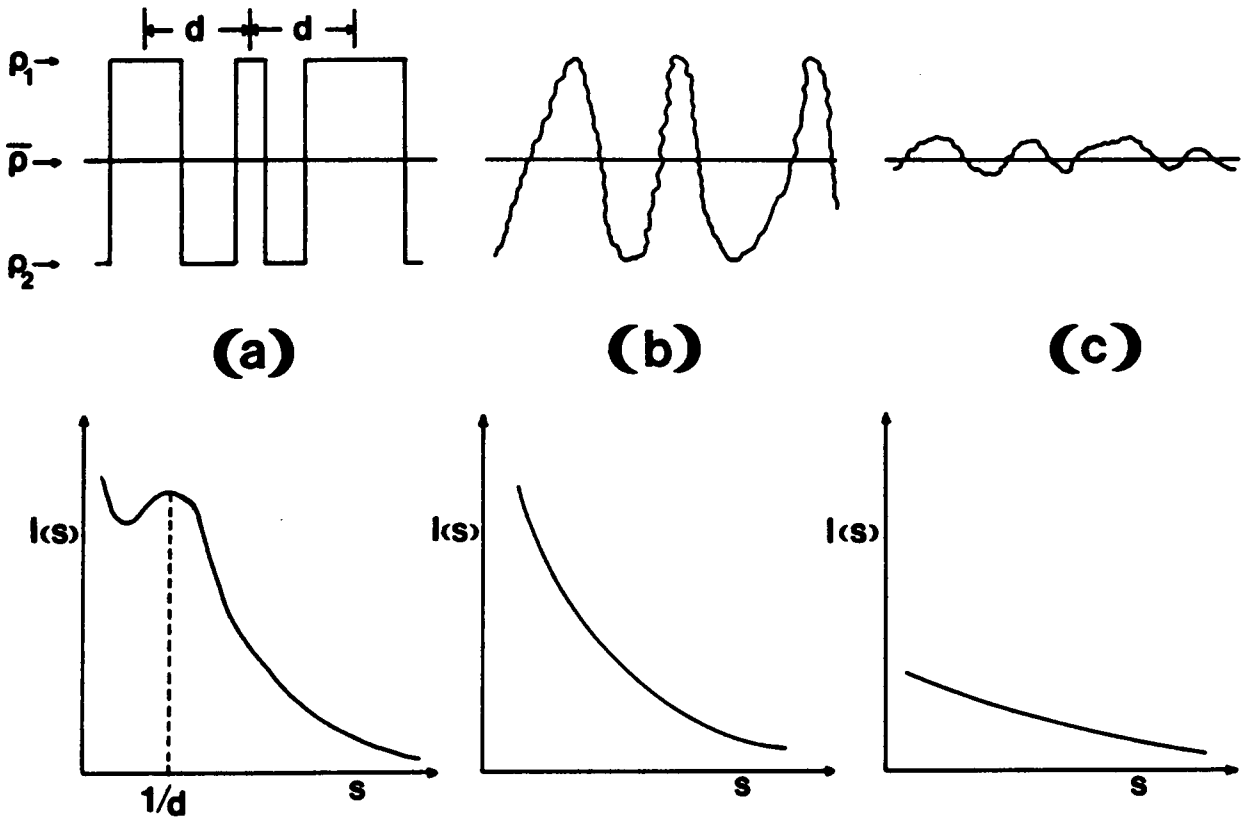
Fig. 3.7 Schematic models for the electron density profile and corresponding SAXS profiles: (a) periodic fluctuation with correlation length "d" (b) random electron density fluctuations (c) random fluctuations with smaller magnitude than for (b) above.

CHAPTER FOUR

HYBRID SYSTEMS BASED ON TETRAORTHOSILICATES

AND FUNCTIONALIZED POLY(DIMETHYL SILOXANES)

The first attempt of preparing hybrid materials through the modified sol-gel route was carried out by using a combination of tetraethoxysilane (TEOS) and functionalized poly(dimethyl siloxane) oligomers. In addition to their rubbery nature, the siloxane oligomers were chosen for the following reasons. First, the backbone structure of these oligomers are similar to that of the silicate network (i.e., the Si-O-Si type of linkage). In fact, the siloxane polymers have been categorized as inorganic polymers (Flory [2]). Therefore, it was hoped that this characteristics could assist in promoting compatibility with the silicates. Secondly, the siloxane polymers are relatively stable at high temperatures. Since the silicates are known to sustain high temperatures too, materials prepared with this combination could hopefully be used for applications which require high thermal stability. Finally, due to the extremely hydrophobic nature of the siloxanes, oligomers were used instead of high molecular weight polymers so that the possibility of large scale phase separation could be reduced.

Several types of PDMS oligomers with different terminal functional groups were available, but the silanol terminated PDMS was chosen for this initial study. This choice can be understood by recalling the reaction scheme of the pure silicate sol-gel process (see page 10). According to that simplified scheme, the silicon alkoxides (TEOS in this case) will first react with water to generate silanol groups. Then, these silanols will self condense to produce Si-O-Si linkages. Eventually, a 3-dimensional network structure will be formed due to the high functionality of silicon alkoxides (i.e., 4). With this

procedure in mind, it is reasonable to postulate that the incorporation of PDMS can likely be achieved by using oligomers with silanol terminal groups. However, this type of oligomer does have the drawback of low functionality (i.e., 2), which will result in dangling ends or free chains in the system if the reaction is not complete. Hence, another form of PDMS which was endcapped with triethoxysilane was also used for the incorporation. The objective of this work was to understand the effect of the oligomeric functionality of the reaction and the properties of the final materials. In addition, if this triethoxysilane endcapping route was successful, it offered a strong possibility of parparing other types of oligomers for incorporation into the sol-gel reaction.

The reaction procedures of preparing these TEOS-PDMS hybrid materials were given in the previous chapter (see section 3.3). All the materials obtained in this part of the study were transparent. Three cast films of these TEOS-PDMS hybrid materials are shown in Fig. 4.1. The diameter of the resulting films was ca. 10 cm, which was the approximate size of the petri dish used to cast the films. Although no larger films were prepared, there is no reason to exclude this possibility. However, as the TEOS content increased beyond 70 wt%, the cracking problem became severe and sufficiently large samples for testing were not obtainable. Shrinkage was observed in most cases and it was more significant for samples of higher TEOS content. This is reasonable considering the large weight loss in the hydrolysis reaction of TEOS. Several important variables of these TEOS-PDMS systems --- acid content, water content, TEOS content, PDMS molecular weight, and PDMS functionality --- were varied to study the effects on the final structure and properties. The results will be discussed accordingly in the following sections.

4.1 EFFECT OF ACID CONTENT

In a pure silicate sol-gel system, it has been shown by previous studies that the catalyst will influence the mechanism of the reaction and, therefore, the final structure and properties [17-27]. For a system without a large excess of water, an acidic catalyst tends to produce more "chain-like" molecules at the beginning stages of the reaction. Subsequently, the driving force of lower surface energy will cause these molecules to coalesce and undergo further curing to form a dense network. In contrast, a base catalyst will promote highly compact silicate particles and result in materials with large pores. Therefore, the choice of catalyst really depends on the desirable final properties. This is also true for the TEOS-PDMS hybrid systems. For example, a base catalyst will be the choice if a system with compact silicate particles is desirable. The previous studies by Mark and coworkers are good examples for these systems (see section 2.3). In their studies, highly condensed and compact silicate particles were observed to be dispersed in a PDMS network. Mark also reported that a higher degree of mixing was observed in their systems when an acid catalyst was used [60]. Since an intimate incorporation of the organic and inorganic components was the goal of the present study, an acidic catalyst was therefore used. Several types of acid were tested in a preliminary study [72], and the results showed that hydrochloric acid was particularly effective in producing useful hybrid materials. However, the question of how the HCl content would affect the final structure and properties was still unknown.

In order to understand the effect of acid content, a series of hybrid materials with various acid contents were prepared with film thicknesses of about 15 mils. The initial TEOS content was 48 wt%; the molecular weight of the silanol terminated PDMS was 1700 g/mole; the amount of water added was 50% of the exact stoichiometry (i.e.,

TEOS(48)-PDMS(1700)-50-X-80C, where X indicates that the acid content is a variable). The acid content, which was arbitrarily expressed as the molar ratio of HCl to TEOS, ranged from 0.022 to 0.111. This range of acid content was relatively high compared to that used in most of the previous pure sol-gel studies. A reaction with a lower acid content (HCl/TEOS = 0.002) was carried out, but an opaque sample with oily surfaces was obtained. This apparently unsuccessful incorporation resulted in the usage of higher acid content. All the solutions in these series were clear without visible incompatibility; this was essential in producing transparent materials. After 20 minutes of agitation under 80°C, the solutions became viscous. Although the viscosity was not measured, it clearly increased with increasing acid content. As might be expected, the shortest gelation time occurred for the system with the highest acidity. Similar observations have been reported for pure TEOS systems [11], and also attributed to a higher reaction rate resulting from a higher concentration of the catalyst.

The mechanical properties were first measured by carrying out the stress-strain experiments after being dried for at least one week. Examples of the resulting stress-strain curves from this acid series are shown in Fig. 4.2. The first thing to notice is that an near linear behavior is displayed by all samples, which is similar to the behaviors of glassy polymers and "stiff" elastomers. Secondly a clear trend is observed for the elongation at break: the value increases from 6% to 15% as the acid content increases from 0.022 to 0.111. Nevertheless, all these values are relatively low compared to pure crosslinked PDMS elastomers. Finally, a trend is also shown by the Young's modulus: the value of the initial modulus decreases as the acid content increases. However, the ultimate stress does not display any distinct tendency in this specific group. To further verify these different trends observed in Fig. 4.2, repetitive experiments were performed. The results of the elongation at break and the Young's modulus at different

acid content are shown in Figs. 4.3 & 4.4, respectively. In spite of some scatter of the data, the trends observed in Fig. 4.2 are again clearly displayed. The elongation at break ranges approximately the same as those shown previously, whereas the Young's modulus decreases from ca. $2x10^7$ to $1x10^7$ Pa. as the acid content increases. These values are relatively higher than those of pure elastomers (i.e., 10^6 Pa.), which further indicates the stiff nature of these hybrid materials. Due to the brittleness of these materials, dogbone samples sometime fractured in the region close to the clamps. This is believed to be the main reason for the observed scatter in the results.

The mechanical properties discussed so far provide information on the macroscopic response; clearly this macroscopic behavior should intimately relate to the microscopic structure. To understand this structure-property relationship, dynamic mechanical experiments were therefore performed to obtain more insight regarding the microscopic structure.

The behavior of the storage modulus, E', is shown in Fig. 4.5 with the corresponding tanδ spectra in Fig. 4.6. By examining the former, a general pattern is shown by all samples. At very low temperatures (lower than -130°C), a plateau with a magnitude of ca. 10^9 Pa. is observed. This value is typical for polymers below their glass transition temperatures (i.e., in the glassy state). As temperature increases, each sample initially goes through a broad transition region showing a gradually decreasing modulus and finally reaches another plateau which has the magnitude of about 10^7 Pa.--the modulus of a reasonably "stiff" elastomer. The broadness of this transition is somewhat different between each sample, but the trend is not easily seen from these spectra. This trend is better noted from the tanδ behavior which will be discussed shortly. The magnitude of the storage modulus in the plateau region increases as the acid content decreases; this

is consistent with the stress-strain results. However, the E′ values are somewhat higher than the modulus obtained from stress-strain experiments. This is reasonable when one considers the high frequency (110 Hz) by which the storage modulus was measured. After reaching the second plateau, the modulus remains almost constant for a range of almost 150°C before it begins to increase. This increasing tendency is smooth at the beginning and, then, becomes much steeper after ca. 250°C. The highest temperature for most of the experiments was over 300°C. Although most of the samples turned yellowish after the experiment, no fracture was observed.

Further information regarding the dynamic mechanical behavior comes from inspecting the corresponding tanδ spectra. As shown in Fig. 4.6, a bimodal type of behavior is displayed by all samples. At very low temperatures (lower than -130°C), the magnitude of tanδ is very low. As the temperature increases further, the intensity increases to a maximum at -106°C and then again decreases to a plateau region. Particularly noticable is that the magnitude of this maximum increases as the acid content decreases. Following this plateau region, another maximum or shoulder in tanδ is observed at high temperatures (-10°C). Contrary to the trend shown in the first maximum, the magnitude of this second maximum increases with the acid content. This bimodal type of tanδ behavior and the change of intensity with acid content are viewed as very important in the following discussion of the results.

As reported earlier, all prepared samples were transparent. This strongly suggested that, in the scale of the wavelength of the visible light (ca. 4000-7000 Å), no phase separation was observed. This absence of large scale separation is further supported by the fact that only one broad transition is shown in the storage modulus spectra. However, this does not exclude the possibility of some microphase separation. In fact, the bimodal type of

behavior observed in the tanδ spectra indicates that some extent of separation does exist. In order to interpret these results, one has to consider the possible ways of the PDMS incorporation and their corresponding physico-chemical environments.

As an oligomeric chain is incorporated into the silicate network, two types of restrictions may be imposed on this moiety:

TYPE 1 —— That caused by connecting both ends of the oligomer to the silicate network.

TYPE 2 —— That caused by interaction with surrounding, lightly condensed, TEOS species, or by possibly being encapsulated in a condensed TEOS network environment.

For a long but phase-separated chain, both types of restrictions should be negligible. As a result, the glass transition temperature (T_g) for this type of chain should be close to that of the pure polymer. For the case of PDMS, this temperature should be ca. -128°C [73]. On the other hand, for a short and phase-mixed chain both types of restrictions should be large. Since higher thermal energy is required in this case to mobilize the chain, the T_g will thus shift to a higher temperature. Therefore, from the value of the glass transition temperature, one can obtain information on the interaction between the oligomeric/polymeric chain and its environment.

Based on these postulations about the interaction, the tanδ behavior given in Fig. 4.6 can possibly be interpreted. First, the presence of a maximum near -106°C suggests that there exist some siloxane rich regions. However, this T_g is about 20°C higher than that reported in the literature for the PDMS polymers. This large difference can be attributed to two factors. First, the value of -128°C was obtained by thermal analysis. Difference

is expected if one compares that with the values obtained by other experiments. In addition, the T_g obtained by taking the temperature where the tanδ maximum occurs is usually higher than other methods [74]. Secondly, Even though type 2 restriction does not exist in a siloxane rich phase, type 1 may still have some effect on the mobility. Therefore, the value is somewhat higher than expected. Nevertheless, the postulation of the presence of a siloxane rich phase should still be reasonable. This point has also been further verified by the sub-ambient DSC experiments, and the results will be given in later discussion.

Regarding the second tanδ maximum, it may be interpreted as the T_g of those more restricted PDMS oligomers. That is to say, both types of restrictions are significant and cause the T_g to increase considerably. Another way to view this situation is that the PDMS oligomers mixes intimately with the partially condensed TEOS species. Due to the stiffness of the latter species, the mobility of these mixed PDMS chains should be reduced. This kind of mixing effect has also been reported by Parkhurst et al. in a titanium containing TEOS-PDMS system [53], in which two transitions were shown by the DSC technique. Since the extent of interaction between PDMS and the environment can vary considerably, the shifting of T_g will thus be quite different. This can, at least partially, explain the broadness of the second tanδ maximum. In addition, the original molecular weight distribution of the PDMS oligomers may also contribute somewhat to the broadening of this second maximum.

According to the rational given above, the effect of the acid content can now be considered. As shown by the mechanical data, the intensity of the first tanδ maximum (-106°C) decreases as acid content increases. Whereas the second tanδ maximum (-10°C) intensifies at the same time. This implies that as the acid content increases, there is a

decrease in the siloxane rich phase while more mixing of PDMS and partially condensed TEOS result. In other words, the siloxane oligomers became better dispersed or incorporated into the silicate network as more acid was used. This better dispersion should result in a more homogeneous structure. To verify this improvement in the homogeneity, small angle X-ray scattering (SAXS) analysis was utilized and the results will be presented and discussed later.

In order to understand the structure and the effect of acid content, one has to examine the reaction scheme and procedure of this modified sol-gel process. As mentioned previously, the TEOS content of this specific acid series was fixed at 48 wt%. However, this does not represent the final weight fraction of the inorganic species due to the large weight loss of TEOS in the hydrolysis step. Table 4.1 provides a conversion between the initial TEOS wt% and the final weight fraction of SiO_2. This final weight fraction is calculated by assuming 100% completion of the hydrolysis and condensation of the inorganic silicates, which is certainly not the actual case. Nevertheless, it can still serve as a low estimation of the organic weight fraction of these systems. Also listed in the table is the molar ratios of TEOS to PDMS, which can be inversely related to the concentration of the silanol group from the PDMS species. As shown in this table, PDMS should be the dominant component in this series of samples. Therefore, the formation of a siloxane rich matrix phase will be almost inevitable. However, in order to interpret the effect of acid content, the growth process of the silicate and the possibility of PDMS self condensation needs to be considered.

As concluded by several previous studies on the pure silicate sol-gel process [18,19,26,27], higher acid content tends to induce more chain-like structures in the beginning stages of the reaction. For the present hybrid systems, this conclusion should

still be valid. As more polymer-like silicate particles are formed, the possibility of mixing between two components will be promoted. This point is confirmed by a previous study on silicate filled PDMS system [75]. The TEM micrographs from that study showed well defined silicate particles dispersed in a PDMS matrix as base was used as the catalyst. Whereas for the acid catalyzed systems, TEM micrographs showed no distinct structure which strongly implied that significant mixing took place. Since the second tanδ maximum (-10°C) has been attributed to the PDMS in the mixed region, higher mixing induced by higher acid content should intensify this maximum. As the magnitude of this maximum increases, the low-temperature maximum caused by the siloxane rich phase should decrease due to the constant PDMS loading of these materials. This interpretation coincides well with the experimental results.

Another factor that may influence the structure is the possibility of PDMS self condensation. It has been documented that the silanol terminated PDMS is rather reactive, and self condensation can take place if catalyst and thermal energy are applied to the system [75]. This possibility can be important in the present systems. At the very beginning of the sol-gel reaction, almost all the silanol groups are from the functionalized PDMS. Any condensation that takes place will most likely result in self extension of the PDMS chains. As the reaction continues, more silanol will be generated by the hydrolysis reaction of TEOS. Since the molar ratio of TEOS to PDMS is 7.5, self condensation of PDMS should become less probable from a statistical point of view. Eventually, this stage of co-condensation will end as the silanol groups from PDMS are exhausted. Then, the self condensation of hydrolysed TEOS will take place and form a 3-dimensional network. Since the siloxane rich phase should be promoted as PDMS self condenses, a shorter first stage (i.e., PDMS self condensation) should result in a decrease of this phase and, consequently, better dispersion of the PDMS oligomers. As more acid

is used, the hydrolysis rate of TEOS increases considerably and, hence, shorten the time for PDMS self condensation. This factor can also contribute to the change observed in tanδ spectra.

Although either of the above two factors can explain the dynamic mechanical data, a combination of both effects is believed to be closer to the real situation. In order to strengthen these postulations, more experiments were carried out on these materials. To verify a higher mixing of the two components, sub-ambient DSC experiments were performed to measure the ΔCp at the transition temperature of pure PDMS. To demonstrate the improvement of homogeneity, SAXS analysis was also utilized. Finally, to test the speculation of self condensation of PDMS, materials with triethoxysilane endcapped PDMS were prepared. All of these results will be reported shortly.

As discussed earlier, the storage modulus shows a plateau region with a magnitude of ca. 10^7 Pa. for all samples. In fact, the modulus is not constant throughout the entire plateau region. A slight increase is observed up to 150°C and, most importantly, this increase is reproducible on the same sample after thermal cycling to 150°C. This increase in storage modulus could be caused by the further curing of the silicate network, resulting from the formation of Si-O-Si linkages by residual silanol groups. However, if this was true, it would not be observed in the second run of thermal cycling. Therefore, the interpretation of rubber elasticity is adapted. According to that, the modulus of a rubbery chain under strain should be proportional to the absolute temperature. On a logarithmic scale, this will result in a slight upturn of the modulus curve. If the siloxane was entrapped in the silicate network, it would not show this special behavior. Hence, this observation of increase in modulus can be used as an indication of a successful incorporation of the elastomeric component.

After the plateau region, the increasing tendency becomes much steeper. This can no longer be attributed solely to the rubber elasticity behavior mentioned above; further curing of the network must have taken place. To investigate this curing process, IR spectroscopy was utilized. The results of these experiments are shown in Fig. 4.7. Three samples of a same material were annealed under different temperatures. The first one was the control sample (without annealing); the other two were heated for 2 hours at 150 and 250°C, respectively. The absorption peak that being monitored is the silanol band around 3400 cm^{-1}, which is pointed out by an arrow in the spectra. For the control sample, a broad band is observed which indicates the existence of a considerable amount of silanol groups. After annealing under 150°C for 2 hours, the absorption is somewhat constant. This observation is quite important since it excludes the possibility of water absorption, which may be caused by any entrapped water. In addition, it also indicates that further curing is not significant up to 150°C, which supports the postulation of rubber elasticity mentioned above. For the sample annealed just under 250°C for 2 hours, however, the silanol band decreases considerably. This significant decrease implies that further formation of the Si-O-Si linkages has taken place. This further curing will result in higher crosslinking density and a denser network and, therefore, a significant increase in the storage modulus.

As explained earlier in the section of reaction procedure, all the samples were dried at ambient conditions to remove the solvent. Some questions were raised about the possibility of residual volatiles, which might influence the mechanical loss behavior (i.e., tanδ). To clarify this, thermal cycling experiments were performed on one of the hybrid materials. For the first run, a fresh sample was taken to measure its dynamic mechanical properties up to 100°C. After cooling down, a second run was carried out on the same sample in the same temperature range. The resulting tanδ spectra of these two

experiments are shown in Fig. 4.8. An almost identical behavior is observed in both cases. Therefore, it is concluded that the trend observed by using various acid contents is caused by the structure, and not by any residual volatiles.

One thing to note at this point is the possible effect of the residual acid. As discussed earlier, the acid content of these systems is relatively high compared to pure sol-gel systems. In addition, it has also been suggested that acid may decrease the stability of the siloxanes. However, from the results of the thermal cycling experiments, one observes no indication of degradation of the network. Furthermore, extractions of some aged samples did not show significant weight loss of the systems. Therefore, it seems that the residual acid does not affect the structure and properties of the systems. Nevertheless, further purification is likely to be necessary if practical applications are considered in the future.

According to the interpretation given above, more siloxane oligomers are dispersed into the silicate network as the acid content increases. As a result of this better dispersion, less oligomers are in the siloxane rich phase. To provide further evidence on this effect, measurements of ΔCp were performed utilizing DSC. The results of sub-ambient DSC experiments on this series of samples are shown in Fig. 4.9. Only one transition is observed in each case; the onset points are approximately the same at -123°C. As the acid content increases, this transition becomes more difficult to define. The ΔCp at the transition temperature is calculated as the normalized energy difference across the T_g. Since the sample weight was approximately the same for all samples, a comparison between these values should be proper (if the sample weight was different, the non-linearity of the instrument might result in a misleading comparison.) The magnitudes of ΔCp for samples with various acid contents are shown in Fig. 4.10, and

it is clear that the ΔCp decreases as the acid content increases. This trend provides support of all the previous interpretations.

For the present systems, a transition at -123°C is observed for all samples. This temperature is close to the reported, pure PDMS glass transition temperature (ca. -128°C.) The small difference may be attributed to the different heating rate used. Therefore, it is reasonable to conclude that a PDMS rich phase exists in these hybrid systems. This confirms the results from the dynamic mechanical studies. Furthermore, from the results of the ΔCp measurements, it is clear that less siloxane molecules are present in this PDMS rich phase as the acid content increases. In other words, more siloxane oligomers have been "mixed" with the silicate network. This result is consistent with the conclusion drawn from the tanδ spectra (i.e., an increase in acid content would result in a better dispersion of the PDMS oligomers.) However, the second transition near -10°C is not observed in the DSC results. This may be due to the broadness of this transition, which makes it difficult to be detected by the thermal analysis.

One crucial assumption being made in analyzing the DSC results is that the weight fraction of PDMS in this series of samples is approximately the same. In other words, the extent of reaction is the same in all cases. Only with the validity of this assumption, can the comparison of the ΔCp and the interpretation be meaningful. In order to verify this important assumption, elemental analysis and some limited Raman spectroscopy were carried out on these materials. The results are supportive and will now be discussed now.

The elemental analysis was performed on three of this series of samples; the weight fractions of silicon, carbon, hydrogen, and oxygen were obtained. The result of this analysis with the corresponding acid content is listed in Table 4.2. From these data, it

is clear that the composition of these materials are essentially the same. This provides additional support to the validity of the assumption made for the DSC studies. However, it should be noted that this analysis is subjected to some degree of error caused by residual solvent. A very small amount of solvent can change the amount of carbon and hydrogen considerably and, consequently, result in a significant error. Therefore, the Raman scattering technique was utilized to further confirm this result and the assumption of equal degree of reaction.

The Raman spectra of this series of samples are shown in Fig. 4.11. The two peaks of the scattering profile that are useful to characterize the degree of reaction are:

1. The 814 cm^{-1} band is caused by the Si-O-Si stretching. Since the structure of PDMS can also result in scattering around the same range, a deconvolution has to be carried out to obtain the part that extends from the silicate network only. The area under the peak after deconvolution can then be related to the extent of network formation.

2. The 1460 cm^{-1} band is caused by the C-H bending from the ethoxy group. The area under this peak can then be related to the residual ethoxy content and the amount of unreacted species in the system.

Due to the difference in background and film thickness, a comparison of the absolute area under a specific scattering peak of different samples is meaningless. Therefore, an internal standardization has to be used. That is, instead of using the absolute area, a ratio of the area under the C-H bending peak to that of the Si-O-Si stretching peak has been taken for comparison. The results of this calculation of all samples are listed in Table 4.3. No significant difference exists with change in the acid content. Although the values of the two lower acid content samples are slightly higher than the others, it has

been attributed to the error in the deconvoluting process of the Si-O-Si stretching peaks. By considering the experimental error involved and the result from the elemental analysis, it is reasonable to conclude that all samples have approximately the same extent of reaction. That is to say, the weight fraction of PDMS in each sample is approximately the same. Therefore, the previous comparison of the ΔCp of different samples is further supported. Moreover, the change of the dynamic mechanical behavior with acid content is also further confirmed to be caused not by composition but by structural variation.

One important implication form the results of elemental analysis and Raman spectroscopy is that the acid functions, in a conventional way, as a catalyst. That is, it accelerates the reaction without affecting the equilibrium state and, therefore, the extent of reaction. To the author's knowledge, this point has not been mentioned in any previous studies on either pure or modified sol-gel processes. This is mainly because that most of those systems were sintered into glass eventually and, hence, the extent of reaction at the gel stage did not matter. In order to understand the details of the relationship between catalyst and equilibrium, further studies on the molecular structure and reaction mechanism should be carried out. However, such studies were beyond the scope of this project. In view of the analytical results presented so far, it will be reasonable to assume there is essentially an equal extent of reaction for the members of the acid series.

Up to this point, all the understanding of these hybrid materials comes mostly from the measurements of either mechanical or thermal properties. Although postulations have been made on the structure, they are all based on indirect information. Therefore, in order to better confirm these postulations and further understand the structure-property

relationships, structural characterization of these hybrid materials was carried out. In this study, structural information has been mainly provided by the utilization of SAXS analysis. However, some results from electron microscopy will also be reported.

As mentioned at the very beginning of this chapter, all the samples of these TEOS-PDMS materials were transparent. This indicated no large scale phase separation. In order to obtain direct evidence of this, scanning electron microscopy was employed to study the fracture surfaces of various hybrid materials. All the samples were fractured in a liquid nitrogen environment so that the deformation of the rubbery phase would be minimized. In this series as well as the others discussed later on, scanning electron microscopy showed no sign of phase separation within the limits of the instrument resolution. An example of a typical fracture surface is shown in Fig. 4.12. It is clear from this micrograph that no domain structure or phase separation exists in this sample -- at least at the scale of the magnification used. In addition, no particulate structure is observed which confirms the nature of an acid catalyzed system. Furthermore, the surface is somewhat glassy but with layered structure. A similar structure was observed for a low water content system [31], and it has been attributed to a low crosslinking density of the system. Since only 50% water was used for most of the present study, this type of structure is somewhat expected.

The utilization of SEM provides structural information in the macroscopic scale, and the result confirms what expected from the transparent appearance of the samples. However, other techniques are needed so that microscopic structure can be understood. In addition, the postulation of developing greater homogeneity of these TEOS-PDMS materials by increasing acid content also needs further confirmation. Both small angle X-ray scattering (SAXS) and transmission electron microscopy (TEM) were applied for

these purposes, however, no distinct structure was observed by the latter. This is somewhat expected due to the similar molecular structure of PDMS and silicate network and, hence, the contrast may be too low to detect by TEM. Therefore, SAXS was utilized as the major technique.

The principles of SAXS analysis have been highlighted in the previous chapter (see section 3.6), and the purpose of utilizing this technique in this acid series is to provide two modes of structural characterization. The first is to detect the existence of any periodicity or "correlated structure" in these TEOS-PDMS materials, which will result in a maximum in the SAXS profile. The second is to obtain information about the homogeneity of these systems through an invariant analysis. The respective scattering profiles obtained for the previously discussed acid series are shown in Fig. 4.13. The first thing to notice is that all these profiles show a monotonic decrease with the scattering vector s (defined as $2\sin\theta/\lambda$), which means that no correlated structure exists in these systems. Another thing to mention is that the overall scattering intensity decreases as the acid content increases. Although not directly, this overall intensity can be related to the homogeneity of the sample. One crucial condition to satisfy before carrying out the invariant analysis is that these materials have approximately the same composition. From the previous discussion of extent of reaction, this condition has proven to be correct in this series. Following correction for background scattering whereby the method of Bonart was utilized [76], the invariant analysis was applied through use of a computer program of Vonk. The mean square electron density fluctuation $\overline{(\Delta\rho)^2}$ was then be calculated for each sample and the results are plotted against the acid/TEOS ratio in Fig. 4.14. It is obvious that for the four samples investigated, $\overline{(\Delta\rho)^2}$ systematically decreases and hence the homogeneity increases as the acid catalyzed reaction is enhanced. This is in direct support of the earlier interpretation of the dynamic

mechanical and DSC data. Similar to the dynamic mechanical data, these SAXS profiles are reproducible by thermal cycling the sample up to 150°C.

Regarding the trends observed in stress-strain data, they may be explained by the oversimplified schematic model shown in Fig. 4.15. The system of Fig. 4.15a is an extreme case for PDMS phase separation, while Fig. 4.15b is for high dispersion of PDMS within the TEOS network. As the former system is deformed, the glassy phase will most likely be somewhat strained. Whereas for the latter case, the dispersed rubbery chains should sustain most of the stress. Another important point is that in the case of higher phase separation, the dispersed regions of pure PDMS may serve as stress concentrators and thereby have a negative effect on obtaining high elongation. Both of these two factors lead to a result of higher modulus and lower elongation at break for the system with more phase separation. Clearly, these results and their interpretation are in parallel with the dynamic mechanical and SAXS data.

In summary of the analysis regarding the effect of the acid content. both the mechanical and thermal analysis and the structural information are in good overall agreement. From the consistence of all the experimental data, it can be concluded with confidence that an increase in acid content improves the homogeneity of the final material. This improvement is caused by a better dispersion of the PDMS oligomers or, in other words, higher mixing between the two components. This higher homogeneity results in an increase in the elongation at break and a decrease in the initial modulus. However, the ultimate strength is approximately the same. In addition, the experimental data also indicates that the extent of reaction is approximately the same among all the samples.

4.2 EFFECT OF WATER CONTENT

The effect of water content on the growth process and final properties of a pure sol-gel system has been studied in several previous investigations [30-32] -- a detailed review being given in chapter two of this thesis. To briefly summarize this effect, it can be generally stated that adding more water will promote the rate and level of the hydrolysis and, consequently, result in particles with rather compact structure. However, for the present hybrid systems, the situation may be more complicated due to the fact that most of the organic species are incompatible with water. Therefore, it is important to understand how water will influence the structure-property relationships of these hybrid materials.

In order to investigate the effect of water content, a series of samples were prepared by adding various amounts of water into the modified sol-gel reaction. The TEOS content was 48 wt%; the molecular weight of the silanol terminated PDMS was 1700 g/mole; the acid to silane ratio was fixed at 0.045. The water content, which was the variable under study, ranged from 25 to 100% of the stoichiometric amount needed for the hydrolysis of TEOS. The reason for using this low range of water content was that PDMS is known to be very hydrophobic. Hence, too much water may result in large scale phase separation. In fact, some difficulty was encountered in preparing the system with exact stoichiometric amount of water (i.e., 100% water content.) In the first attempt, 100% water was added. The solution was turbid throughout the entire period of reaction and, as a result, the cast films were opaque and the surface was oily. This indicated that the incorporation of PDMS was not successful and a large scale phase separation had taken place. In order to improve the incorporation and produce useful samples, the reaction procedure was slightly modified. Instead of adding 100% water to the system, only 50%

was added in the beginning so that a homogeneous solution could be obtained. After 10 minutes of mixing under 80°C, the other 50% of water was then added. The resulting material of this modified procedure was transparent and without visible phase separation.

The collective results of the elongation at break and Young's modulus are illustrated in Figs. 4.16 & 4.17. Similar to those shown previously, some scatter of the data is observed. Nevertheless, trends are clearly displayed in both properties. In Fig. 4.16, the elongation at break decreases from ca. 13% to 5% as the water content increases from 25 to 100%. In fact, the dependence is almost linear. Young's modulus (Fig. 4.17) increases with the water content, ranging from 5 to 20 MPa. Interestingly, these trends are the same as that shown in the acid series.

In order to further understand the microscopic behavior, dynamic mechanical experiments were carried out. The storage modulus spectra of these series of samples are shown in Fig. 4.18, and these will be examined first. In general, the behavior is similar to that observed earlier in the acid series. A glassy stage with a modulus around 10^9 Pa. is displayed by all samples. This is followed by a broad transition, after which a plateau with a modulus of 10^7 Pa. is observed. However, it should be pointed out that a slight increase still exists. Finally, as the temperature increases beyond 150°C, this increase again becomes steeper. The important thing to notice is that the modulus of the plateau region increases with the water content. This is consistent with the results of the stress-strain experiments. The tanδ spectra of these samples are shown in Fig. 4.19. All of these show a bimodal type of behavior, which has been observed in the previous acid series. At very low temperature, a sharp maximum is observed (-106°C). The intensity of this maximum is approximately the same for all three spectra. Furthermore, a second,

broad maximum is observed at a higher temperature (-10°C). However, the intensity of this peak decreases as the water content increases. As the temperature increases further, this second maximum eventually decays to almost zero and remains constant thereafter.

To interpret the experimental results, it is necessary to recall some of the ideas mentioned on the growth process of the sol-gel reaction. It has been suggested, by several previous studies on the pure sol-gel process [18,30-32], that particles with more compact structure will be produced as the water content increases. The rationale of this tendency is as follows. For every silicon alkoxide molecule, there are four reactive sites to undergo hydrolysis reaction. However, the reactivity of these four sites will depend on the order of hydrolysis. In an acidic environment, the first alkoxide group will have the highest reactivity, which means it is the easiest one to react with water. After the first one is hydrolysed, the reactivities of the other three alkoxide groups will be lowered (see section 2.1 for detail on reaction mechanisms.) With the same logic, the other two alkoxides will have even lower reactivities after the second one is reacted, and so on. Therefore, if the water content is low, most of the silicon alkoxides will only be partially hydrolysed. As the condensation takes place between these molecules, chain-like particles will be formed. However, if sufficient water is supplied to the reaction, the third and even the fourth alkoxide groups on the silicon are likely to be hydrolysed according to LeChatelier's principle. As a result, the probability of forming branched and compact particles will be promoted. This line of deduction is supported by experimental data too [18,30-32].

In addition to the growth process, the factor of solubility may be affected by water content for the present TEOS-PDMS systems. The reported solubility parameter for PDMS is about 7.3 whereas the water has a value of 23.4 [73]. This large difference in

the solubility parameter results in the extremely hydrophobic nature of the siloxanes. For the modified sol-gel reaction suggested in this study, this inherent nature may induce phase separation. In fact, the large scale separation observed in the system with 100% water content confirmed this point. Although no visible separation was observed for systems with lower water content, an increase in water content should still promote the probability of microphase separation. This consideration is very important in the following discussion.

With this background, the experimental results can now be interpreted. As the water content increases, more compact structure of condensed TEOS should be formed due to the change in the growth process. In other words, the probability of forming chain-like, partially condensed TEOS species should decrease. Since the phase mixing was postulated to be between PDMS and chain-like TEOS species, this decrease should result in lower mixing. Furthermore, due to the extremely hydrophobic nature of PDMS, an increase in water content should also cause the extent of phase mixing to be reduced. As a result of both these factors, the PDMS should be less dispersed and the final material should be less homogeneous. As discussed earlier (see section 4.1), the second maximum (ca. -10°C) of the $\tan\delta$ spectrum was attributed to the dispersed or phase-mixed PDMS oligomers. Therefore, as the phase mixing is suppressed, this maximum should also be lowered. This is exactly what the $\tan\delta$ behavior shows in Fig. 4.19. In addition, following the same argument given earlier (see Fig. 4.15), less homogeneous sample should show higher modulus and lower elongation at break. This is also in line with the stress-strain results and the storage modulus behavior. To further strengthen this interpretation, some structural information concerning the homogeneity was obtained.

Small angle X-ray scattering was again utilized for the structural characterization of these materials, and the results are shown in Fig. 4.20. The first thing to notice is that the scattering intensity decrease monotonically with increasing values of s; this behavior is similar to that shown earlier by the acid series (see Fig. 4.13.) This absence of any maximum indicates that no periodic structure exists in these systems. Furthermore, the overall scattering intensity increases as the water content increases. This may be an indicative that the structure or, more specifically, the homogeneity is different between these materials. To further confirm this point, the invariant analysis was carried out and the results are shown in Fig. 4.21. As expected, the mean square electron density fluctuation $(\overline{\Delta\rho^2})$, increases with water content. Since the homogeneity of the system is inversely related to this fluctuation, such result implies that the system becomes less homogeneous as more water is added. This implication is consistent with that concluded from the mechanical properties and tanδ behavior.

One important point to mentioned is that all the SAXS data were obtained on samples that had been aged under ambient conditions for at least one year. Therefore, the behavior observed were caused by structural differences, which were not affected by the long time exposure to humidity. This invariance with respect to aging may not be true for other sol-gel hybrid systems as will be discussed in the oncoming chapter.

To summarize this section, it is reasonable to state that the amount of water added to the reaction will significantly influence the dispersion of the PDMS oligomers. As a result, the homogeneity and the final properties will be affected. Within the range of this study, an increase in water content results in lower homogeneity, lower elongation at break, and higher modulus. This result can be attributed to a change in the growth process of TEOS and the hydrophobic nature of the PDMS oligomers. As the water .

content increases to 100% or beyond, a large scale phase separation was observed and the incorporation was unsuccessful. However, this limitation may not be applied to other systems prepared with different types of oligomers.

4.3. EFFECT OF TEOS CONTENT

In the previous sections, the initial weight fraction of TEOS was fixed at 48wt%. Although some glassy nature was observed in the final properties, these materials were predominantly PDMS in final composition. Since one of the objectives was to investigate the cracking problem that generally occurs in the preparation of inorganic sol-gel materials, it was of interest to see at what amount of TEOS content could be used without leading to fracture of the cast film. Also important was to study how the change in TEOS loading affected the structure and properties.

To understand the effect of TEOS content, several materials with a TEOS content higher than 48 were prepared. First, a series of samples with 60 wt% TEOS and various acid content were produced. The water content was fixed at 50%; the PDMS molecular weight was 1700 g/mole; the reaction temperature was 80°C. The purposes of this series were (i) to understand how the TEOS content affect the structure and properties and (ii) to study how the TEOS content influence the effect of acid content. With the understanding of the latter, some of the conclusive remarks in the previous acid series (see section 4.1) could be confirmed. In addition to this series, another sample with 70 wt% TEOS was prepared. This material was compared with the other two samples that had the same acid content but lower TEOS loadings. It was hoped that by this comparison, the effect of TEOS content could be better understood.

As for the other hybrid materials, the samples prepared for this part of study were transparent. Although no viscosity was measured, the time of gelation tended to increase with TEOS content. In fact, a pure TEOS sample was made with the same procedure and it showed the longest gelation time. Since gelation can be viewed as the point where the molecular weight reaches infinity, this trend in gelation is reasonable considering the high molecular weight of PDMS oligomers compared to TEOS. Another observation was that as the TEOS content increased, the resulting sample became stiffer, more brittle, and warped. In fact, for the sample prepared with 70 wt% TEOS, no stress-strain data was obtained due to the difficulty in cutting dogbone samples. The cracking problem became rather significant as the TEOS content reached 70%, however, considerably large pieces were still obtainable so that dynamic mechanical test could be performed. Shrinkage became more significant as TEOS content increased. This is reasonable due to the large weight loss in the hydrolysis step of the TEOS.

Stress-strain experiments were first carried out on the acid series which were made with 60 wt% TEOS. Examples of the resulting curves are shown in Fig. 4.22. The data show that the range of elongation at break is approximately the same as that shown in the lower TEOS content series -- which is somewhat surprising. However, the range of tensile strength (i.e., the stress at break) is almost 3 times as high as that shown before (see Fig. 4.2). For the two samples made with lower acid contents, the behavior is almost linear which are similar to those shown in the 48 wt% TEOS series. However, as the acid content increased to 0.067, a different behavior is observed. At low strain, the modulus is high and the curve is almost linear. As the strain increases further, the modulus suddenly drops to a lower value and the curve bends to another linear region. Although the bending point is not as sharp as a yield point, the general behavior is similar. This may be an indication that the glassy phase has become somewhat continuous in the

system. For the two samples with even higher acid contents, similar behavior was also observed. Although only one example is shown for each acid content, its behavior is typical for all samples. Repetitive experiments were carried out for statistical reasons, and collective data of the mechanical properties are shown in Figs. 4.23 & 4.24. Instead of showing an increasing trend like the earlier series, a two-step type of behavior is observed in the elongation at break. The two materials with lower acid contents are in one group which has a value ca. 5%, whereas the other three materials display a greater value of ca. 15%. This distinction is the same as that concluded from the stress-strain curves. The magnitude of Young's modulus is scattered about 60 MPa for all samples; this value is about 3 times greater than the highest shown by the earlier series. This high value of modulus also results in the high tensile strength observed in the stress-strain behavior (Fig. 4.22).

After observing this significant change in the mechanical properties, one would expect that the microscopic properties may be quite different from those shown before. Dynamic mechanical tests were thus carried out, and the results are shown in Figs. 4.25 & 4.26. For the two samples with lower acid contents, the storage modulus behaves similar to those shown before. However, the magnitude of the plateau region after the broad transition is now ca. 10^8 Pa. This is one order of magnitude higher than the previous samples. In addition, the temperature range of this plateau becomes somewhat shorter before the modulus begins to increases. As the acid content increases further, however, the behavior changes considerably. First, the temperature range of the transition is now even broader and the magnitude continues to decrease until ca. 130°C. Secondly, instead of going through a plateau region, the modulus begins to increases immediately after the transition. The modulus at ambient temperature does not show a clear trend, which is consistent with that observed in the stress-strain results. However,

at higher temperatures, an increasing tendency in stiffness (i.e., modulus) is shown as the acid content decreases. This is similar to what the previous acid series shows. An important point to note from these storage modulus spectra is that, the threshold value of acid content at which the behavior changes is the same as when the "bending" in stress-strain curve begins to appear -- recall Fig. 4.22.

To understand the change in storage modulus, one has to examine the corresponding tanδ spectra. As shown in Fig. 4.26, the behavior becomes rather complicated now. The intensity is, in general, lower than that shown in Fig. 4.6. This is reasonable since there is less PDMS oligomers in these materials than that in the 48 wt% TEOS series. Another change in the general behavior is that tanδ loss spreads over a much wider temperature range. For example, the tanδ value decays to very low values at 200°C for the high acid content cases. This is about 100°C higher than that shown in the 48% series. Such a wide spread in loss behavior implies that the PDMS oligomers, at least some of them, are under much higher restriction. Regardless of these changes, a trend with acid content is still observed and it is explained as follows. For the material with the lowest acid content (0.022), the tanδ behavior is quite similar to the bimodal curves shown before except that an additional maximum at -90°C is now observed. As the acid content increases to 0.045, the loss at low temperatures somewhat decreases whereas the part between 0°C and 100°C rises considerably. As the acid content increases further, the maximum at -106°C shifts completely to -90°C and its magnitude decreases to even lower values. Meanwhile, another maximum at 90°C begins to show. The important point to note is that the threshold acid content at which this 90°C maximum occurs is again consistent with that shown by the mechanical data. This observation is crucial to the following arguments.

In order to interpret the data, it is necessary to recall the two types of restrictions mentioned earlier in this chapter. The first type is caused by the end-linking of the oligomers to the silicate network, and the second type is caused by either the interaction between partially condensed TEOS and PDMS or the encapsulation of the oligomeric chains. In the systems with 48 wt% TEOS, the siloxane is most likely the continuous phase. Therefore, the possibility of encapsulation is very low or even none. However, as the TEOS content increases to 60 wt%, this situation may become more probable. If this occurs, the T_g for this type of PDMS will be shifted to very high temperatures due to the highly restricted environment. Another point needs to be taken into account is the molar ratio between TEOS and PDMS. As the TEOS content increases to 60 wt%, this ratio increases from 7.5 to 12.3 (see Table 4.1). As a result, the probability of PDMS self condensation should decrease considerably. This will suppress the formation of a siloxane rich phase and, therefore, promote the mixing and encapsulation.

With these considerations, the tanδ behavior can now be rationalized. For the samples made with low acid content, the hydrolysis rate of TEOS is relatively slow. Therefore, the time period for PDMS self condensation is long. In addition, the particles formed through the growth process is less chain-like and the extent of phase mixing is low. Both of these factors cause the tanδ behavior to be similar to that shown earlier by the 48 wt% series. Nevertheless, the magnitude of the loss is lower due to less oligomeric content. Compared to the sample with same acid content but 48 wt% TEOS, the spread of the loss is still wider due to the larger molar ratio of TEOS/PDMS. As the acid content increases to 0.067 or beyond, the hydrolysis rate is so fast that the PDMS rich phase is largely suppressed. This results in the shifting of the low temperature peak from -106°C to -90°C. Furthermore, the encapsulation becomes possible at this point due to the growth process and high glass content. Therefore, a maximum at 90°C begins to

grow. Also because of this high temperature transition, the material continues to soften and results in the absence of plateau region in the storage modulus.

Another important change may occur with an increase in encapsulation is that the glassy phase becomes more continuous. This partial continuity can sustain only a low strain but may be broken at higher strains. This breaking of silicate continuity should result in a drop in the stiffness of the sample. This postulation can be adapted to explain the bending of the stress-strain curves for samples with high acid contents. If this continuity was observed over the entire structure, then a yield point would be observed. Although this point was never observed for this TEOS-PDMS system due to the brittleness of the 70 wt% TEOS sample, it will be shown later in the hybrid system prepared with oligomers possessing pendent functional groups.

Following the same argument as that given before, the material should become more homogeneous as the PDMS oligomers are more dispersed into the silicate network. Therefore, the acid content should promote the homogeneity of the system. To verify this point, SAXS analysis was utilized and the resulting profiles are shown in Fig. 4.27. A monotonic decrease with respect to s is again observed, and the overall intensity decreases considerably as acid content increases. After removing the background, the invariant analysis was carried out on each sample. The values of the mean square electron density fluctuation at various acid contents are shown in Fig. 4.28. The postulation of an improvement in homogeneity is again confirmed.

It should be pointed out, though, that a direct comparison of the scattered intensities from this series versus the earlier series shown in Fig. 4.13 is not a valid one. This is due to the fact that there is also a change in the relative volume fractions of the two components (TEOS and PDMS) and, hence, the general scattering intensity levels are

expected to be somewhat different. For example, it is well known that in the case of a two component system having sharp phase separation, the mean square fluctuation in electron density is proportional to the product of the volume fractions of the two components and the electron density difference between the two components [70]. Therefore, as the volume fractions change, the electron density fluctuation should change also. While indeed the present systems do not have such sharp phase separated components, the same argument can be utilized accordingly. Even so, the reader will note that the absolute values of the mean square fluctuation in electron density are of the same order of magnitude as observed in the previous systems.

Up to this point, the effect of TEOS content is probed by using only two compositions -- 48 and 60. It seems reasonable to have at least one more point so that a trend can be established. Therefore, a sample with 70 wt% TEOS was prepared and the dynamic mechanical test was carried out. The results of the storage modulus and tanδ are shown in Figs. 4.29 and 4.30, respectively. Also shown are two other spectra which have exactly the same reaction conditions but different TEOS content; one is 48 and the other one is 60. From this comparison, it is obvious that an increase in TEOS content results in higher modulus and lower tanδ loss. This is reasonable considering the high stiffness of the inorganic glasses. In addition, the temperature spread of the tanδ loss tends to increase with TEOS content. This is also understandable due to the corresponding increase in the molar ratio of TEOS/PDMS.

In this section, the effect of TEOS content has been discussed. It can be generally concluded that an increase in TEOS loading will result in further dispersion of the PDMS oligomers, higher stiffness, and higher tensile strength. However, the shrinkage, brittleness, and cracking problem will also become more significant. Encapsulation of

PDMS and partial continuity of the glassy phase begin to show in materials prepared with high acid contents. These changes result in a "bending" in the stress-strain curves and the appearing of a high temperature (90°C) tanδ peak. This encapsulation should become more probable as the PDMS molecular weight decreases, and this point will be studied in the next section.

4.4 EFFECT OF PDMS MOLECULAR WEIGHT

For the modified sol-gel process suggested in this work, a change in the oligomeric molecular weight is expected to have an effect on the final structure and properties. For example, the probability of encapsulation should be higher for a system made with lower molecular weight oligomers. On the other hand, phase separation should be promoted as the oligomeric or polymeric molecular weight increases. In fact, Parkhurst et al. did report that in a titanium containing TEOS-PDMS system, the final materials made with various molecular weight of PDMS do appear to be different [53]. In particular, samples prepared with low molecular weight PDMS (MW = 1700) were always clear, whereas those with higher molecular weight (MW = 36000) were typically opaque. However, no mechanical properties were measured and no structural characterization were given. In view of the data given earlier in this thesis on the 1700 molecular weight materials, and the limited but interesting data by others, it was decided that further investigation of this variable was worthwhile.

All the materials studied so far were prepared with TEOS and silanol terminated PDMS oligomers having a number average molecular weight of 1700 g/mole. In order to understand the effect of oligomeric molecular weight, another silanol terminated PDMS with the molecular weight of 550 g/mole was used. The TEOS content was 60 wt%; the

water content was 50%; the reaction temperature was 80°C. The acid content ranged again from 0.022 to 0.111.

The final materials were also transparent. However, the stiffness was higher than those samples made with 1700 molecular weight PDMS. To quantify this difference, stress-strain experiments were performed. Examples of the resulting curves are shown in Fig. 4.31. All five curves show more or less a bending as the strain increases, which is either an indicative of encapsulation (PDMS), some partial continuity of TEOS, and/or simply a rubber elasticity effect caused by a lower M_c between crosslinks. The tensile strength is somewhat higher than the materials with 1700 molecular weight PDMS, however, no clear trend is observed for this property. The modulus, on the other hand, tends to increases while the elongation decreases as the acid content decreases. To further clarify this behavior, repetitive experiments were carried out and the collective results are shown in Figs. 4.32 and 4.33. Except for the sample with 0.09 acid content, the increasing trend of elongation at break with acid content is rather clear. The range is comparable to what the earlier series showed. This is somewhat surprising since one would expect a lower extendibility for materials made with lower PDMS molecular weight. However, This may be a result of better oligomeric dispersion. Regarding Young's modulus, a slight decreasing trend with acid is observed. This is consistent with all the previous series (see Fig. 4.4 and 4.24). The magnitude of the modulus is ca. 80 MPa, which is the highest value observed so far for these TEOS-PDMS systems.

The dynamic mechanical results from these materials are illustrated in Figs. 4.34 & 4.35. The behavior of the storage modulus is similar to that shown in the PDMS(1700) series (see Fig. 4.25.) However, for the samples with high acid contents (above 0.067), the modulus continue to decrease to almost 180°C before increasing at very high

temperatures. For the PDMS(1700) series, this decrease was never beyond 150°C. To further understand this behavior, the corresponding tanδ spectra should be examined.

As shown in Fig. 4.35, three maxima are observed in each case. The first one is at -90°C, and the second one is at 0°C. These two peaks were also observed in the cases with 1700 MW PDMS (see Fig. 4.26). However, the intensity of the peak at -90°C is lower in this series. The third maximum is at 100°C except for the case of 0.111 acid content, which shows a broad maximum ca. 130°C. In addition, the intensity of this third maximum increases with the acid content. This higher temperature tanδ response has been attributed to more restricted or encapsulated PDMS. Another point to noted about this third maximum is that it is observed even for the material made with the lowest acid content (i.e., 0.022), whereas in the PDMS(1700) series it was not observed until the acid content increased to 0.067. Incidentally, this is consistent with the fact that all five materials in this series show a bending in stress-strain curve, whereas the PDMS(1700) series does not show this bending until the acid content reaches 0.067. Finally, the tail of this third maximum extends to almost 250°C which is much higher than previous cases.

In this PDMS(550) series, the average oligomeric chain length is much shorter than that of the 1700 molecular weight PDMS. Although self-condensation can still occur, the chance of forming a siloxane rich phase should be reduced whereas the phase mixing between the two components should be promoted. Therefore, there should be less siloxane rich phase in these materials. This postulation is confirmed by the fact that the intensity of the tanδ peak at -90°C of these materials is always lower than that of the PDMS(1700) systems. Furthermore, since this peak (or T_g) is caused by the PDMS in a siloxane rich phase, one would not expect its position to change by varying the

molecular weight. In fact, both the pure PDMS(550) and PDMS(1700) showed a T_g at -123°C in sub-ambient DSC experiments. Regarding the 0°C peak which is attributed to PDMS in a mixed phase, the T_g should also be rather constant with respect to the molecular weight. This is because that type 2 restriction (i.e., interaction between partially condensed TEOS and PDMS) is the dominant factor in this case, and it should not be sensitive to the length of the chain. However, for the encapsulated PDMS chains, the situation may be quite different. For a encapsulation to take place, the chain must be rather isolated in an environment filled with relatively highly condensed TEOS. Therefore, both ends of this chain are most likely connected to rigid crosslinks. In this case, the type 1 restriction may become more crucial. With this speculation, it is suggested that as the short 550 chains are encapsulated, the end-linking effect should be higher than that for the 1700 chains. Therefore, the T_g for this encapsulated short chain should also be higher than that of a longer chain. This rationale can explain why the "tail" of the tanδ extend to higher temperature in this series than that in the previous series. Another important point is that the probability of encapsulating a chain should be promoted as the length of the chain shortens. Indeed, all five materials in this series suggests stronger signs of encapsulation (see stress-strain curves and tanδ spectra), whereas no sign is observed in the lower acid content samples of the PDMS(1700) series.

To complete the study of this series, SAXS experiments were carried out to obtain structural information. The scattering profiles from these experiments are shown in Fig. 4.36. In general, the overall scattering intensity decreases as the acid content increases. This is consistent with the SAXS behavior of all the previous series. Another important point to note that, for the same acid content, the scattering intensity of the sample made with PDMS(550) is always lower than that of the PDMS(1700) (compare Fig. 4.27 and Fig. 4.36). Although this may be an indication of higher homogeneity in the former

systems, a conclusive remark can not be made until the invariant analysis is carried out. Also of interest is the fact that there seems to be a very broad, diffuse but reproducible maxima in most profiles. Its origin is still unclear. In order to confirm the postulation about homogeneity with acid variation, the invariant analysis was performed. The values of the mean square electron density fluctuation at various acid contents are shown in Fig. 4.37. As in the earlier results for the 1700 series, it is again obvious that the system becomes more homogeneous as the acid content increases. This can be, as mentioned earlier, attributed to better dispersion of the PDMS oligomers. To see the effect of PDMS molecular weight on the final structure, one can compare this result with that shown in Fig. 4.28. (Since these two series have approximately the same composition, a direct comparison of these values should be valid). Obviously, the system with PDMS(550) always show a lower electron density fluctuation than that with PDMS(1700). Therefore, it can be concluded that the homogeneity has been improved by using a lower molecular weight oligomer.

This low molecular weight oligomer series provides very useful information. First, the trend that was observed previously with respect to the acid content is also shown in this case. Therefore, the improvement of the homogeneity by increasing acid content is further confirmed. Secondly, the materials prepared using this shorter PDMS chains tend to show higher modulus without losing extendibility. This is likely caused by the increasing connectivity of the glass network and the better dispersion of the oligomers. Thirdly, a decrease in the oligomeric molecular weight promotes the probability of encapsulation. In fact, signs of encapsulation are observed even for the material made with the lowest acid content. Finally, the homogeneity of the final material can be improved by using a lower molecular weight PDMS.

4.5 EFFECT OF PDMS FUNCTIONALITY

In the previous sections, all the materials were prepared by using TEOS and silanol terminated PDMS oligomers. Since the functionality was 2 for this species, two important factors should be considered:

1. Noll has suggested that silanol terminated PDMS is among the most reactive silica compounds [75]; this is especially true in an acidic environment and under high temperature. Furthermore, since TEOS will have to undergo hydrolysis to generate silanol groups, all the silanol groups of the system in the very beginning come from PDMS. Therefore, it is reasonable to postulate that some self condensation of PDMS may occur in these modified sol-gel reactions. The result of this will be to form longer PDMS chains and, possibly, promote phase separation. In addition, since water is necessary in the present reactions, this separation might be even more probable due to the hydrophobic nature of PDMS.

2. As suggested by the Raman scattering and elemental analysis, the overall degree of reaction was never 100%. Therefore, from the statistical point of view, some of the silanols may not react with other species. Furthermore, due to the high molecular weight and coil-like nature of the chain, the end may be shielded by steric hindrance. Both of these situations would result in the existence of dangling ends. This may not affect the transparent appearance of these materials, however, it would be expected to influence the mechanical properties considerably.

To minimize the two situations mentioned above, the functionality of the PDMS oligomers was increased from 2 to 6 by endcapping the PDMS with triethoxysilanes. With this change, the initial stage of "all silanol" ends from the PDMS could be eliminated since the triethoxysilane endcapped PDMS also needed to undergo

hydrolysis. However, it should be noted that Schmidt et al. suggested that the reactivities of the ethoxy groups on triethoxysilane were higher than those on TEOS [5,51]. However, even though self condensation of PDMS might still take place, there were four reactive sites left to condense, possibly, with hydrolysed TEOS. Therefore, phase mixing should be promoted. In addition, due to the similar structure of the endcapping triethoxysilane with the TEOS, the compatibility of the organic and inorganic components should be promoted. This would likely result in a better dispersion of the endcapped oligomers. Furthermore, since the functionality is now 6, the probability of leaving a dangling end should be considerably lowered. The result of these considerations was that the PDMS rich phase should be greatly minimized, and the mechanical properties should change significantly.

Following the logic given above, hybrid materials with TEOS and triethoxysilane endcapped PDMS were prepared (see Fig. 3.2 for the endcapping reaction). Two different kinds of PDMS were used: the molecular weight before endcapping was 1000 and 2400 g/mole, respectively. The TEOS content was 50 wt% for both systems. However, by adding the endcapping triethoxysilane, the initial silane contents were approximately 60 wt% for the PDMS(1000) system and 55 wt% for the PDMS(2400) system. The water content was 50% and the acid content was 0.045. Due to the fast gelation of these systems, reactions were carried out at ambient temperature. Even so, the comparison with previous systems should still provide some information.

The gelation time for these systems was much shorter than that of previous systems. Since all the other factors were basically the same as before, this fast gelation should most likely be caused by the high functionality of the oligomers. The system with PDMS(1000) was transparent and rigid. However, the system with PDMS(2400) was

opaque and with oily surfaces. This might indicate that the molecular weight of the endcapped PDMS was sufficiently high so that a large scale phase separation took place. Similar result was reported by Parkhurst et al. [53]. Since the actual glass content for the latter can not be determined, only the system with PDMS(1000) will be reported and discussed.

The stress-strain data could not be obtained due to the difficulty in cutting the dogbone samples without fracturing the material. Even so, this result can still be viewed as an indication of the high stiffness of this material. However, it was possible to obtain sample for dynamic mechanical analysis. The results are shown in Fig. 4.38. Obviously, the behavior is quite different from all the earlier PDMS(1700) or PDMS(550) systems. The storage modulus shows a much slower decrease over the entire temperature range of the experiment, which confirms the implication about the high stiffness. This higher and nearly constant modulus also implies that the network structure is rather dense. The first thing to notice from the tanδ spectra is that the intensity is rather low throughout the entire temperature range of experiment. In fact, this magnitude is lower than all the previous series with comparable glass contents. Although a small loss is observed at low temperatures, the intensity is rather insignificant which indicates very little siloxane rich phases. On the other hand, relatively high loss is shifted to higher temperatures which indicates a good dispersion of the oligomers. A maximum is observed at 80°C and it can be attributed to highly dispersed PDMS according to previous arguments. Interestingly, this T_g is between those shown by the PDMS(550) and PDMS(1700) samples (see Figs. 4.26 and 4.35). This is reasonable since for the encapsulated species, T_g should depend on its molecular weight due to the type 1 restriction (see section 4.4).

The SAXS experiment was also performed on this material and the result is shown in Fig. 4.39. A monotonic decrease of intensity is observed, which is similar to those shown before. However, A rather high intensity is observed at small value of s. Since the overall intensity is related to the invariant and the homogeneity of the system, this greater scattering indicated a larger mean square electron density fluctuation in this system than the previous silanol terminated PDMS systems.

As discussed earlier, PDMS self condensation is quite possible in the system prepared with silanol terminated PDMS and, hence, the probability of forming a siloxane rich phase will be finite. For the systems with triethoxysilane endcapped PDMS, however, this self condensation should be less likely since the oligomers now will also need to be hydrolysed to generate silanol groups. In addition, one of the possible cause for poor dispersion of the oligomers is that the two reacting components are not compatible. Even though reaction media is used, localized separation may still be possible. This also promotes the self condensation of the silanol terminated PDMS. However, for the triethoxysilane endcapped PDMS, the structure of the endcapping groups are very similar to TEOS. Obviously, this should improve the compatibility and, hence, the dispersion of the oligomers. These two considerations may well be the reason for the insignificant intensity of the low temperature tanδ peak. Furthermore, this increase in PDMS functionality also greatly decrease the possibility of leaving dangling oligomeric ends in the final network. This "tightening" effect on the oligomers apparently causes the stiffness of the final material to increase considerably. In addition, this "tightening" also causes the oligomeric mobility to decrease and, therefore, results in the low overall tanδ intensity. However, the reason for the SAXS behavior is still not clear.

To summarize, the effect of the functionality of the PDMS is quite significant. The stiffness of the final materials increases significantly, which may be attributed to the tightening effect of the PDMS oligomers. Furthermore, the increase of functionality and the change in the endgroup structure minimize the possibility of PDMS self condensation. As a result, the oligomers are better dispersed into the final network. This improvement in incorporation by endcapping also provokes the possibility of using this same endcapping chemistry to prepare other types of oligomers for incorporation.

Table 4.1   The initial weight fractions of TEOS and the corresponding molar ratios of TEOS/PDMS and calculated final weight fractions of SiO_2.

wt% of TEOS	molar ratio of TEOS/PDMS		wt% of SiO_2 in the final product†
	MW = 1700	MW = 550	
48	7.5	2.4	21.0
60	12.3	4.0	30.2
70	19.1	6.2	40.2

†assuming reaction is 100% complete

Table 4.2 The results of elemental analysis on the acid series of TEOS(48)-PDMS(1700)-50-X-80C.

molar ratio of HCl/TEOS	final weight fraction (%)			
	C	H	O	Si
0.022	25.1	6.4	34.2	34.3
0.045	25.4	6.5	33.5	34.6
0.111	26.5	6.7	32.9	33.9

Table 4.3   Ratios of the areas under the Raman scattering peaks of the C-H bending mode and the Si-O-Si stretching mode for the   acid   series   of TEOS(48)-PDMS(1700)-50-X-80C.

molar ratio of HCl/TEOS	area ratio of C-H/Si-O-Si
0.022	1.439
0.045	1.541
0.067	1.185
0.09	1.118
0.111	1.246
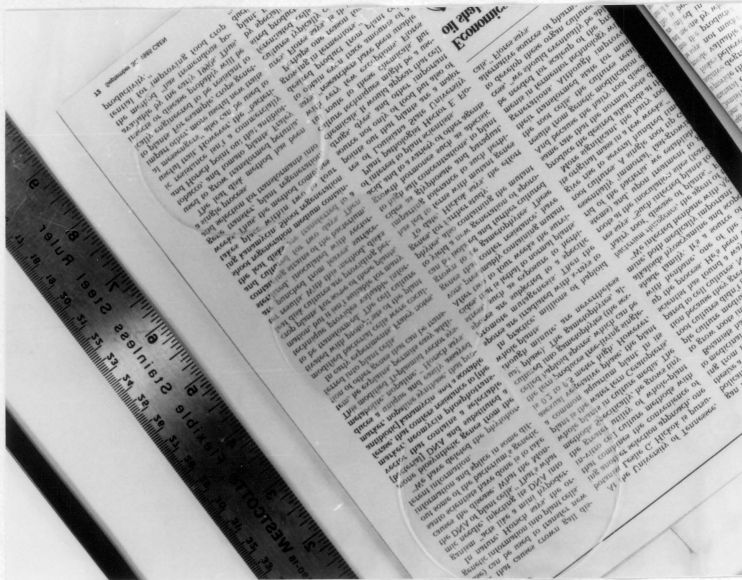
Figure 4.1   Cast films of hybrid materials prepared with 48 wt% TEOS and silanol terminated PDMS (MW = 1700).
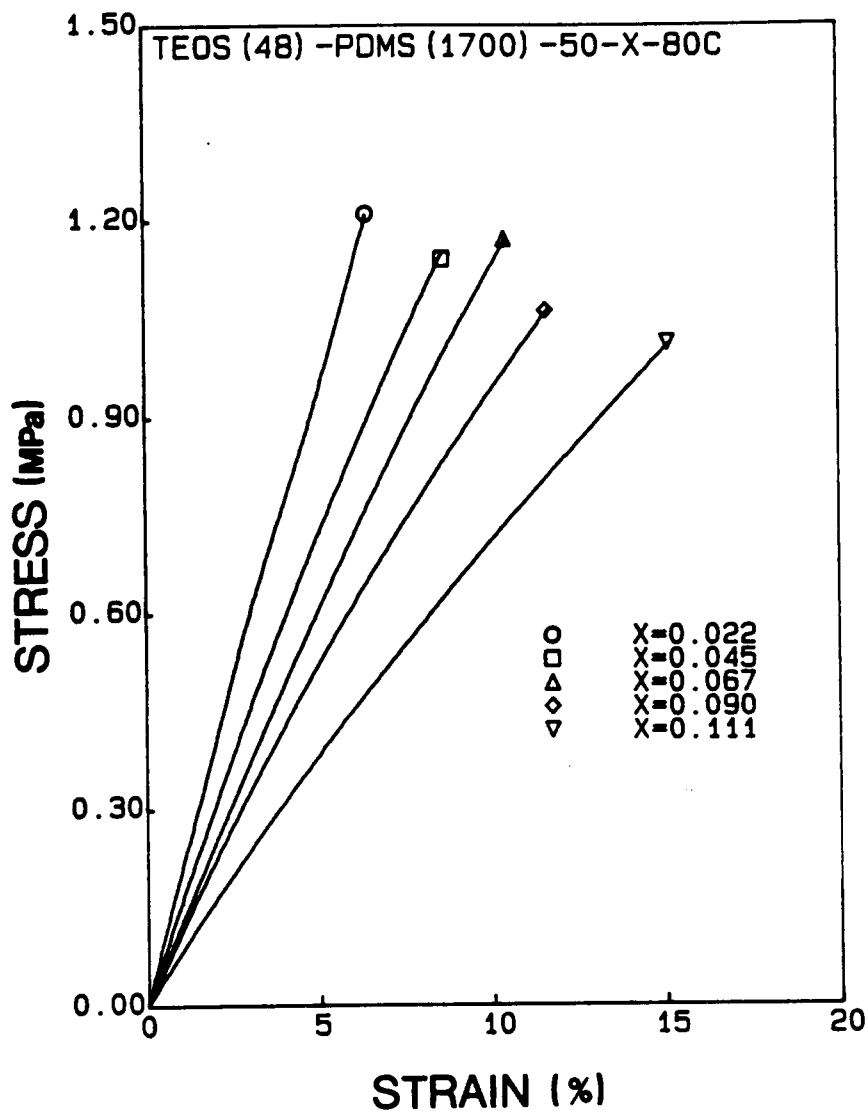
Figure 4.2 Stress-strain behaviors of materials prepared with various acid content, 48 wt% TEOS, 1700 MW PDMS, 50% water content, and 80°C reaction temperature.
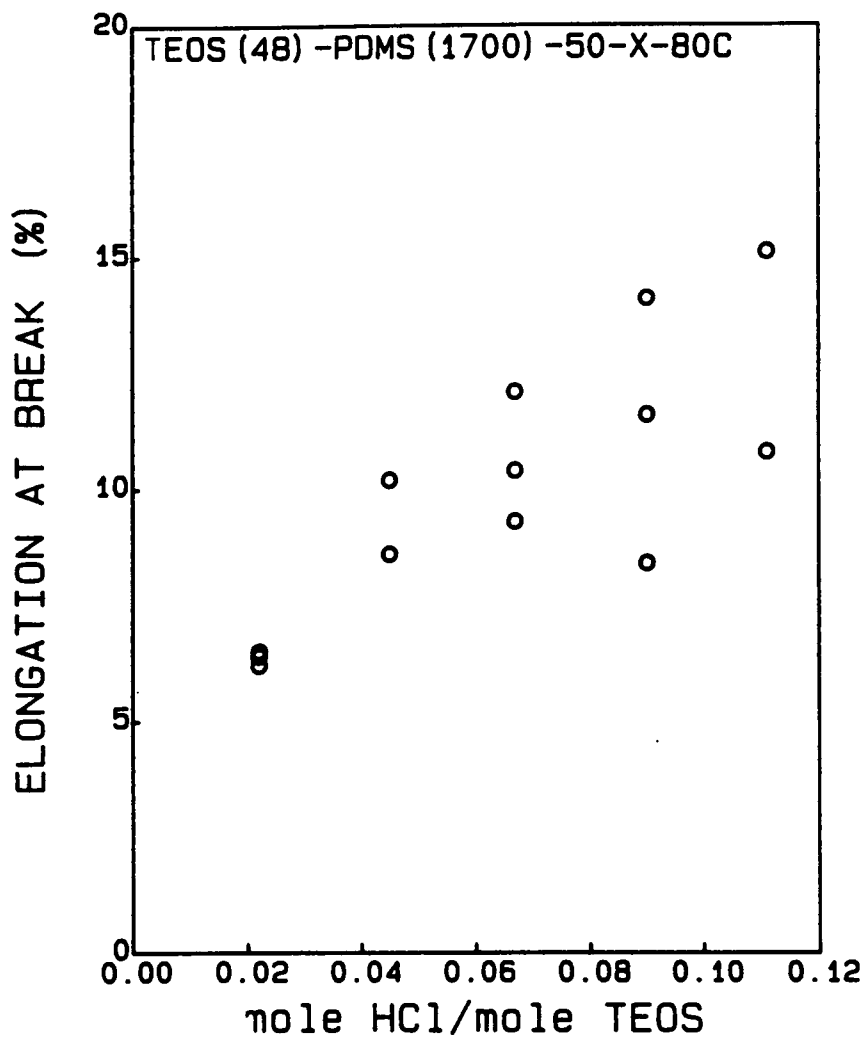
Figure 4.3   Effect of acid content on the elongation at break of materials prepared with 48 wt% TEOS, 1700 MW PDMS, 50% water content, and 80°C reaction temperature.
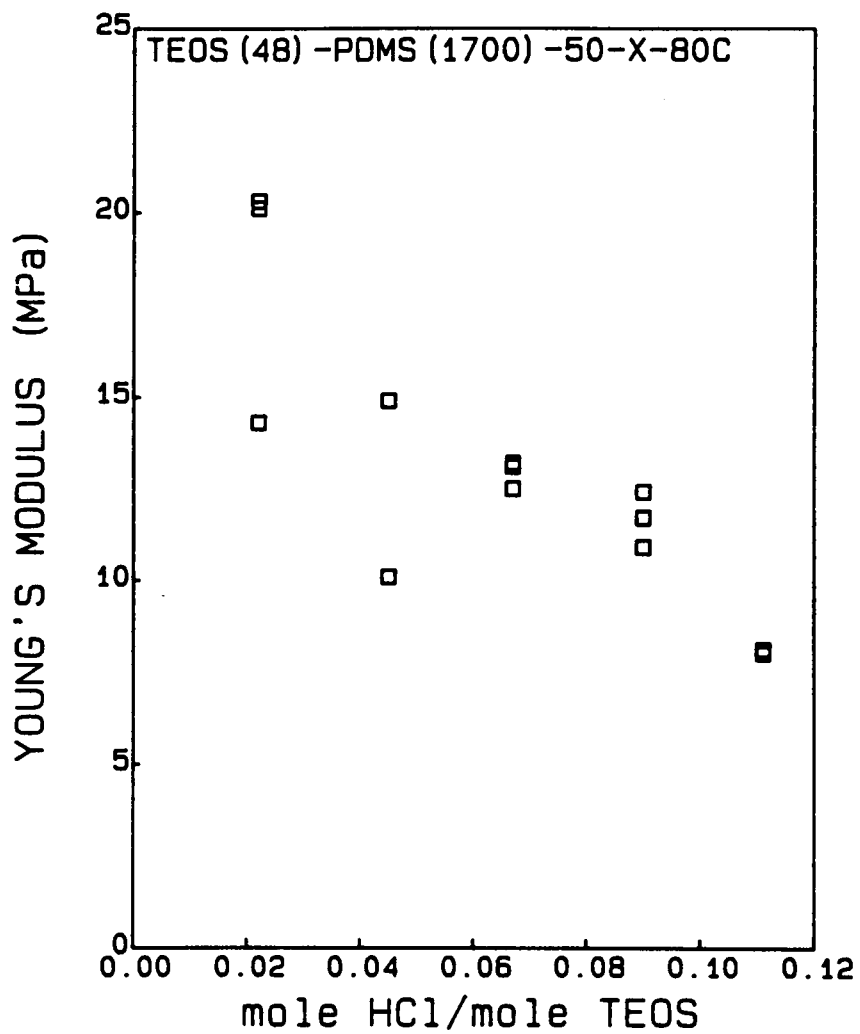
Figure 4.4 Effect of acid content on the Young's modulus of materials prepared with 48 wt% TEOS, 1700 MW PDMS, 50% water content, and 80°C reaction temperature.
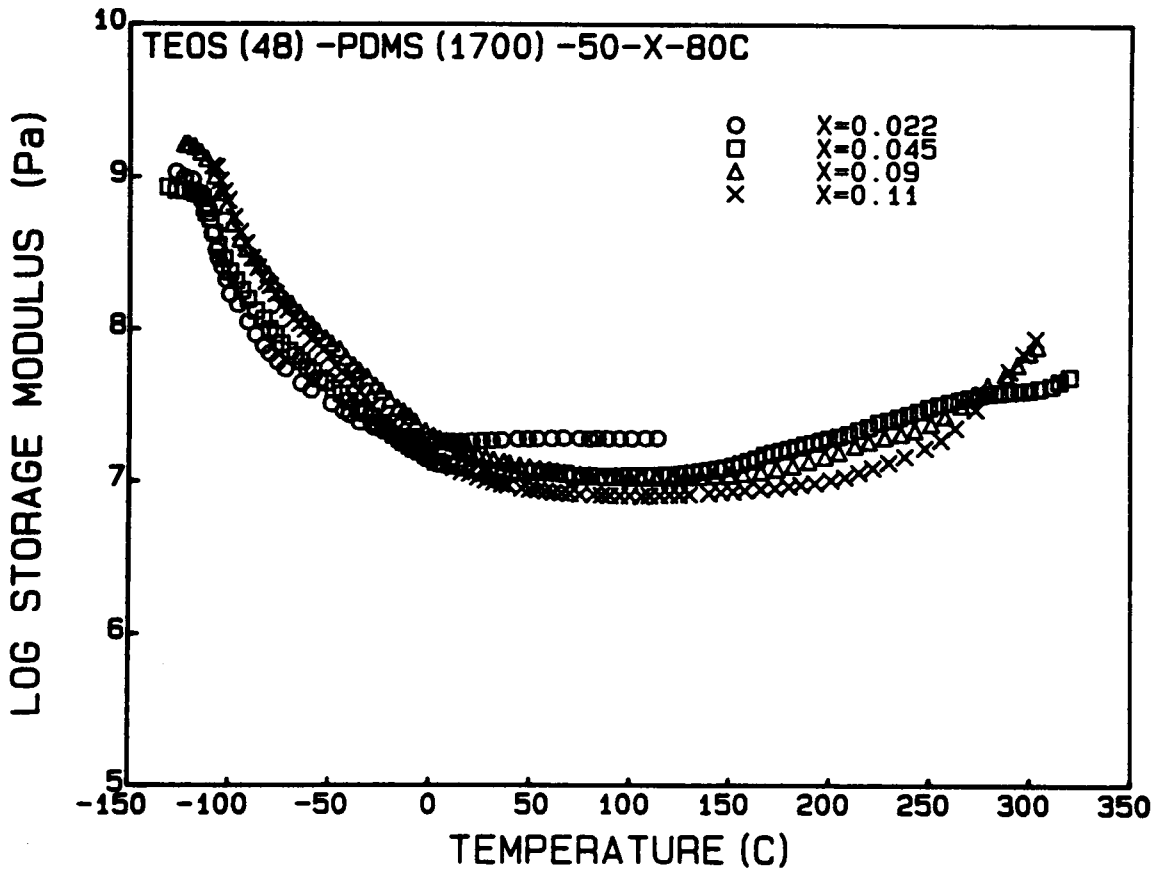
Figure 4.5 Spectra of storage modulus of materials prepared with various acid content, 48 wt% TEOS, 1700 MW PDMS, 50% water content, and 80°C reaction temperature.
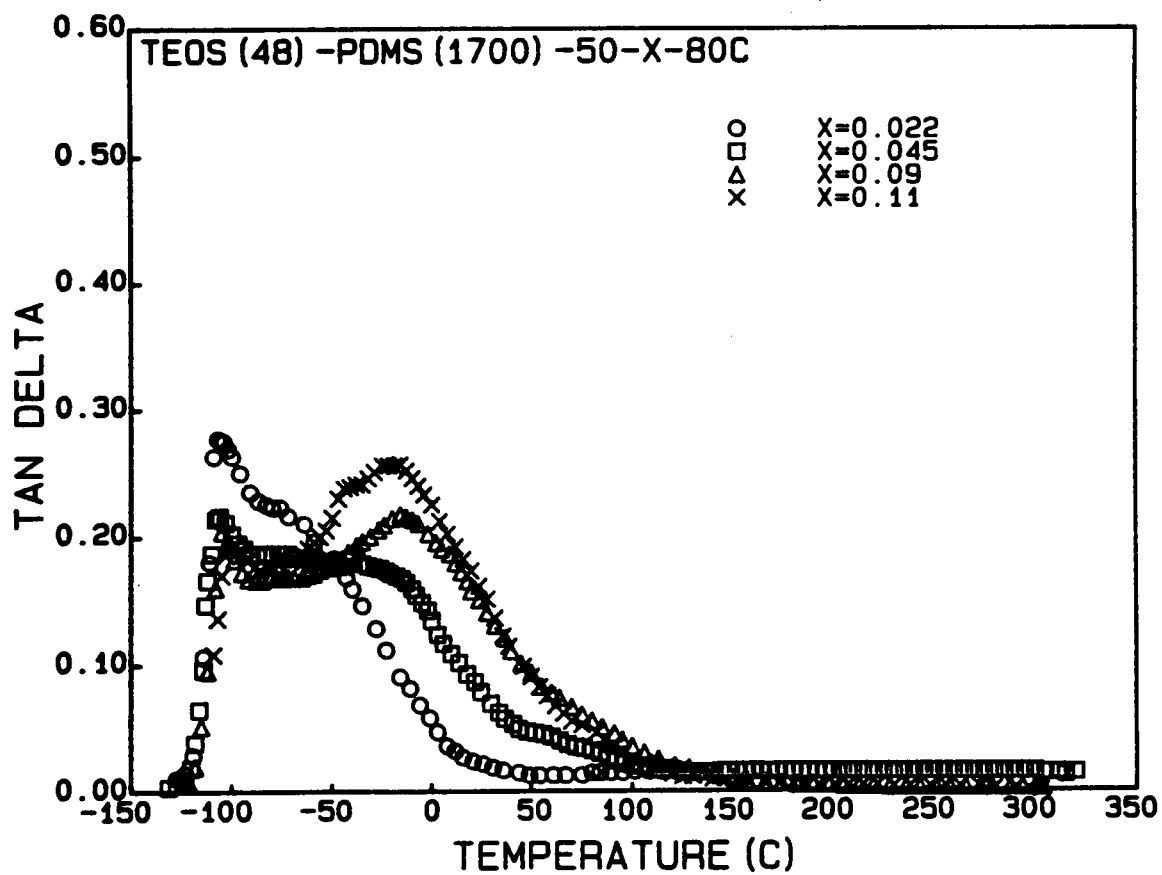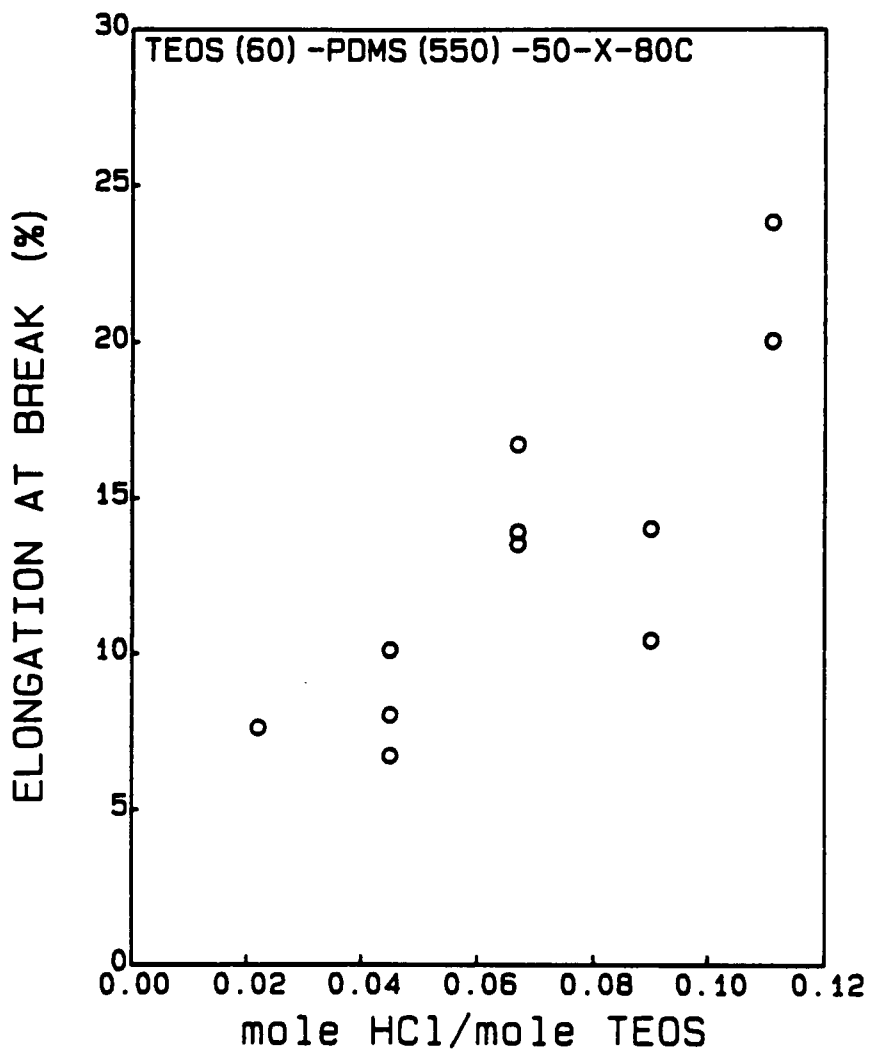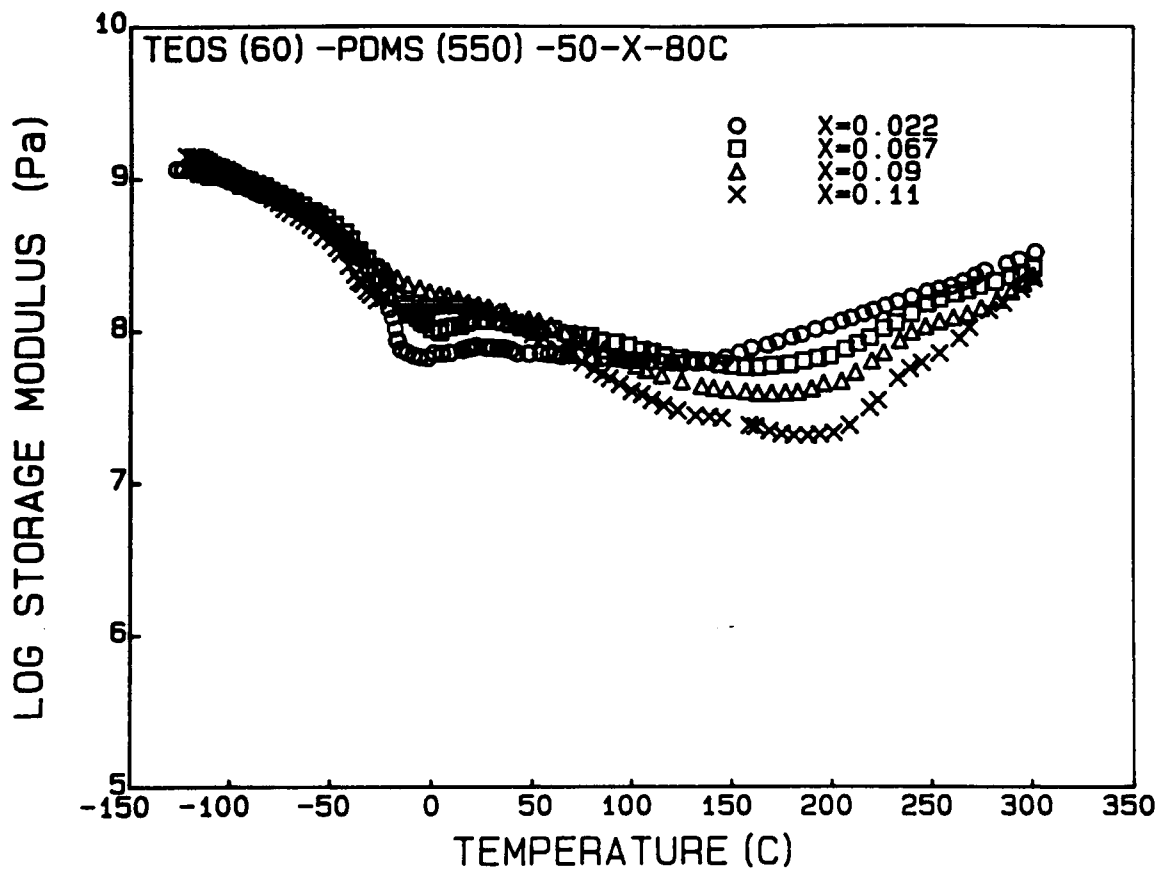
Figure 4.6 Spectra of tanδ of materials prepared with various acid content, 48 wt% TEOS, 1700 MW PDMS, 50% water content, and 80°C reaction temperature.
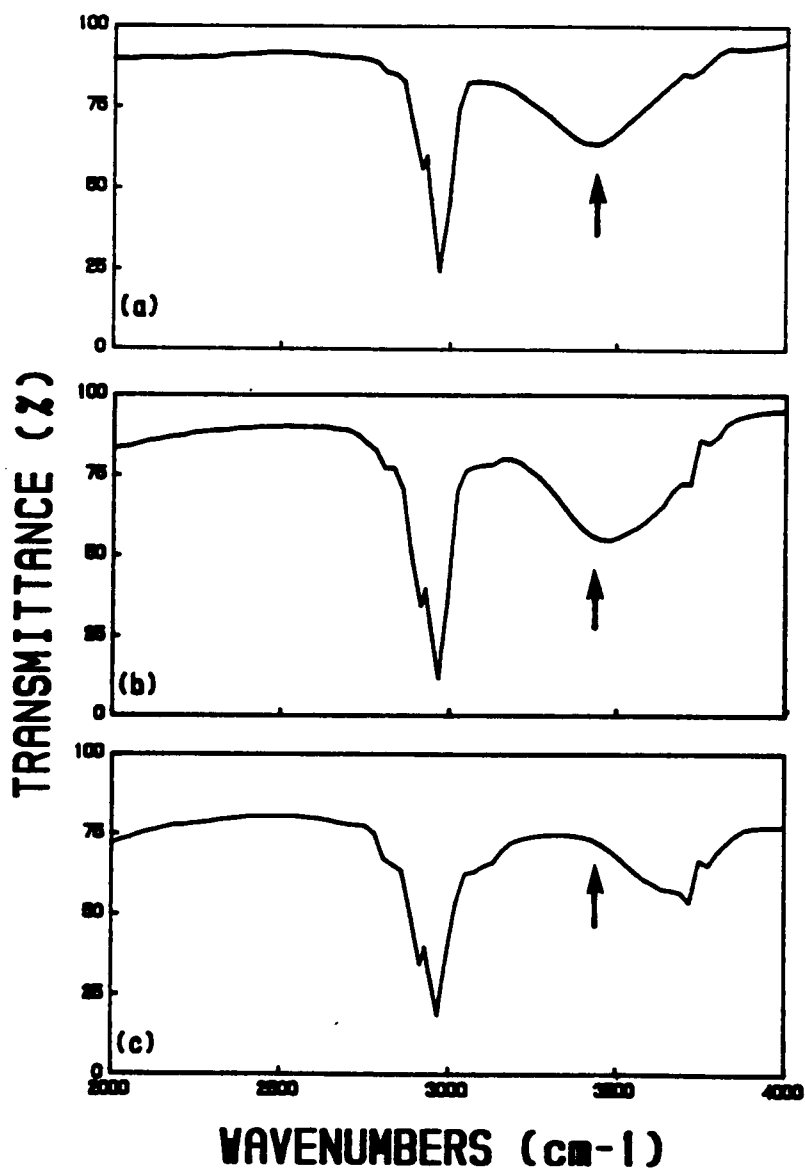
Figure 4.7 Infrared spectra of a TEOS-PDMS material treated at different temperatures. (a) without thermal treatment, (b) 150°C for 2 hours, (c) 250°C for 2 hours.
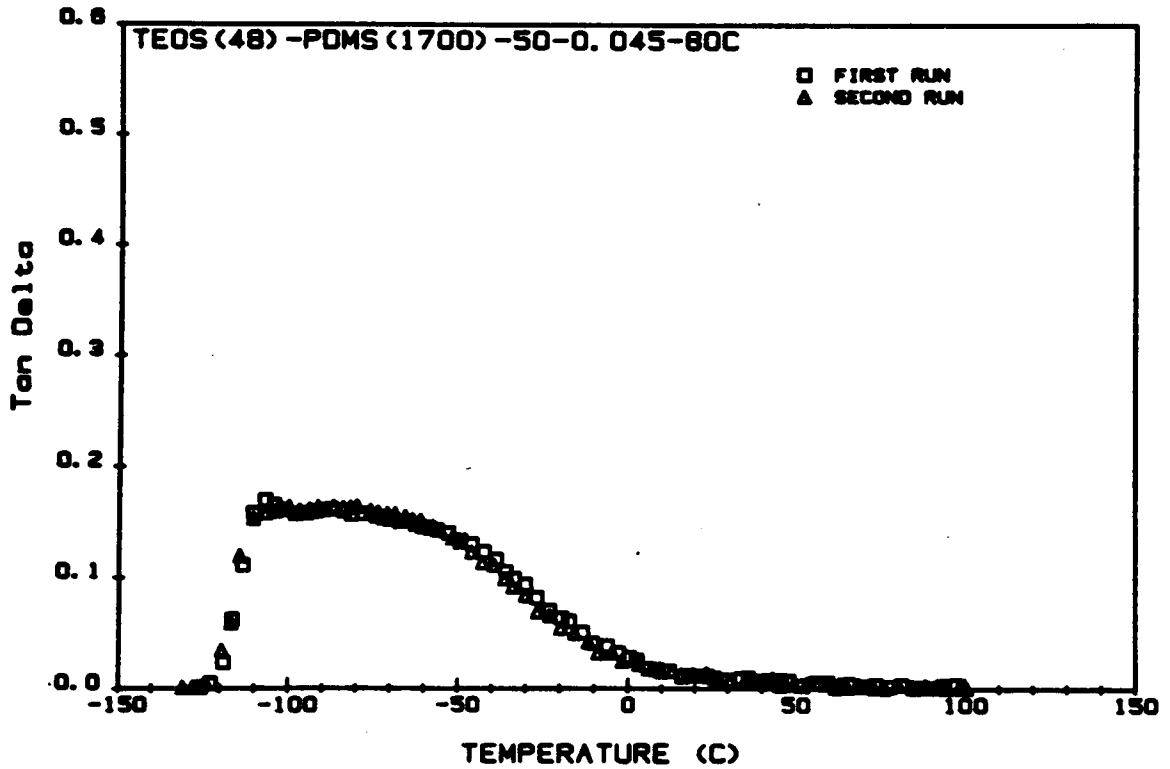
Figure 4.8 Comparison of tanδ spectra of two consecutive runs on the same sample prepared with 48 wt% TEOS, 1700 MW PDMS, 50% water content, 0.045 acid content, and 80°C reaction temperature.
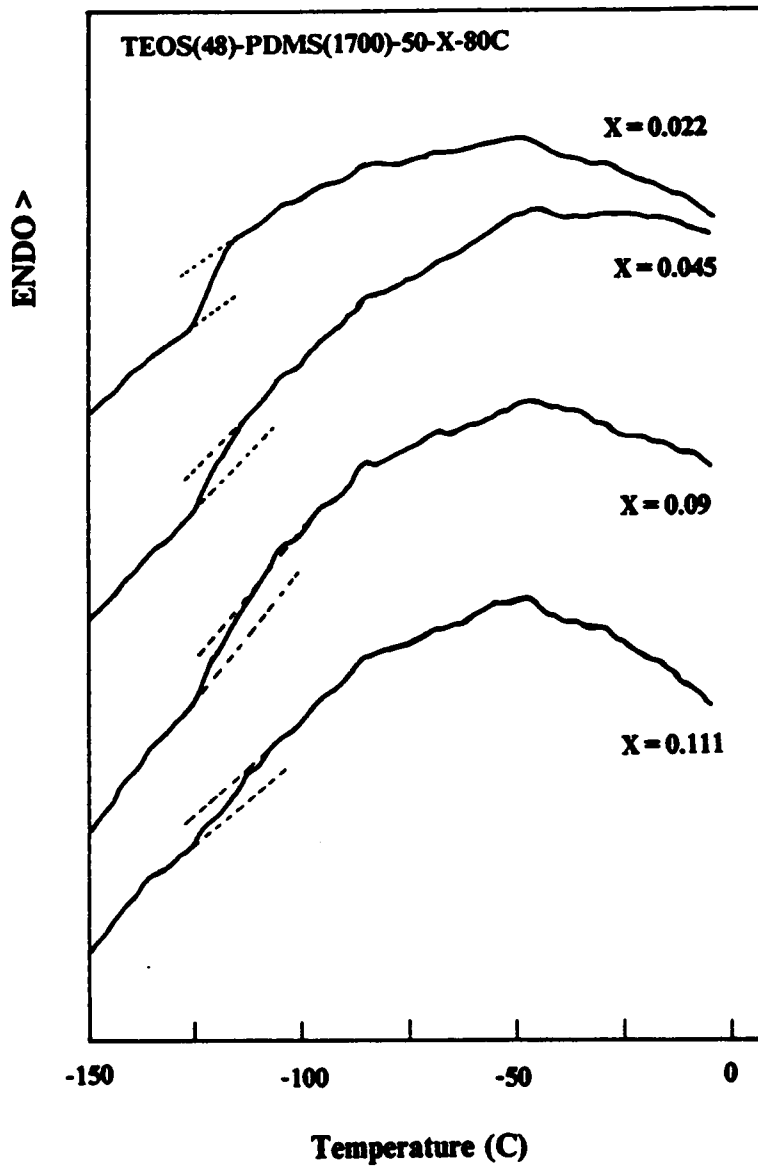
Figure 4.9 Results of DSC experiments for materials prepared with various acid content, 48 wt% TEOS, 1700 MW PDMS, 50% water content, and 80°C reaction temperature.
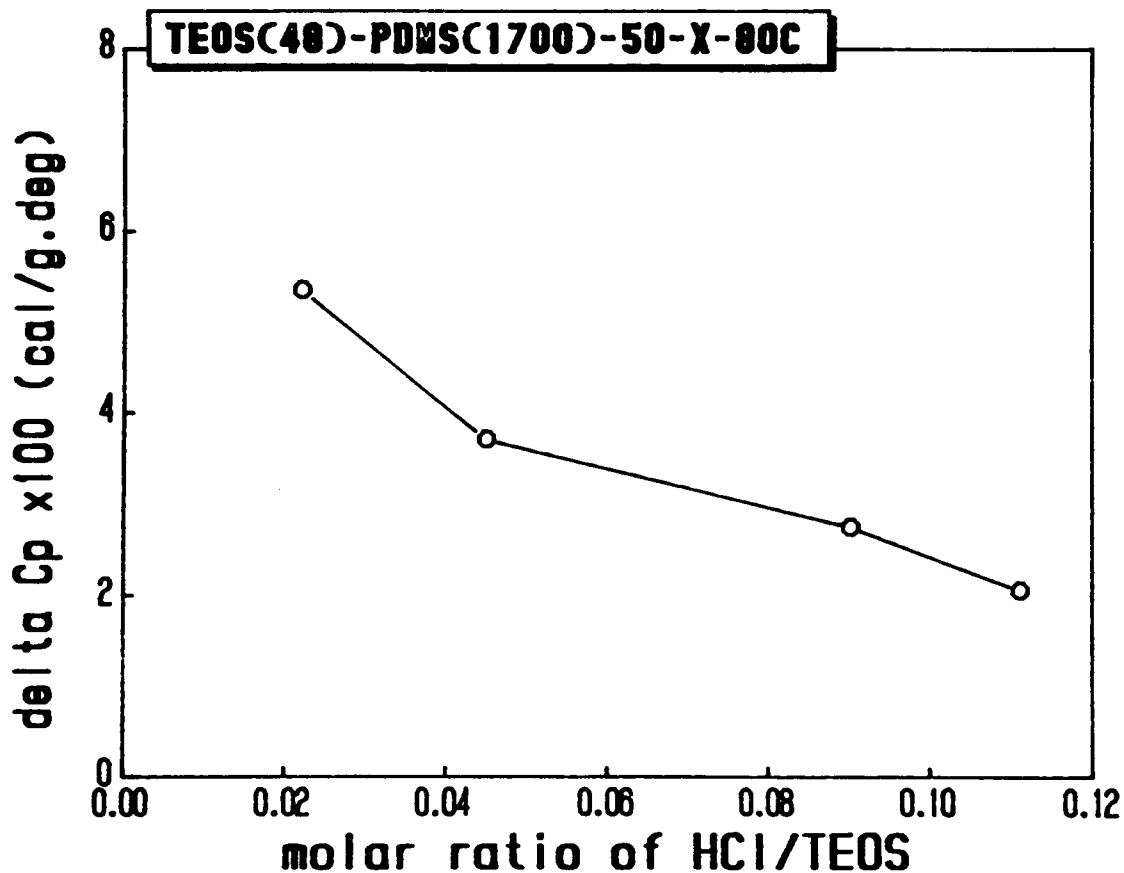
**Figure 4.10**   Effect of acid content on the change of specific heat (ΔCp) at the transition temperature (-127°C) of materials prepared with 48 wt% TEOS, 1700 MW PDMS, 50% water content, and 80°C reaction temperature.
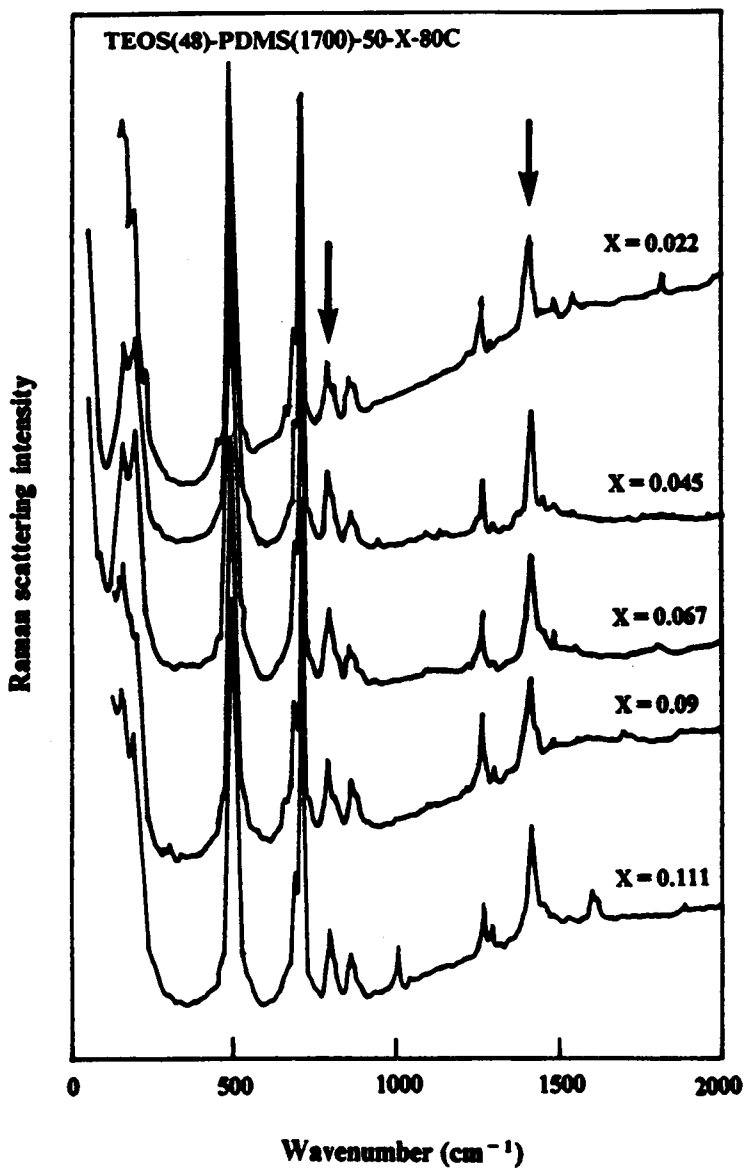
Figure 4.11   Raman spectra of materials prepared with various acid content, 48 wt% TEOS, 1700 MW PDMS, 50% water content, and 80°C reaction temperature. The acid content increases from (a) to (e).
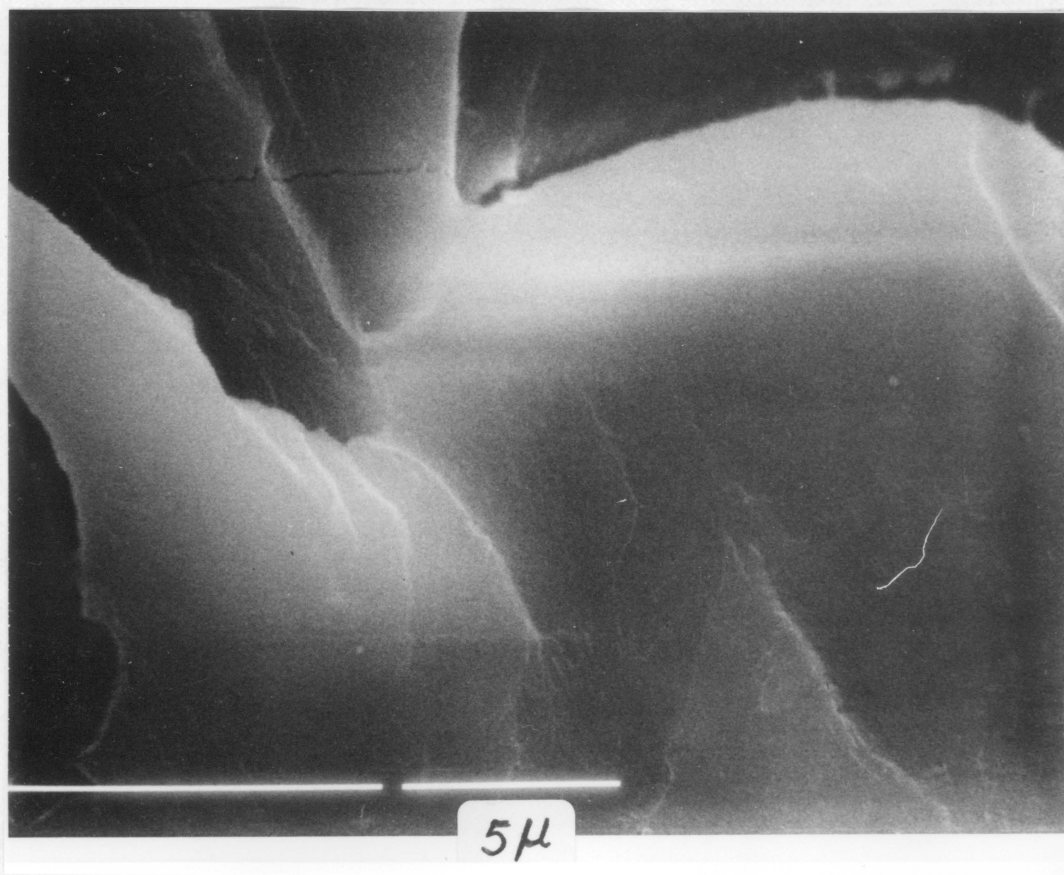
Figure 4.12   An example SEM micrograph of a TEOS-PDMS hybrid material.
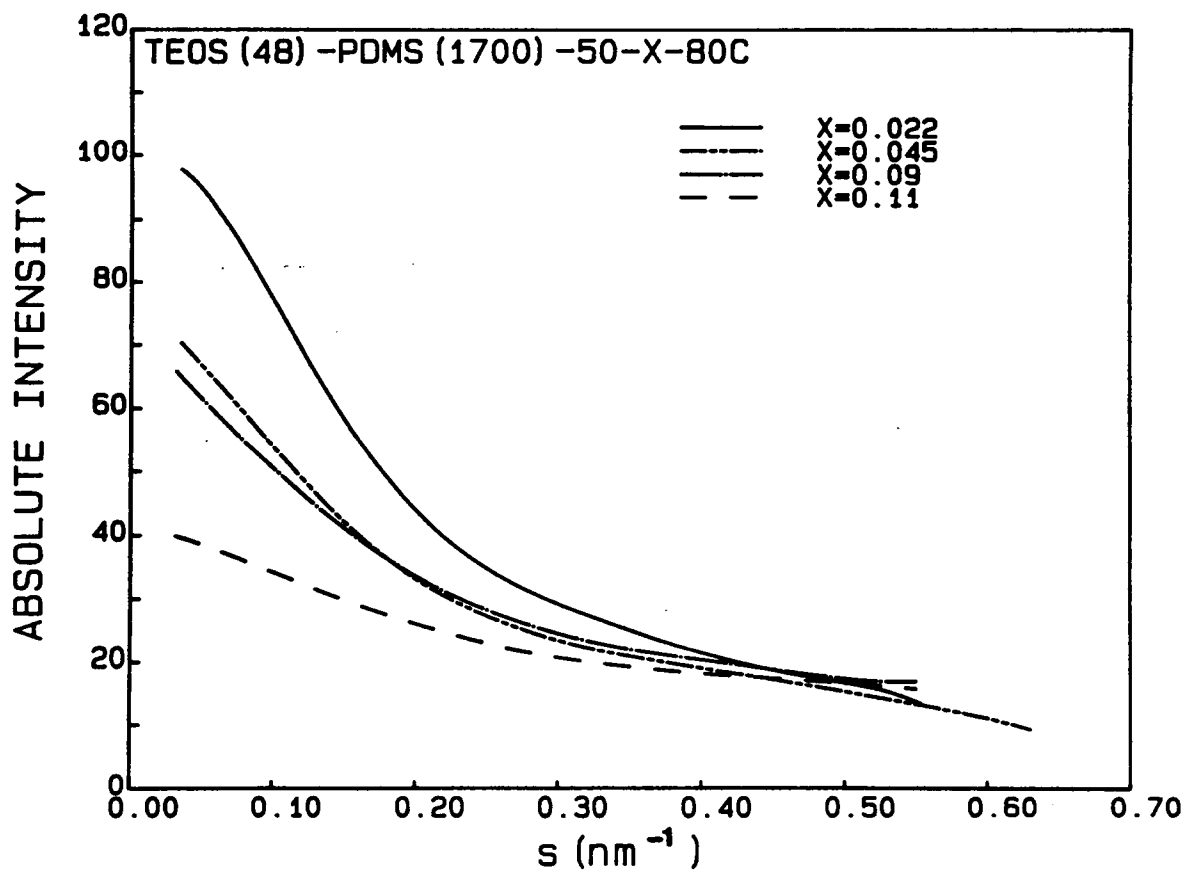
Figure 4.13   SAXS profiles of materials prepared with various acid content, 48 wt% TEOS, 1700 MW PDMS, 50% water content, and 80°C reaction temperature.
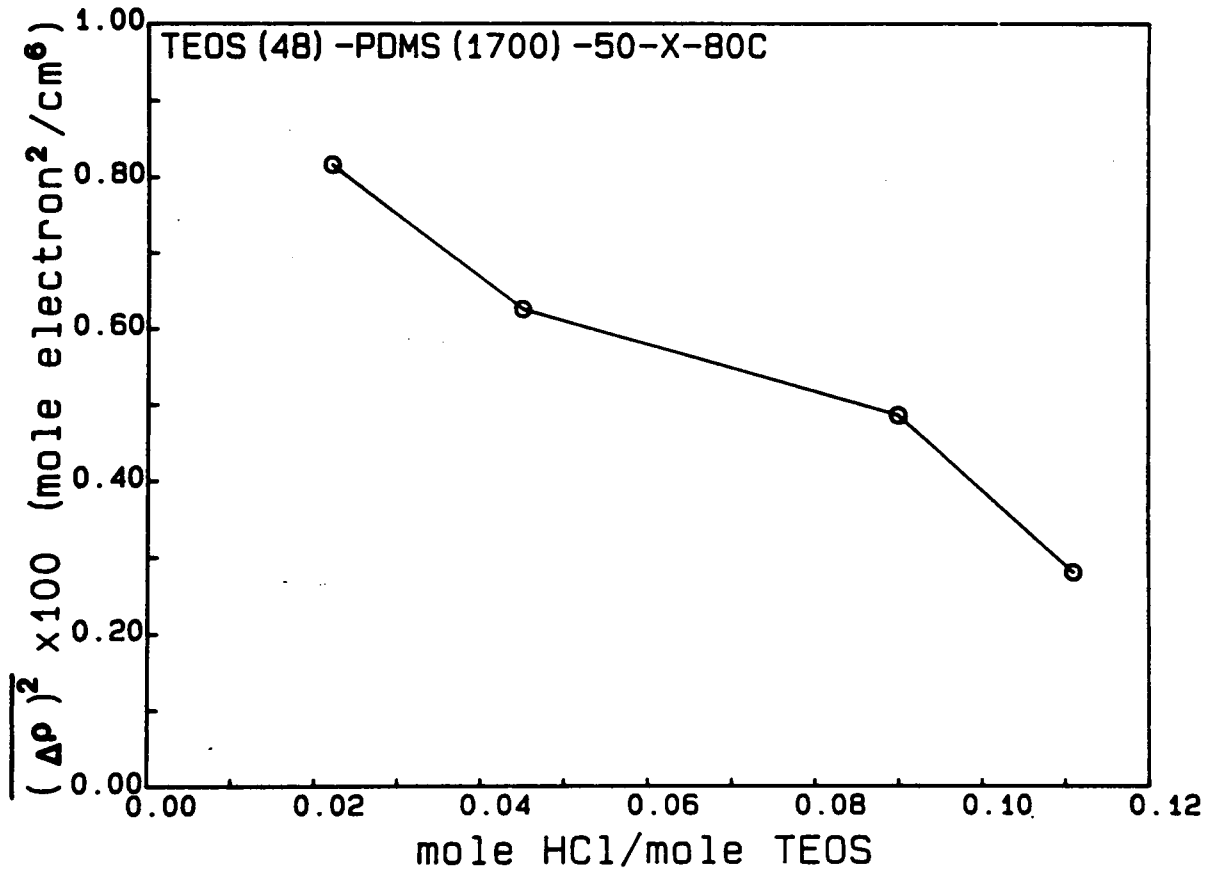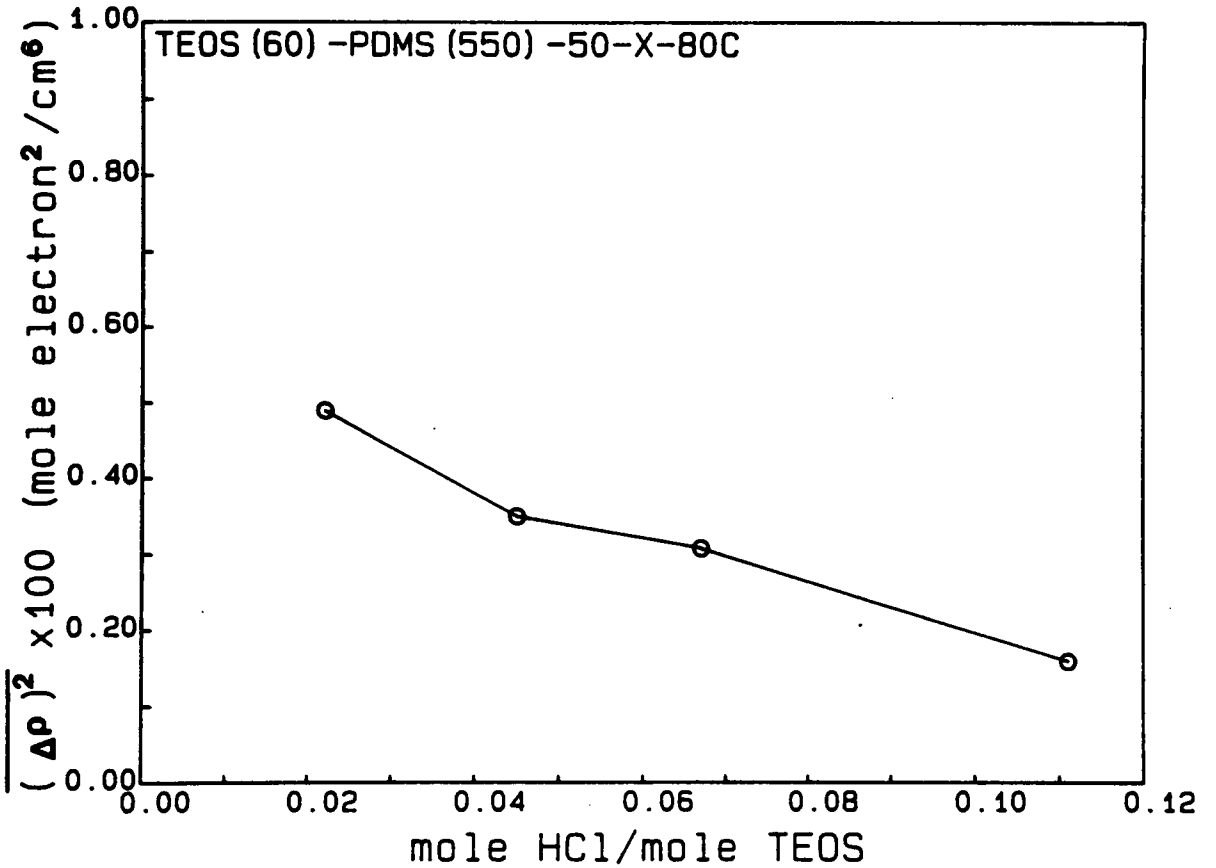
Figure 4.14 Effect of acid content on the mean square electron densityÖ fluctuation of materials prepared with 48 wt% TEOS, 1700 MW PDMS, 50% water content, and 80°C reaction temperature.
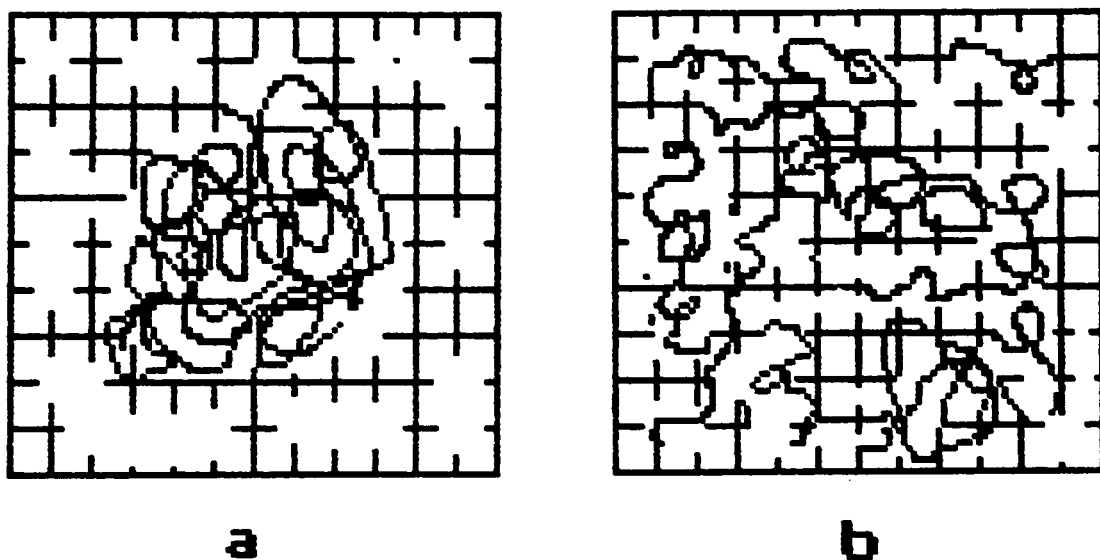
Figure 4.15   Simplified schematic models for the TEOS-PDMS hybrid systems: (a) phase separated oligomers, (b) better dispersed oligomers.
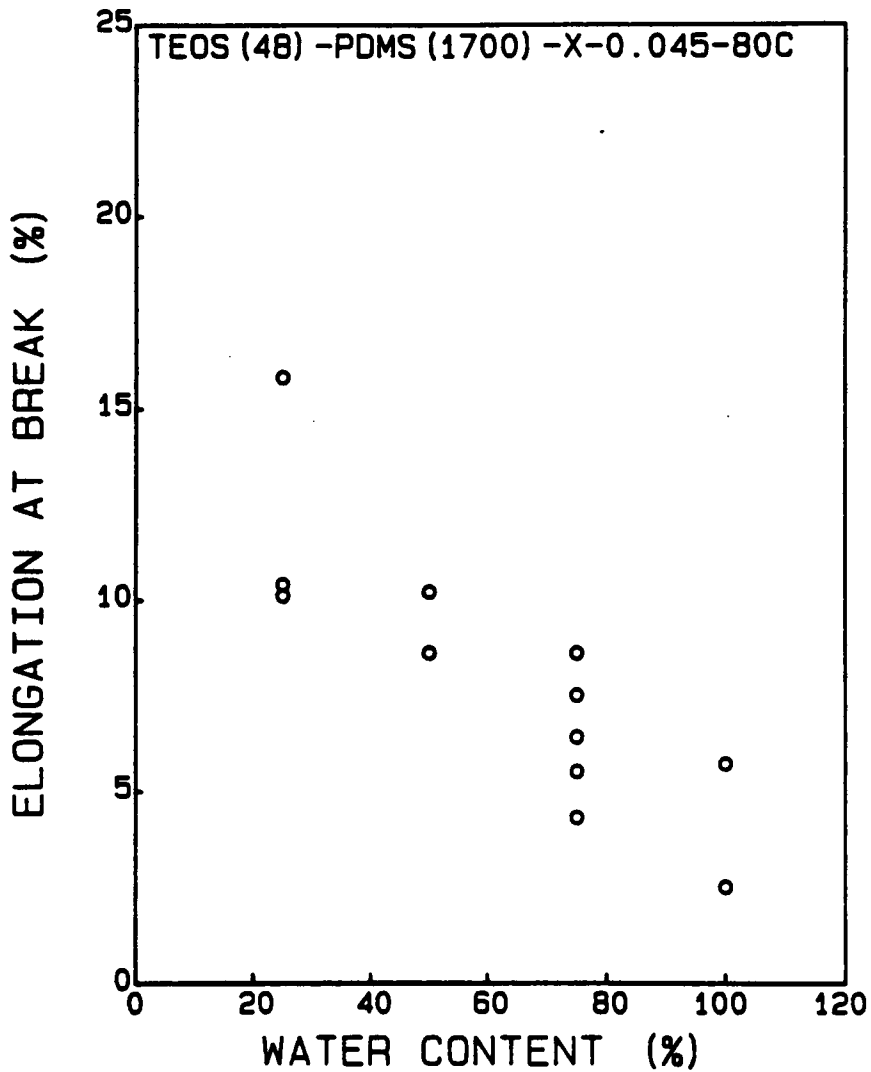
Figure 4.16 Effect of water content on the elongation at break of materials prepared with 48 wt% TEOS, 1700 MW PDMS, 0.045 acid content, and 80°C reaction temperature.
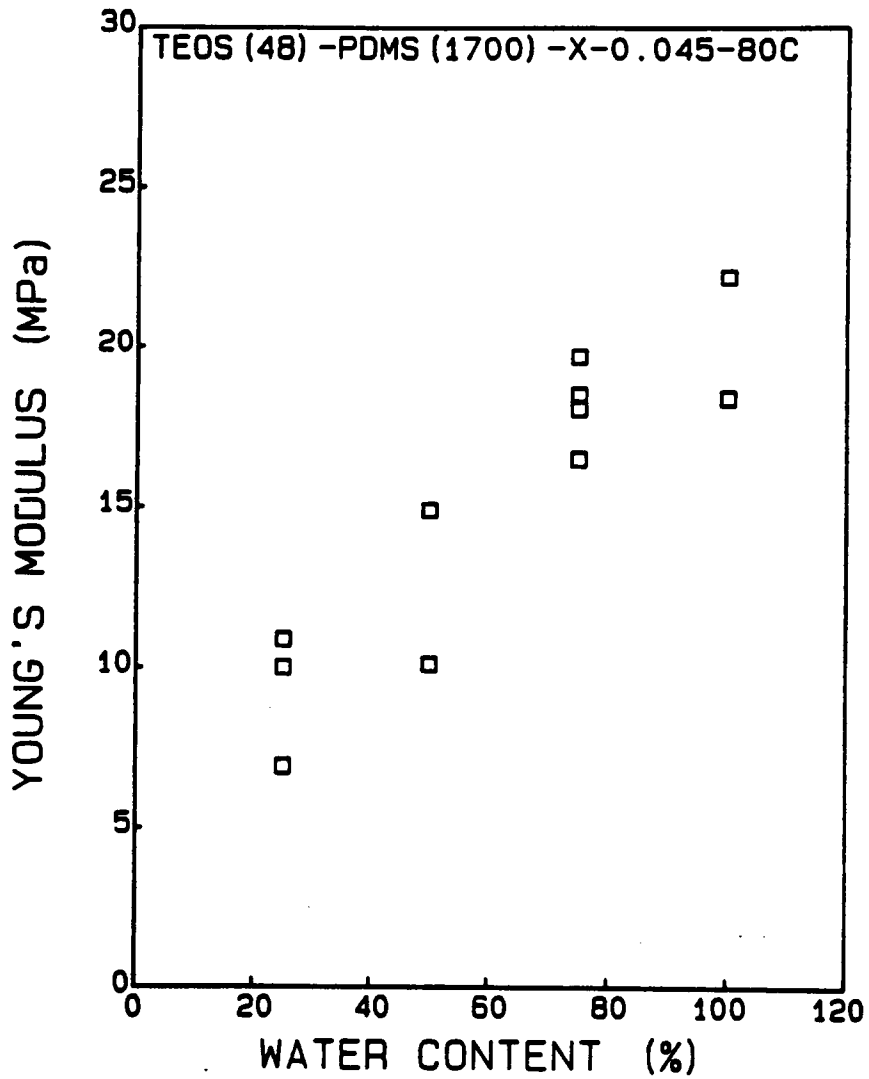
Figure 4.17   Effect of water content on the Young's modulus of materials prepared with 48 wt% TEOS, 1700 MW PDMS, 0.045 acid content, and 80°C reaction temperature.
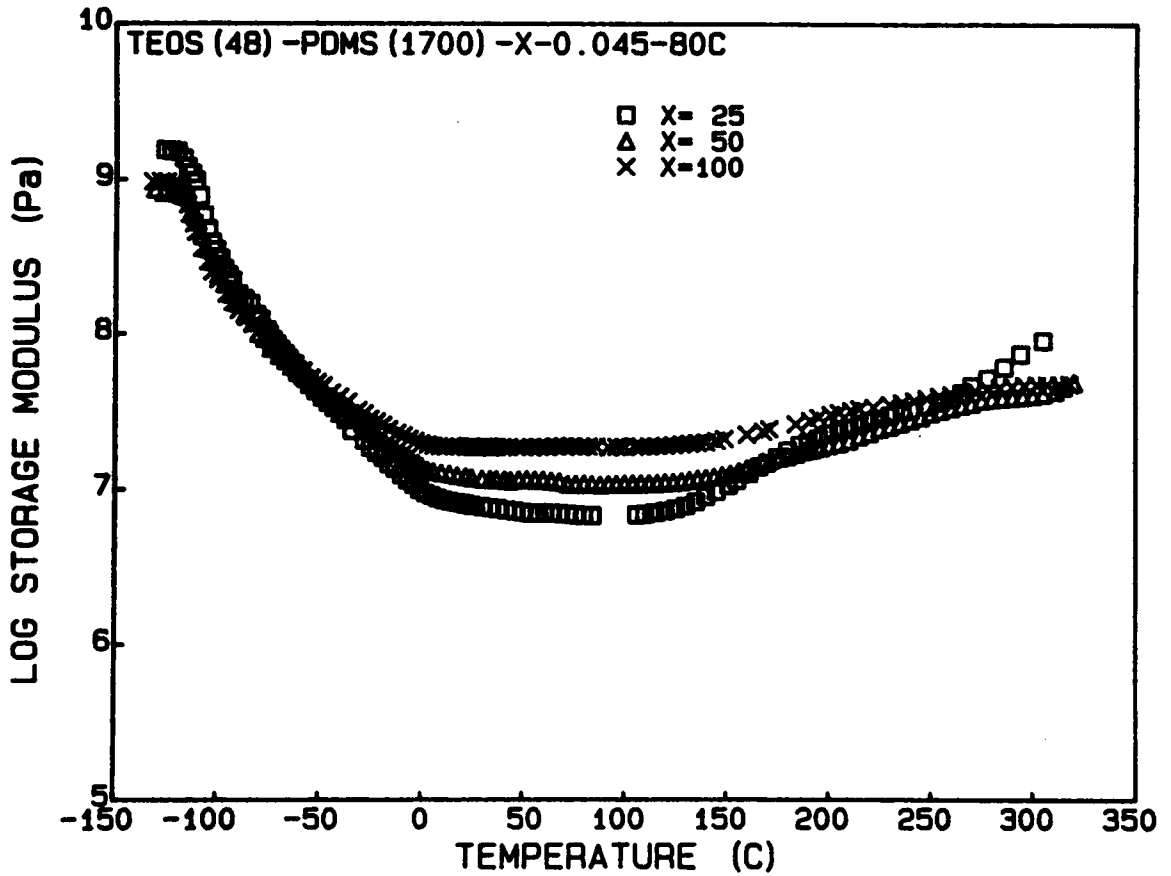
Figure 4.18 Spectra of storage modulus of materials prepared with various water content, 48 wt% TEOS, 1700 MW PDMS, 0.045 acid content, and 80°C reaction temperature.
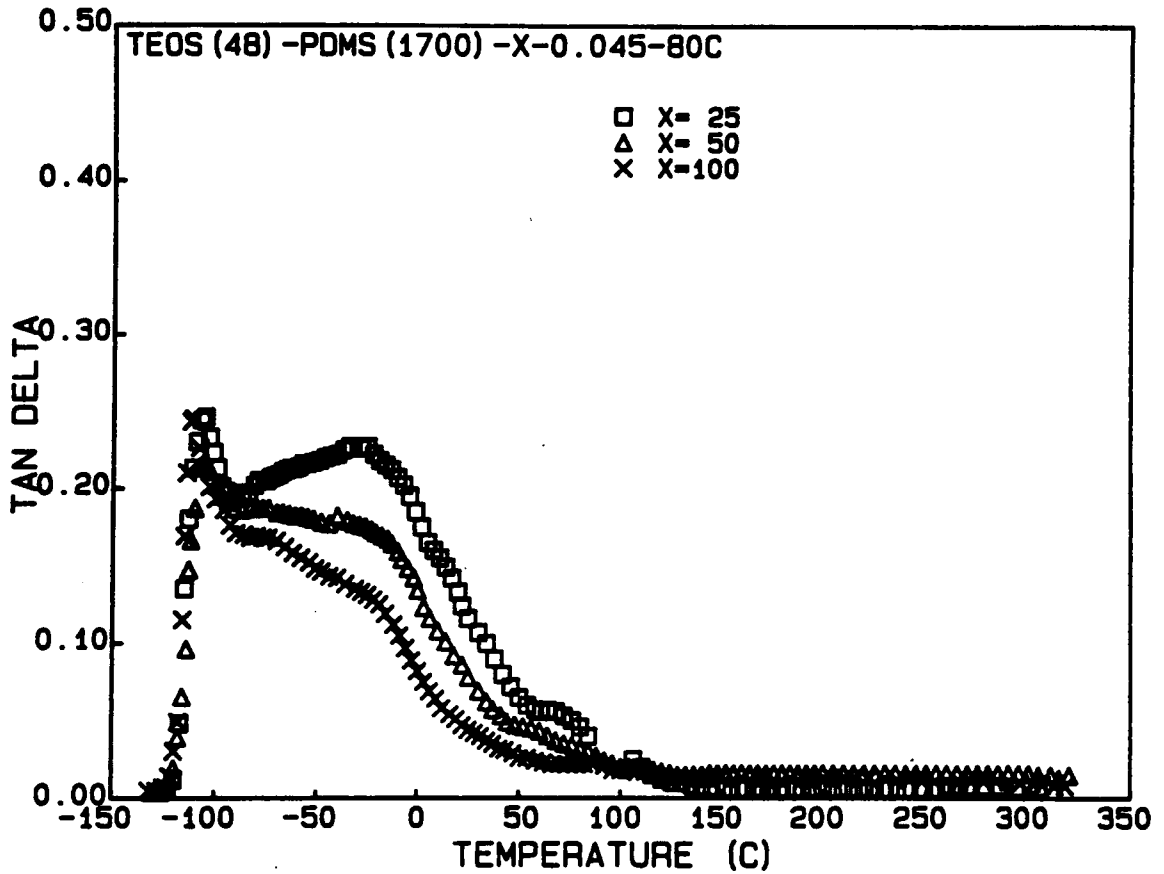
Figure 4.19 Spectra of tanδ of materials prepared with various water content, 48 wt% TEOS, 1700 MW PDMS, 0.045 acid content, and 80°C reaction temperature.
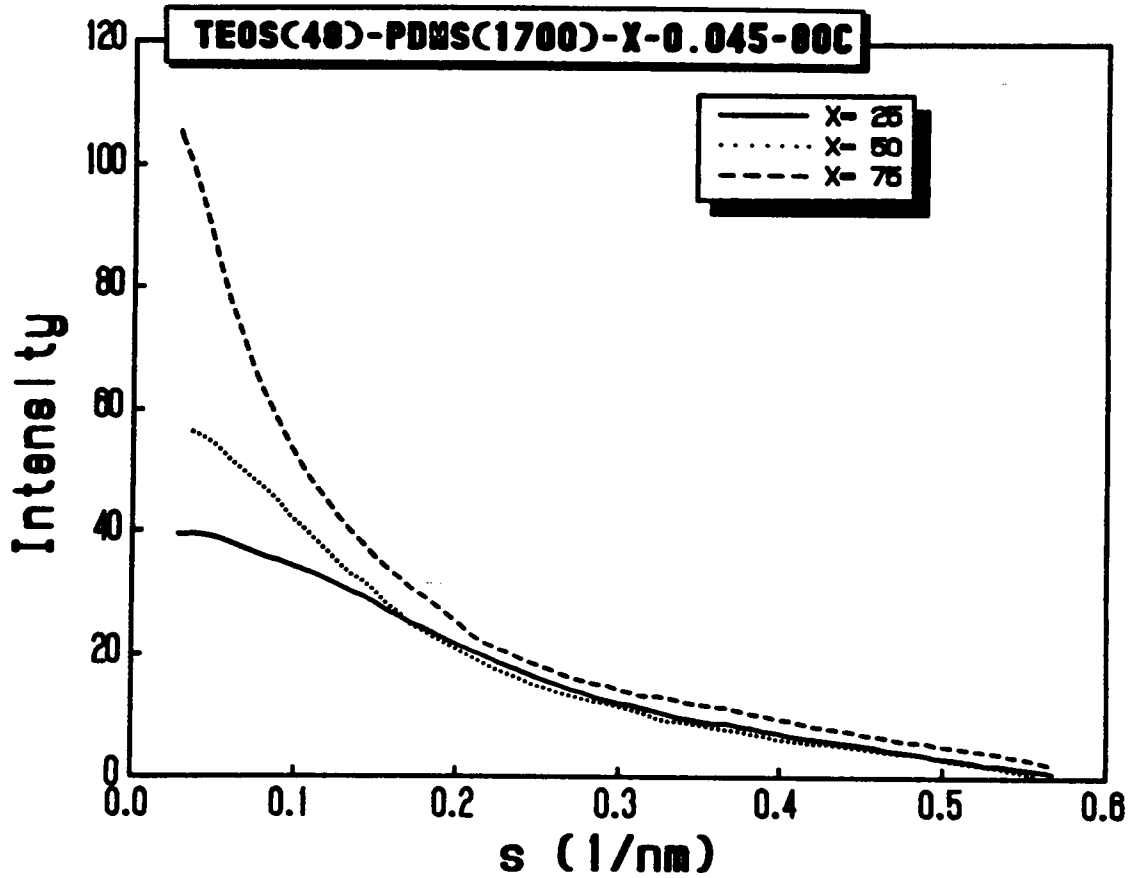
Figure 4.20 SAXS profiles of materials prepared with various water content, 48 wt% TEOS, 1700 MW PDMS, 0.045 acid content, and 80°C reaction temperature.
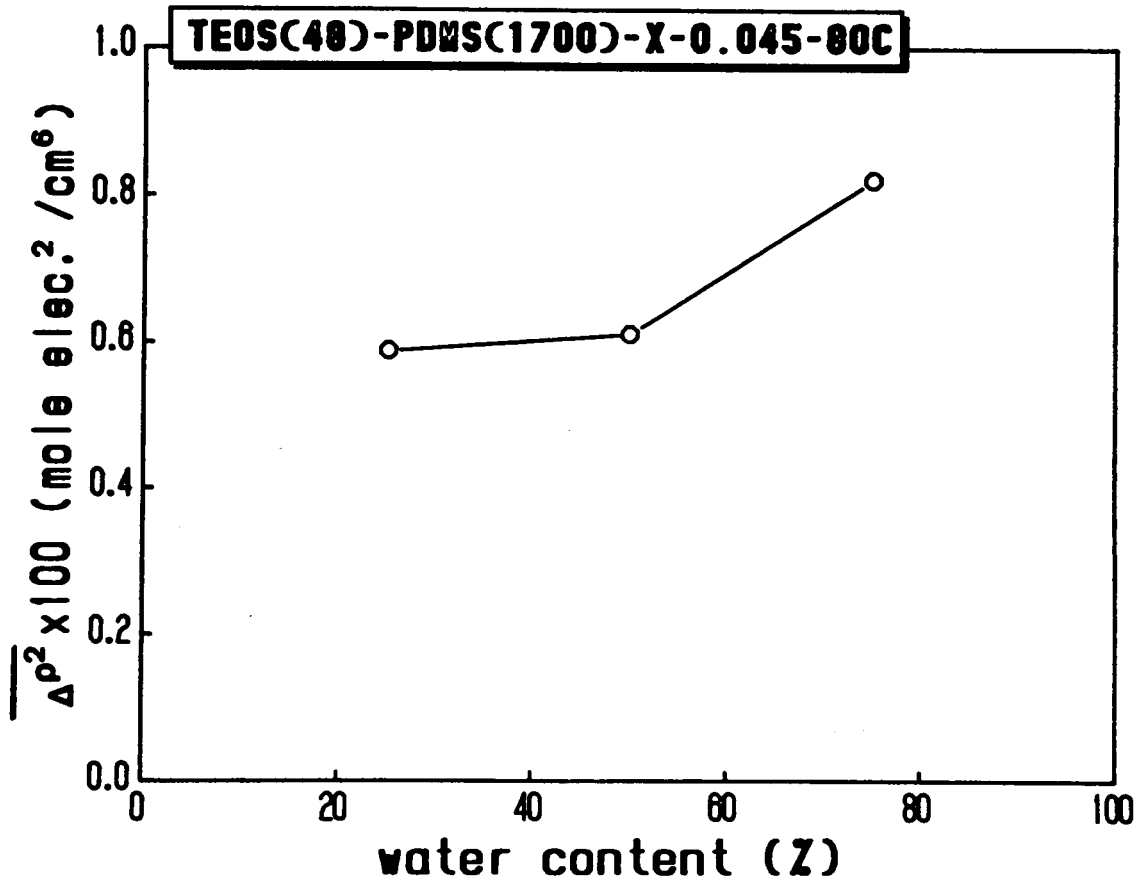
Figure 4.21 Effect of water content on the mean square electron density fluctuation of materials prepared with 48 wt% TEOS, 1700 MW PDMS, 0.045 acid content, and 80°C reaction temperature.
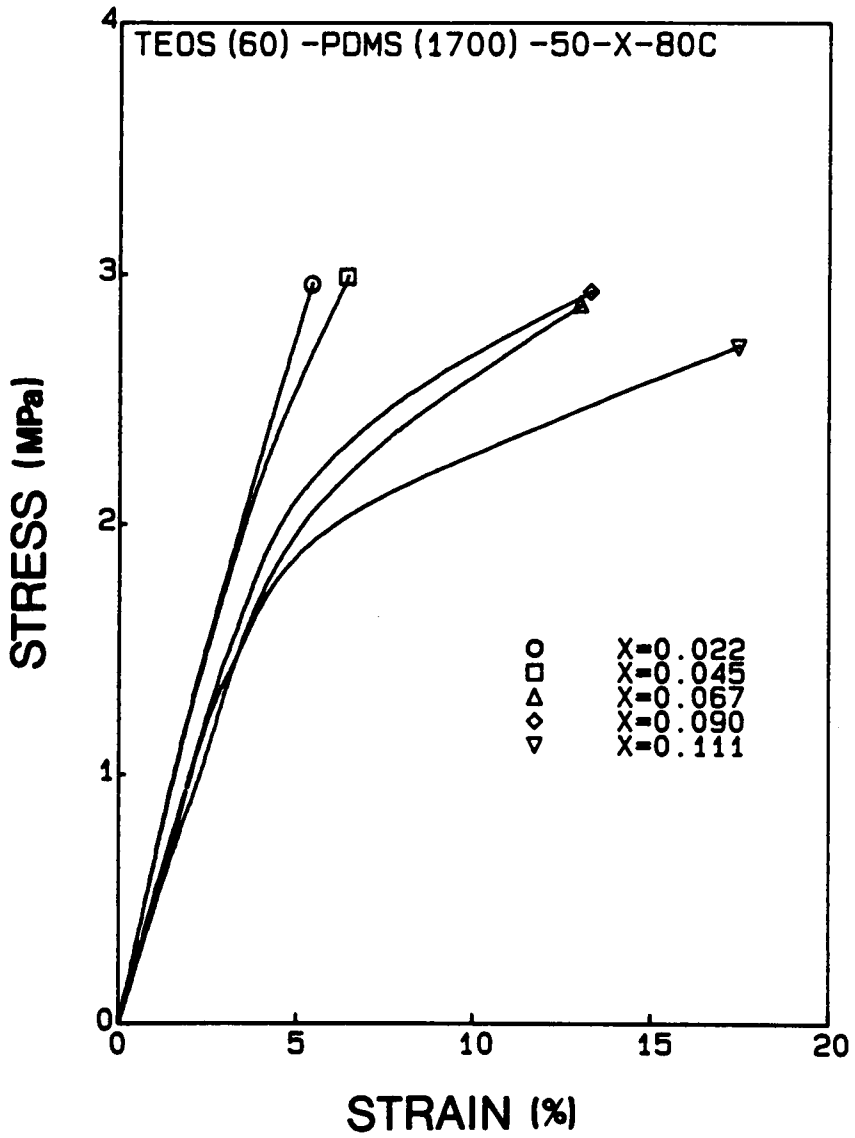
Figure 4.22   Stress-strain behaviors of materials prepared with various acid content, 60 wt% TEOS, 1700 MW PDMS, 50% water content, and 80°C reaction temperature.
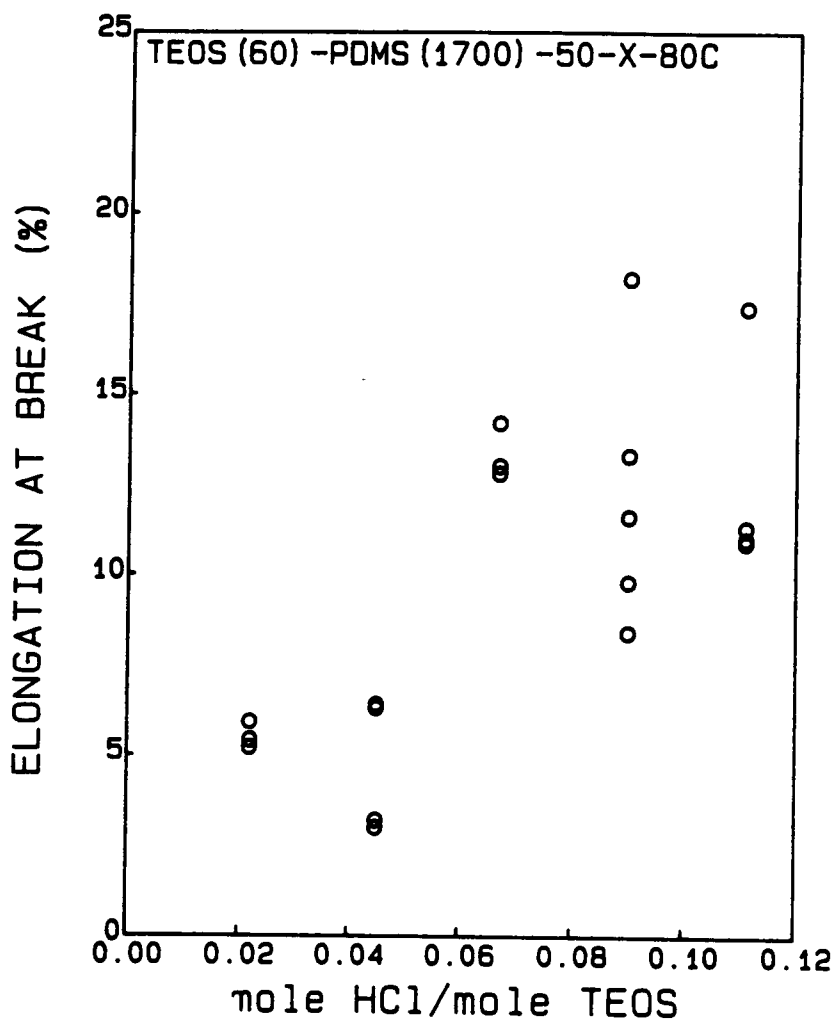
Figure 4.23   Effect of acid content on the elongation at break of materials prepared with 60 wt% TEOS, 1700 MW PDMS, 50% water content, and 80°C reaction temperature.
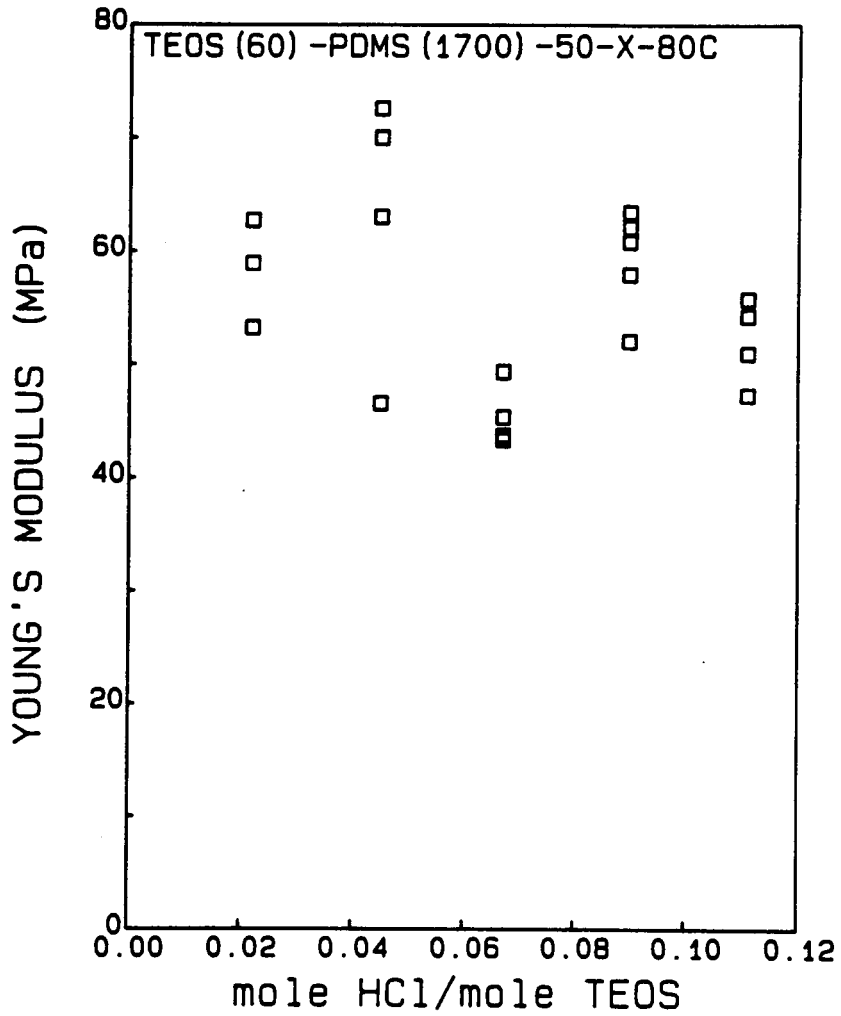
Figure 4.24 Effect of acid content on the Young's modulus of materials prepared with 60 wt% TEOS, 1700 MW PDMS, 50% water content, and 80°C reaction temperature.
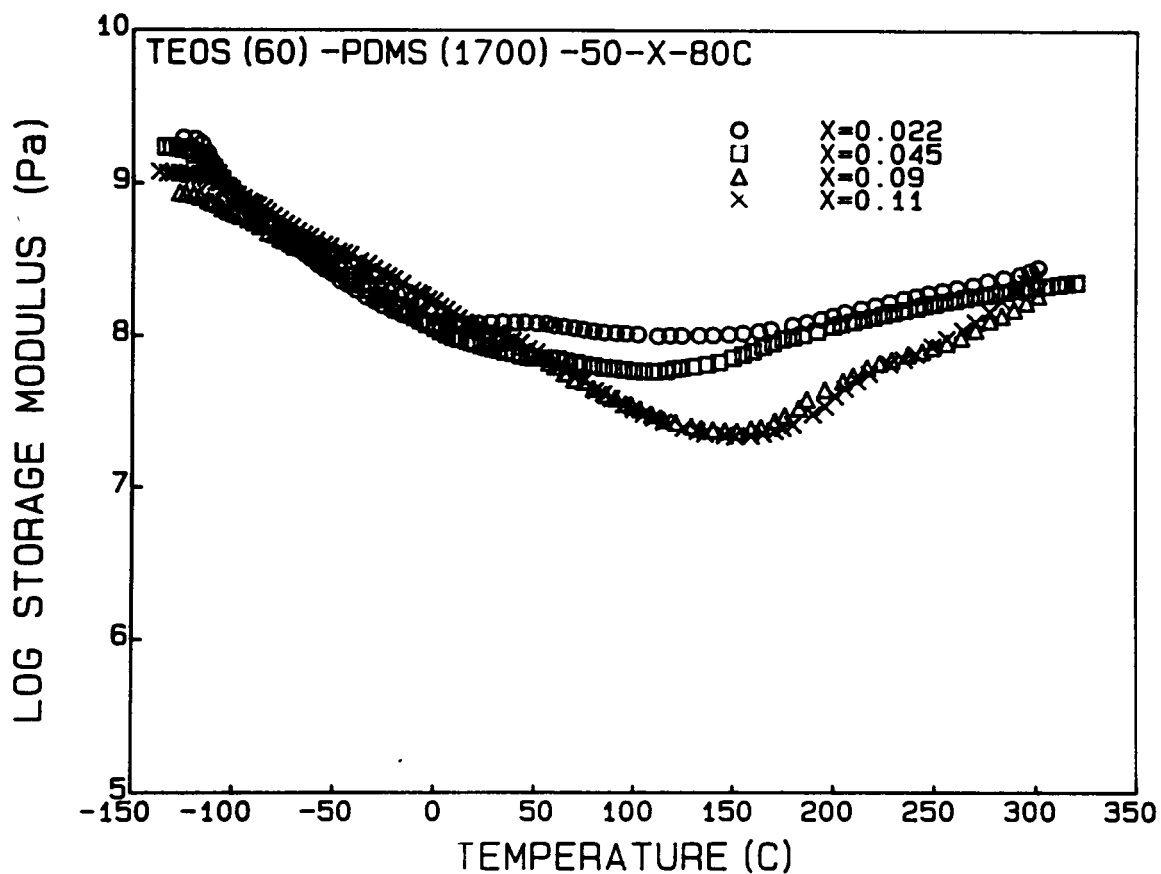
Figure 4.25   Spectra of storage modulus of materials prepared with various acid content, 60 wt% TEOS, 1700 MW PDMS, 50% water content, and 80°C reaction temperature.
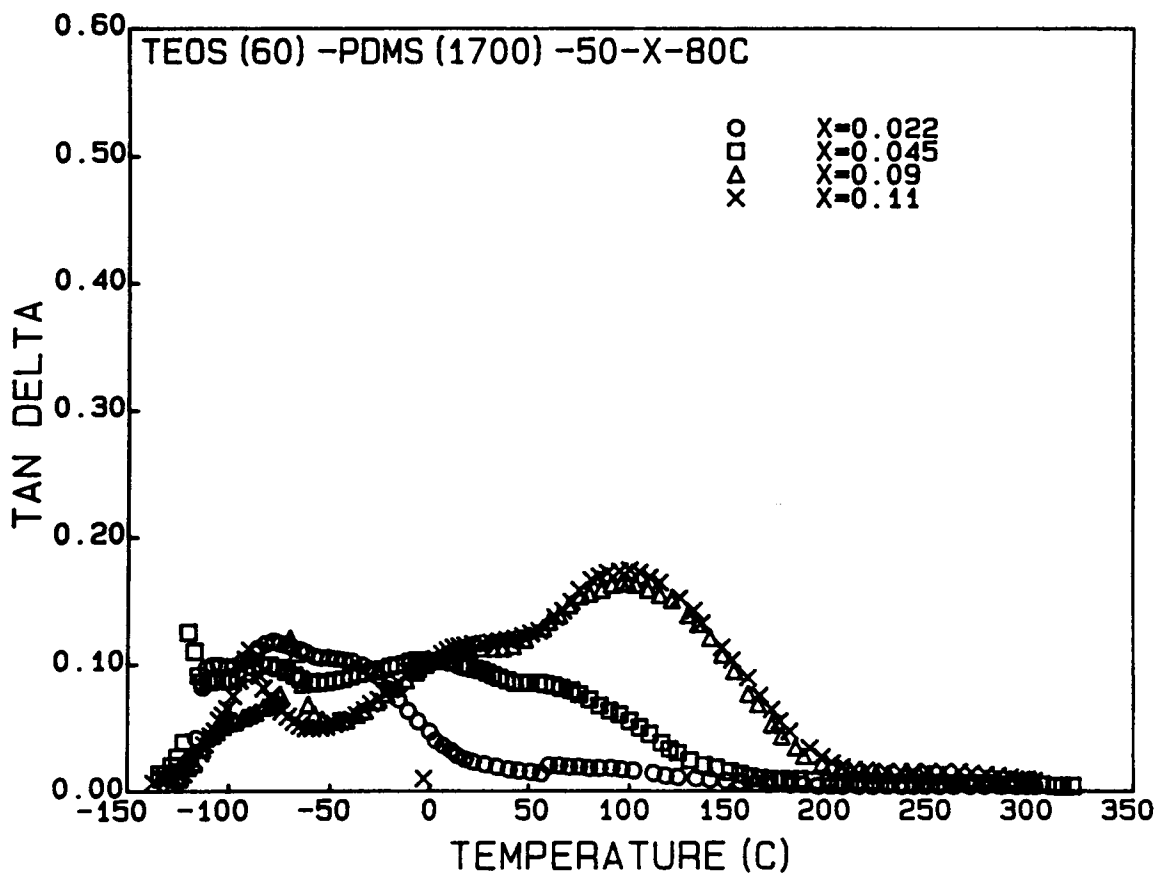
Figure 4.26 Spectra of tanδ of materials prepared with various acid content, 60 wt% TEOS, 1700 MW PDMS, 50% water content, and 80°C reaction temperature.
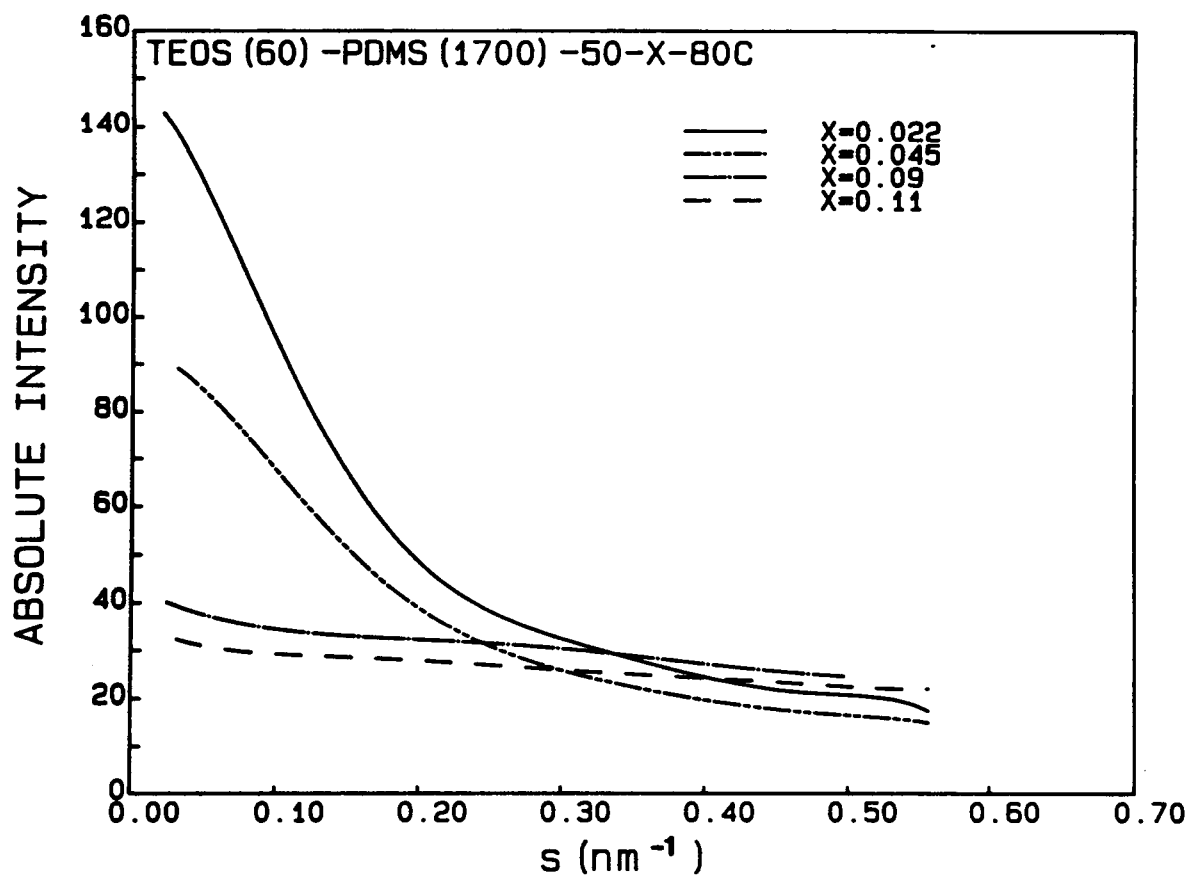
Figure 4.27 SAXS profiles of materials prepared with various acid content, 60 wt% TEOS, 1700 MW PDMS, 50% water content, and 80°C reaction temperature.
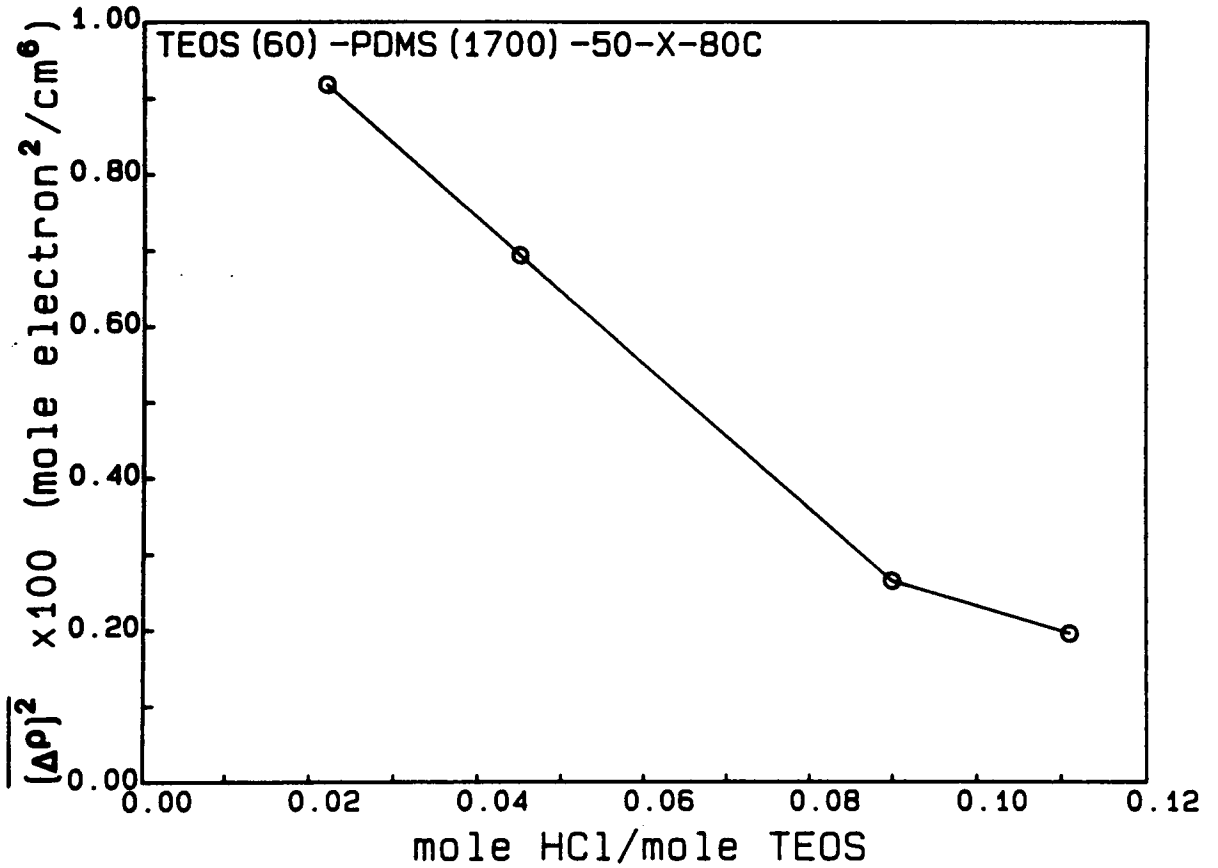
Figure 4.28 Effect of acid content on the mean square electron density fluctuation of materials prepared with 60 wt% TEOS, 1700 MW PDMS, 50% water content, and 80°C reaction temperature.
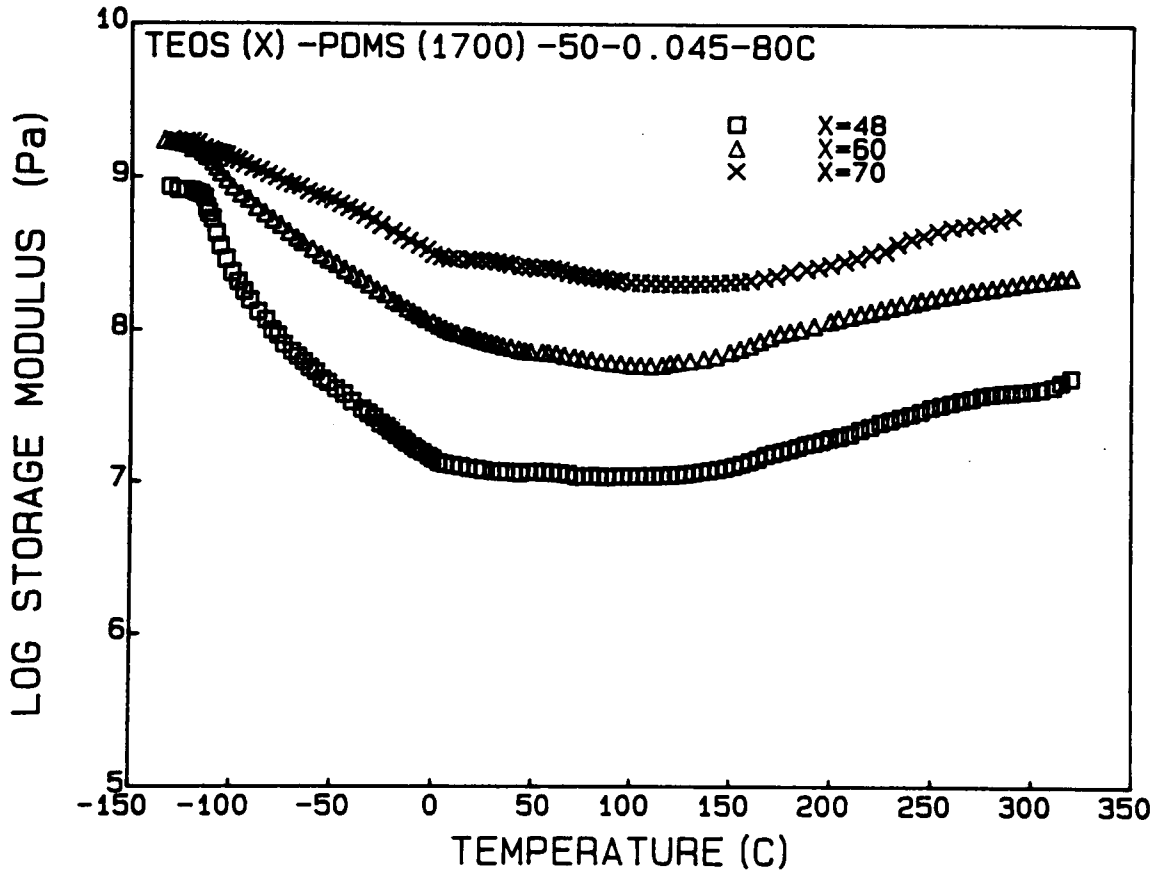
Figure 4.29   Spectra of storage modulus of materials prepared with various TEOS content, 1700 MW PDMS, 50% water content, 0.045 acid content and 80°C reaction temperature.
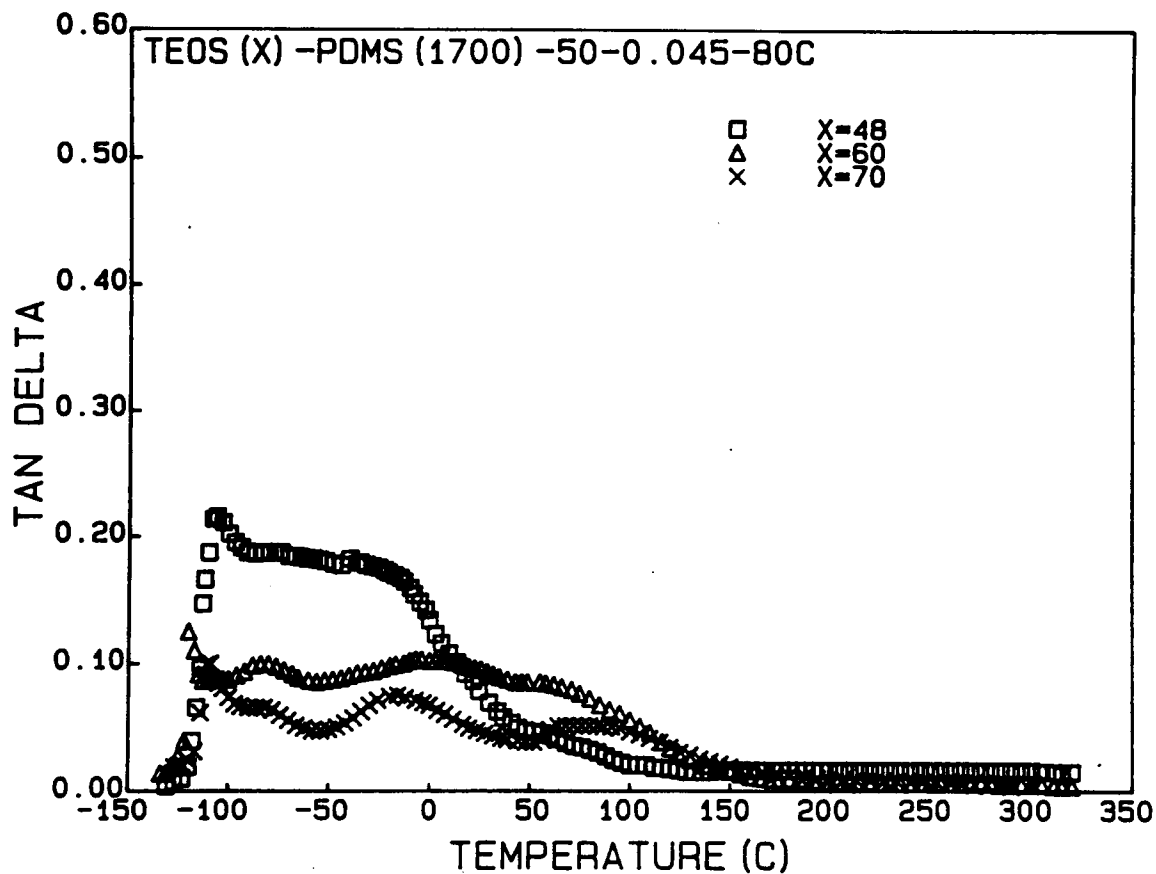
Figure 4.30   Spectra of tanδ of materials prepared with various TEOS content, 1700 MW PDMS, 50% water content, 0.045 acid content and 80°C reaction temperature.
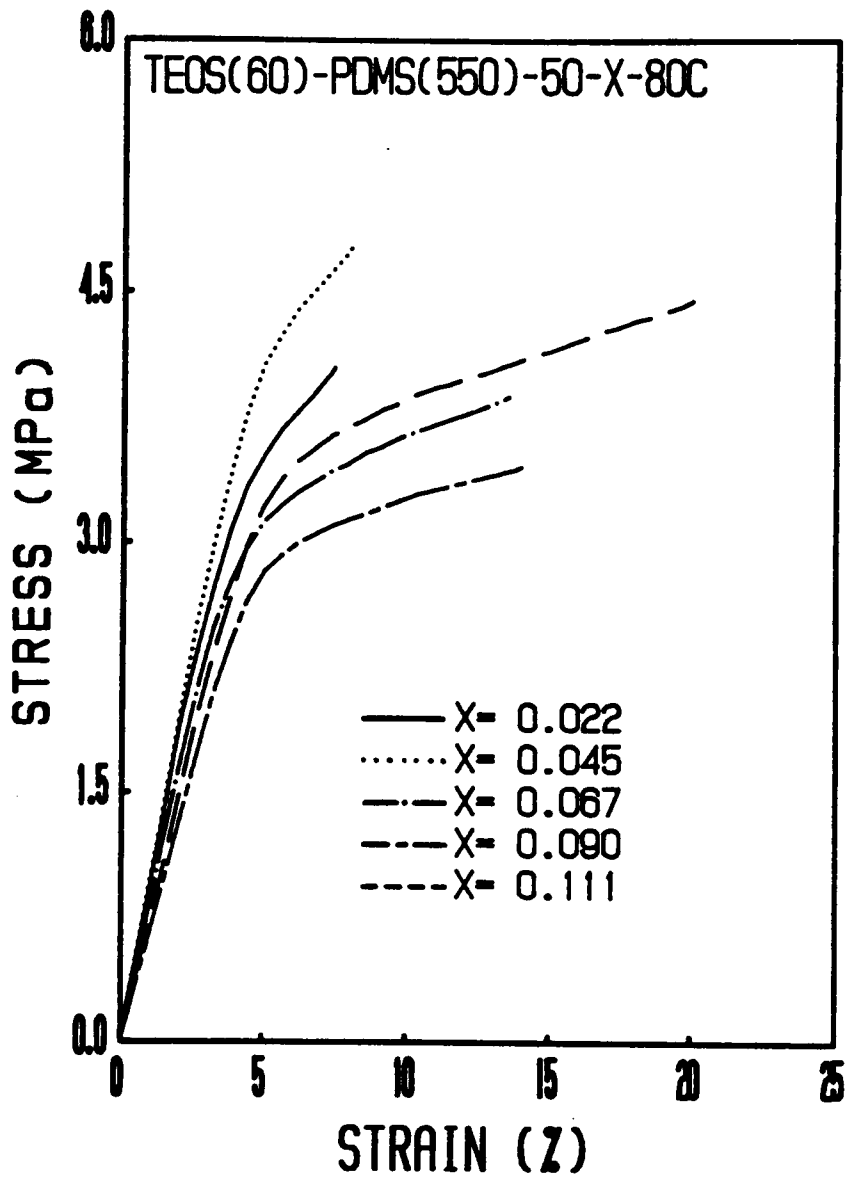
Figure 4.31 Stress-strain behaviors of materials prepared with various acid content, 60 wt% TEOS, 550 MW PDMS, 50% water content, and 80°C reaction temperature.

Figure 4.32 Effect of acid content on the elongation at break of materials prepared with 60 wt% TEOS, 550 MW PDMS, 50% water content, and 80°C reaction temperature.
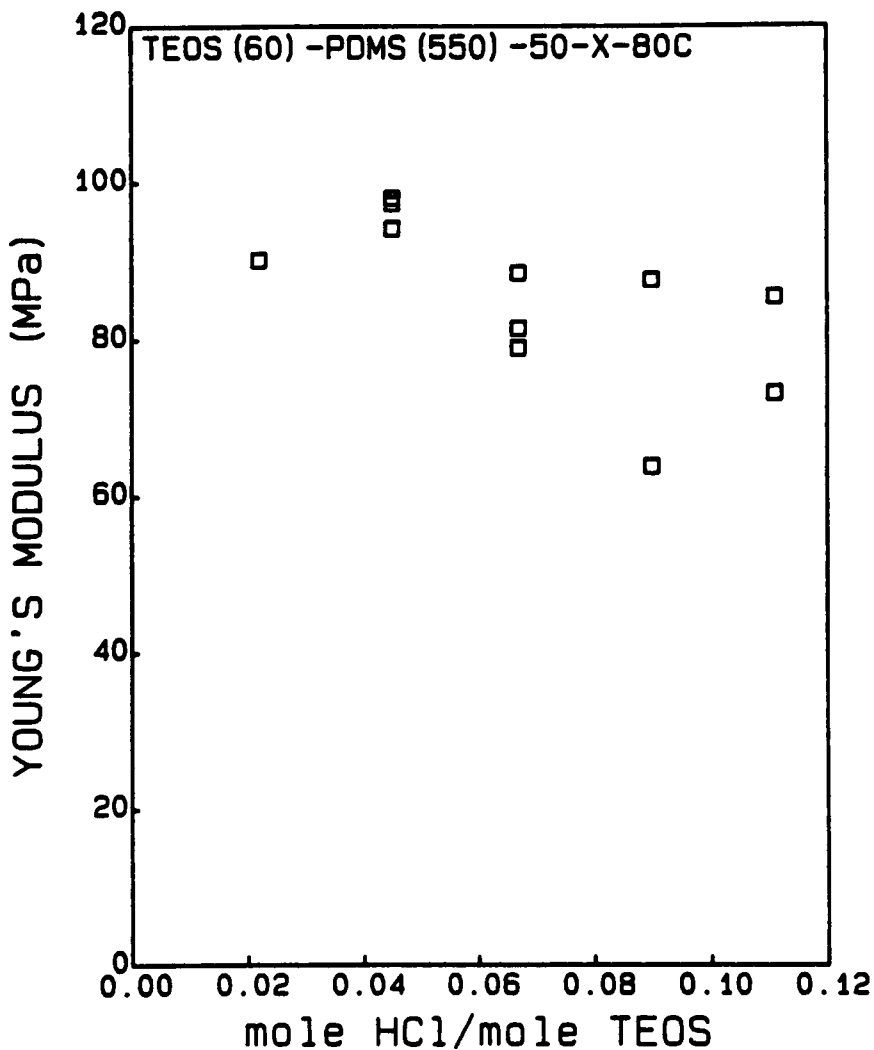
Figure 4.33 Effect of acid content on the Young's modulus of materials prepared with 60 wt% TEOS, 550 MW PDMS, 50% water content, and 80°C reaction temperature.

Figure 4.34 Spectra of storage modulus of materials prepared with various acid content, 60 wt% TEOS, 550 MW PDMS, 50% water content, and 80°C reaction temperature.
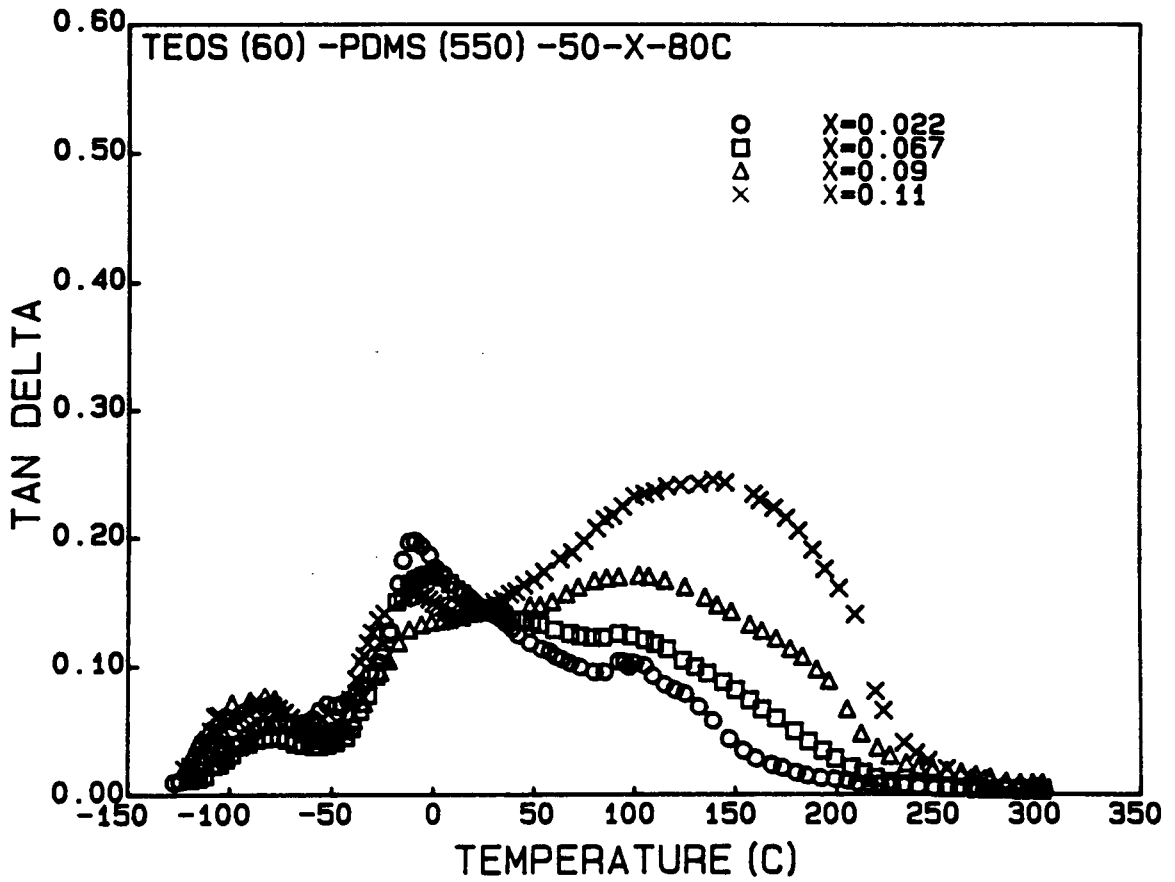
Figure 4.35   Spectra of tanδ of materials prepared with various acid content, 60 wt% TEOS, 550 MW PDMS, 50% water content, and 80°C reaction temperature.
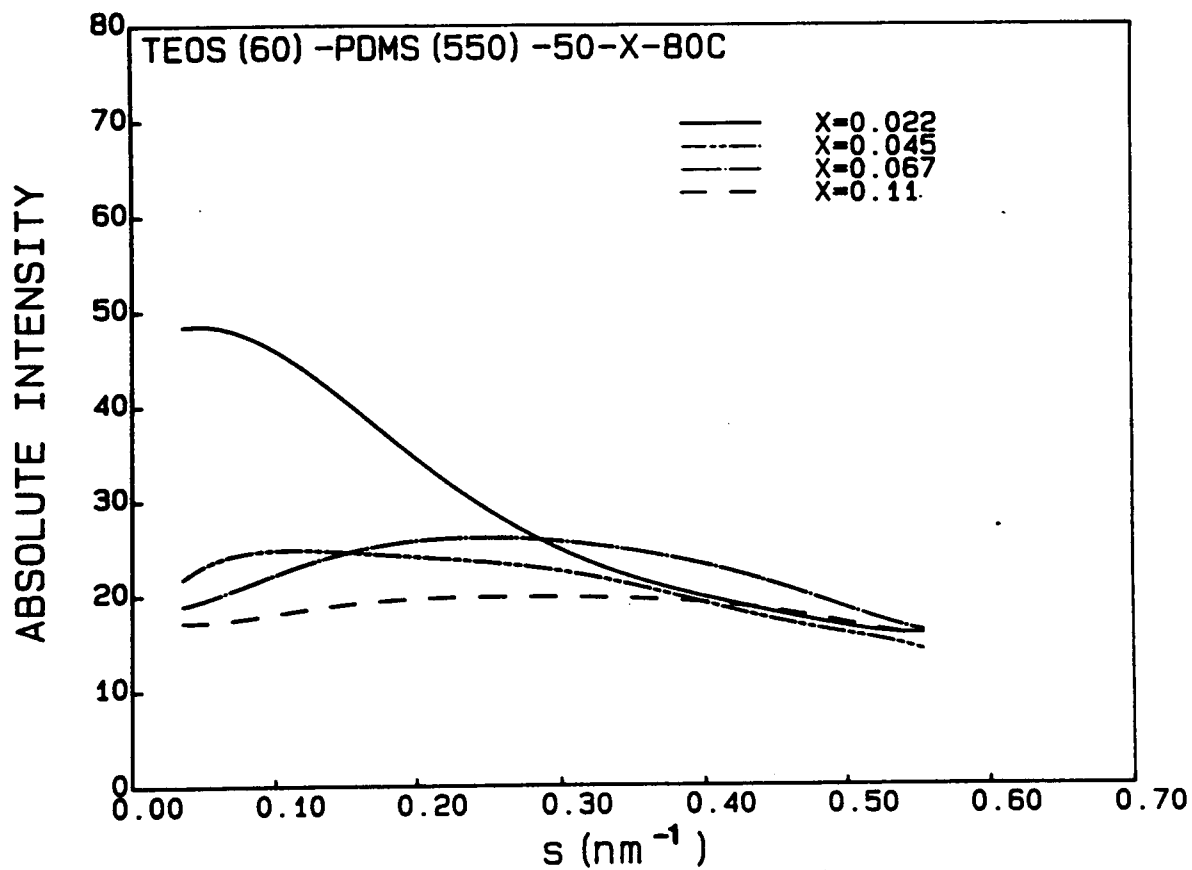
Figure 4.36   SAXS profiles of materials prepared with various acid content, 60 wt% TEOS, 550 MW PDMS, 50% water content, and 80°C reaction temperature.

Figure 4.37 Effect of acid content on the mean square electron density fluctuation of materials prepared with 60 wt% TEOS, 550 MW PDMS, 50% water content, and 80°C reaction temperature.
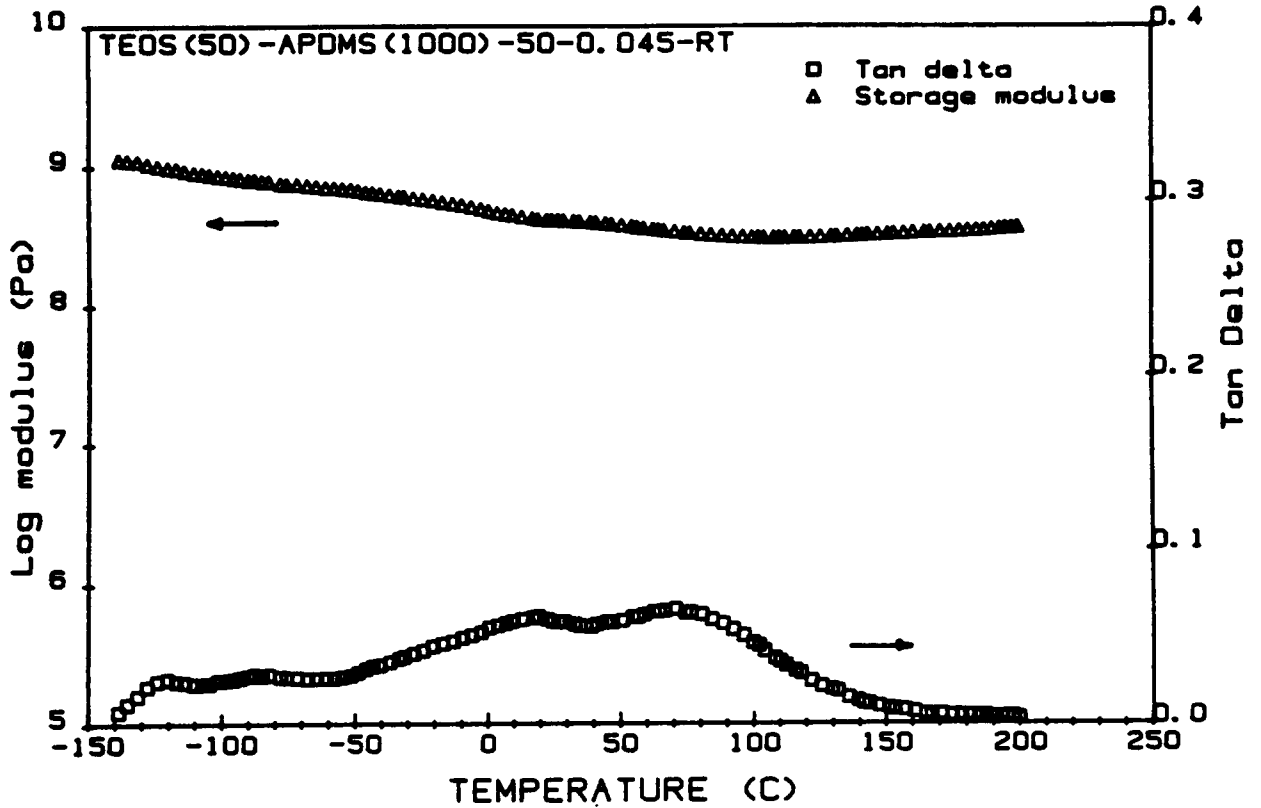
Figure 4.38   Dynamic mechanical spectra of a material prepared with 50 wt% TEOS, 1000 MW triethoxysilane endcapped PDMS, 0.045 acid content, and 50% water content at ambient conditions.
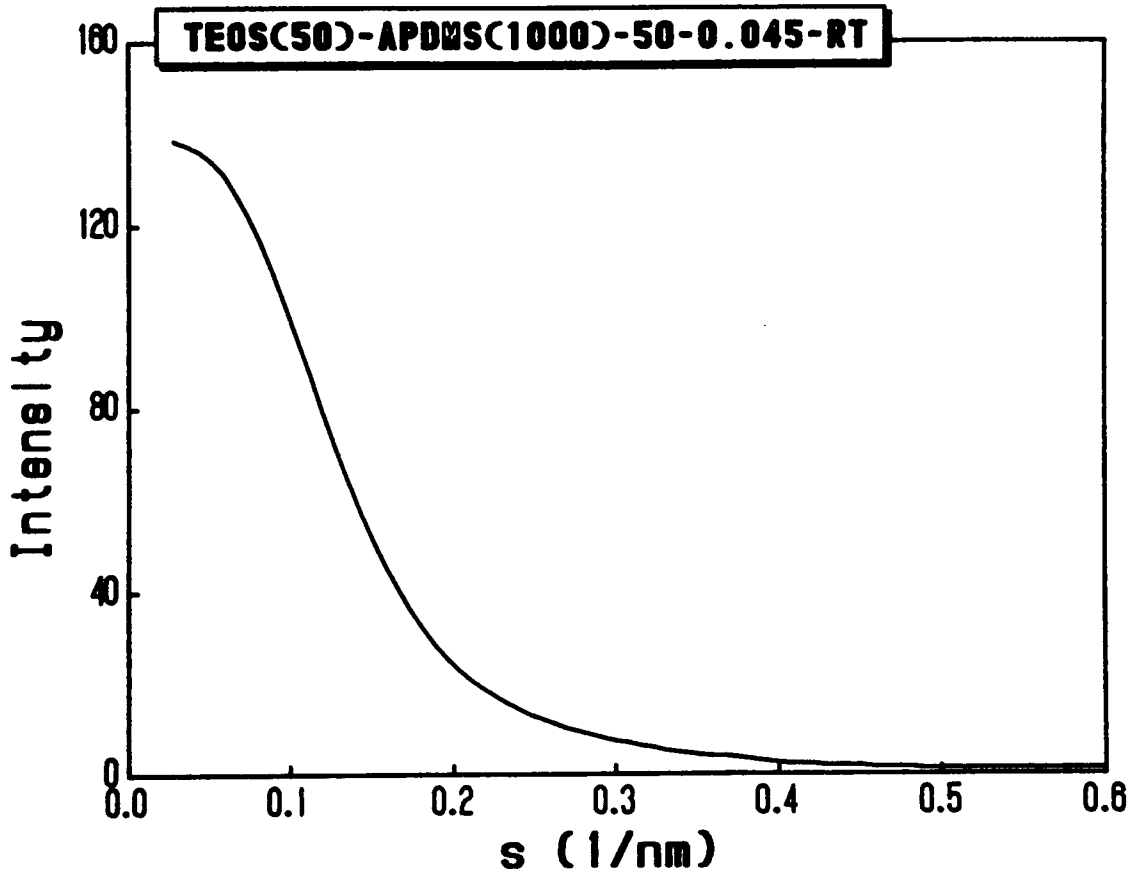
Figure 4.39 The SAXS profile of a material prepared with 50 wt% TEOS, 1000 MW triethoxysilane endcapped PDMS, 0.045 acid content, and 50% water content at ambient conditions.

CHAPTER FIVE

HYBRID SYSTEMS BASED ON TETRAORTHOSILICATES

AND FUNCTIONALIZED POLY(TETRAMETHYLENE OXIDE)

It was demonstrated in the previous chapter that hybrid materials could be prepared by incorporating PDMS with inorganic silicate by a modified sol-gel process. All the final products of these TEOS-PDMS systems were transparent, implying the absence of large scale phase separation. However, some level of non-periodic, microphase separation was suggested in all these materials by the dynamic mechanical experiments. This was attributed to the low functionality and the extremely hydrophobic nature of the silanol terminated PDMS oligomers. However, the degree of oligomeric dispersion was also shown to be dependent on acid content. Unfortunately, the tensile strength of these hybrid materials was not impressive. However, the modulus was relatively high compared to pure PDMS elastomers as was expected. This latter parameter indicated the effect of those incorporated silicates, which caused the stiffness to increase. Several important variables were studied and each one had a significant influence on the final structure and properties of these hybrid materials. Above all, this first attempt has provided considerable insight to this new process.

As discussed in the previous chapter, the choice of PDMS oligomers was based in part upon its partially inorganic nature (i.e., the -Si-O-Si- type of backbone.) It was hoped that this characteristic might not only result in a more compatible system, but also provide higher thermal stability, UV resistance, and other advantages of this relatively stable backbone. With the success of TEOS-PDMS systems, it was then reasonable to investigate some functionalized organic oligomers so that the versatility of this new

process could be expanded. To accomplish this purpose, the organic oligomers must also possess appropriate functional groups to react with the silanols generated by the hydrolysis of silicates. In this study, the functional groups were generated by endcapping PTMO oligomers with triethoxysilanes.

An example of this endcapping reaction was shown and discussed in chapter three (see Fig. 3.3.) As shown by the reaction scheme, a urethane or urea linkage was formed between the oligomer and the endcapping triethoxysilane. This route of generating functional groups had the advantages of a simple reaction procedure with commercially available reactants. However, another very important reason was that it generated oligomers with high functionality (i.e., 6.) As discussed in the last section of the previous chapter (see section 4.5), this high functionality could drastically change the incorporating process and potentially result in good dispersion of the oligomers. Therefore, this endcapping reaction was chosen for all the oligomers in this part of the study. Obviously, this endcapping route is not the only option. Other types of reactions may serve the same purpose or, in some cases, be required for a specific type of oligomer. Although this search for possible routes is beyond the scope of the present study, it should be viewed as a potential area for future research.

From the previous results on the TEOS-PDMS systems, it was found that the tensile strength of these materials was not impressive. This may partially be due to the inherent nature of these PDMS oligomers. It was hoped that this property might be improved by using other types of oligomers. At first, several compounds (including polyethylene glycol, polytetramethylene oxides, and butanediol) were endcapped with the triethoxysilane and "tested" by the sol-gel reaction. A preliminary investigation showed that the materials prepared with endcapped PTMO possessed the most impressive

properties. As a result, all the subsequent studies were carried out using this type of oligomer.

Regarding the inorganic component, TEOS was still used for most of the reactions. However, tetramethoxysilane (TMOS) was used in some cases. As illustrated in the sol-gel reaction scheme, the metal alkoxides have to undergo hydrolysis so that condensation may take place. Therefore, a large fraction of weight is lost in the process. In fact, this is mainly why considerable shrinkage is always observed in these systems. As TMOS is used instead of TEOS, the fraction of weight loss will be lowered considerably. Hence, a smaller shrinkage may be expected. In addition, TMOS has been reported to have a much higher hydrolysis rate than that of TEOS [51,79,80]. Therefore, it was decided to be worthwhile to investigate how the type of silane would influence the final structure and properties of these hybrid materials.

Besides changing the type of oligomers, modification was also made to the reaction procedure of this new system. The first thing to change was the order of addition of the reacting compouunds. In the TEOS-PDMS systems, the mixture of cosolvents, acid, and water was mixed first before adding the reactants (i.e., TEOS and PDMS). Whereas in this TEOS-PTMO system, the silicate and oligomer were mixed thoroughly in the cosolvents first before adding a mixture of acid and water. This change was made due to the following consideration: In the preliminary study, the gelation time for these TEOS-PTMO systems was observed to be very short (usually within a few minutes.) Furthermore, the viscosity of some of high molecular weight PTMO oligomers was much higher than that of PDMS. If the same procedure were used, it would be possible that the system might have gelled before being mixed thoroughly. This could result in a less homogeneous material and nonreproducible properties. Therefore, with the pre-mixing

procedure of TEOS and PTMO, this situation was better avoided. Another difference was in the reaction temperature, which was changed from 80°C to ambient temperature. As observed in the preliminary study, the system would gel almost immediately after the addition of water and acid if 80°C were used. Since a short period of mixing time (usually 20 to 30 seconds) was needed for the solution to become homogeneous after the addition of the acid and water, this fast gelation might result in non-uniform materials. Hence, in order to assure that the system became homogeneous before gelation took place, all the reactions were carried out at ambient conditions so that the reaction rate could be reduced.

The details of this modified reaction procedure for these PTMO containing sol-gel systems was given in chapter three. All the materials prepared in this study were transparent and, without being quantitative, more extendible than the previous TEOS-PTMO systems. Those cast onto polystyrene petri dishes were usually very transparent due to the smooth surfaces of these dishes. However, this method could not be used for the TEOS-PDMS systems because of the cracking usually took place in the drying process. This advantage of the present PTMO containing systems may become important as one considers the processability of these hybrid materials.

Before investigating the effects of reaction variables on the final structure and properties, some expected differences between these PTMO containing and the TEOS-PDMS systems should be pointed out:

1. The solubilities of these two oligomers are quite different. The solubility parameter of PTMO is approximate 9.1 $(cal/cm^3)^{1/2}$, while that of PDMS is 7.3 $(cal/cm^3)^{1/2}$. As discussed earlier, the microphase separation observed in the TEOS-PDMS systems was partially attributed to the extremely hydrophobic nature of the PDMS.

Therefore, as the oligomer becomes more soluble, the formation of an organic rich phase is expected to be suppressed. In other words, the oligomers may be better dispersed.

2. The functional group of the endcapped PTMO oligomers is silicon ethoxide, while it is silanol for the PDMS. Therefore, the self condensation of these PTMO oligomers should become less likely since it also needs to undergo hydrolysis first. This factor also favors the suppression of macrophase separation of the PTMO.

3. The two components are thoroughly mixed before adding the acid and water to initiate the reaction. Therefore, the probability of self condensation should be further decreased due to the large molar ratio of TEOS to PTMO (or TMOS/PTMO).

4. The functionality of these endcapped PTMO oligomers is 6, while that of the silanol terminated PDMS is 2. This increase in functionality has been shown to favor the dispersion of the PDMS oligomers and, therefore, should have the same effect on the present PTMO containing systems. In addition, this high functionality should be the main reason for the much shorter gelation time of these systems compared to that observed earlier.

All of the differences mentioned above indicate that the two components in this new hybrid system should be highly mixed, and the formation of macrophase separation of the PTMO should be greatly suppressed. These points are important to remember as the discussion of experimental results continues.

In this chapter, the effects of six reaction variables on the structure and mechanical properties will be discussed. Among these variables are PTMO molecular weight, TEOS content, water content, type of silicate, type of reaction medium, and aging under

ambient conditions. Furthermore, a schematic model of these PTMO containing systems will be suggested to account for the experimental results from various techniques.

5.1 EFFECT OF PTMO MOLECULAR WEIGHT

In a multicomponent system, the molecular weight of each component is always a crucial factor to be considered. In general, high molecular weight tends to promote phase separation and cause the final product to be less homogeneous. However, whether this is an advantage will depend on the desirable properties of this product. For the TEOS-PDMS hybrid systems, it was demonstrated in the previous chapter that the oligomeric molecular weight could significantly influence the final structure and properties of these hybrid materials. As the oligomeric molecular weight decreased, the dispersion of the oligomers was improved and, thus, resulted in a more homogeneous system. This change in structure caused both the modulus and tensile strength to increase significantly without a loss in the extendibility.

In order to understand the effect of PTMO molecular weight, a series of samples with various PTMO oligomers were prepared. The number average molecular weights of these PTMO oligomers before endcapping ranged from 650 to 2900 g/mole. The silicate used was TEOS, and its initial weight fraction was 60% for all the samples. The water content was 100%, indicating that the exact stoichiometric amount of water for the hydrolysis (both the TEOS and the endcapping silanes) was used. The acid content, which was expressed as the molar ratio of HCl/TEOS, was fixed at 0.04. Shrinkage was observed in all samples, however, only the material made with PTMO(650) showed some cracking. Even so, it was still possible to obtain sufficiently large pieces for all characterization methods. The stiffness of these materials seemed to increase with decreasing PTMO

molecular weight, and the materials seemed to be stronger than the TEOS-PDMS systems. However, conclusive remarks about the mechanical properties could not be made until the stress-strain experiments were carried out.

For the PDMS oligomers used in the previous chapter, the molecular weight was always too low to form any crystalline structure. Therefore, no effort was made to detect the possibility of crystallization. However, the situation is different in the PTMO containing systems. Not only can the oligomer with very low molecular weight crystallize, but its melting point is also in the range of room temperature (ca. 40°C [73].) In fact, two of the higher molecular weight PTMO oligomers (i.e., MW=2000 and 2900) were crystalline in pure form. If the incorporation of these oligomers was not successful, some PTMO crystalline structure might be expected. Therefore, it was important to investigate the possibility of crystallization in these hybrid materials, especially the ones made with PTMO(2000) and PTMO(2900).

Wide angle X-ray scattering (WAXS) is one of most sensitive methods of detecting the existence of crystallinity, and it was therefore used. The results of WAXS experiments on the two samples made with higher molecular weight PTMO are shown in Fig. 5.1. It is noted tha only an amorphous halo is observed, which indicates the absence of any crystalline structure. This observation not only implies that the incorporation was successful, it also indicates that the environmental restrictions on these PTMO chains were significant.

Examples of the stress-strain curves of these PTMO containing samples are shown in Fig. 5.2. For the sample made with PTMO(650), the behavior is similar to a glassy or stiff polymer. An almost linear curve is observed before the sample breaks at a low strain (ca. 7%). As the PTMO molecular weight increases, the elongation at break

increases but the stiffness (modulus) decreases. Compared to the TEOS-PDMS systems discussed earlier, these materials generally show higher values of tensile strength and elongation at break. To further understand the effect of PTMO molecular weight on the mechanical properties, repetitive stress-strain experiments were carried out and the results are listed in Table 4.1. As shown in the second column of this list, the elongation at break increases from 7 to 54% as the PTMO molecular weight increases from 650 to 2900 g/mole. The Young's modulus, however, shows a decreasing trend as the oligomeric molecular weight increases. These trends imply that as the molecular weight of PTMO increases, the resulting material becomes softer and more flexible. One point should be noted, that an inversion in modulus is observed between the two samples made with higher PTMO molecular weight. The reason for this exception is still not clear, however, it does not invalidate the general trend shown by the entire series. Finally, the tensile strength is much more impressive than that of the TEOS-PDMS materials. In particular, a value of 33 MPa is obtained for the sample made with PTMO(2900), which is much higher than the highest strength (ca. 6 MPa.) shown by the PDMS materials.

To provide further information on the structure and properties of these new hybrid systems, dynamic mechanical experiments were carried out. Several spectra of the storage modulus are shown in Fig. 5.3. In spite of some differences in the magnitude, the general behavior is similar among all the samples. At low temperatures, a glassy region with a modulus of ca. 10^9 Pa. is observed. Depending on the PTMO molecular weight, each sample then goes through a broad transition at different temperature ranges after which the modulus decreases to ca. 10^8 Pa.. Finally, an upturn of the modulus is displayed at high temperatures. This behavior of modulus is, in fact, similar in some ways to that shown by the earlier TEOS(60)-PDMS series. However, several important differences should be noted. First, for most of the samples, no decrease in modulus is

observed at temperatures below -50°C. Since the T_g of pure PTMO has been reported to be -84°C [78], this extended glassy region indicates the absence of a pure PTMO rich phase. Secondly, it is quite obvious that the modulus of the sample made with PTMO(650) is considerably higher than the others. This is also observed in the results of the stress-strain experiments. Finally, the inversion of modulus between the two materials with higher PTMO molecular weight is again observed. However, the difference is not very great.

The corresponding tanδ spectra of this series of samples are shown in Fig. 5.4. Compared to the previous TEOS-PDMS systems, the tanδ behavior is very different. Generally speaking, only one broad maximum is observed in every sample and it increases as the PTMO molecular weight decreases. Although a broad maximum is also shown at low temperature (-65°C), its intensity is rather insignificant. This is probably why the storage modulus shows almost no decrease at that temperature. Therefore, it can be concluded that there is very little pure PTMO rich phase exists in these materials. Furthermore, the transition temperatures indicated by the major peaks are considerably higher than the T_g of pure PTMO (-84°C by calorimetry). This implies that the PTMO chains in these systems are quite highly dispersed or mixed with the rigid silicate network, which imposes significant restrictions on the mobility of these oligomers.

As discussed in the beginning of this chapter, changes in functionality, functional groups, and reaction procedure were made in this new hybrid system to improve the incorporation process. In the solution stage, the addition of a pre-mixing process of all the reactants should assist in making the system rather homogeneous before the reaction. Therefore, as the reaction was initiated by adding the acid and water, the possibility of two oligomeric chains to promote "chain extension" should be low due to

the high molar ratio of TEOS/PTMO. As a result, these oligomers should be well dispersed into the silicate network and the formation of PTMO rich regions should be very much suppressed. Furthermore, It has been suggested that in an acidic solution, the reactivity of the ethoxide increases considerably with the number of substituents on the silicon atom [5,51]. Therefore, the ethoxide groups of the triethoxysilane should be much more reactive than those of the TEOS. The result of this is that most of the ethoxide groups on the endcapped oligomers should be hydrolysed to generate silanol groups. Subsequently, as the condensation takes place, these endgroups of the oligomers should be connected into the silicate network through more than one site (as that in silanol terminated PDMS.) This line of deduction leads to the conclusion that both ends of these functionalized oligomers would be incorporated tightly into the network and, therefore, the restrictions caused by endlinking should be significant. This tight connection and the good dispersion mentioned above should cause the T_g of these PTMO oligomers to increase (and likely broaden) considerably, which is exactly what the tanδ spectra showed.

Regarding the increasing and broadening trend of the tanδ maximum with decreasing PTMO molecular weight, two factors need to be considered. First, the endlinking effect is expected to be influenced by the PTMO molecular weight. As discussed in the previous chapter, the type 1 restriction (endlinking) should be more significant as the chain length decreases. In addition, as this chain length decreases, the possibility of "chain encapsulation" by the silicate should be promoted. Assuming that all the oligomeric chains possess a coil like nature, then, the size of the coil (or the radius of gyration) should increase with the molecular weight. Since it is easier to encapsulate a small coil than a large one, the probability of encapsulation should therefore increase as the PTMO molecular weight decrease. For the sample made with PTMO(650), this

encapsulation effect may have become sufficient to cause the material to display a very glassy nature at ambient temperatures. This is why the material made with PTMO(650) shows a very high stiffness and low strain at break.

The second factor to be considered for the effect of PTMO molecular weight on the mechanical response is the initial silane content. Although it has been stated that the initial TEOS content was fixed at 60 wt%, that did not mean the initial silane content was the same. The amount of silane from the endcapping triethoxysilane of the oligomers also has to be taken into account. Doing so leads to the fact that the actual initial silane content should always be higher than that shown by the TEOS weight fraction. The important point here is that this contribution of silane content from the triethoxysilane varies with the PTMO molecular weight; it increases with the number of oligomer chains (i.e., the number of moles). Since the weight fraction of PTMO was fixed at 40 wt%, the higher the PTMO molecular weight was, the lower the amount of triethoxysilane would be. The total molecular weight of each endcapping group is 252 g/mole, and the molecular weight of triethoxysilane is 163 g/mole. Therefore, the actual initial silane content can be estimated. The results of these calculations are shown in Table 5.2. As the PTMO molecular weight increases, the initial silane content decreases. Since the initial silane content is directly related to the final glass content, the material should become stiffer as a lower molecular weight PTMO is used.

To conclude from the two considerations given above, the material should be stiffer and the T_g should increase as the PTMO molecular weight decreases. This is consistent with the experimental data. However, one point should be noted that this effect should be a combination of both factors (i.e., the PTMO molecular weight and actual initial silane content.) As shown by the TEOS-PDMS materials, the T_g increased with the TEOS

content. However, a shift of 20°C in T_g can not be solely attributed to a 3 wt% difference in the initial silane content (compare samples with PTMO(650) and PTMO(1000).) Therefore, the PTMO molecular weight must also be responsible for the increase of T_g. Regarding the effect of TEOS content in this PTMO containing system, it will be addressed later in this chapter.

Up to this point, all the interpretations were given based on the results from measurements of properties. Although some postulations were made about the structure of these hybrid materials, no structural characterization (except WAXS) has yet been reported. In order to provide further structural information, SAXS analysis was preformed on these PTMO containing materials. The resulting profiles of this molecular weight series are shown in Fig. 5.5. The first and most important point to notice is the observation of a maximum or shoulder in every sample, which is distinctly different from what shown by the TEOS-PDMS materials. According to the scattering theory (see section 3.6), the presence of a maximum indicates the existence of a correlation distance. Furthermore, the value of s at which the maximum is observed increases as the PTMO molecular weight decreases. Since the correlation distance can be estimated as the reciprocal of s, this means that such distance decreases as the PTMO molecular weight decreases. Finally, the overall intensity increases with the oligomeric molecular weight. Since this intensity is related to electron density fluctuations, this trend indicates a decreasing homogeneity as the PTMO molecular weight increases.

To further clarify the relationship between the correlation distance and the PTMO molecular weight, the former is plotted against the latter in Fig. 5.6. Also shown in this figure is a curve of the root-mean-square end-to-end distance of PTMO calculated by the Flory-Fox equation given below

$$< r^2 >^{1/2} = a(M_v)^{1/2}$$

where $< r^2 >^{1/2}$ is the root-mean-square end-to-end distance in nm, **a** is an empirical constant that corresponds to theta conditions, and M_v is the average molecular weight obtained from intrinsic viscosity measurements. It has been shown that isopropanol is a theta solvent for PTMO at 44.6°C [81], and the value of **a** for this specific system is 0.093. It is obvious that the PTMO chain may be perturbed in the present reaction, however, the Flory-Fox equation can be used as first order approximation of the end-to-end distance. From Fig. 5.6. one can see that a difference exists between the correlation distance obtained by SAXS and the calculated end-to-end distance. In fact, the magnitude of this difference increases with the PTMO molecular weight.

In order to interpret the above SAXS results, one has to recall the reaction procedure and some of the postulations suggested before. As reported in chapter three, the reaction medium of this modified sol-gel process was a mixture of isopropanol and THF with a volume ratio of 4:1. Although this is different from the theta conditions for PTMO chains, It should still be reasonable to assume a near coil-like behavior for the oligomers due to the large volume fraction of isopropanol. Furthermore, since a pre-mixing period was added to these PTMO containing systems, the oligomers should be rather uniformly dispersed in the solution. Based on these two postulations, a possible situation for the solution before adding the acid and water is suggested and shown in Fig. 5.7. Several important points about this scheme should be noted. First, due to the coil-like nature of the oligomers, most of the TEOS molecules will be in the interstitial space of these coiled chains. As the sol-gel reaction is initiated later on, these TEOS molecules will begin the network-forming process. At first, a linear or lightly branched growth will be the dominant species due to the acidity of the solution. However, the local exhaustion

of silicates will occur with time. Therefore, further growth will have to take place between these linear or branch molecules. As a result, clusters with ring-like structures will most likely be formed. In fact, Raman spectroscopy on these PTMO containing materials did show significant scattering intensity caused by 3- or 4-member rings. However, there should still be some linear or lightly branched silicate molecules between these clusters that form a mixed region with the PTMO oligomers.

The second point to noted about Fig. 5.7 is that the interstitial space of PTMO coils should depend on the size of these coils and the composition of the system. To illustrate this point, a highly simplified drawing is shown in Fig. 5.8. Each circle in the figure represents a coil-like particle, and the shaded area is the interstitial space mentioned above. As shown by this drawing, this interstitial space becomes greater as the particle becomes larger. It should be noted, though, that a hard sphere model is assumed for the polymer particles and the packing is arbitrarily chosen. However, it should help to at least illustrate the point. Since the size of the particle is proportional to the molecular weight, the clusters which are formed in the interstitial space should also become larger as the PTMO molecular weight increases. The compositional effect on this suggested scheme will be discussed in the next section. Finally, due to the good dispersion and the high functionality of the oligomers, each end of these endcapped PTMO should most likely be connected to one of the clusters formed in the interstitial space. In other words, the distance between two interstitial spaces should scale approximately with the end-to-end distance of a PTMO chain.

After the acid and water are added to the system, the sol-gel reaction will be initiated. The solution will eventually gel as an infinite network structure is formed. Following the scheme and arguments mentioned above, the final structure of the hybrid system may

be represented by the model suggested in Fig. 5.9. Several possible regions are illustrated in this model. First is a cluster formed by the growth process of the silicates in the interstitial space of the PTMO molecules. The exact molecular structure of these clusters needs further characterization. Another possible region consists of PTMO chains and partially condensed TEOS species, which should be either linear or lightly branched. The oligomers in this region will be restricted by the interaction between itself and the linear TEOS species and, therefore, should show a higher T_g than pure PTMO. Finally, it is also possible that some of the PTMO chains are surrounded by some highly condensed TEOS species. This will result in the encapsulation of these oligomers and a considerable increase in T_g. With the understanding of these possible structures in this simplified model, the experimental results can now be interpreted.

As mentioned earlier, each end of the endcapped PTMO should be connected to a cluster due to its high functionality and good dispersion. Therefore, the distance between two adjacent clusters should be rather regular and close to the end-to-end distance of the PTMO chain. This regularity results in the observation of a maximum in every SAXS profile which indicates the existence of a correlation distance. As the PTMO molecular weight increases, the end-to-end distance should also increase and so should the correlation distance observed by SAXS. This explains the increasing trend shown in Fig. 5.6. With regard to the difference between the SAXS correlation distance and the calculated end-to-end distance, it can be realized by considering the following:

1. According to SAXS theory, the correlation distance is an estimate of the average length from the center of one region to the center of another region which possesses the same electron density. In this case, it should be the center-to-center distance between two adjacent clusters. Since the size of these clusters is finite, this distance

should always be larger than the end-to-end distance of PTMO. In fact, it should be close to the sum of the average size of the cluster and the PTMO end-to-end distance.

2. As the PTMO molecular weight increases, not only its end-to-end distance increases, the size of the clusters should also increase due to a larger interstitial space (see Fig. 5.8.) Since the correlation distance from SAXS corresponds to the center-to-center distance of adjacent clusters, its increment should be the sum of both increments from PTMO chain length and cluster size. This is mainly the reason for the increasing difference between the SAXS correlation distance and the calculated end-to-end distance (see Fig. 5.6.)

3. Another possible factor is deviation from the Gaussian behavior of the PTMO oligomers. As mentioned earlier, the PTMO chains in these system may well not be at the theta conditions. Therefore, some deviation from the Gaussian behavior is expected. Furthermore, the value of 0.093 (recall Flory-Fox equation) was obtained by using high molecular weight PTMO polymers [81]. Therefore, the extrapolation to low molecular weight oligomers may be questionable. This may be another reason for the low values of the calculated end-to-end distance.

In addition to these interpretations, there are two additional points to mention. First, each maximum in the SAXS profiles is rather broad. This could be caused by (i) the molecular weight distribution of the PTMO oligomers, (ii) the size distribution of the clusters, and (iii) the irregular shape of these clusters. Secondly, as the PTMO molecular increases, less mixing of the two components will take place and result in an increase in the electron density difference between the cluster and the mixed region. Therefore, an increase in the overall scattering intensity is observed as the PTMO molecular weight increases.

To further confirm this suggested model, the mechanical and dynamic mechanical results will have to be reexamined. It has been postulated that mixing will be promoted as the PTMO molecular weight decreases. In addition, one can understand from the model that encapsulation should be more possible as PTMO chain becomes shorter. This results in a higher continuity of the glassy phase (more connectivity between clusters.) and, consequently, an increase in the modulus. Since glassy linkages formed by condensed TEOS are not as extendible as the oligomers, a lower elongation at break should be observed. Regarding the tanδ behavior, a higher mixing should result in higher type 2 restrictions and, thus, a higher T_g.

In general, these PTMO containing hybrid materials show a better defined structure due to several changes made in both the reaction procedure and the nature of the oligomers. The results of stress-strain experiments showed that the elongation at break and tensile strength were considerably higher than those of the TEOS-PDMS systems. Also, both properties showed an increasing trend with the PTMO molecular weight. Dynamic mechanical results showed that the modulus and the T_g increased as the PTMO molecular weight decreased. This has been attributed to the difference in the physico-chemical environment of the oligomers in the silicate network. A correlation distance was observed by SAXS for all samples, and this distance increased with the PTMO molecular weight. After considering all the experimental results, a schematic model has been given in Fig. 5.9 to represent the structure of the final gels. Although this model is an oversimplified representation of the actual structure, it does explain the experimental results quite well. The next step for the further verification of this model will be to study the effect of system composition (TEOS content), as will now be addressed.

5.2 EFFECT OF TEOS CONTENT

As illustrated in the TEOS-PDMS systems, the initial compositions of these hybrid materials were important to the final product (see section 4.3.) According to the experimental results, a change in the TEOS content would affect the gelation time, the mechanical behavior, the glass transition temperature of the oligomers, and the homogeneity of the final materials. However, for the PTMO containing systems, the same argument may not be valid due to the significant change in the procedure and oligomer nature. Therefore, it should be important to investigate this effect on these new hybrid materials. Furthermore, it is also crucial to use these new systems to provide further verification about the schematic model suggested in the previous section.

To study the effect of TEOS content, a series of samples with various loadings of TEOS were prepared. The initial weight fraction of TEOS ranged from 0 to 80 wt%. As stated earlier, this study concentrated on hybrid materials with a TEOS loading higher than 50 wt%. However, several lower TEOS content samples were prepared in this case. The purpose was to obtain a more complete trend of the glass transition behavior and to test the validity of the suggested model. The PTMO molecular weight was 2000 g/mole; the water content was 100%; the acid content was 0.042. The samples made with TEOS contents less than 50 wt% were very rubbery and had sticky surfaces. As the TEOS content increased to 50 and 60 wt%, the samples became stiffer and possessed smooth and glassy surfaces. This visual difference indicated that the product had changed from a "inorganic crosslinked" organic elastomer to a material which possessed certain inorganic glass characteristics. Due to the large weight loss of silicates in the reaction, the organic species was still be the dominant component. However, as the TEOS content increased beyond 70 wt%, the products became very stiff and cracking problem began

to occur. However, compared to the pure inorganic sol-gel glasses, these materials still possessed considerable flexibility. This indicated the toughening effect of the oligomeric component on the glass network. For the sample made with 80 wt% TEOS, the material was too stiff and brittle to cut dogbone samples for the stress-strain experiment. However, It was possible to obtain samples for dynamic mechanical and SAXS analysis.

The results of stress-strain experiments on three high TEOS content samples are given in Table 5.3. As the TEOS content increases from 50 to 60 wt%, the elongation at break remains approximately the same. However, the Young's modulus increases from ca. 14 to 37 MPa., which is somewhat expected since TEOS is the stiff component of the system. Furthermore, the tensile strength also increases with the TEOS content. Interestingly, this increase in tensile strength was also observed in the previous TEOS-PDMS systems as the TEOS content increased from 50 to 60 wt%. One thing to note is that although the data shows an increase in modulus, the values are of the same order of magnitude. However, the mechanical properties change considerably as the TEOS content increases further to 70 wt%. The elongation at break decreases by a factor of two, whereas the Young's modulus increases from ca. 37 to 430 MPa., which is close to that of a glassy polymer. Although an increase in modulus is expected as the TEOS content increases, this drastic increase (by an order of magnitude) indicates that a significant change in structure must have taken place. To further investigate this point, dynamic mechanical experiments were performed on these materials.

The spectra of storage modulus are shown in Fig. 5.10. A wide span of TEOS content, ranging from 10 to 80 wt%, was used so that a better understanding of this effect could be achieved. For the sample made with 10 wt% of TEOS, a distinctly different behavior is observed. After the glassy plateau region at low temperatures, the modulus begins to

decrease, indicating the onset of the glass transition of PTMO. However, after about 20°C, this decreasing tendency is disrupted and the modulus begins to increase with the temperature. After increasing to a maximum, the modulus begins to decrease again but in a steeper trend and, eventually, it reaches another plateau with a magnitude similar to a rubbery polymer. This peculiar behavior of modulus can be attributed to crystallization and melting of the PTMO oligomers, respectively. This will be addressed in detail in later discussion. As the TEOS content increases to 30 wt%, no peculiar behavior is observed and the modulus decreases gradually from a glassy plateau to a rubbery plateau. However, the magnitude of modulus in the rubbery plateau region is slightly higher than that of the 10 wt% TEOS sample. As the TEOS content increases further, the onset of the glass transition (the point where the modulus begins to decrease from the glassy plateau) shifts toward higher temperatures and the modulus also becomes higher. For the sample made with 70 wt% TEOS, the transition is very broad (about 130°C) and the modulus is always higher than 10^8 Pa.. Finally, for the sample made with 80 wt% TEOS, the modulus is ca. 10^9 Pa. and almost shows no decrease in the entire temperature range of the experiment.

The corresponding tanδ spectra of these materials are shown in Fig. 5.11. For the sample with 10 wt% TEOS, a sharp maximum is shown at -68°C and followed by another less intense maximum at -15°C. The first peak is caused by the glass transition of PTMO oligomers, and the second one is attributed to the melting of the PTMO crystals. This appearing of a melting peak in the tanδ spectrum has also been reported before [74]. As the TEOS content increases to 30 wt%, a single maximum is again observed and the temperature is about 30°C higher than that of the 10 wt% TEOS sample. Apparently, no crystallization is observed and this is consistent with the disappearing of the peculiar behavior in the storage modulus. As the TEOS content increases further, the T_g

dispersion continues to shift toward higher temperatures and, meantime, the overall intensity of the spectrum becomes lower. For every sample, a very weak maximum is observed at -130°C. In fact, the magnitude somewhat decreases as the TEOS content increases. This peak has also been reported by previous workers, and they attributed it to the rotational motion of the methylene groups in PTMO [82].

As suggested earlier, the mobility of the oligomers will be considerably restrained as they are combined into the silicate network. These restrictions can be caused by both the endlinking and mixing effects, and they are expected to be higher as the glass content of the system increases. This point has been clearly illustrated by this series of samples. As mentioned in the experimental section, the endcapped PTMO oligomer with a molecular weight of 2000 g/mole will crystallize under ambient conditions. Therefore, it is possible for materials containing this component to show some crystallinity. However, as these oligomers are combined into a system which imposes high restrictions on their mobility, the crystallization is suppressed. As a result, the absence of crystallinity for a crystallizable compound may be used as an indication of higher restrictions on the molecular mobility. As shown in Fig. 5.10, the modulus of the sample made with 10 wt% TEOS increases at low temperatures after the T_g of PTMO. This increase strongly implies a stiffening effect caused by crystallization. This is reasonable since only a small amount of glass component exists in the system, the interactions are not expected to be high. However, as the TEOS content increases to 30 wt%, no crystallization is observed in the spectrum. This may be viewed as an indication of greater environmental restrictions on these oligomeric chains (i.e., type 2 restriction), thus, the crystallization process is suppressed.

Another implication of this result is that, besides the endlinking effect, the mixing effect (type 2 restriction) must be important too. This can be understood by the following argument. Assuming no mixing takes place in these hybrid systems, then, the increase of TEOS content would result in more glassy region. Therefore, the mobility of the oligomers should not be significantly affected, which means that the crystallization observed in the 10 wt% TEOS sample should also be observed in the 30 wt% material. However, this is not the case as shown by the experimental data. Hence, the postulation of type 2 restriction is strongly supported. As the TEOS content increases further, the mixing and interactions become higher and cause the T_g dispersion to broaden and the maximum shifts to even higher temperatures. This change in structure also causes the stiffness of the materials to increase due to higher content of the glass component. One point to note about the shifting of maximum is that as the TEOS content increases by 10 wt%, the maximum shifts approximately 20°C toward higher temperatures. Therefore, the large difference shown in the previous section between samples with various PTMO molecular weights should not be caused only by the small increase of silicate content (see Table 5.2). The molecular weight must also be a crucial factor.

To obtain a clear picture of the change in structure with TEOS content, the model suggested before is again utilized. As shown in Fig. 5.9, part of the TEOS molecules will react with the endgroups of the endcapped PTMO and form clusters. However, the rest of these TEOS molecules will be partially hydrolysed and condensed to form lightly branched or linear species. These species will be mixed with the oligomers and induce some interactions which cause the mobility of PTMO to decrease. As the TEOS content increases, the size of clusters will most likely increase too. Eventually, the glass content becomes so high that the clusters will be connected together and form the continuous phase. This phase inversion will result in a drastic change in the structure and properties.

The first sign of this inversion is the significant change of the Young's modulus, which increases by one order of magnitude as the TEOS content increases from 60 to 70 wt%.

To provide more evidence for the phase inversion and structural changes suggested by the schematic model, SAXS analysis was performed. First, the profiles of samples with up to 60 wt% TEOS are shown in Fig. 5.12. As those shown earlier, a maximum is observed in every sample which indicates the existence of a correlation distance. Furthermore, the scattering angle at which the maximum is observed decreases as the TEOS content increases. This means that the correlation distance indicated by these profiles increases with increasing glass content. These profiles also show that the overall scattering intensity increases as the TEOS content increases. However, a different behavior begins to show as the TEOS content increases beyond 60 wt%, especially in the tail region of the scattering curve. The results of the three samples with higher TEOS contents are shown in Fig. 5.13. In order to illustrate the change in the tail region, the range of the scattering vector under investigation was expanded to the value of 1.0 (instead of 0.6 for the earlier SAXS data.) Obviously, significant changes have taken place with changes in TEOS content. First, the position of the maximum shifts toward the right (higher angles) as the TEOS content increases, indicating a "decrease" in the correlation distance. Secondly, the intensity at small angles decreases while that at higher angle increases with TEOS content. Although the origin for this high angle scattering is still not clear, the shape of the scattering profile does become more similar to that of a pure sol-gel glass as the TEOS content increases.

To understand these SAXS results, the model suggested earlier will be utilized again. According to this oversimplified model, the correlation distance obtained by SAXS should be directly related to the sum of PTMO end-to-end distance and the cluster size.

Therefore, for systems with a fixed PTMO molecular weight, the change in SAXS correlation distance should reflect the change in the cluster size. For a system with very small size of clusters, the SAXS correlation distance should be close to the root-mean-square end-to-end distance of the PTMO oligomers. Hence, one can test the validity of this model by extrapolating the correlation distance to 0% TEOS content and compare this value with the calculated end-to-end distance. To facilitate this comparison, the correlation distance obtained by SAXS is plotted against TEOS content and the result is shown in Fig. 5.14. Also shown in this plot is the end-to-end distance of PTMO(2000) calculated by the Flory-Fox equation. At 0 wt% TEOS, the difference between these two values is 1.3 nm. However, two points should be noted:

1. The SAXS experiments were carried out on a slit camera and, therefore, smearing effects are present. With respect to the position of the maximum, this smearing effect usually causes it to shift toward smaller angles. Therefore, the correlation distance calculated from a smeared profile is always somewhat higher than the actual value.

2. The end-to-end distance calculated by the Flory-Fox equation is for PTMO(2000) without endcapping groups. Therefore, the actual value of this end-to-end distance should be somewhat higher than what obtained from the calculation.

With these two considerations, it is reasonable to say that the experimental value agrees quite well with that from the approximate theoretical calculation which assumes Gaussian behavior. This agreement provides strong support for the validity of the suggested model.

Another important point to note is the increasing trend of the correlation distance with the TEOS content. From the hypothetical solution shown in Fig. 5.7, it is clear that the

PTMO molecules should be further apart as the TEOS content increases (remember that PTMO content decreases at the same time.) This will result in larger interstitial spaces and, therefore, larger clusters in the final gel. This postulation is consistent with the trend shown in Fig. 5.14, which also supports the suggested model. However, all the above conclusions are based on the series of samples containing PTMO(2000). To further verify these remarks, another series of samples with PTMO(650) and various TEOS content were prepared, and the SAXS analysis was again applied on these materials. The result of the correlation distances for various TEOS content is shown in Fig. 5.15. Obviously, the increasing trend is again shown in these samples. However, the most encouraging observation is that the difference between the correlation distance at 0 wt% TEOS and the calculated end-to-end distance is also 1.3 nm. Since the endcapping groups are the same for all PTMO oligomers, these results again provide additional support for the proposed morphological model.

The increasing trend mentioned above reaches a maximum at 60 wt% TEOS and, then, the SAXS behavior begins to change. Although a maximum is still shown, its origin may not be the same as before. As speculated above, the size of clusters will grow with the TEOS content. However, as the glass content increases to a critical value, the clusters become so large that they may connect to form the continuous phase. This phase inversion will obviously invalidate the suggested model, and the correlation distance will no longer represent the inter-cluster distance. Nevertheless, the point at which the SAXS behavior begins to change can serve as an indicative of the onset of a phase inversion. In fact, for this series of PTMO(2000) samples, the phase inversion point observed by SAXS behavior is consistent with that shown by the stress-strain and dynamic mechanical results. In order to further verify this postulation of phase inversion, several other experiments were carried out.

To obtain a first approximation of the TEOS content at which phase inversion may occur, one can calculate the volume fraction of each component in the final gel. The phase inversion point should be close to the composition where the glassy phase becomes the dominant component (i.e., over 50 vol%.) However, due to the complexity of the present system, several assumptions will have to be made before carrying out the calculation:

1. To estimate the PTMO volume fraction, the densities of pure PTMO oligomers are used. Due to the amorphous nature of these incorporated oligomers, this assumption should be close to the actual case. In addition, the final volume fraction of PTMO always refers to that of the pure oligomers only, that is, not including the endcapping groups.

2. To simplify the process of estimating the final glass content, a value of overall degree of reaction is used. This value represents the fraction of ethoxy groups that is hydrolysed and condensed.

3. To estimate the final glass volume fraction, a density of 2.2 g/cc is used for the part that converts into SiO_2 according to the overall degree of reaction. Whereas the density of pure TEOS is used for the rest of the glass phase. Due to the high density used, this assumption may cause the underestimation of final glass volume fraction. However, this should be sufficient for a first approximation.

4. It is also assumed that the PTMO and condensed TEOS are the only two components in the final gel. That is to say, the sum of the two volume fractions will always be equal to unity.

With these assumptions, the final volume fractions of the two components can now be estimated. The result of this calculation for a TEOS-PTMO(2000) system is shown in

Fig. 5.16. In this figure, the calculated final volume fraction of PTMO is plotted against the initial weight fraction of the endcapped PTMO oligomers. To obtain the initial TEOS content, one can simply subtract the PTMO wt% from unity. There are five curves in this plot, and each one represents the calculated final PTMO vol% based on a specified degree of reaction. For a fixed amount of initial PTMO wt%, a higher degree of reaction will result in higher final PTMO vol% and, hence, lower final glass vol%. One point to note is that according to this plot, the vol% of PTMO for a sample made with pure endcapped oligomers (i.e., 100 wt% PTMO loading) is always less than unity. This is because the finite volume of the endcapping groups being considered in the calculation. The usage of this figure can be illustrated by the following example. First, one will have to choose a value for the degree of reaction. According to the previous TEOS-PDMS systems, a value between 70 and 80% should be a reasonable estimation. Therefore, 70% will be used for this example. With this number, one can thus fine the intercept of the vertical line at 30 wt% PTMO and the curve marked 70% degree of reaction. The y-axis value of this intercept will be the estimated final PTMO vol%, which is 56% in this case. If this value is higher than 50%, it means that this material will likely have a dispersed glassy phase and a continuous PTMO matrix. Following the same procedure, one can obtain a value of 43% final PTMO vol% for a system made with 80 wt% TEOS. According to the argument given above, these two observations indicate that a phase inversion is likely to take place between these two initial TEOS content (i.e., 70 and 80 wt%.) However, this transition should most likely occur in a gradual way. Hence, it should not be surprising to observe some indications of this inversion at a TEOS content near 70 wt%.

One thing to bear in mind is that this calculation is simply a first approximation of the final composition of these hybrid materials. Several assumptions have been made, and

some of them may cause certain extent of error. In particular, the assumption of using 2.2 g/cc as the density for the SiO_2 species. Nevertheless, the results of this approach is in parallel with other characterization data. Also, the composition becomes more sensitive to the initial TEOS content as this value increases. For example, the final glass content increases about 13% as the initial TEOS content changes from 70 to 80 wt%, whereas it only increases by 6% as the initial TEOS content changes from 10 to 20 wt%. This observation matches well with the rising trend shown in Fig. 5.14.

To provide further support on the validity of this calculation, a similar plot for the system with PTMO(650) is shown in Fig. 5.17. Following the same procedure described above, one can see that a phase inversion should occur between 50 and 60 wt% of initial TEOS content. This is again in agreement with what the SAXS data given earlier in Fig. 5.15. Furthermore, the dependence of the final composition on the initial TEOS content does not change as much throughout the entire range as that shown in the case of PTMO(2000). This is again consistent with the less pronounced upturn at higher TEOS content shown in the SAXS result (see Fig. 5.15.) From the good agreement observed in both series, not only the calculation is validated, the suggested model is once again further strengthened.

In addition to the theoretical calculation described above, two other experimental techniques were utilized to investigate this effect of TEOS content and the postulation of phase inversion. The first method is the swelling experiment. Two samples of each composition were immersed overnight in THF and the swelling ratio was then calculated based on the average of percent weight gained for these two samples. The results of these swelling experiments are shown in Fig. 5.18. The curve marked "overall" is the swelling ratio calculated based on the total weight of the starting material, which is the swelling

ratio generally used in the literature. While the other curve represents the "normalized" swelling ratio. The procedure of normalization is to divide the overall swelling ratio by the weight fraction of PTMO in the final gel, assuming that only the PTMO containing phase can swell.

For the material made with 10 wt% TEOS, the normalized swelling ratio is ca. 500%, which indicates the crosslinked, elastomeric nature of this sample. As the TEOS content increases to 30 wt%, this ratio decreases to ca. 200%. This large drop in the swelling ratio indicates a considerable decrease in M_c of this network system. This decrease in M_c can be attributed to a more effective crosslinking process and higher environmental restrictions on the oligomers. Recalling the storage modulus spectra, this is also the range where crystallization is completely suppressed. As the TEOS content increases further, the swelling ratio continues to decrease. However, the decreasing tendency is much lower than before. This slow decrease implies that mixing must have been a factor, otherwise, the normalized swelling ratio should be the same. Finally, as the TEOS content reaches 80 wt%, there is almost no swelling shown by the sample. Obviously, the crosslinked TEOS, which can not swell in any medium, has become the dominant component. From this result, one can once again conclude that a phase inversion has occurred between the TEOS contents of 70 and 80 wt%.

Another remark about the swelling experiment is that it can also be used to provide indirect support for the suggested model. As illustrated in the schematic model, the SAXS correlation length corresponds to the distance between two highly condensed TEOS clusters. Therefore, as the materials are swollen with a good solvent, an increase of the SAXS correlation distance should be observed. To verify this point, a sample prepared with 50 wt% TEOS and PTMO(2000) was immersed in THF overnight. The

swollen sample was then sealed between two Mylar films (which would not cause small angle scattering) and studied by SAXS. The result showed that the correlation distance increased from 11 nm (for the unswollen sample) to 12.8 nm, which further supported the simplified model suggested before.

In addition to the swelling experiments, another technique to provide indirect evidence for this significant change in structure was TGA. The results of TGA experiments of some materials in this TEOS content series are shown in Fig. 5.19. All the experiments were carried out under dry air and with a temperature range from 50 to 750°C; the heating rate was 10°C/min. All samples show almost no weight loss up to 250°C, which is relatively high considering the low thermal stability of PTMO. As the temperature increases further, the materials with 50 and 60 wt% TEOS begin to show considerable weight loss and lose almost all the organic species as the temperature reaches 450°C. However, for the 70 wt% TEOS sample, this onset of large weight loss is delayed for about 25°C. Whereas for the sample with 80 wt% TEOS, this onset is not observed until almost 400°C. After this loss of the majority of the organic component, each sample shows a slight decrease of weight until the end of the experiment.

After the point of phase inversion, the inorganic species should become the continuous phase. Therefore, the oligomers in this type of system will most likely be isolated in a highly encapsulated environment, This entrapment may well cause the oligomer to show a noticeable increase in its degradation temperature. According to this argument, the degradation temperature can be used as an indicator for detecting phase inversion. As shown by the TGA results, a small increase in the onset of major weight loss is observed as the TEOS content increases from 60 to 70 wt%. This can be viewed as an early sign for a structural change. As the TEOS content increases further to 80 wt%, an increase

of 70°C of the onset is observed. This drastic increase in the degradation temperature is likely caused by a great change in the environment of the oligomers. Therefore, it can be concluded that a phase inversion must have occurred between 70 and 80 wt% TEOS contents.

Other information that can be obtained from these TGA results is the final weight fraction of PTMO. As shown in Fig. 5.19, a slight decreasing trend is observed at both low and high temperatures for every sample. This small weight loss has also been reported by a previous study on pure silicate sol-gel systems, and it has been attributed to the small amount of water and organic species trapped in the network [9]. Therefore, one can use the same reason for the present systems and attribute only the major weight loss to PTMO. With this assumption, the final PTMO weight fraction can be obtained by measuring the percent weight loss in the period where a drastic weight loss is observed. The resulting PTMO weight fractions are shown in Table 5.4. Although the exact final volume fraction still can not be calculated due to the unknown density of the glassy phase, one can at least have an estimation by assuming that (i) PTMO has a density equal to the pure oligomer, and (ii) the glassy phase has a density between 0.93 (TEOS) and 1.7 (typical gel density). The volume fractions obtained by using both these two extremes are also listed in Table 5.4. Once again, the range for the phase inversion to take place should be between 70 and 80 wt% TEOS.

To summarize this section, the effect of TEOS content has again been shown to be very important to the final structure and properties of these hybrid materials. An increase of TEOS content would result in higher modulus, lower strain at break, higher T_g, and larger SAXS correlation distance. From the mechanical tests, it seemed that the samples made with 60 and 70 wt% TEOS had the highest tensile strength. A similar result was

also observed in the TEOS-PDMS systems. A phase inversion was observed by several experimental techniques, and the ranges where this took place were very consistent between different methods. For the PTMO(2000) systems, it took place between 70 and 80 wt% TEOS. Whereas for the PTMO(650) systems, it was between 60 and 70 wt%. After this phase inversion, the sample became very stiff and showed almost no mechanical loss. Also suggested by the TGA results, this phase inversion caused the thermal stability of PTMO to increase. Finally, the schematic model suggested in the previous section has been further supported. In particular, the SAXS results showed an increase in the cluster size with TEOS content. Also, the correlation distance at 0 wt% TEOS agreed very well with the end-to-end distance calculated by the Flory-Fox equation. This confirmation has strengthened the confidence of utilizing this model for the study of other variables.

5.3 EFFECT OF TYPE OF SILICATE

As discussed earlier, the choice of TEOS for preparing these hybrid materials was based on the commonly recognized fact that the TEOS possesses a relatively low hydrolysis rate. This characteristic facilitates the mixing between components and prevents the problem of preferential precipitation, which often occurs in inorganic multicomponent systems [7,9]. However, this should not exclude the possibility of using other type of silicates, especially tetramethoxysilane (TMOS). Since TMOS is known to have higher reactivity and lower weight loss compared to TEOS, it should be interesting to see how this type of silicate will affect the structure and properties of these hybrid materials. In addition, the result may also be utilized to provide further verification for the suggested model.

In this part of study, the results from two series of materials will be discussed. The first series was prepared with 50 wt% TMOS and various molecular weights of triethoxysilane endcapped PTMO, ranging from 650 to 2900 g/mole (before endcapping). The second one was prepared with PTMO(2000) and various contents of TMOS, ranging from 50 to 80 initial wt%. Basically, these are the same two series discussed in previous sections. However, due to the difference in composition, the final glass content will not be the same for two systems with the same loading but different types of silicates. Hence, systems with the same molar ratio of silicate to PTMO should be used as the basis for comparison. Following this argument, the corresponding TMOS and TEOS contents are calculated and listed in Table 5.5. According to this conversion table, the glass content of a 50 wt% TMOS system is close to a 58 wt% TEOS hybrid system. Therefore, the results of the molecular weight series prepared for this part of study can roughly be compared with those shown in section 5.1.

All the materials prepared using TMOS were transparent, and no visual difference existed between these and the TEOS based materials. The rate of reaction seemed to be higher since it took a very short time for the solution to become viscous. Consequently, the gelation time was also generally shorter than the corresponding TEOS based systems. From the fact that the TMOS has been reported to have the highest reactivity among all the silicon alkoxides [79,80], these observations were somewhat expected. For the first series which used various molecular weights of PTMO, the stiffness tended to be higher as the PTMO molecular weight decreased. As for the second series which various TMOS contents were used, both the stiffness and brittleness apparently increased with the TMOS content. In fact, dogbone samples for the stress-strain experiments were not obtainable for the 70 and 80 wt% materials due to the serious cracking occurred in the cutting procedure. However, it was manageable to obtain large

enough pieces of both materials for SAXS analysis. This was a clear indication of the toughening effect of the organic oligomeric species, considering the very high glass content of the 80 wt% TMOS sample (see Table 5.5.) In the following discussion, the series with various PTMO molecular weights will be addressed followed by those the TMOS series.

From the results of the TEOS based materials, one would expect no crystallization in these systems. However, WAXS experiment was still carried out on a sample prepared with PTMO(2900) for further confirmation. The result is shown in Fig. 5.20. As expected, the WAXS results confirms that no crystalline phase exists in this material. In addition to the amorphous halo, some scattering is observed in the small angle region which has been studied further by SAXS and the result will be shown later. Also shown in this figure is a WAXS pattern for the same material but was strained by 50%. A similar result is displayed, indicating the absence of strain induced crystallization. Of course, both of these two results implies that considerable restriction has been imposed on the oligomers.

The mechanical properties of this molecular weight series are shown in Table 5.6. The elongation at break increases from 8% to 80% as PTMO molecular weight increases from 650 to 2900 g/mole, which is a first indication of the difference in the characteristics of final products. As PTMO molecular weight increases from 650 to 2900 g/mole, the Young's modulus decreases from 490 MPa, which is close to that of glassy materials, to ca. 60 MPa, which is similar to stiff elastomers. However, the materials made with the two higher molecular weight PTMO (2000 and 2900) show almost no difference in modulus. Interestingly, this is similar to what observed in the TEOS containing series (see Table 5.1.) The tensile strength, on the other hand, is roughly constant for these

materials except the one with PTMO(2900), which has a value of 33 MPa. This is again consistent with the previous results of the TEOS based materials, and it can be important when considering practical applications.

To continue probing the effect of PTMO molecular weight on the final properties, dynamic mechanical experiments were performed on these materials. The storage modulus spectra are shown in Fig. 5.21, and the corresponding tanδ spectra are shown in Fig. 5.22. Generally speaking, an increase in PTMO molecular weight will result in a decrease in both the storage modulus and the T_g dispersion. These trends are especially clear as one examines the behavior below ambient temperature. In this region, the decreasing trend of modulus with increasing PTMO molecular weight is clearly shown in Fig. 5.20. Meanwhile, the onset of the tanδ maximum shifts to higher temperatures as the PTMO molecular weight decreases. Both of these effects are similar to those discussed in the TEOS based systems. However, one difference to note is that the temperatures at which the tanδ peaks are observed tend to be lower than those shown in Fig. 5.4 (i.e., the corresponding TEOS based materials.) Furthermore, an inversion between the storage moduli of PTMO(2000) and PTMO(2900) materials is observed for temperatures higher than 20°C. The reason for this inversion in the storage modulus is not clear, however, it was also observed in the TEOS based materials.

In order to have further insight on the structural differences between this series and the earlier one, SAXS analyses were again carried out. The resulting profiles of these TMOS based materials are shown in Fig. 5.23. The first thing to notice is that a maximum is again observed in every sample, and the angular variable s at which this maximum occurs decreases as PTMO molecular weight increases. This means that the correlation distance increases with the PTMO molecular weight, which is the same as that concluded

from the TEOS based materials. However, the magnitudes of these correlation distances are somewhat different from those shown earlier. To better illustrate this point, the SAXS correlation distance of this series is plotted against the PTMO molecular weight and shown in Fig. 5.24. Except the sample with PTMO(650), the TMOS based material always shows a greater distance than the corresponding TEOS based material. These differences in both the SAXS behavior and the T_g indicates that the type of silane used does influence the structure and properties.

Although the type of silicate is different from the TEOS based systems, the reaction procedures are the same as before. There is still a pre-mixing period, and the solution is homogeneous before adding the water and acid. Therefore, one would not expect great difference between these two types of systems except the reactivity. Since the models suggested before does not depend on the reaction rate, they should also be valid for the TMOS based systems. Furthermore, for the results of SAXS correlation distances, the dependence on the PTMO molecular weight is the same as that shown before (compare Fig. 5.24 with 5.6.) In addition, the trends in mechanical properties and dynamic mechanical spectra are also similar to what observed in the TEOS based systems (compare Fig. 5.22 with 5.4.) All of these experimental results also strongly suggest the validity of the simplified models shown earlier. Therefore, those models will still be used in this section to interpret the experimental results.

With this assumption in mind, the SAXS results will be first examined. As mentioned earlier, the correlation distances obtained for this series of samples are always higher than the corresponding TEOS based materials. Since the correlation distance has been postulated as the center-to-center distance between clusters, this difference must have been caused by a change in either the cluster size or the PTMO end-to-end distance.

From the similarity of the two reaction procedures, it seems reasonable to assume that the behavior of the oligomeric chain has not been significantly affected. Hence, the coil-like nature and the end-to-end distance should be approximately the same in both cases. This means that the change in the SAXS correlation distance must have been caused by the difference in the cluster sizes. In other words, the cluster size in a TMOS based system is always higher than that in the corresponding TEOS based system. This result can be explained by the following arguments. Due to the less bulky structure of the TMOS, the number of silicate molecules in the interstitial space mentioned in the solution model should be higher in the TMOS case than that in the TEOS case. This will result in, after the sol-gel reaction, larger size of clusters in the final system which, therefore, causes the SAXS correlation distance to increase.

Another direct result of this increase of silicate molecules in the interstitial spaces is that there will be less such molecules in the mixed region, knowing that the overall molar ratio between the silicate and the PTMO is the same in both cases. Therefore, the restrictions imposed on the PTMO chains by the environment should be lower. This may partially explain the lower T_g observed in the TMOS based systems compared to the corresponding TEOS based materials. Also important is the interaction between the residual or unreacted alkoxide groups and the oligomers. To demonstrate the significance of this interaction, the dynamic mechanical result of a TEOS based sample after soaking in water for a long period of time will be utilized.

In Fig. 5.25, two $\tan\delta$ spectra of materials prepared with 50 wt% TEOS and PTMO(2000) are shown. One is a sample after soaking in water for 27 days, and the other one is without soaking. Two important changes should be noted. First, the overall intensity of this $\tan\delta$ spectrum is reduced after soaking in water, which implies that the

system is tightened by further curing of the glass phase. Secondly, the T_g shown by the first maximum shifts from -5°C to -15°C. Since this glass transition temperature has been postulated as the result of a mixing effect between PTMO and partially condensed TEOS, the lowering indicates some changes in this mixed region. As suggested in the model, it is possible that some of the ethoxy groups are still unreacted in this mixed region. However, after soaking in water for a long time (27 days in this case), these unreacted species should most likely be converted into hydroxyl groups. Since these hydroxyl groups are less bulky than the ethoxy groups, the interactions between them and the oligomers should be lower. This decrease in interactions may result in less restrictions on the mobility of PTMO and, therefore, a decrease in the glass transition temperature.

Returning to the TMOS based systems, there should be some unreacted methoxy groups in the mixed region too. According to the same logic suggested above, the interactions between methoxy groups and PTMO should also be lower than that of the ethoxy groups due to its less bulky structure, Hence, the glass transition temperature should be somewhat lower in these TMOS based systems compared to the corresponding TEOS based systems.

In addition to this series of PTMO molecular weight, a second series of samples with various TMOS contents were also prepared. The mechanical properties are listed in Table. 5.6. Due to the difficulty in cutting dogbone samples, stress-strain results were not obtainable for materials with TMOS content higher than 60 wt%. However, the brittleness of the samples did provide a first indication of a change in the characteristics of the material. By comparing the properties of samples with 50 and 60 wt% TMOS, it is obvious that a higher glass content results in a significant decrease in the elongation

at break and a drastic increase in Young's modulus. From the experience of the TEOS based materials, these changes seem to indicate the beginning of a phase inversion.

To provide further insight on these materials, dynamic mechanical experiments were carried out. The results of samples with TMOS contents ranging from 50 to 70 wt% are shown in Figs. 5.25 and 5.26. Generally speaking, the effect of glass content is similar to what shown by the TEOS based materials. The storage modulus shows systematic increase with the TMOS content, and the tanδ maximum shifts toward higher temperatures as the TMOS content increases. Both of these tendencies indicate that the environmental restrictions on the PTMO oligomers become higher and the final material becomes more glassy. However, the glass transition temperatures shown by the tanδ spectra are still somewhat lower than that of the corresponding TEOS based materials. The SAXS profiles of this series of materials are shown in Fig. 5.28. Similar to what was observed before, the maximum in the profile becomes somewhat diffuse as TMOS content increases to 60 wt% and finally disappears at 70 wt%. Meanwhile, the scattering intensity systematically decreases in small angles while increases in higher angles with the TMOS content. This can again be used as an indicative of a possible phase inversion, and this is consistent with what shown by the mechanical data. Also, this phase inversion point is approximately the same as that concluded from the TEOS based materials.

To summarize, all the models and conclusions suggested from the previous TEOS based materials are still valid for these TMOS based materials. The PTMO molecular weight still shows significant influence on the final structure and properties, and so is the TMOS content. By comparing the tanδ spectra of these TMOS based materials with the corresponding TEOS based materials, the T_g dispersion tends to be lower for the former.

Furthermore, the SAXS results shows that, for a same silicate content, the TMOS based materials show larger correlation distances than the corresponding TEOS based materials. Both of these results have been attributed to the less bulky structure of the methoxy group of the TMOS with respect to the ethoxy group on the TEOS.

5.4 THE EFFECT OF WATER CONTENT

One of the important differences between the previously discussed PDMS oligomers and those of PTMO is the respective solubility parameter values. As mentioned earlier, the solubility parameter of PDMS is 7.3 and that for the PTMO is 9.1 (cal/cm^3). However, the endcapping groups of the functionalized PTMO are very reactive in terms of hydrolysis, which may also affect its solubility. In any event, the result of these factors is that the endcapped PTMO oligomers is not that hydrophobic and, thus, a considerable amount of water can be used for the sol-gel reaction without inducing a large scale phase separation. Although the reaction is expected to be more complete if a large amount of water is added, the structural changes are still unknown. Therefore, there is a need for carrying out a study on the effect of water content on the final structure-property relationships for these hybrid materials.

In this part of study, a series of materials were prepared by adding various amount of water into the reaction, ranging from 25 to 200% exact stoichiometry. The silicate employed was TEOS, the oligomer was functionalized PTMO with a molecular weight of 2000 g/mole, the acid content was 0.042, and the reaction was carried out under ambient conditions. The solutions were clear in all cases, which indicates the absence of visible phase separation. Also, the gels obtained after the drying procedure were always transparent. However, it should be noted that in the case of 200% water content,

the solution was first turbid and became clear after a considerable amount of mixing. Although no viscosity was measured, this specific system tended to be less viscous than the cases of 75 and 100% water contents. In addition, the stiffness of the final material seemed to be lower than all the other cases.

Mechanical properties obtained from stress-strain experiments are listed in Table 5.7. The elongation at break first decreases as the water content increases from 25 to 75%, then, it shows an increasing trend as the water content increases further. On the other hand, the Young's modulus increases to a maximum at 75% water content and then decreases to a minimum at 200% water content. Although these trends are observed, the differences between various samples are not very significant. Regarding the tensile strength, it is approximately constant throughout the entire range of water content under investigation. All of these changes seem to indicate that the sample made with 75% water content possesses a more lighly crosslinked network structure than others, though the difference is not that significant. Also interesting to note is that the sample made with 200% water content is less stiff, more extendible than all other samples (even the 25% water content sample). This is somewhat surprising since one would expect that higher water content should promote the hydrolysis reaction and, hence, result in a denser network. To further verify this trend, dynamic mechanical tests were performed on these materials.

The storage modulus spectra are shown in Fig. 5.29. Generally speaking, the behavior is almost identical in this water series. A plateau with a glassy modulus is observed at very low temperatures, after which the modulus goes through a broad transition and reaches another plateau eventually. Although the magnitude of the modulus at this plateau region is approximately 20 MPa. for all samples, small differences do exist. In

fact, the sample made with 200% water content again shows the lowest modulus among all the samples, which is consistent with the stress-strain experiments. This consistency indicates that this high water content indeed has an effect on the final properties. Regarding the corresponding tanδ behavior of these samples, the results are shown in Fig. 5.30. Once again, all the spectra are rather similar to each other. A high intensity maximum is observed at 0°C and, then, followed by a low intensity shoulder near 40°C. The sample made with 75% water content tends to show the lowest overall intensity, while the 200% sample tends to be the highest. Nevertheless, the difference is not that pronounced. Regarding the corresponding structural difference of this general observation, it will be discussed further in the next section concerning aging effects. The important point to note in the present case is that the positions of these two maxima are the same for different samples. With this observation and the fact that all the mechanical properties are rather similar, it is reasonable to postulate that the structural variation caused by the water content is mild.

To obtain further support on this remark, SAXS analyses were carried out on all the samples. The resulting profiles of this water series are shown in Fig. 5.31. Like all the other profiles shown so far, a broad maximum is observed for all materials. This is a first indication of the validity of the earlier suggested model. Furthermore, the value of s at which the maximum occurs is approximately the same for different samples, which implies that the general structures are very similar. Nevertheless, the overall scattering intensity does show an increasing tendency as the water content increases from 25 to 200%. This increase is important in the forthcoming discussion.

As the water content of the present systems varies, there are two important changes should be considered. The first one is the extent of reaction, which is expected to be

higher as more water is used. The second possible change is the growth process of the silicate network, which has been reported to be more compact as an excess amount of water is present in a sol-gel reaction [18,30,31]. To provide an idea of how the water content affects the extent of reaction, TGA experiments were carried out. Since the initial composition of these materials were the same, a higher degree of reaction should result in less glass content and, therefore, a lower residual fraction of weight. Although the absolute extent of reaction is not obtainable this way, a relative order of all the samples can be determined by comparison.

The results of TGA experiments are shown in Fig. 5.32. Basically, the general behavior of these materials are similar, which means the stability of the organic species is not affected by the water content. The residual weight fractions of both the samples made with 25 and 75% water contents are 28.5, where as the one with 100% water is 27.5. This might at first imply that these three samples have approximately the same glass content and, thus, similar extents of reaction. However, one important to bear in mind is that this does not necessarily mean the structure is identical. For the sample made with 200% water content the residual fraction is 23.5, which is almost 5% lower than all the other samples. Although 5% may not be a great difference, it is quite significant is this case considering the low overall glass content of these materials (i.e., approximately 26%.) Therefore, the extent of reaction in this particular sample should be considerably higher than other cases. With this information and the conclusions reported by other workers on the growth process, one can now try to explain the data.

In the system with 25% water content, the structure of the glassy phase should be rather open due to the unreacted ethoxy groups. As the sample is strained, this more open structure can also provide some level of flexibility. This has been suggested by other

studies on systems with not only the tetrafunctional silicates, but also some di- and trifunctional species [7]. This may explain the lowering of the modulus and the increase of elongation at break compared to the cases of 75% water content. Another result of this more open structure is that the electron density of these region, which related to the physical density, will also decrease. This decrease will cause the electron density difference between the cluster and the mixed region to decrease as well and, therefore, the overall SAXS scattering intensity is lower than other cases.

Regarding the case of 200% water content, the clusters should be rather compact and dense. Keefer [18] has suggested that even though the solution is acidic, the growth of compact structure can still take place if a large excess of water is provided. In addition, the higher degree of reaction from the TGA results also favors this postulation. Since the density of the cluster is directly related to its compactness, it should also increase as an large excess of water is added. This will result in an increase in the electron density difference and, therefore, a rise in the SAXS scattering intensity. One point should be mentioned is that this increase in SAXS intensity has also been observed for an aged sample, which implies a densification effect of the clusters caused by further curing (this aging effect will be discussed in detail in the next section.) However, the increase of SAXS scattering intensity in the aging process always accompanied by an increase in modulus and decrease in extendibility. Whereas for the present case (i.e., 200% water content), a reversed change is observed. This indicates that as more water is added, there is less linear inorganic species between clusters to sustain the strain. As a result, the final properties become closer to the elastomeric component, i.e., lower modulus and higher elongation at break. Although the reason for this effect is not clear, the TGA results do support this postulation.

One important point to mentioned is that although a maximum in stiffness is observed for the 75% water content sample, it does not mean that one can extrapolate this result to other type of systems. For example, the situation is different for a water series prepared with PTMO(650). Instead of showing a decreasing tendency as the water content increases from 100 to 200, these systems display an increase in stiffness with water content. The results of mechanical properties for these materials are shown in Table 5.8. Since the PTMO chains in this case are quite short, encapsulation of these oligomers by the TEOS based species is possible. If so, then the increase of water content will simply provide a greater encapsulation and cause the entire network to be stiffer. With this line of argument, one may expect to see the same trend for a system with PTMO(2000) but of much higher TEOS content. Another important point for PTMO(650) series is that similar to the other water series, the effect of water on the mechanical properties is not that significant.

To summarize, the effect of water content on the systems made with functionalized PTMO is noticeable but not very significant. For the water series in this work, which was prepared with 50 wt% TEOS and PTMO(2000), the material shows a maximum in modulus at 75% water content. Although higher water content (up to 200%) can be used for these systems without inducing large scale phase separation, the modulus of the final material is relatively low. The result from SAXS shows that the correlation distance is approximately the same for all samples, however, the overall scattering intensity increases with water content. This increase can be explained by the formation of more highly compact silicon containing clusters. This postulation is supported by the TGA results.

5.5 EFFECT OF AGING

According to Flory [2], the gel point is where the molecular weight of the system reaches infinity. At this point, the viscosity of the system becomes so high that flowing motion is suppressed. Furthermore, the diffusion rate of molecules will be reduced significantly. However, in spite of this drastic decrease of molecular mobility, further reaction can still take place until the vitrification point is reached. This slow but additional crosslinking of the system with time is termed as "aging". Gillham and coworkers have studied this aging phenomenon extensively by using epoxy systems and a torsional pendulum technique [77], and they usually reported the data by utilizing a time-temperature-transformation (TTT) diagram. A typical example of this diagram is shown in Fig. 5.33. As shown in this figure, a complete reaction can only be achieved if the network is taken to its infinite glass transition temperature. Any temperature lower than that will cause the reaction to be limited by the diffusion and, therefore, leaves unreacted species in the system. If given sufficient time, some of these species may eventually react and result in an aging process.

For a sol-gel system, the situation should be similar to the epoxy materials or related network-forming systems when in the vicinity of T_g. The metal alkoxide will undergo hydrolysis to generate silanol groups, and these reactive groups will then go through a polycondensation reaction to form a 3-dimensional network. After the gel is formed, the system will be very glassy and the diffusion rate of residual unreacted groups will be low. Even though the gel is usually allowed to dry for a long time, organic species are always present. These species may continue to react and, accordingly, result in an aging process. For a pure sol-gel system, this aging effect is not crucial since most of them will undergo a sintering process and consume all the organic species. However, for the modified

sol-gel process suggested in this thesis, this aging effect may be important since the final materials were dried under ambient temperatures.

For the PDMS containing systems, the gelation time was usually in the order of several hours. Although this was shorter than for pure sol-gel systems, the aging effect did not seem to be significant from the property and structural studies. However, for the hybrid systems prepared using triethoxysilane endcapped PTMO, the gelation usually occurred in a few minutes. From the fact that pure sol-gel systems usually take several days to gel, one would expect that there still be considerable amount of unreacted species in these PTMO containing systems due to the short gelation time. Therefore, the aging effect should be quite significant. With aging time, the structure and properties may well be expected to change due to the formation of further crosslinks. Hence, a study on this aging process was carried out so that its effect on the final characteristic of the material could be understood.

To study this aging effect, a series of samples with 60 wt% TEOS and various molecular weights of PTMO were prepared. The water content was 100% and the acid content was 0.042. As usual, all systems gelled within a few minutes under ambient temperatures. After the regular drying procedure, the samples were exposed under ambient conditions so that the aging process can take place. The structure and properties of these materials were monitored with respect to the aging time by the stress-strain, dynamic mechanical experiments and SAXS. It was noticed that the materials tended to become stiffer and less flexible with aging time.

To obtain quantitative result for the observed change of sample stiffness, stress-strain experiments were carried out after samples were aged for different periods. The results of these experiments are listed in Table 5.9. Regardless of the difference in PTMO

molecular weight, all samples show significant changes in both the elongation at break and Young's modulus, but not the tensile strength. For example, the average elongation at break for the material made with PTMO(2900) is 141% when measured 7 days after the reaction. Whereas after 45 days of aging, the average decreases to 53% which is about one third that of the fresh samples. On the other hand, the modulus for this material increases from an average of 26 MPa. after 7 days to 91 MPa. after 45 days of aging. These significant changes indicate that the network may have been tightened considerably after 45 days, and this causes the material to become more glassy and large deformation of the sample becomes more difficult. Although this is only the result from a particular material, all the other three materials in this series show similar behavior. However, one important thing should be noted. Even though the aging process affects the mechanical properties, the trend reported earlier concerning the effect of PTMO molecular weight is still valid. For example, after 7 days of aging, the modulus decreases from 123 MPa. to 26 MPa. as PTMO molecular weight increases from 650 to 2900 g/mole. Whereas after 45 days, the modulus still shows a decreasing trend (from 275 MPa. to 91 MPa.) with increasing PTMO molecular weight. Therefore, as long as the comparison is made between samples aged for a same period of time, the earlier conclusions should still be valid.

To further confirm this increase of modulus with aging and to understand the change in the transition behavior, dynamic mechanical experiments were performed on these materials. To illustrate the changes with aging, the results of the material prepared with PTMO(2900) are shown in Figs. 5.34 & 5.35 as examples. From the results of storage modulus, one can see that its magnitude increases with time, which is consistent with the stress-strain results. Furthermore, the transition range becomes broader with aging time. It is clear that the oligomers become more restricted with time, resulting in a shifting of

T_g toward higher temperatures. However, this change can be observed more clearly by examining the tanδ spectra given shortly. Finally, there is one perplexing point about this result should be mentioned. The storage modulus behavior of the sample aged for 8 days shows a slight increase above 30°C. After reaching a maximum, the modulus decreases again as the temperature increases further. The reason for this increase in modulus is not clear. However, this behavior has been observed in some other samples and it is thermally reversible. More importantly, it is usually not observed in aged samples.

Regarding the tanδ results, two maxima are observed in all three spectra. However, the behavior is somewhat different. The first thing to notice is that the overall intensity of the spectra decreases with time, indicating a tightening effect of the silicate network. This decrease of intensity with time has also been observed for all the PTMO containing systems. Furthermore, from the spectra shown in Fig. 5.35, it seems that the two maxima tend to merge into a broad maximum by shifting part of the first peak toward higher temperatures. This corresponds to the observation in the storage modulus spectra, which shows a broadening effect of the transition range. This behavior is very important in interpreting the results.

To further support the behavior observed in the above example material, the dynamic mechanical spectra for the systems made with PTMO(650) are shown in Figs. 5.36 & 5.37. All the changes mentioned above for the storage modulus are also observed in Fig. 5.36, i.e., an increase of modulus and a broadening of the T_g transition range. In fact, even the perplexing maximum is also observed in the fresh sample (i.e., 7 days.) As to the tanδ behavior, it is even more pronounced in this case that the low temperature maximum tends to shift to higher temperatures with time. In addition to these similarity,

one important reason for showing these spectra is to demonstrate that the effect of PTMO molecular weight is not changed by aging. To compare the corresponding spectra between these two materials, one can see that the modulus increases as PTMO molecular weight decreases regardless of the aging effect. This is consistent with what was concluded from the stress-strain results. Also, the T_g observed in the tanδ spectra increases with decreasing PTMO molecular weight regardless the aging effect. Therefore, the discussion given previously on various effects should not be affected by the aging process.

The structural change during the aging process was also monitored by SAXS. The resulting profiles for the two materials discussed above (i.e., prepared with PTMO(2900) and PTMO(650), respectively) are shown in Figs. 5.38 & 5.39. The important feature to note is that the overall scattering intensity increases with time, which can be a result of either an increasing amount of "scatterers" or an increasing electron density difference between the earlier existing phases. Nevertheless, the value of s at which the maximum is observed does not change with time, which means that the correlation distance is not affected by the aging process. These results are observed in both examples and, in fact, they have also been shown by all the PTMO containing systems. According to these observations, the trend reported before concerning the effect of PTMO molecular weight on the SAXS behavior should still be valid.

To interpret the experimental data on the aging effect, the schematic model suggested earlier for the hybrid gels will again be utilized. After 7 days of aging, the general structure suggested by the model should already be formed. This point is supported by the fact that the SAXS correlation distance has already reached a constant value, and further aging only causes the intensity to increase but not a change in this distance.

However, due to the large amount of unreacted species, some of the clusters may still be rather open. This can be used to explain the appearing of a low temperature tanδ maximum in this series of samples. Also due to these open structures, the materials can be strained further and the modulus is relatively low. As the aging process continues, these unreacted species may form more linkages and tighten or densify those loose structures. Since the high extendibility and low modulus have been partially attributed to these loose structures, its densification should obviously cause the elongation at break to decrease and modulus to increase. In other words, the materials are stiffened by these further crosslinks. Furthermore, as these clusters become denser, the mobility of the oligomers connected to them should be restrained considerably. This results in the shifting of the low temperature maximum toward higher temperatures. Regarding the SAXS behavior, it may be explained by the following argument. Before the aging process, the open structure suggested above will provoke less electron density contrast to the observed X-ray scattering due to their low electron densities. However, after being aged and exposed to humidity, further reaction will cause these structures to densify considerably. In other words, forming more of the clusters shown in the model. As a result, the amount of scatterer should effectively increase and, therefore, cause the SAXS intensity to increase.

To summarize, the aging effect is rather noticeable in these PTMO containing systems. This can be attributed to the short gelation time and the high glass transition temperatures of the oligomers in the final gels. Due to this aging process, the structure and properties of these hybrid gels will change with time. The elongation at break decreases while the modulus increases with aging, meanwhile, the low temperature maximum shown in the tanδ spectra tends to shift toward higher temperatures with time. The structural change has been monitored by SAXS, and the results show that the

scattering intensity increases with time without changing the correlation distance. All of these experimental results of aging effect can be explained by the densification of some loosely connected structures, which was formed due to the fast gelation of these systems. The important point to note is that, in spite of this aging process, all the effects discussed in the previous sections should still be valid as long as the comparison was made between samples with a similar aging history.

5.6 EFFECT OF REACTION MEDIA

According to the survey of previous studies on pure sol-gel systems, alcohol has been a commonly used reaction medium. Depending on the type of silicates, this medium can be either methanol of ethanol. This is mainly because that alcohol is a product of the hydrolysis reaction and, therefore, compatibility will not be a problem if alcohol is also used as the solvent. Nevertheless, there are some concern about the degree of reversed hydrolysis reaction as large amount of alcohol is used [50]. As a result, a few studies have been carried out to test the possibility of using other types of solvents and, if feasible, to study its effect on the final structure and properties [46-50]. As mentioned in the chapter of literature review, formamide has been one of the alternatives [46-48]. The usage of this so called diffusion control chemical additives (DCCA) will affect not only the reaction rate but, more importantly, the drying process so that the production large monoliths have been reported to be possible [46]. In addition, McGrath et al [50] has studied a pure silicate sol-gel system with dimethyl formamide (DMF) and concluded that the hydrolysis rate is higher than systems using alcohol.

In all the systems discussed above, a mixture of isopropanol and THF with a volume ratio of 4:1 was used as the reaction medium so that homogeneous solutions and

transparent samples could be obtained. The isopropanol was chosen because alcohol had been commonly used in pure sol-gel systems as a reaction medium, whereas THF was used for it was a good solvent for the oligomers used. However, this combination is obviously not the only choice. From the fact that other solvents can also be used and will affect the final materials, it seems reasonable to assume that this solvent effect should also be significant for the present hybrid systems. In particular, the mechanical properties and structural information from SAXS should display noticeable changes.

In an attempt to better understand the changes caused by the usage of different reaction media, a series of samples were prepared. In this series, four different solvents were chosen as the basic components of the reaction media. These include isopropanol, THF, formamide, and DMF. All the combinations that being used and the appearance of the final products are listed in Table 5.10. From these results, one can see that some of the reaction media induced large scale phase separation and precipitation of the silicates. For these systems, the final materials were not uniform and possessed very weak strength. In order to obtain a homogeneous solution and a transparent material, alcohol seemed to be the required component for the reaction medium (except the case of pure THF.) All the transparent materials prepared in this part of study seemed to have a higher stiffness than the corresponding previous system (i.e., using a mixture of isopropanol and THF as the medium.), especially the one with a mixture of isopropanol and DMF. The materials prepared with a medium containing formamide were always very stiff and brittle. However, the cracking and warping problem that often observed in some of the high glass content systems was considerably minimized in these formamide containing systems. In this study, only the transparent samples were studied (i.e., the systems with reaction media of pure THF, pure isopropanol, a mixture of 50/50 formamide and isopropanol, and a mixture of 50/50 DMF and isopropanol.)

The mechanical properties of these materials are shown in Table 5.11, and these experiments were carried out 48 days after the reaction. Also listed is a sample made with the regular procedure (i.e., 80/20 mixture of isopropanol and THF) and aged for 45 days, which should provide an approximate comparison with this solvent series. Due to the high brittleness, only one dogbone sample was obtained for the formamide containing system. In general, the materials made with media of pure THF and pure isopropanol show similar properties. The elongation at break is approximately the same, whereas the modulus and tensile strength are slightly higher for the former. More importantly, these properties are comparable to those of a sample made by the regular procedure. For the pure isopropanol system, this similarity is not surprising since the only difference is a small amount of THF. However, for the pure THF system, a significant effect was expected since no alcohol was present in the system, meaning that the extent of reaction might be promoted. Nevertheless, for the system contains formamide or DMF, the properties show significant changes. Compared to the regular sample, the elongation at break decreases and the modulus increases considerably for these two materials. Although there is only one data point for the system with formamide, the low elongation at break should be approximately the actual value due to the brittleness of this material. Anyhow, these noticeable changes in mechanical properties indicate a significant change in the structure.

To provide further insight on these materials, dynamic mechanical experiments were performed. The results of the storage modulus behaviors are shown in Fig. 5.40. First, the trend shown in these results is consistent with what observed in the stress-strain data. Secondly, most of the materials show some sign of aging and an upturn at high temperatures. However, the material contains formamide shows no significant increase at the end which indicates relatively less unreacted species in the system. The

corresponding tanδ spectra are shown in Fig. 5.41. Obviously, there are some changes in the structure as the reaction medium varies. The sample with pure isopropanol shows an almost identical behavior as that made by the regular procedure, which is consistent with what observed in mechanical data. The sample with pure THF shows a similar behavior as the former, however, the overall intensity is somewhat lower. According to the previous section, this implies a tightening effect of the network. This tightening usually causes the modulus to increase as well, which is in line with the stress-strain results. Regarding the system containing DMF, the spectrum is quite different from the two mentioned above. An increase of intensity in the low temperature end of this spectrum is observed, which indicates an increase of rich PTMO phase. Furthermore, the high temperature maximum is shifted slightly to a higher temperature (ca. 50°C.) The peak at 0°C is likely caused by loose clusters and the intensity should decrease with aging (see section 5.5.) The combination of these two changes seem to imply that the addition of DMF causes the phase mixing to reduce and, meanwhile, causes the glass phase to densify even further. Finally, for the system containing formamide, the overall intensity decrease further and the first maximum shifts to a lower temperature (ca. -15°C.) According to previous interpretations (see section 5.3 & 5.5), these data indicate a further completion of the reaction, which may be the reason why there is almost no upturn of modulus at high temperatures.

The structural information is provided by SAXS analysis, and the resulting profiles of these materials are shown in Fig. 5.42. Due to the large difference in intensity, these profiles are presented in two separated charts. The system containing pure isopropanol again shows a similar profile with the sample made by regular procedure, except that the intensity is slightly lower. This similarity means the SAXS correlation distance is basically unchanged and, hence, the general structure is not affected. The intensity is

most likely to increase with aging. For the system containing formamide, the SAXS profile is also similar to the regular sample except a higher intensity. However, the system containing pure THF shows a somewhat larger SAXS correlation distance than the others. Nevertheless, the general shape and overall intensity are comparable to those from other samples. This similarity among all these four profiles strongly implies that the general structure is not significantly changed by using various reaction media, and this is the same conclusion obtained from the dynamic mechanical data. However, the system containing DMF shows an entirely different behavior. First, the overall intensity increases to almost 3 times as high as those shown in (a). Secondly, the maximum now becomes rather narrow although the correlation distance is still approximately the same.

As mentioned earlier, it is not so different between the system with pure isopropanol as reaction medium and the one made with regular procedure. For about 30 ml of solution, the former has no THF while the latter has 2 ml of THF. Therefore, no large changes are expected with such a small difference. However, the system with pure isopropanol does show a sign of less tightness of the final network. This indicates that alcohol indeed can slow down the reaction rate. For the system containing pure THF, it seems that the general structure suggested by the earlier model is still valid. However, due to the good solvent-polymer interaction, the oligomeric chains seem to somewhat extend and causes the correlation distance to increase. Also because of this extension, the modulus becomes slightly higher and tanδ loss becomes lower. Regarding the system containing formamide, less phase mixing would be expected. This is partially due to its high solubility parameter -- 19.2 $(cal/cm^3)^{1/2}$, which results in a less homogeneous system. This argument is supported by the fact that a non-uniform, precipitated material was obtained as pure formamide was used as the solvent. Furthermore, according to the previous results on pure sol-gel process, formamide tends to generate compact,

particulate structure. This should reduce the possibility of mixing and enhance the extent of reaction. As a result, higher modulus and a lower tanδ is observed. However, due to the tightness of the silicate network, the extendibility decreases and the material becomes more brittle. As to the behavior of DMF containing system, the exact reason for the presence of PTMO rich phase is still not clear. It may somehow be related to the higher hydrolysis rate of this system. Nevertheless, materials produce this way does show a considerably higher modulus and relatively high tensile strength.

To summarize, the addition of formamide or DMF to the reaction can significantly change the structure and properties of the final products. The formamide containing system has the advantage of minimum warping and cracking problems, however, the brittleness is high. Whereas for the DMF containing systems, both the modulus and tensile strength are superior to the others. With more understanding of the actual structure, this may be a promising route to produce materials for practical applications.

Table 5.1   Mechanical properties of materials prepared with 60 wt% TEOS and various   molecular   weights   of   PTMO   ---   a   series   of TEOS(60)-PTMO(X)-100-0.04-RT.

PTMO MW	elongation at break (%)	ultimate strength (MPa)	Young's modulus (MPa)
650	6	14	252
	8	15	268
			305
1000	22	15	141
	21	15	136
			153
2000	35	19	74
	40	16	57
			72
2900	52	34	100
	54	24	69
			106

Table 5.2   The actual silane content of materials prepared with 60 wt% initial TEOS content and various molecular weights of PTMO --- a series of TEOS(60)-PTMO(X)-100-0.04-RT.

PTMO MW	actual silane content (wt%)
650	71
1000	69
2000	65
2900	64

Table 5.3 Mechanical properties of materials prepared with PTMO(2000) and various TEOS contents --- a series of TEOS(X)-PTMO(2000)-100-0.04-RT.

initial TEOS content (wt%)	elongation at break (%)	ultimate strength (MPa)	Young's modulus (MPa)
50	81	10	15
	73	11	14
60	91	33	35
	79	29	39
70	30	19	405
	23	33	431

Table 5.4   Final weight and volume fractions of PTMO estimated from TGA results of materials prepared with PTMO(2000) and various TEOS contents --- a series of TEOS(X)-PTMO(2000)-100-0.04-RT.

initial TEOS content (wt%)	estimation of final PTMO wt%	estimation of final PTMO vol%	
		$\rho(SiO_2) = 0.93$ g/cc	$\rho(SiO_2) = 1.7$ g/cc
50	63	62	75
60	58	57	71
70	48	47	62
80	34	33	48

Table 5.5   The TMOS content and its corresponding TEOS content based on the same molar ratio of silane to PTMO

TMOS content (wt%)	TEOS content (wt%)
50	58
60	67
70	76
80	85

Table 5.6   Mechanical properties of TMOS based hybrid materials --- a series of TMOS(X)-PTMO(Y)-100-0.04-RT.

TMOS content	PTMO M.W.	elongation at break (%)	ultimate strength (MPa)	Young's modulus (MPa)
50	650	9	18	490
		8	17	451
	1000	28	14	102
		22	13	113
				125
	2000	34	12	58
		49	18	52
		43	18	65
	2900	83	33	66
		73	27	70
60	2000	11	20	287
				277
				305

Table 5.7   Mechanical properties of materials prepared with 50 wt% TEOS, PTMO(2000), and various water contents --- a series of TEOS(50)-PTMO(2000)-X-0.04-RT.

water content (%)	elongation at break (%)	ultimate strength (MPa)	Young's modulus (MPa)
25	74	11	17
	57	11	18
			17
75	46	10	24
	54	13	26
100	81	10	15
	73	11	14
200	91	12	12
	102	16	11

Table 5.8 Mechanical properties of materials prepared with 50 wt% TEOS, PTMO(650) and various water contents --- a series of TEOS(50)-PTMO(650)-X-0.04-RT.

water content (%)	elongation at break (%)	ultimate strength (MPa)	Young's modulus (MPa)
50	81	10	15
	73	11	14
60	91	33	35
	79	29	39
70	30	19	405
	23	33	431

Table 5.9 Effect of aging on the mechanical properties of materials prepared with 60 wt% TEOS and various PTMO molecular weight --- a series of TEOS(60)-PTMO(X)-100-0.04-RT.

PTMO M.W.	days of aging	elongation at break (%)	ultimate strength (MPa)	Young's modulus (MPa)
650	7			141
				107
	15	46	14	127
		59	23	147
	21	30	14	215
		23	18	199
	45	6	14	252
		8	15	268
1000	7	28	21	128
		46	24	77
		45	39	75
	15	25	17	119
		27	18	126
	21	27	15	103
		15	14	147
		19	14	143
	45	22	15	141
		21	15	136
2000	7	127	27	18
		110	23	20
	15	79	24	31
		56	12	25
		70	18	32
	21	40	9	32
		49	10	30
		51	15	38
	45	35	19	74
		40	16	57
2900	7	112	27	25
		183	29	27
		127	30	23
	15	90	30	48
		102	24	24
		111	23	25
	21	63	27	53
		57	18	42
		94	23	35
	45	52	34	100
		54	24	69

Table 5.10 Charasteristics of materials prepared with 60 wt% TEOS, PTMO(2000), 100% water content, and various reaction media

solvent 1	solvent 2	vol. ratio	characteristic
isopropanol			transparent
THF			transparent
formamide			non-uniform, precipitated
DMF			non-uniform, precipitated
THF	formamide	50/50	non-uniform, precipitated
THF	DMF	50/50	non-uniform, precipitated
isopropanol	formamide	50/50	transparent
isopropanol	DMF	50/50	transparent

Table 5.11   Mechanical properties of materials prepared with 60 wt% TEOS, PTMO(2000), 100% water content, and various reaction media.

reaction medium	elongation at break (%)	ultimate strength (MPa)	Young's modulus (MPa)
THF	36	24	86
	39	25	57
	32	17	78
isopropanol	39	17	58
	31	14	56
			51
isop./formamide	6	9	148
isopropanol/DMF	17	31	253
	13	23	234
	9	15	216
isopropanol/THF	35	19	74
(4/1 regular)	40	16	57
			72
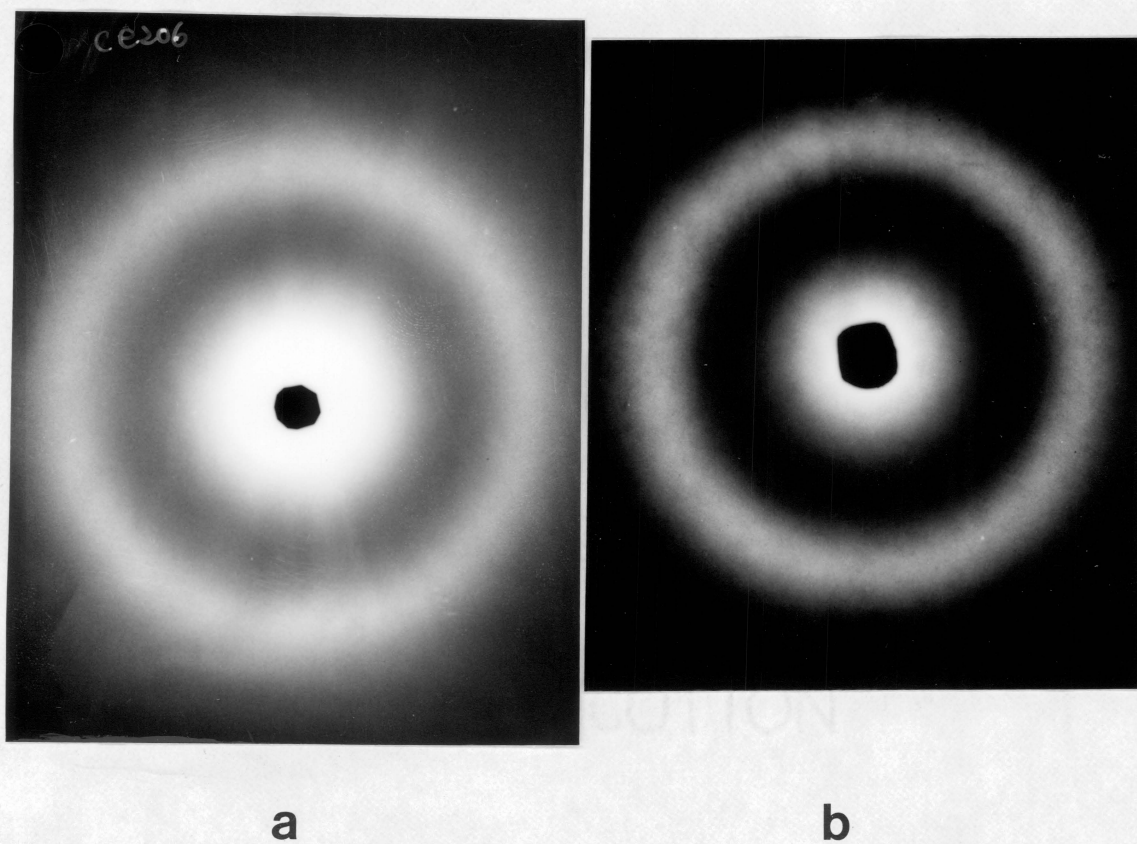
Figure 5.1 WAXD patterns of two samples prepared with 60 wt% TEOS and (a) PTMO(2000) and (b) PTMO(2900), respectively.
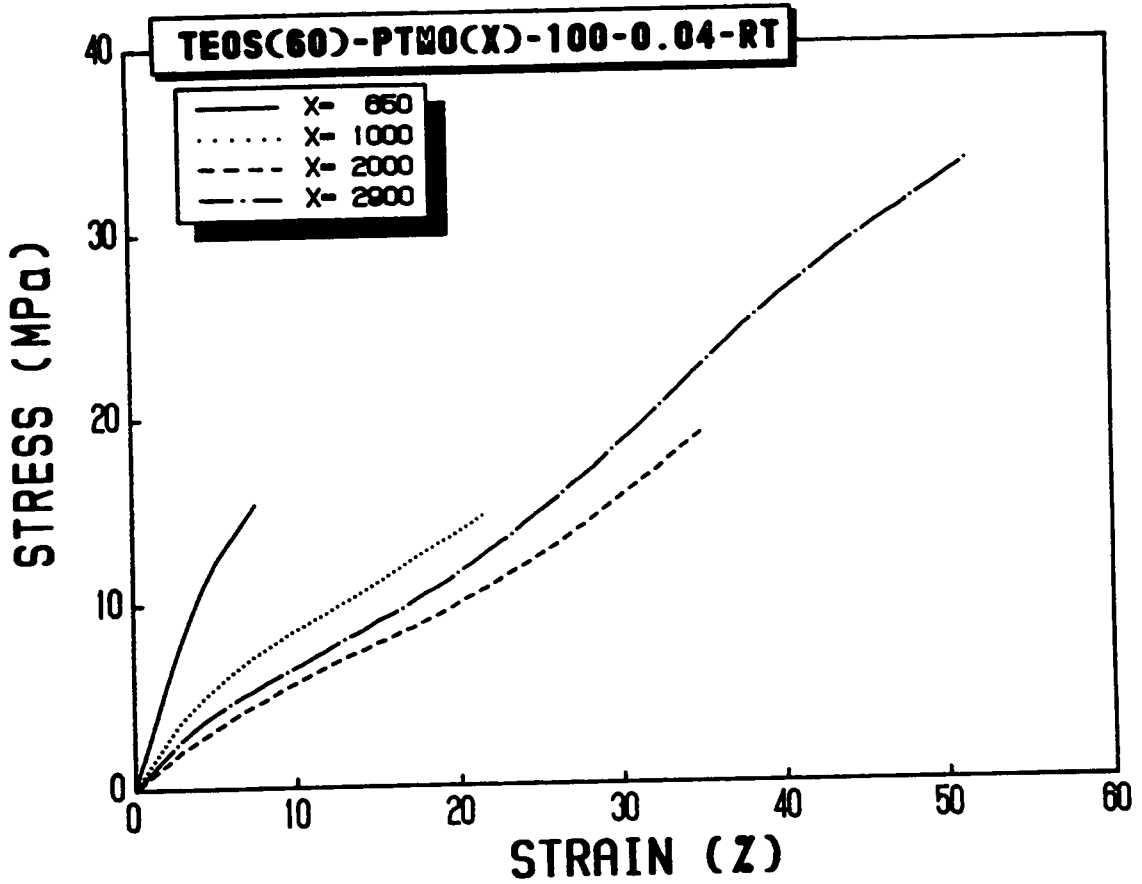
Figure 5.2 Stress-strain behaviors of materials prepared with 60 wt% TEOS and various molecular weights of PTMO.
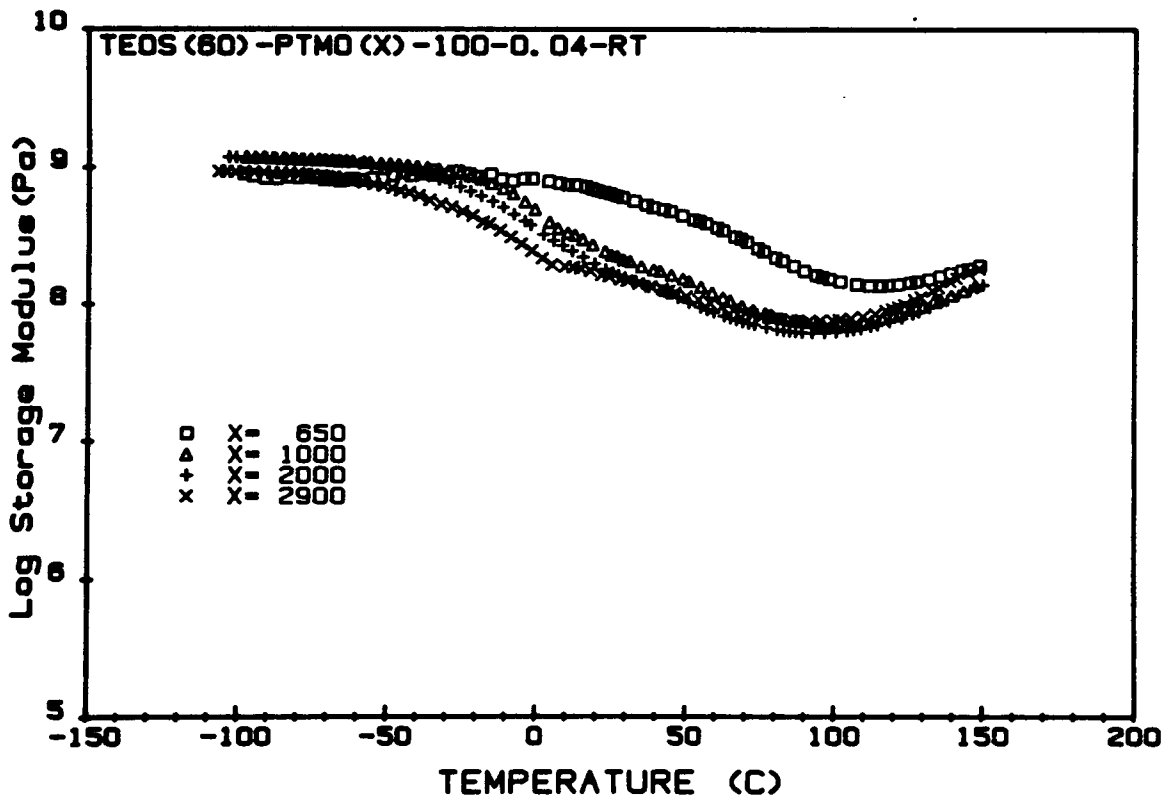
Figure 5.3 Spectra of storage modulus of materials prepared with 60 wt% TEOS and various molecular weights of PTMO.
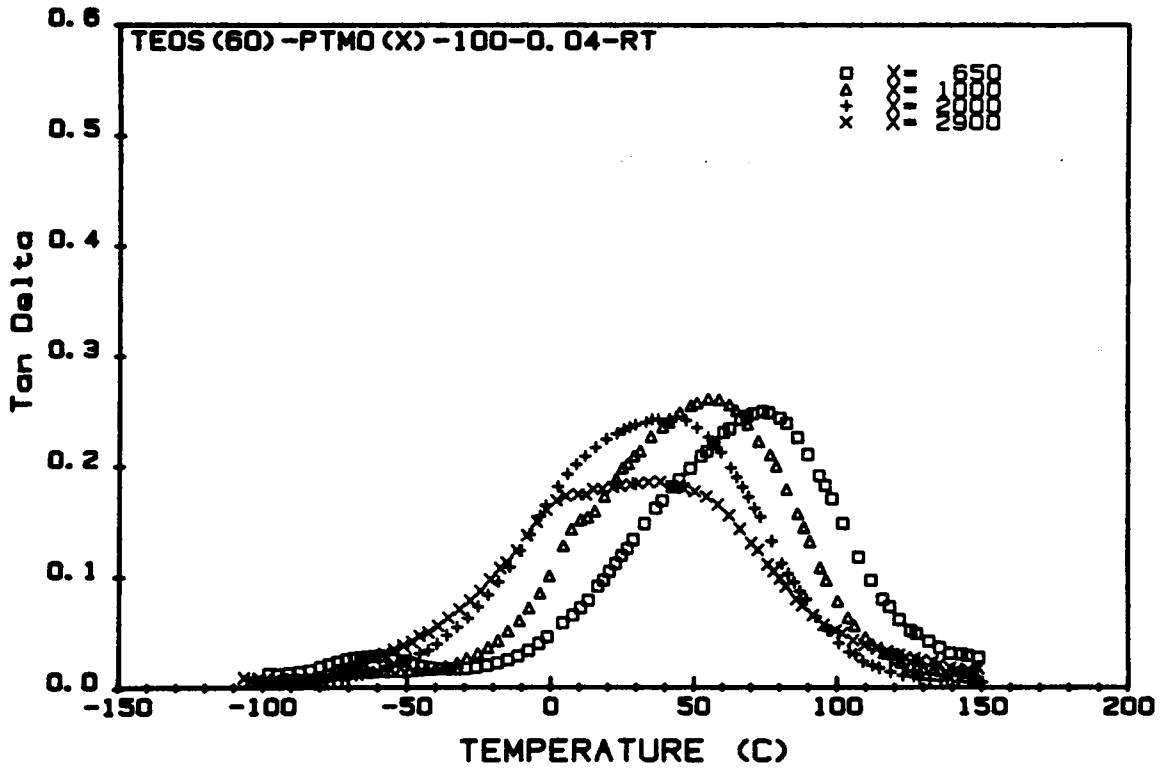
Figure 5.4   Spectra of tanδ of materials prepared with 60 wt% TEOS and various molecular weights of PTMO.
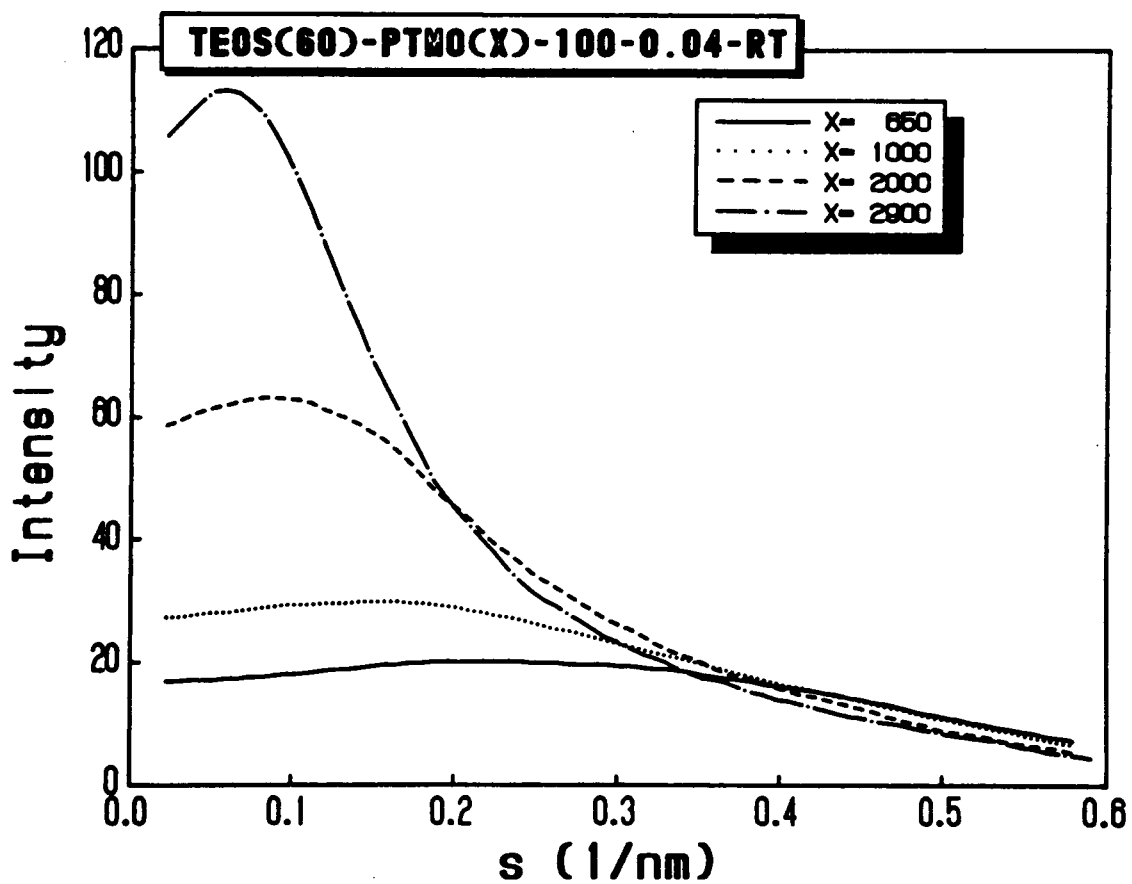
Figure 5.5 SAXS profiles of materials prepared with 60 wt% TEOS and various molecular weights of PTMO.
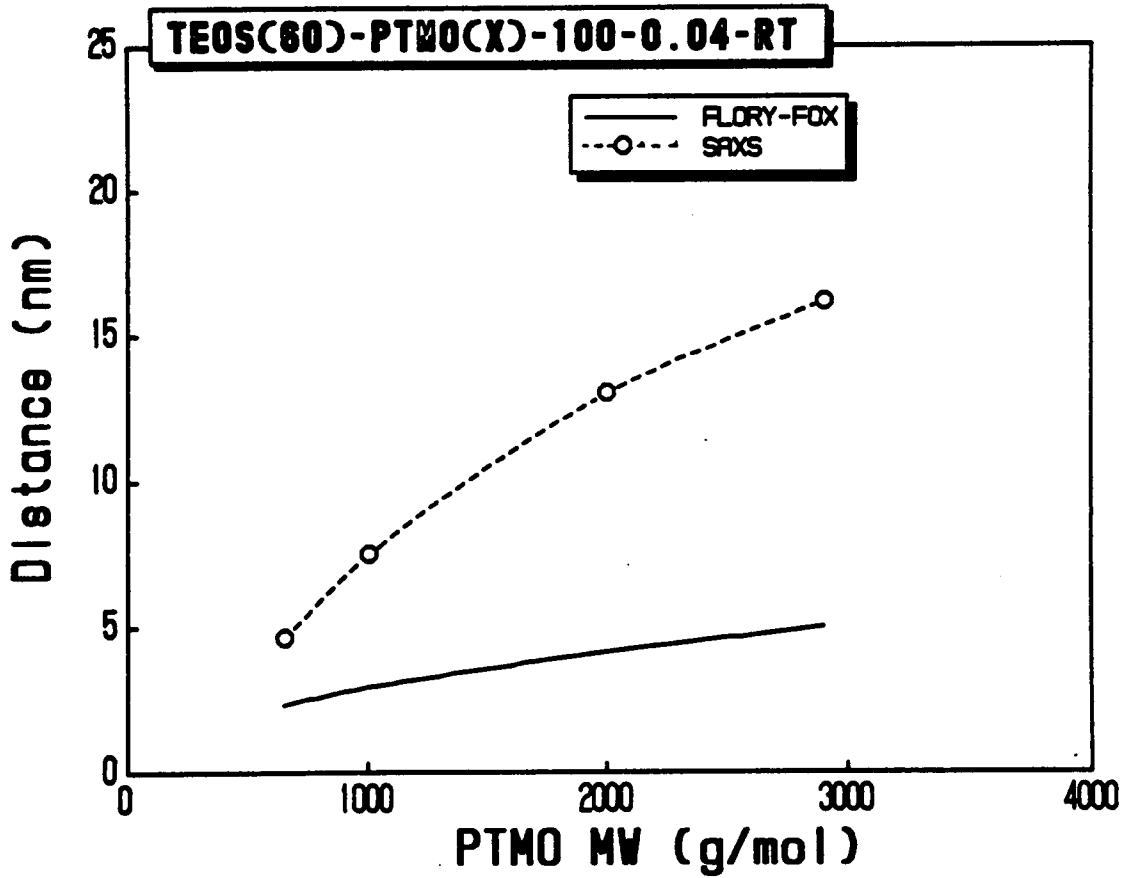
Figure 5.6 The effect of PTMO molecular weight on the SAXS correlation distance and calculated end-to-end distance for materials prepared with 60 wt% TEOS.
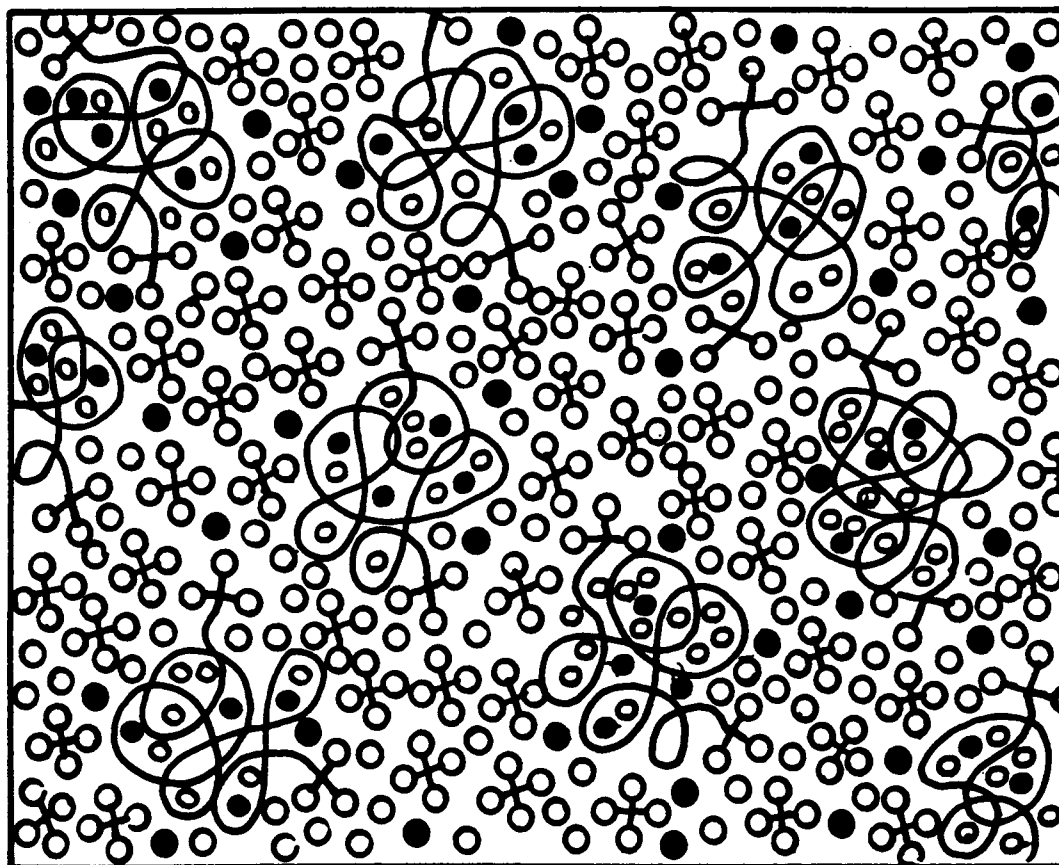
Figure 5.7 A hypothetical scheme for the solution stage of the modified sol-gel reactions before adding the water and acid.
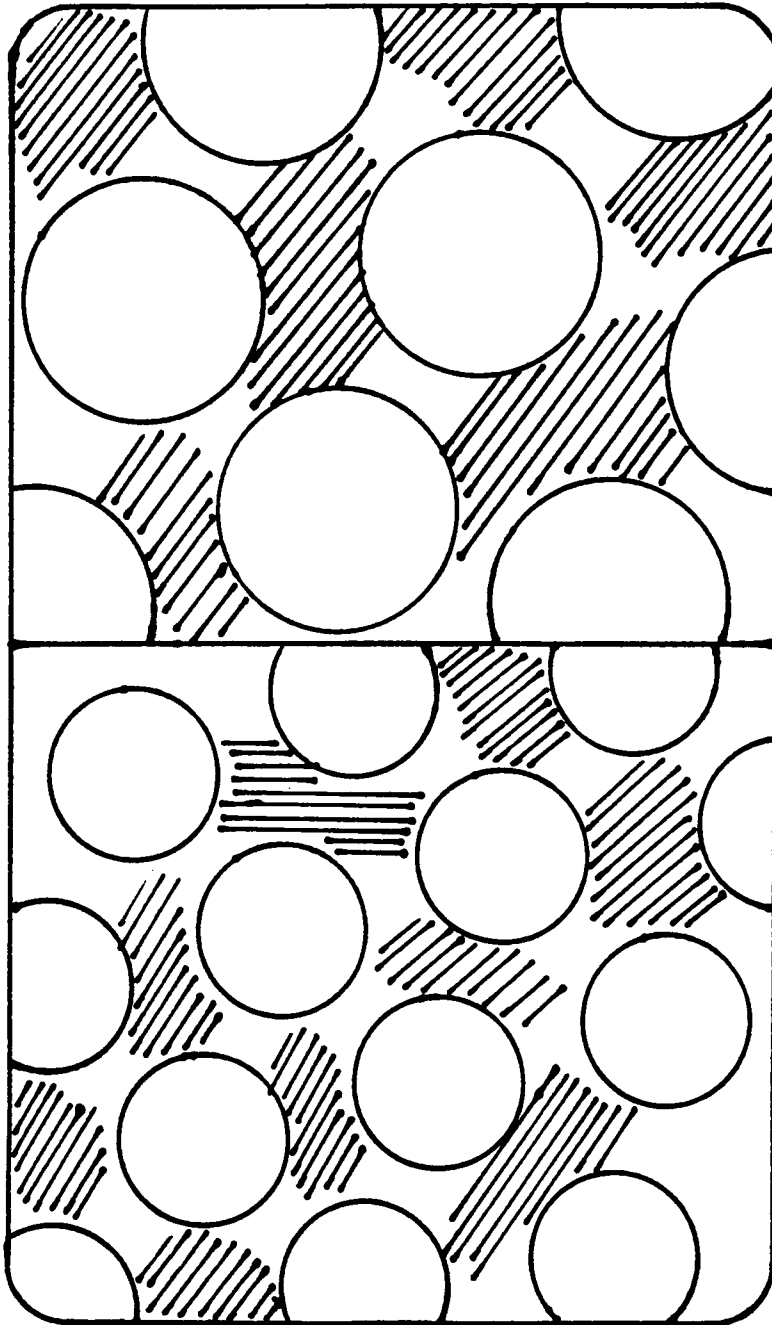
Figure 5.8 A simplified drawing to illustrate the dependence of the interstitial space (shaded area) on the particle size.
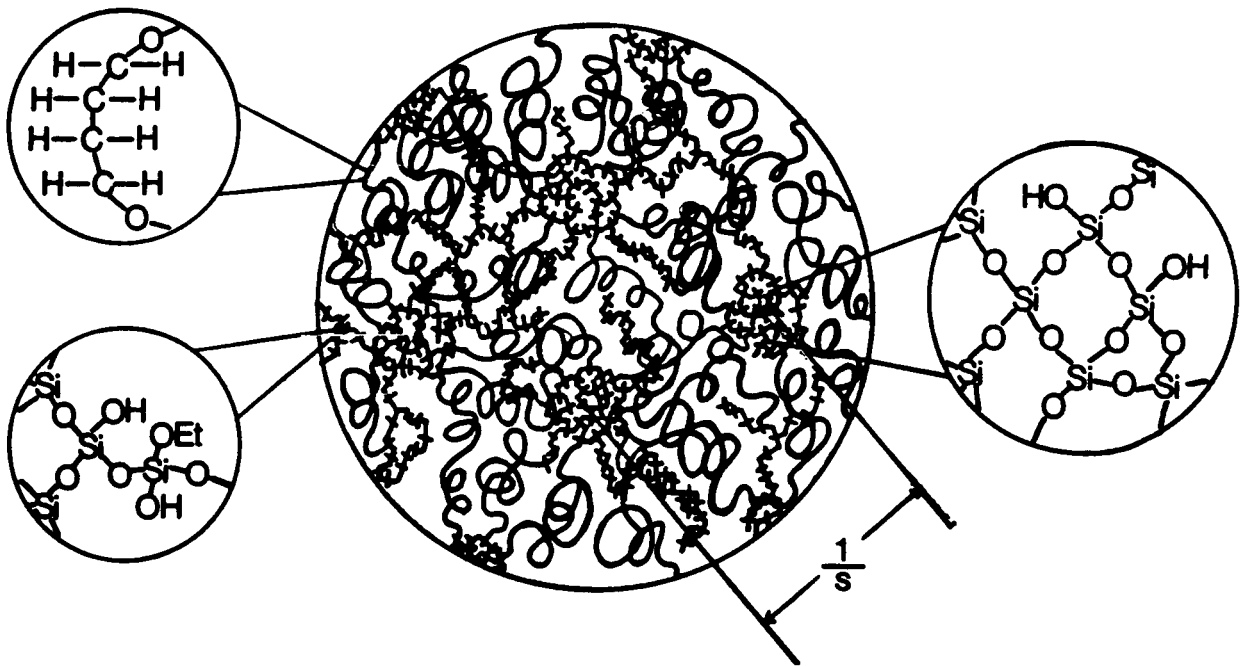
Figure 5.9   A simplified model for the final gels of the TEOS-PTMO hybrid systems, where s is the scattering vector defined as $2sin\theta/\lambda$ and $1/s$ is the correlation distance observed by SAXS.
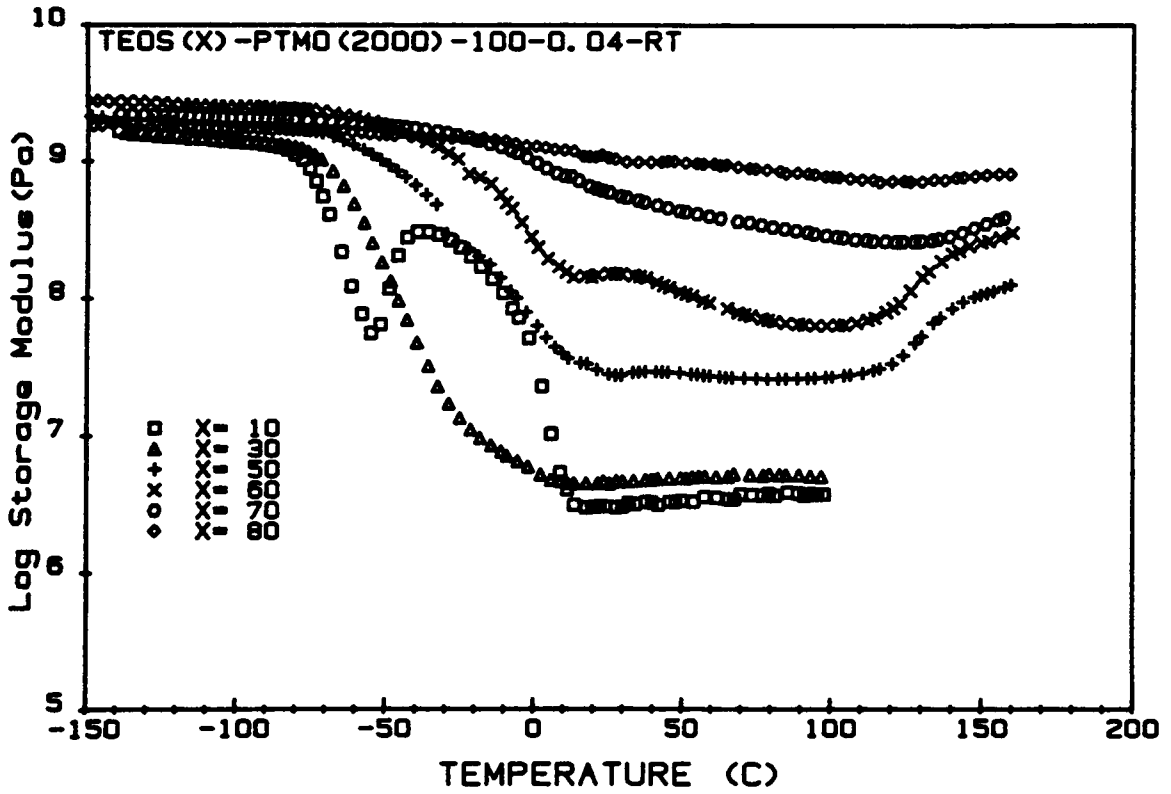
Figure 5.10 Spectra of storage modulus of materials prepared with PTMO(2000) and various TEOS contents.
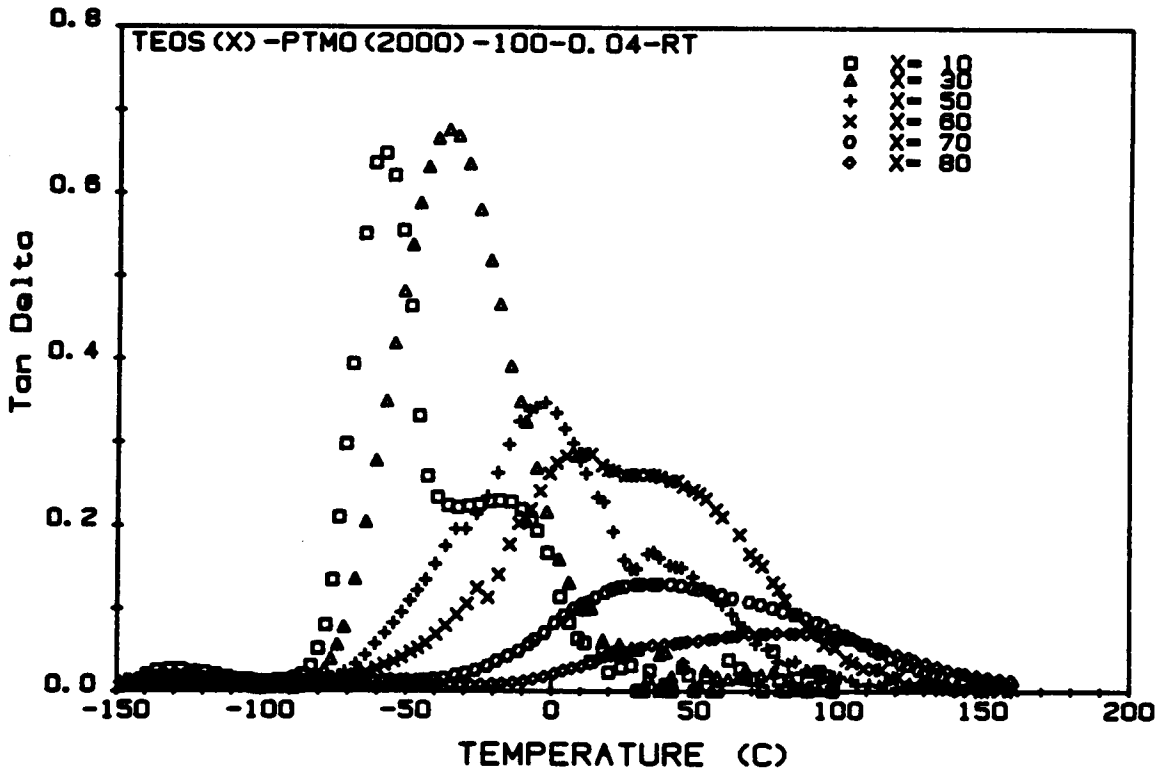
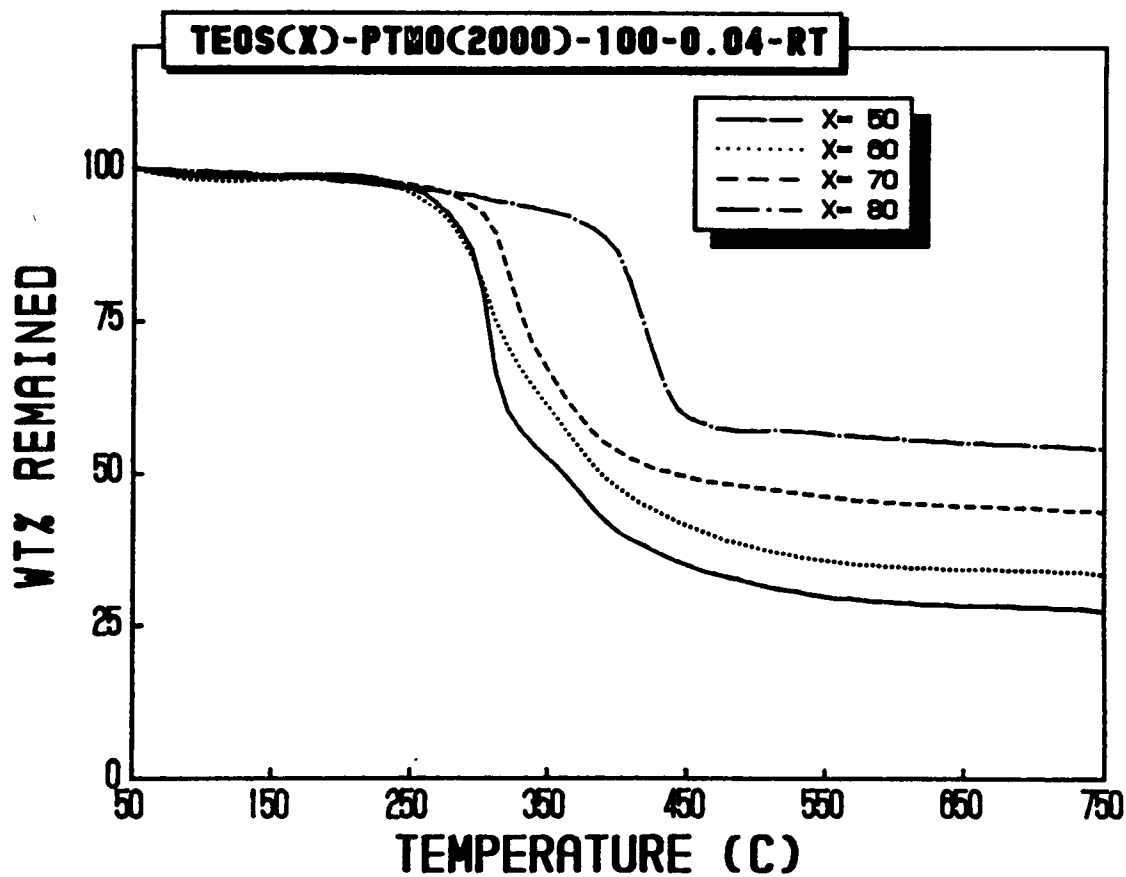**Figure 5.11** Spectra of tanδ of materials prepared with PTMO(2000) and various TEOS contents.
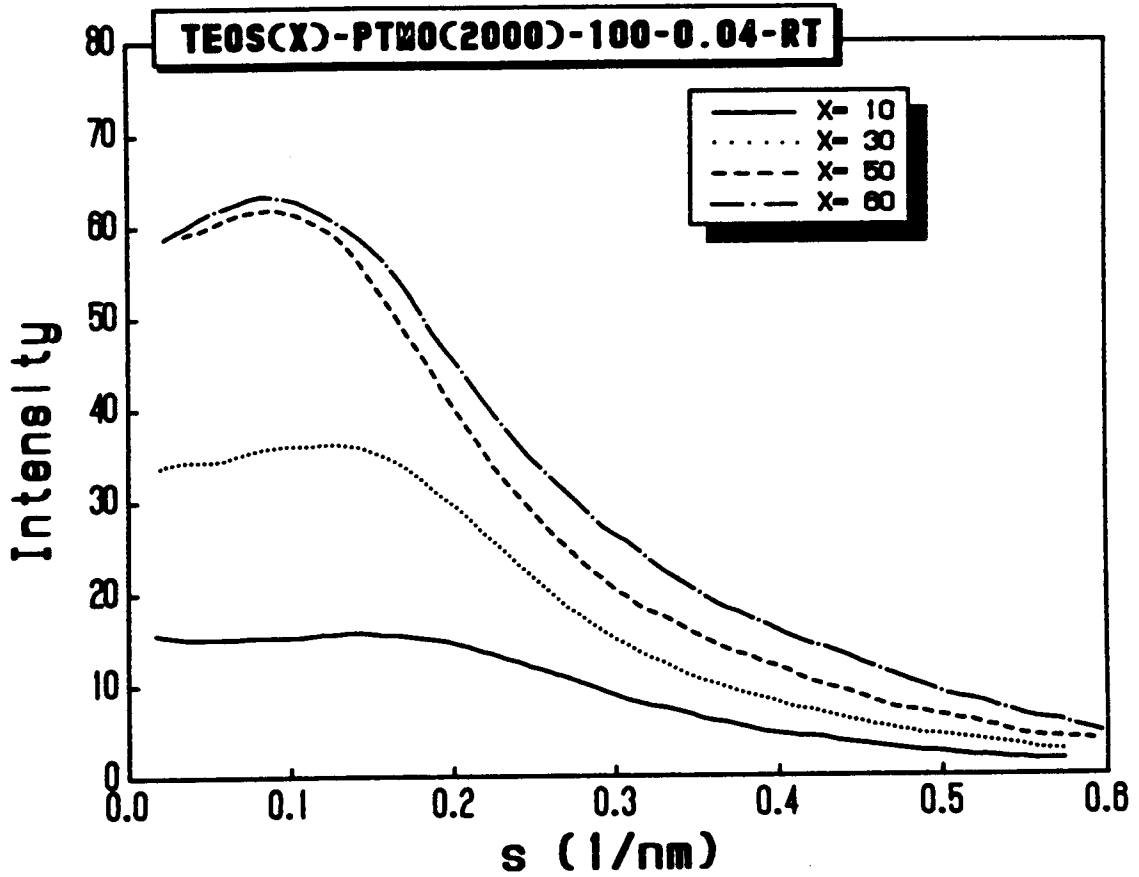
**Figure 5.12** SAXS profiles of materials prepared with PTMO(2000) and various TEOS contents, ranging from 10 to 60 wt%.
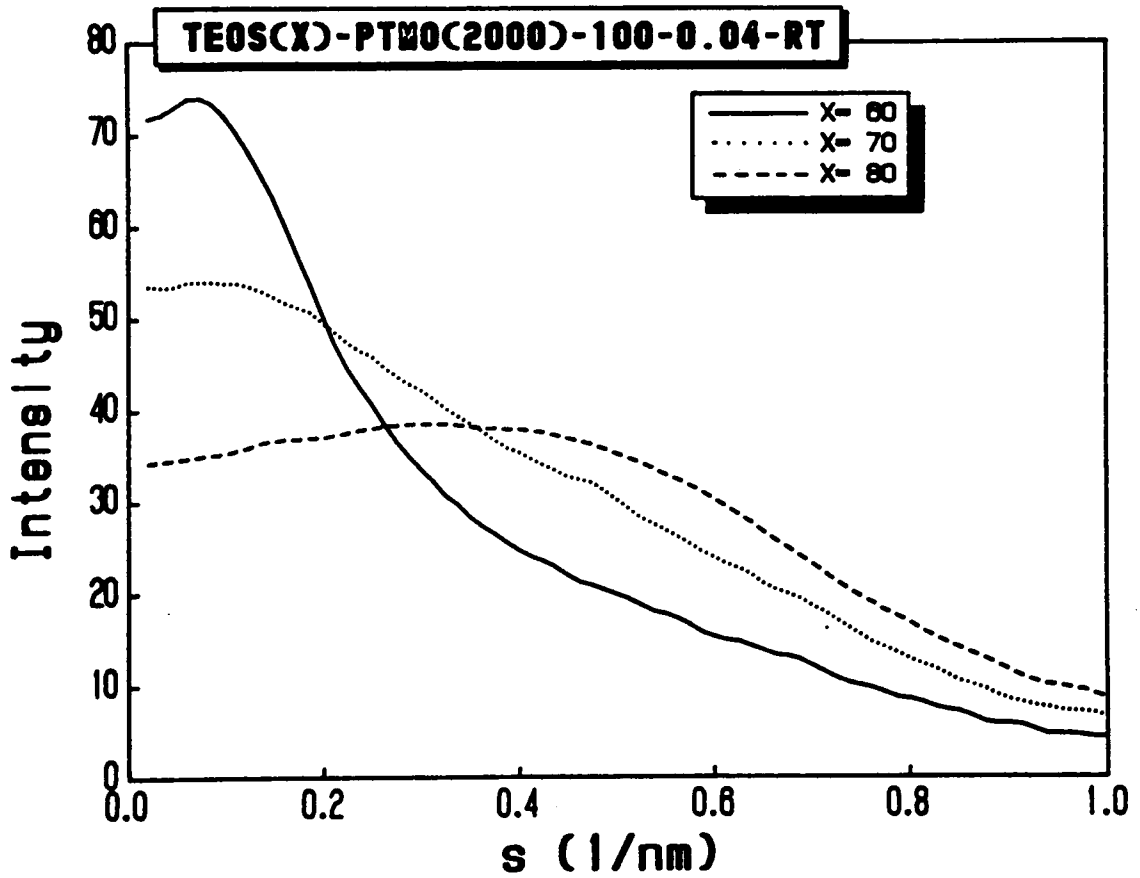
**Figure 5.13** SAXS profiles of materials prepared with PTMO(2000) and various TEOS contents, ranging from 60 to 80 wt%.
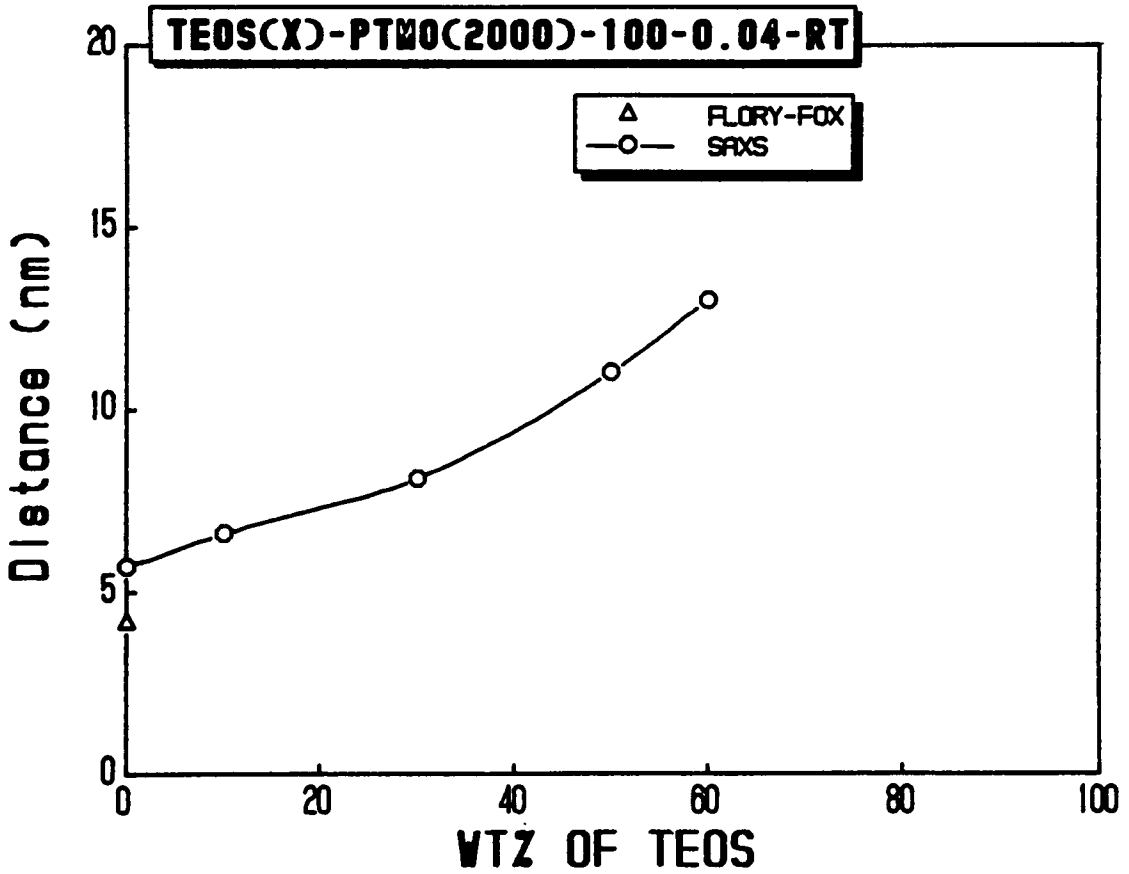
Figure 5.14 The effect of TEOS content on the SAXS correlation distance of samples prepared using TEOS and PTMO(2000).
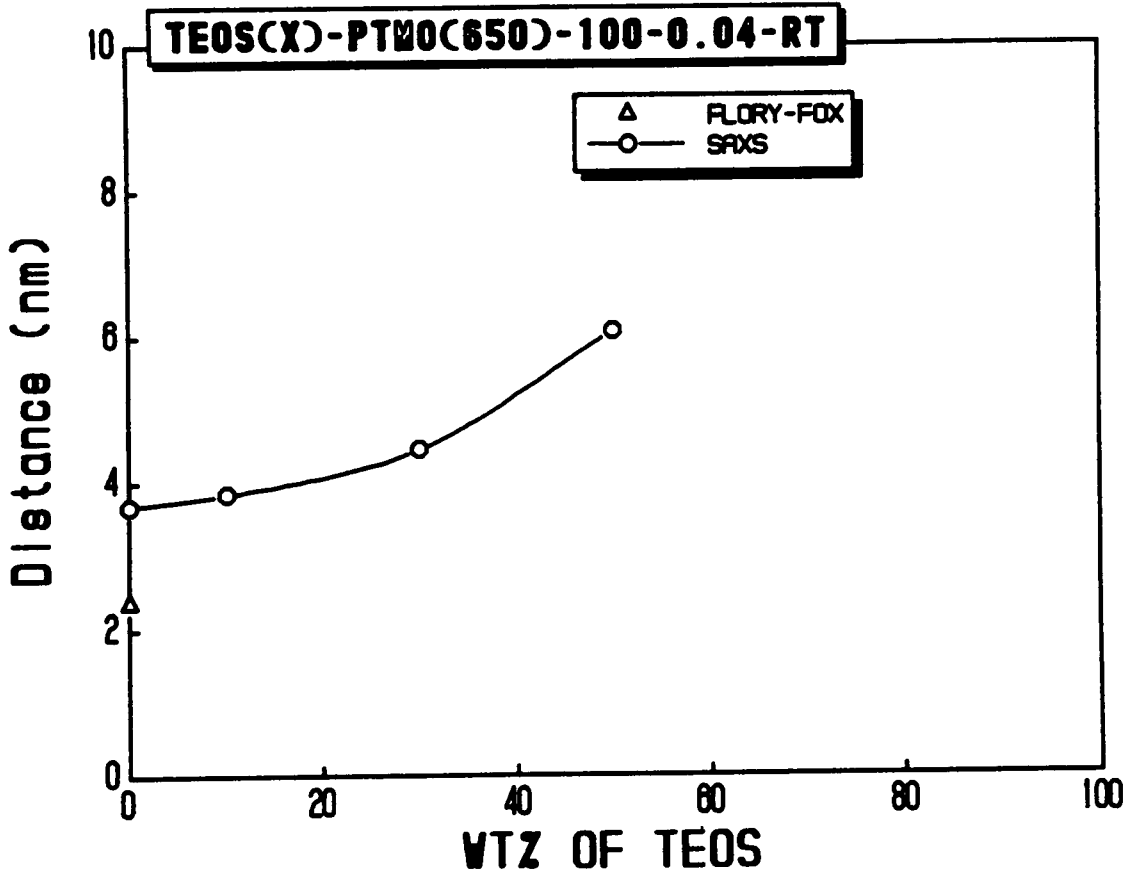
Figure 5.15 The effect of TEOS content on the SAXS correlation distance of samples prepared using TEOS and PTMO(650).
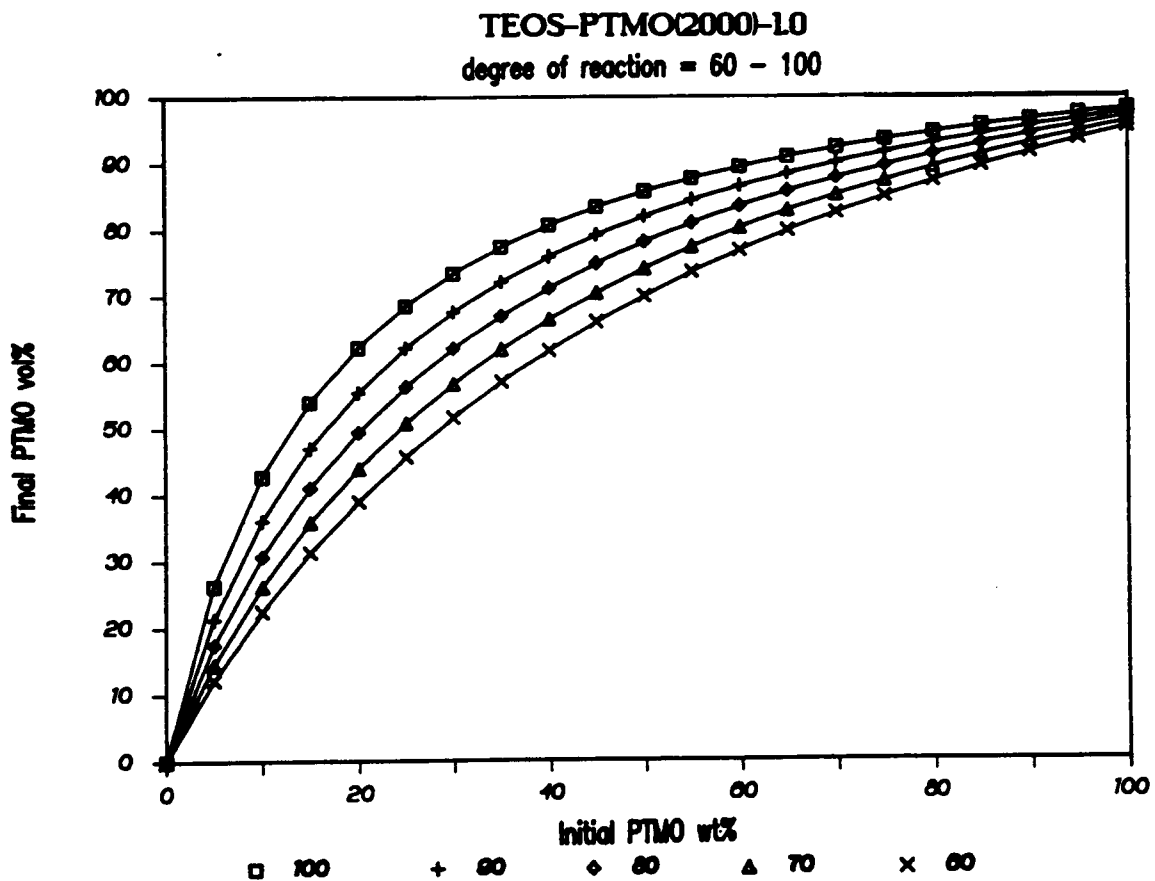
Figure 5.16 Estimations of final PTMO volume fractions in materials prepared with PTMO(2000) and various TEOS contents. Each curve represents an estimation based on a specific overall degree of reaction.
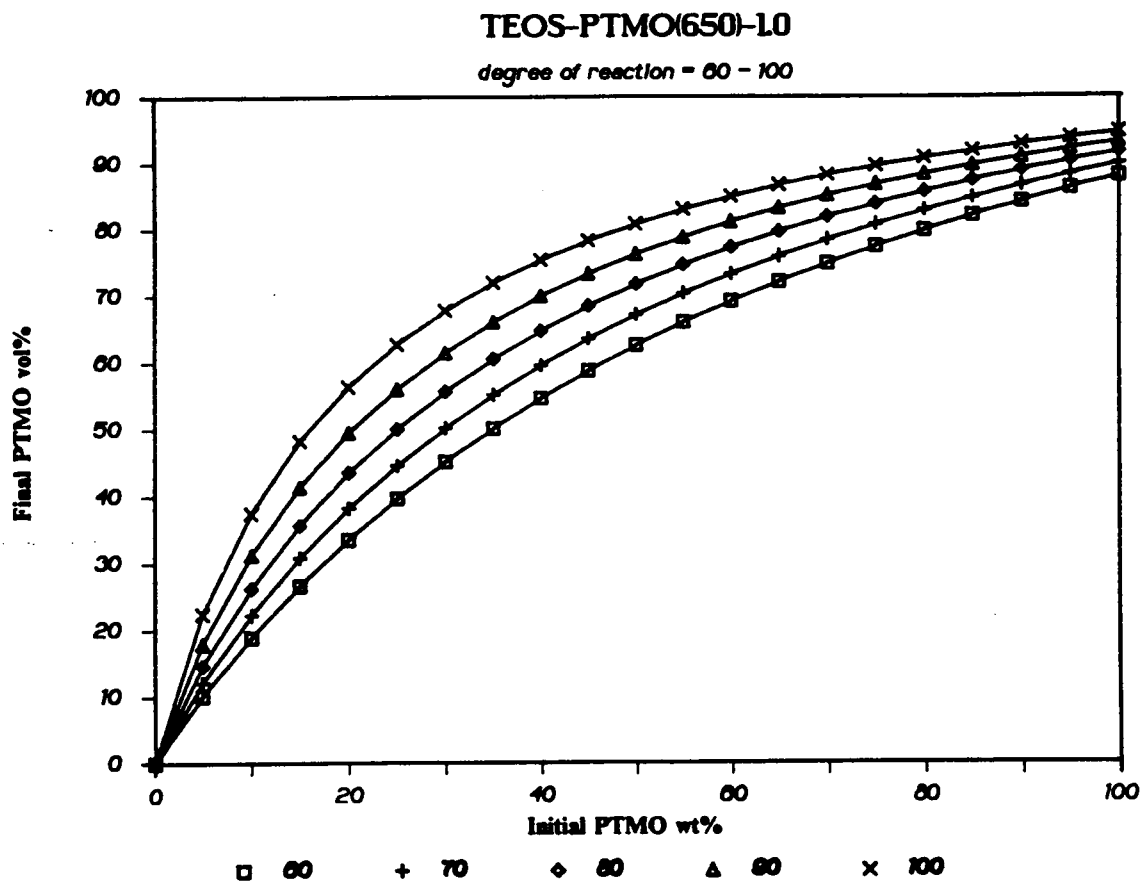
Figure 5.17 Estimations of final PTMO volume fractions in materials prepared with PTMO(650) and various TEOS contents. Each curve represents an estimation based on a specific overall degree of reaction.
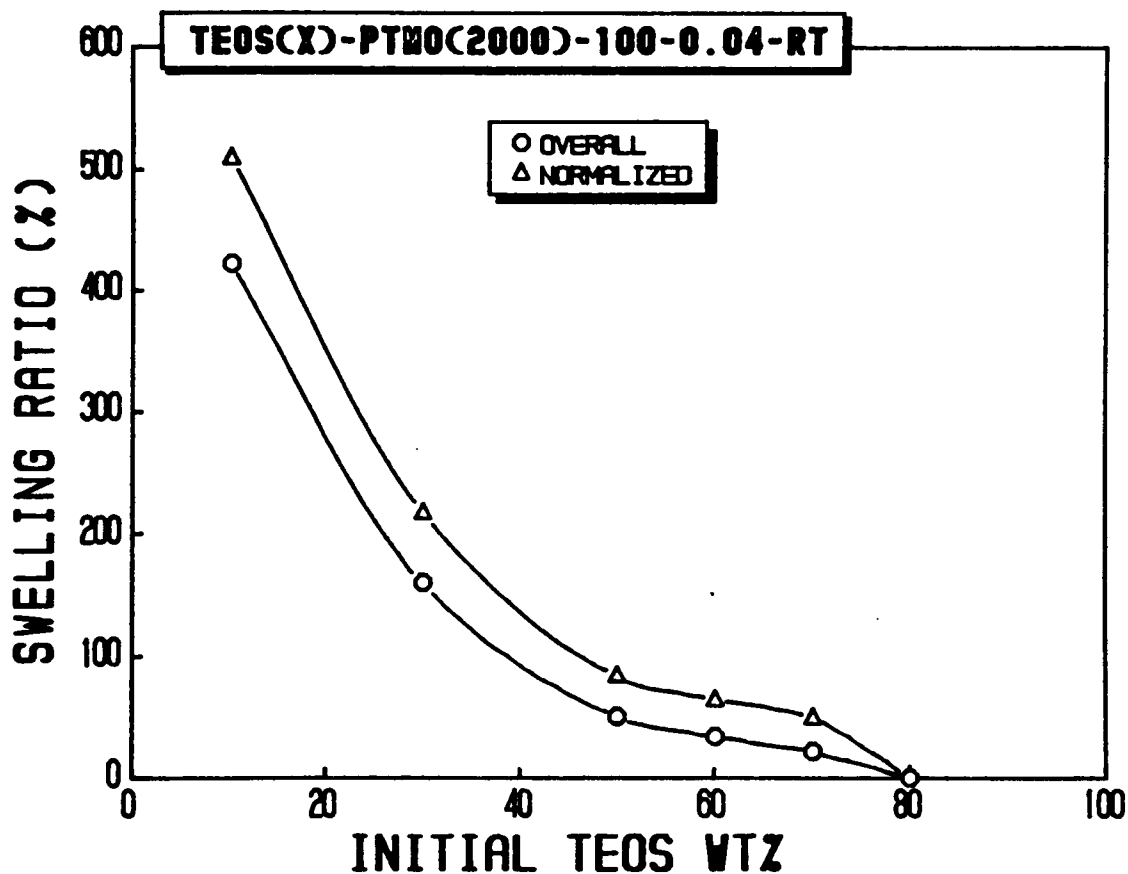
Figure 5.18 The effect of TEOS content on the swelling ratio of materials prepared with TEOS and PTMO(2000). The overall swelling ratio is based on the total weight of the material, and the normalized swelling ratio is based on the estimated weight of PTMO in the sample.

Figure 5.19 TGA results of materials prepared with PTMO(2000) and various TEOS contents, ranging from 50 to 80 wt%.
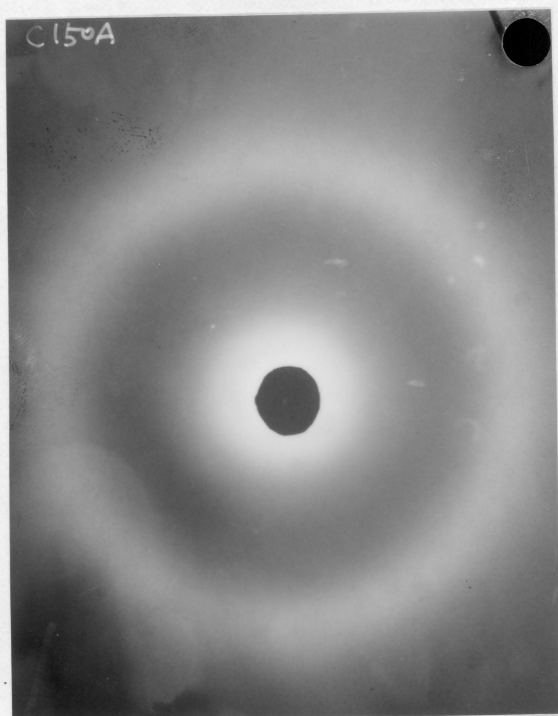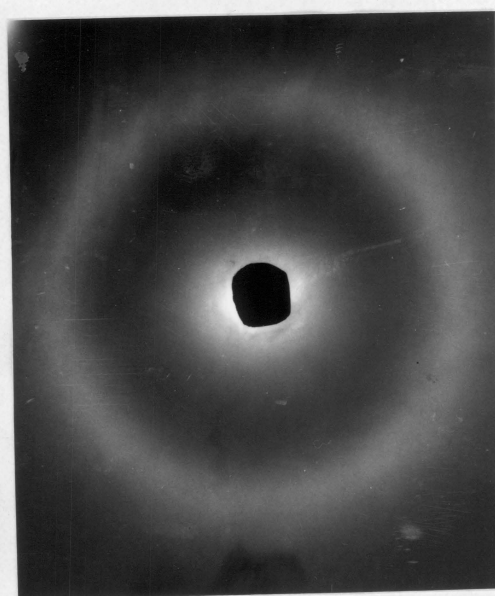
Figure 5.20   WAXD patterns of a material prepared with 50 wt% TMOS and PTMO(2900). (a) unstrained, (b) 50% strain.
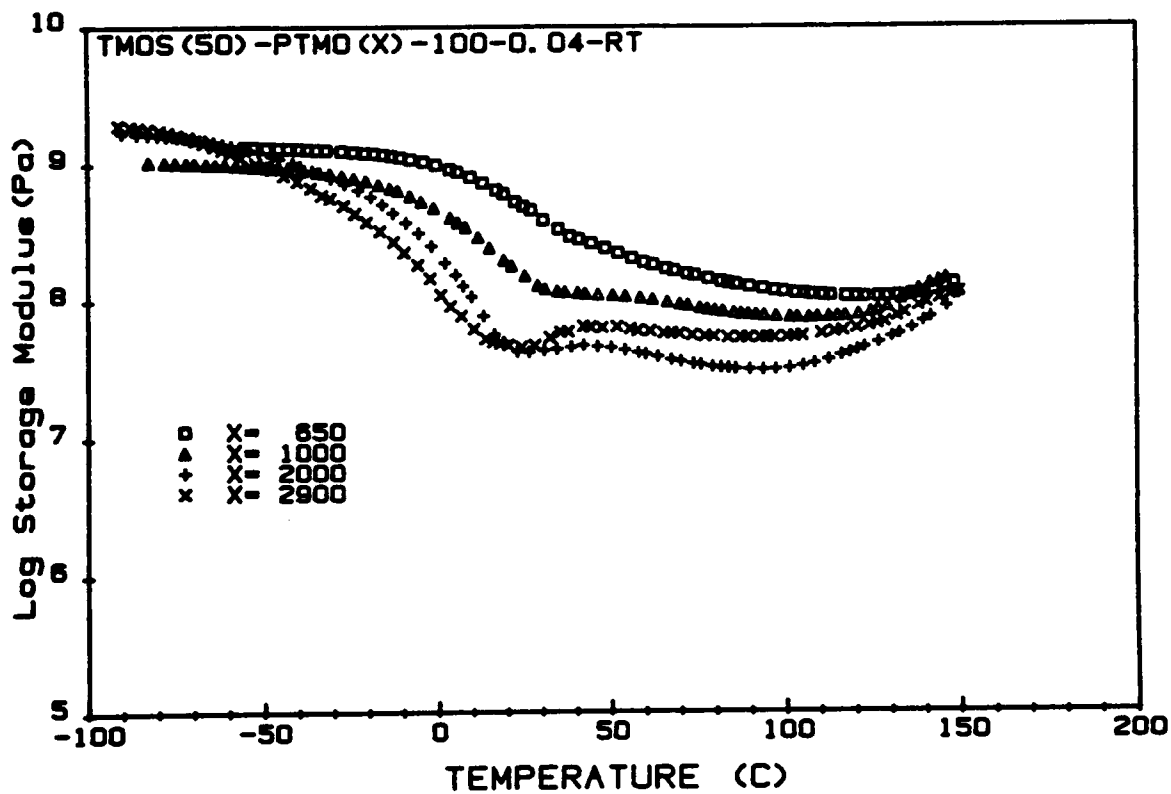
Figure 5.21   Spectra of storage modulus of materials prepared with 50 wt% TMOS and various molecular weights of PTMO.
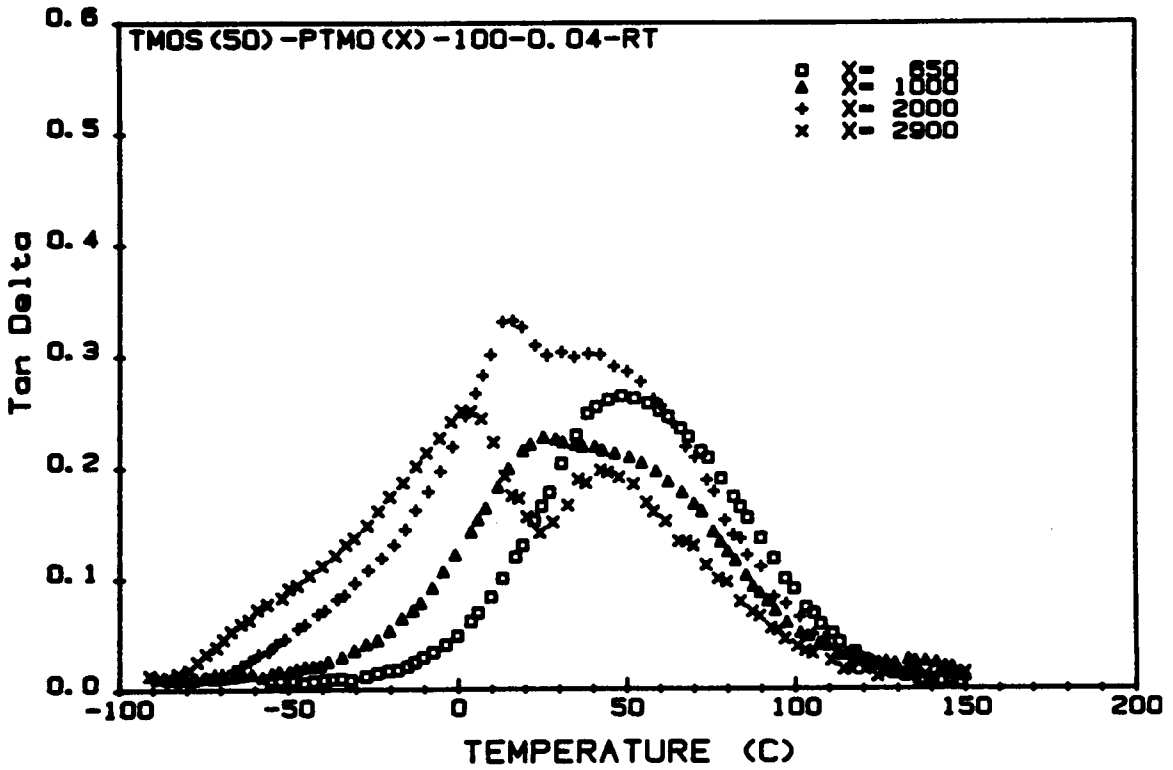
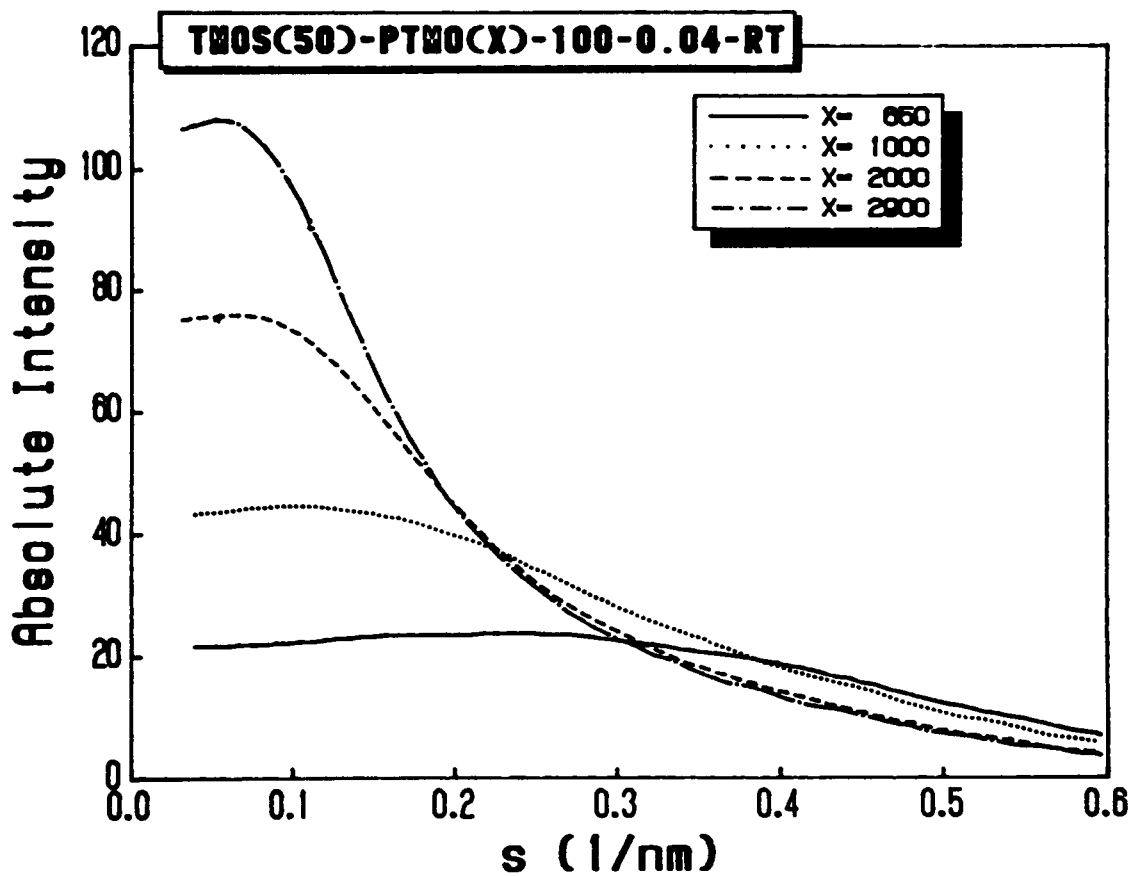**Figure 5.22** Spectra of tanδ of materials prepared with 50 wt% TMOS and various molecular weights of PTMO.
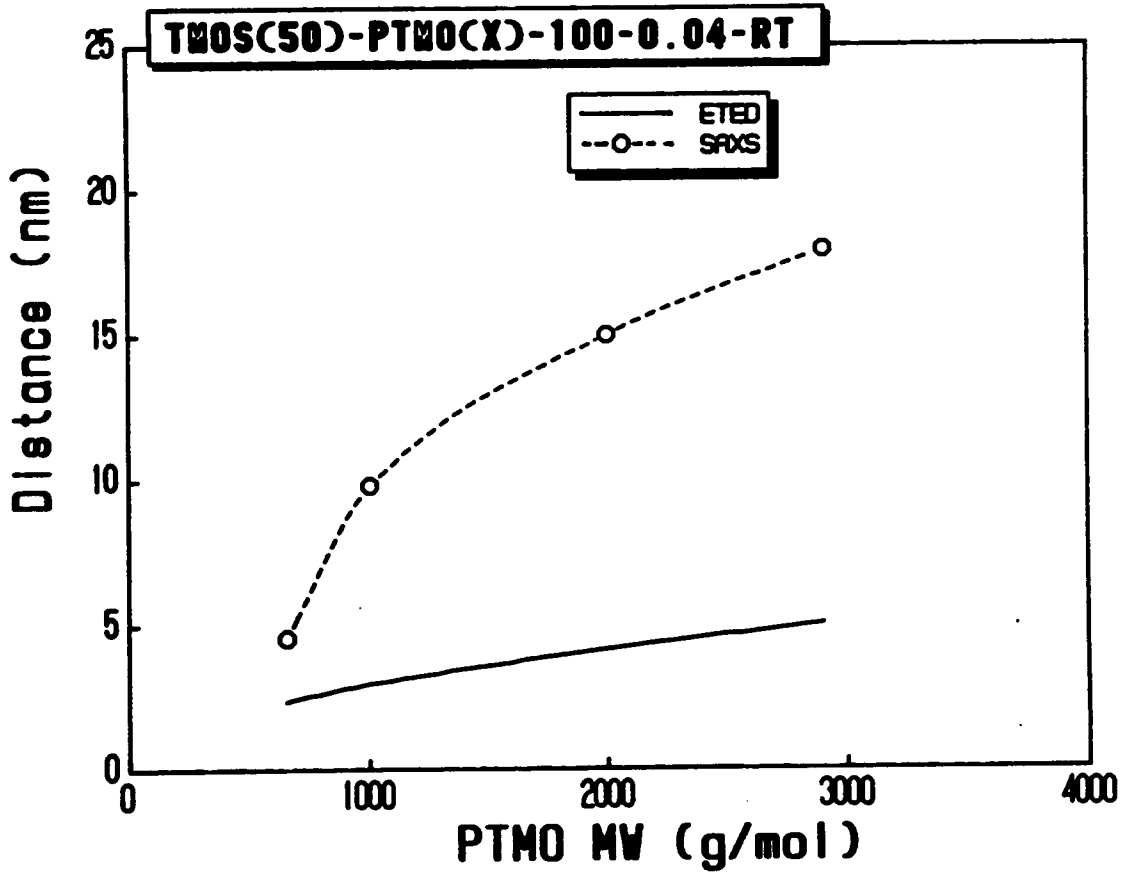
Figure 5.23 SAXS profiles of materials prepared with 50 wt% TMOS and various molecular weights of PTMO.

Figure 5.24 The effect of PTMO molecular weight on the SAXS correlation distance and calculated end-to-end distance for materials prepared with 50 wt% TMOS.
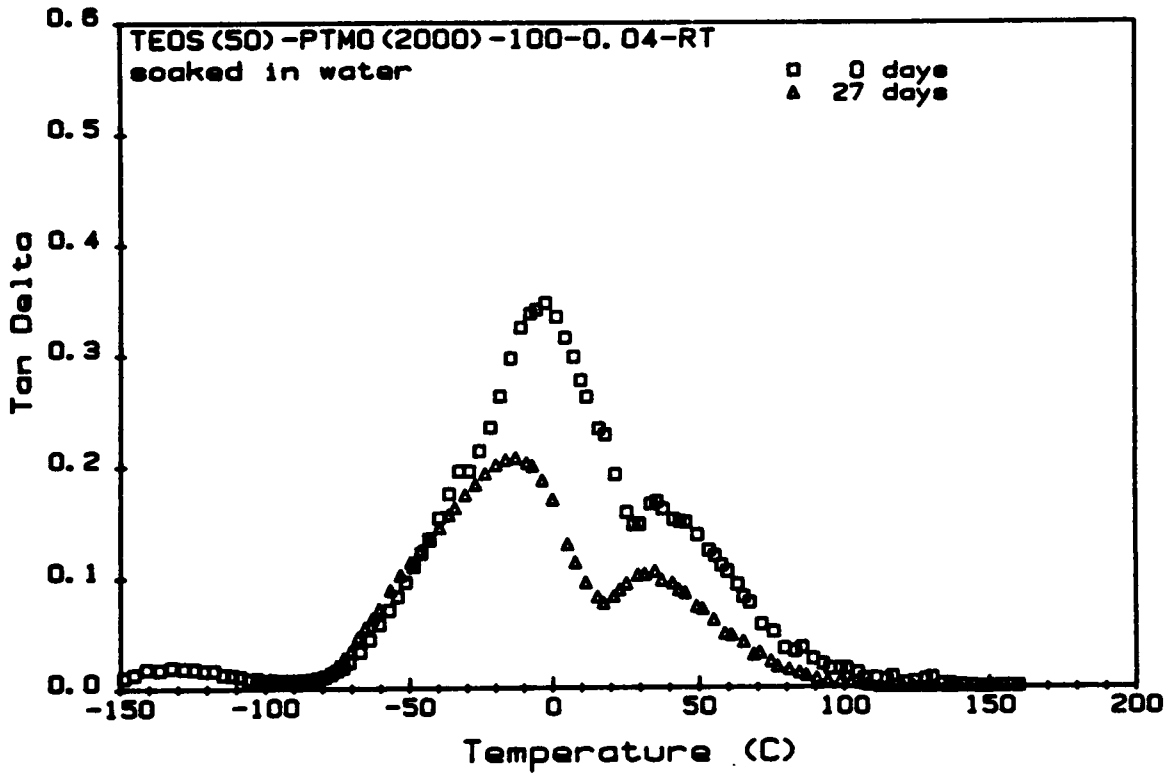
Figure 5.25   Effect of water soaking on the tanδ behavior of a material prepared with 50 wt% TEOS and PTMO(2000).
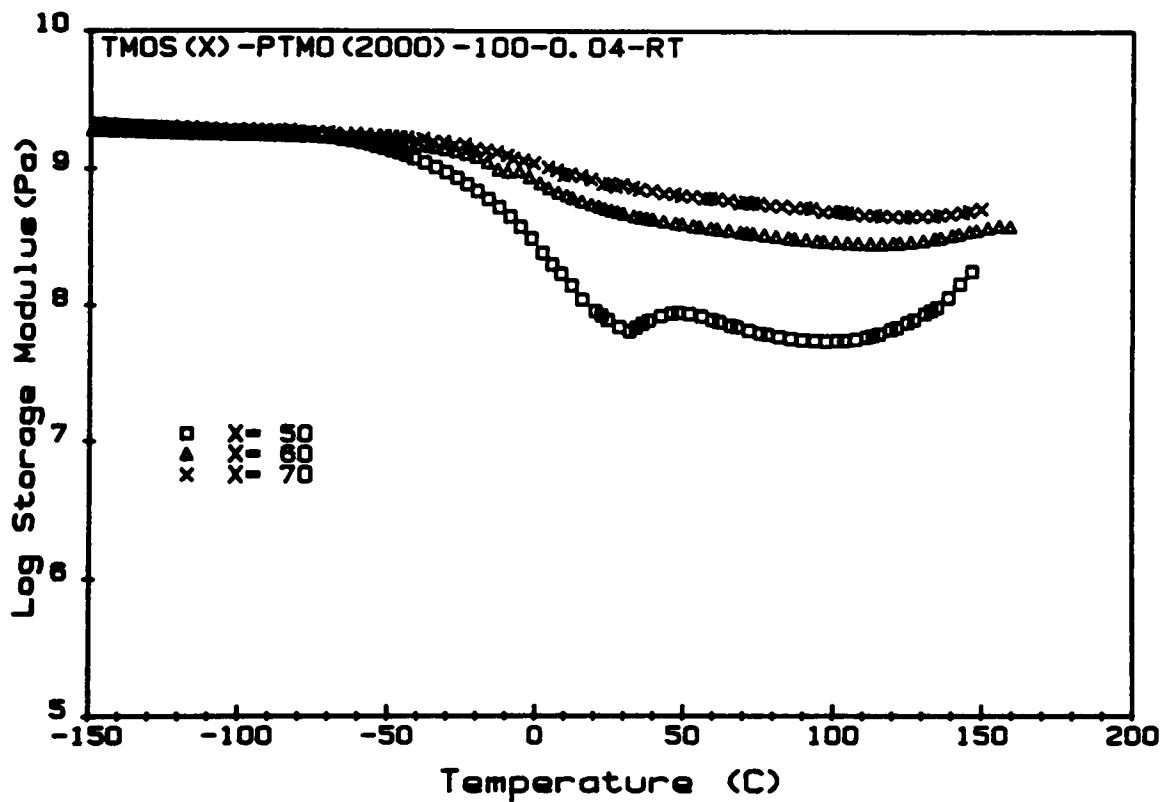
Figure 5.26 Spectra of storage modulus of materials prepared with PTMO(2000) and various TMOS contents.
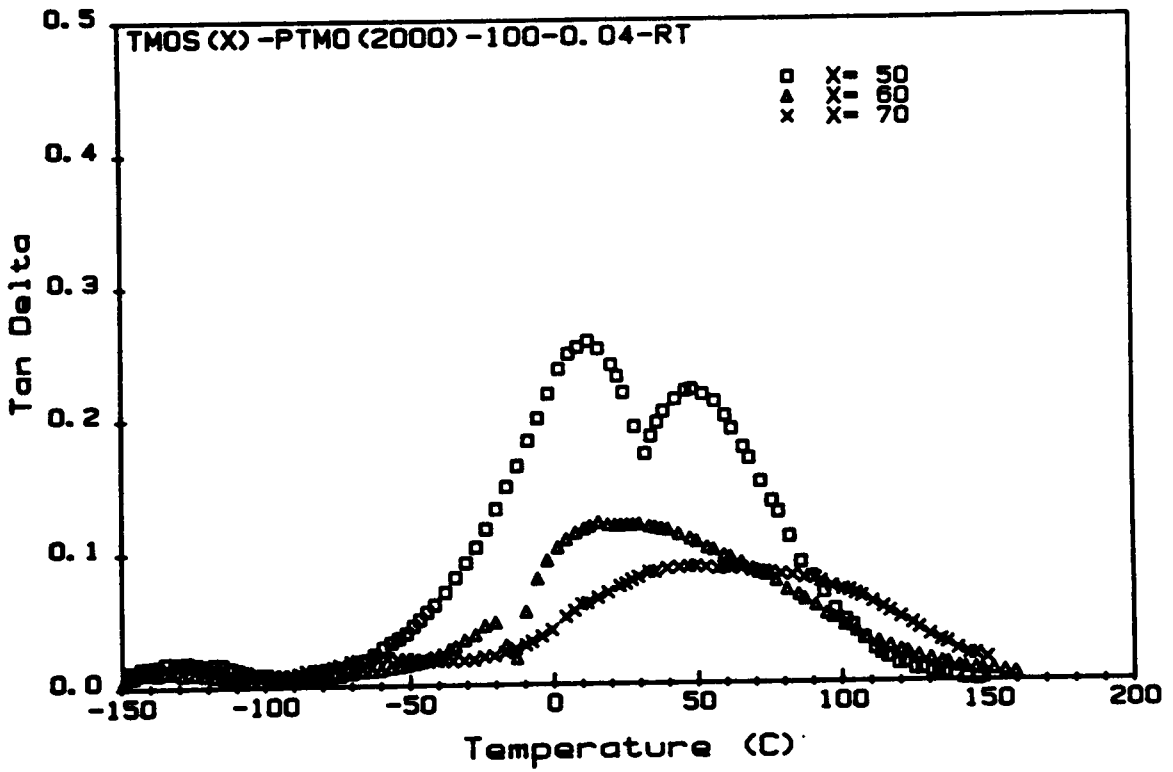
Figure 5.27 Spectra of tanδ of materials prepared with PTMO(2000) and various TMOS contents.
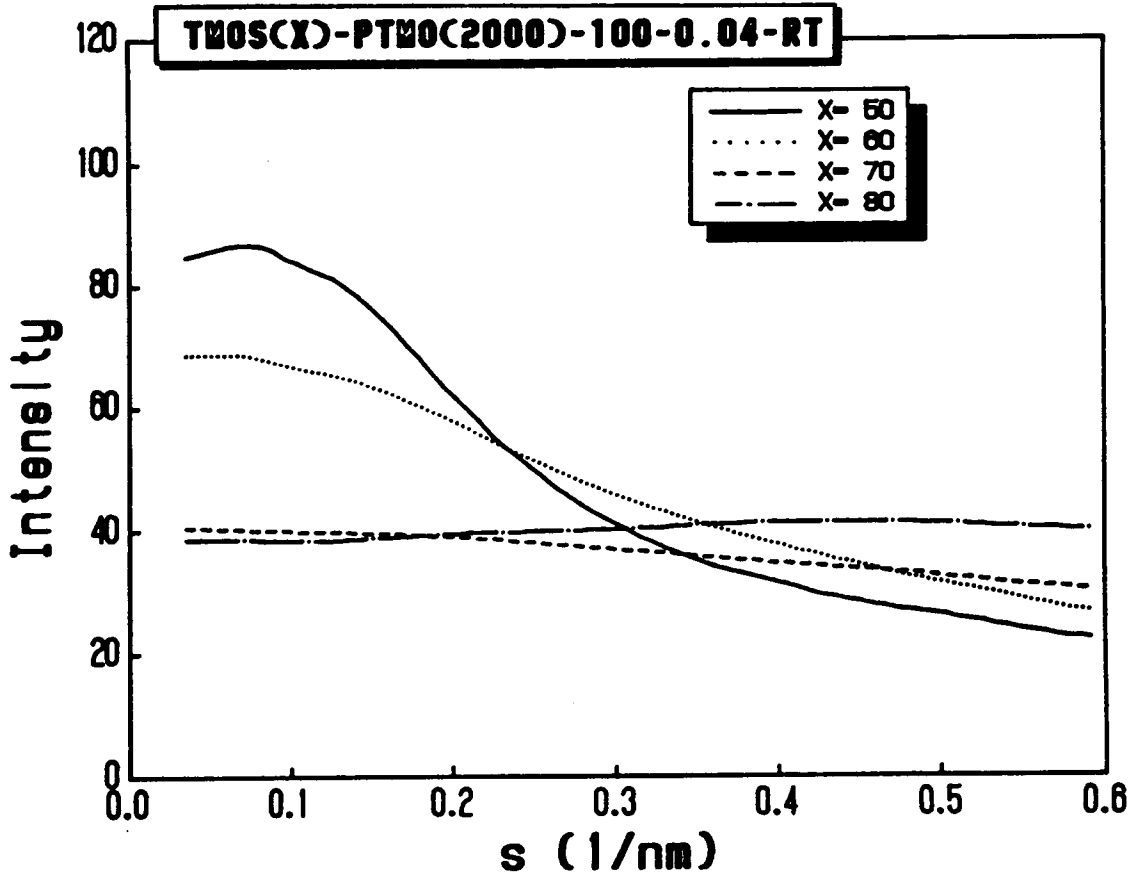
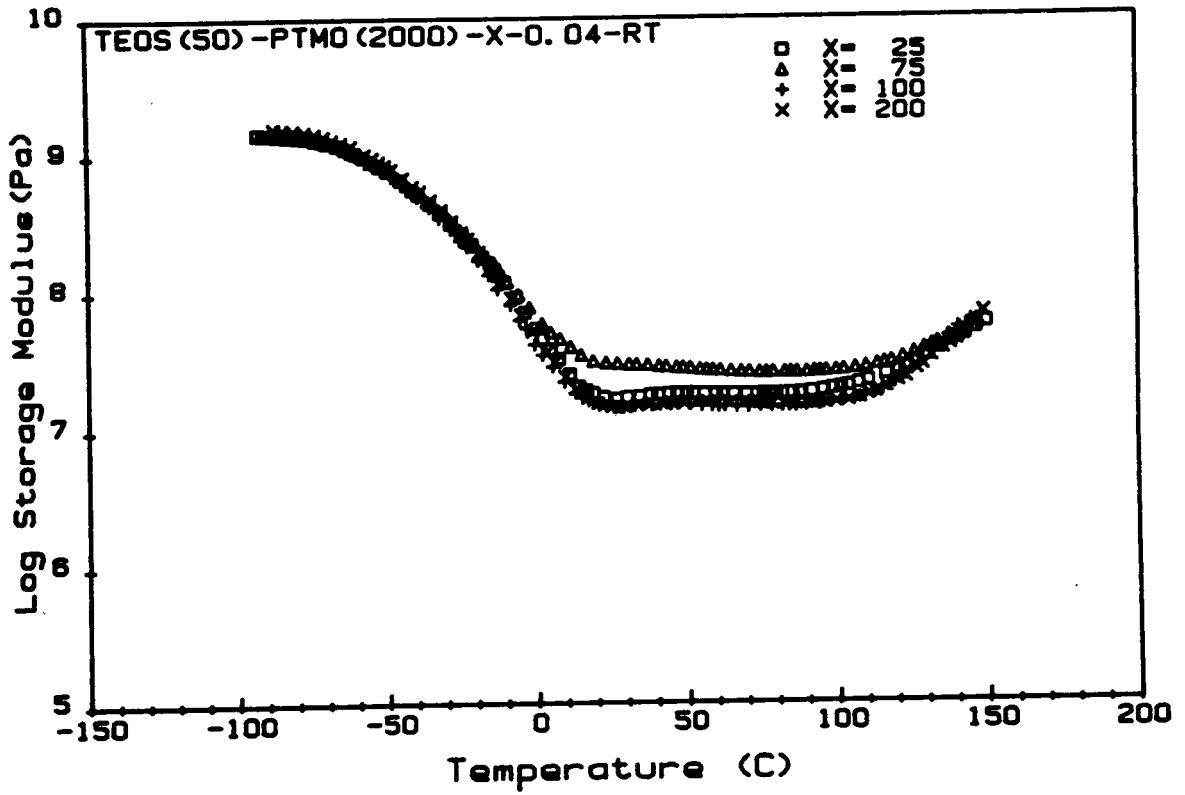**Figure 5.28** SAXS profiles of materials prepared with PTMO(2000) and various TMOS contents.

Figure 5.29 Spectra of storage modulus of materials prepared with 50 wt% TEOS, PTMO(2000), and various water contents.

Figure 5.30 Spectra of tanδ of materials prepared with 50 wt% TEOS, PTMO(2000), and various water contents.
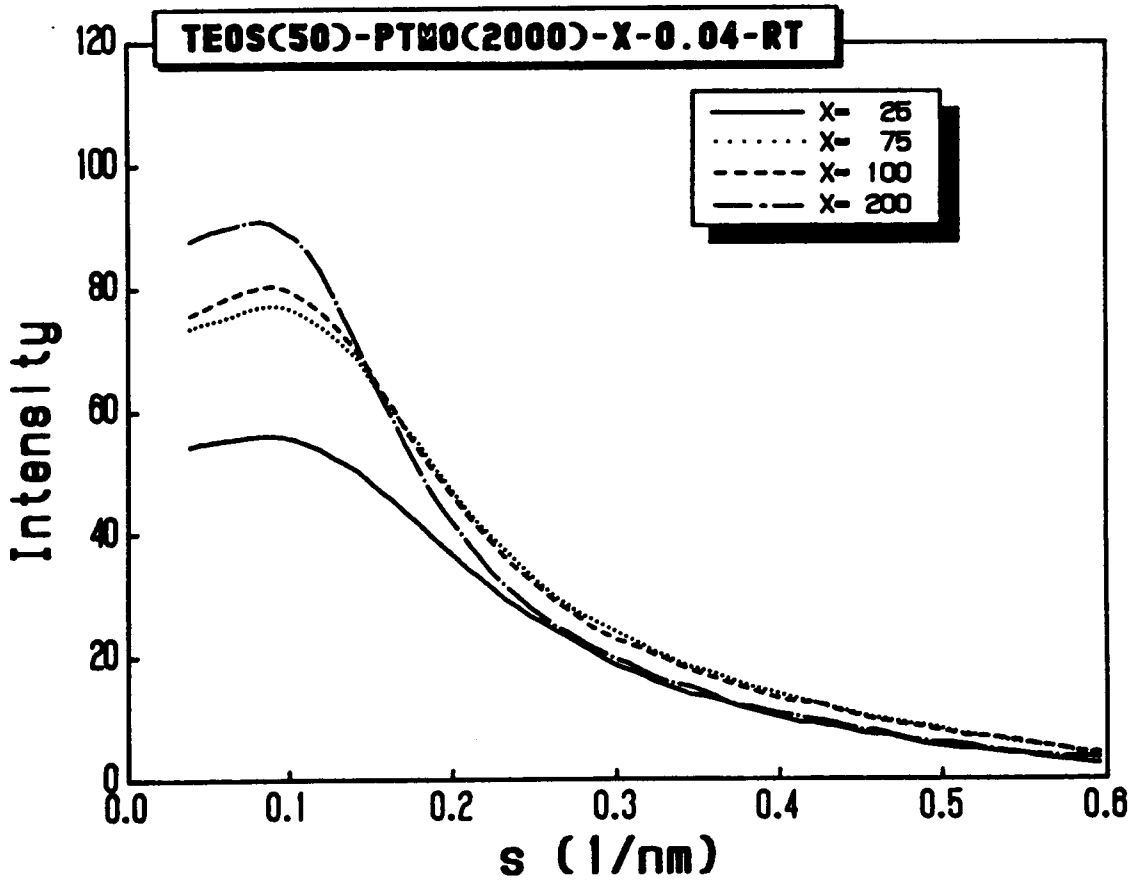
Figure 5.31 SAXS profiles of materials prepared with 50 wt% TEOS, PTMO(2000), and various water contents.
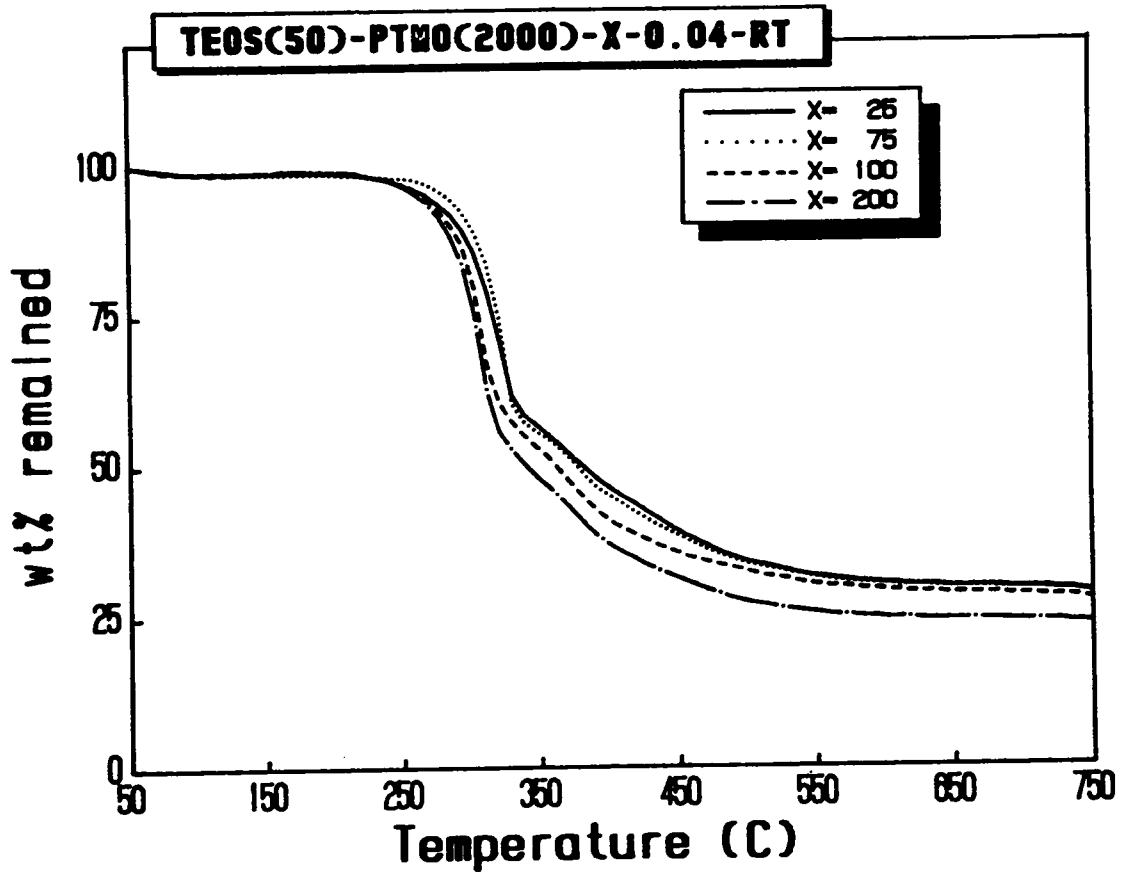
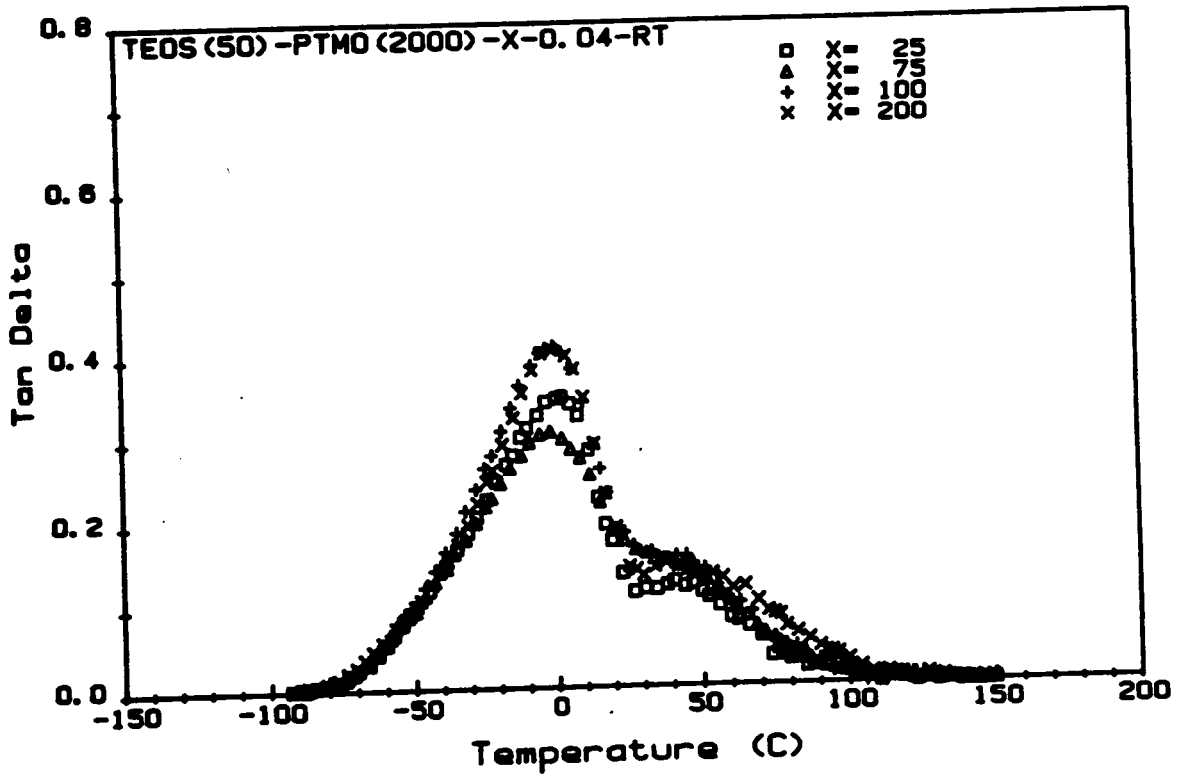**Figure 5.32**   TGA results of materials prepared with 50 wt% TEOS, PTMO(2000), and various water contents.

THE THERMOSETTING PROCESS:
TIME-TEMPERATURE-TRANSFORMATION DIAGRAM
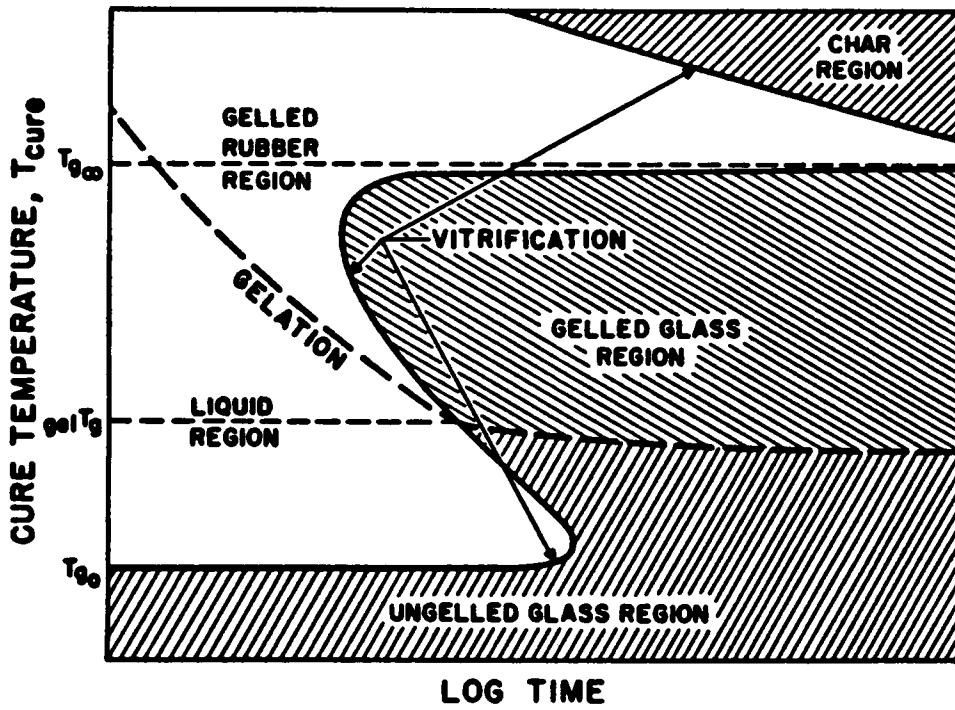
Figure 5.33 A typical time-temperature-transformation (TTT) diagram [77].
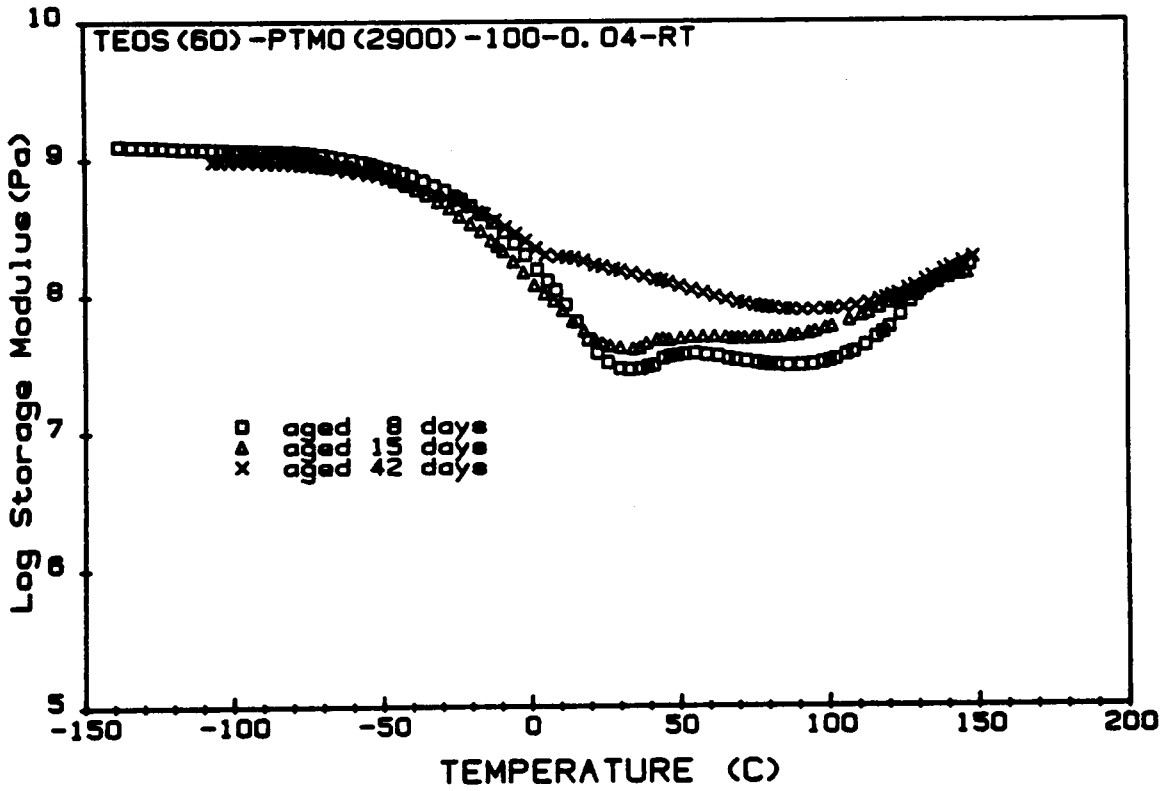
Figure 5.34 Aging effect on the storage modulus behavior of a material prepared with 60 wt% TEOS and PTMO(2900).
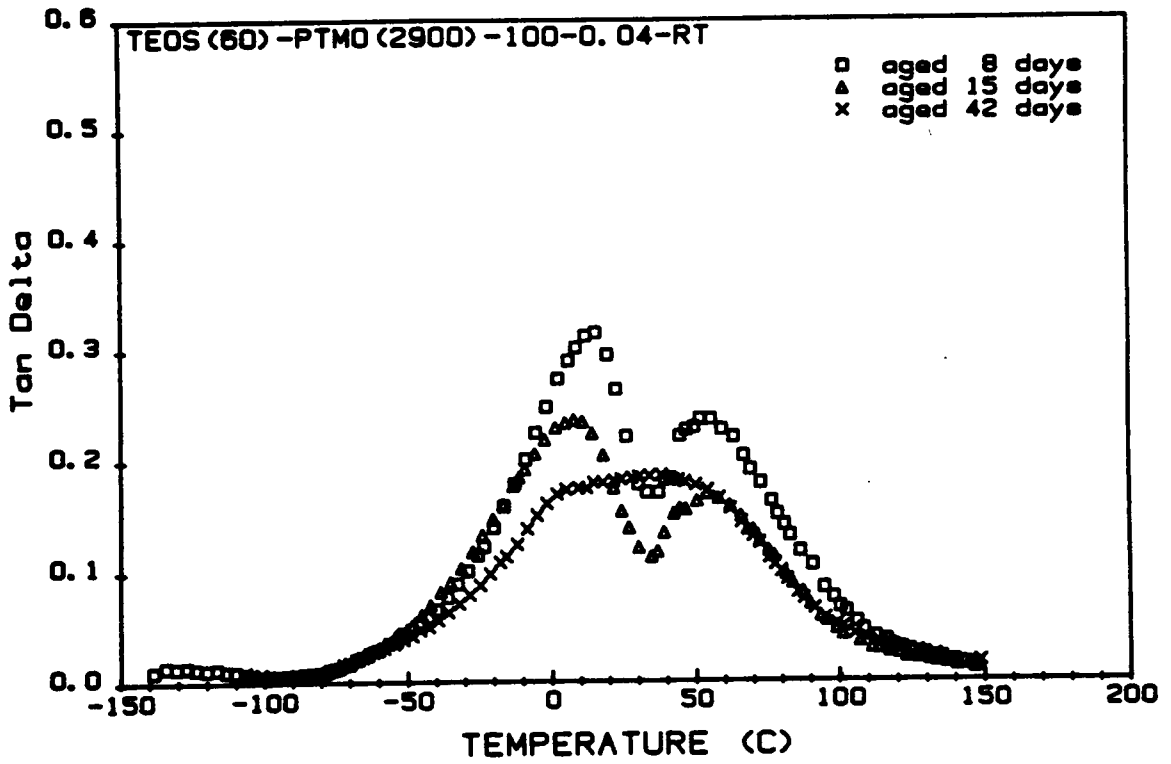
Figure 5.35   Aging effect on the tanδ behavior of a material prepared with 60 wt% TEOS and PTMO(2900).
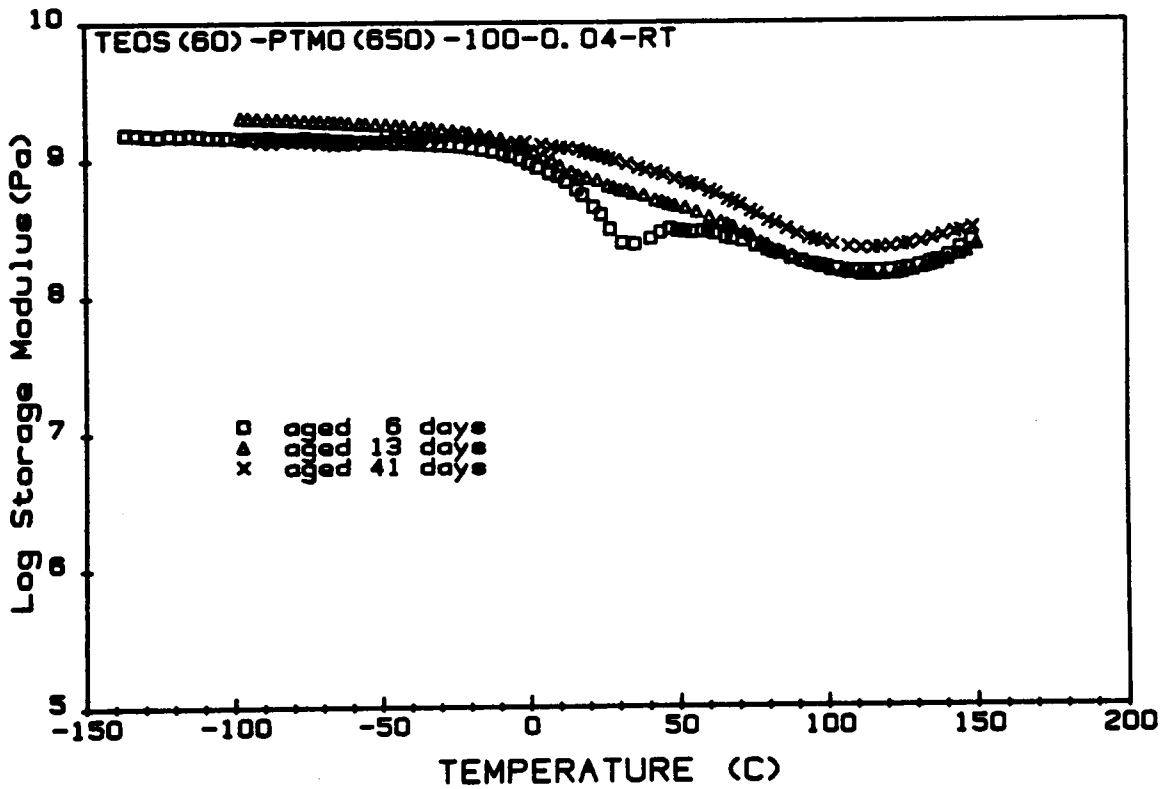
Figure 5.36 Aging effect on the storage modulus behavior of a material prepared with 60 wt% TEOS and PTMO(650).
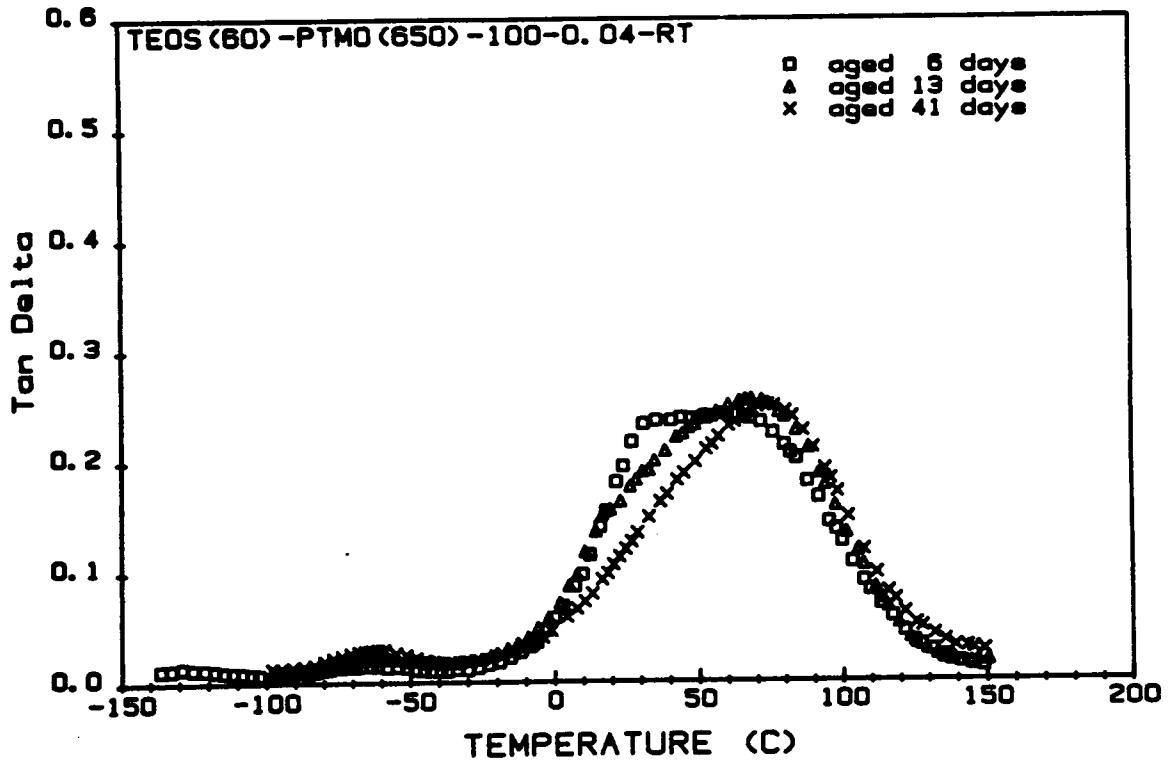
Figure 5.37 Aging effect on the tanδ behavior of a material prepared with 60 wt% TEOS and PTMO(650).
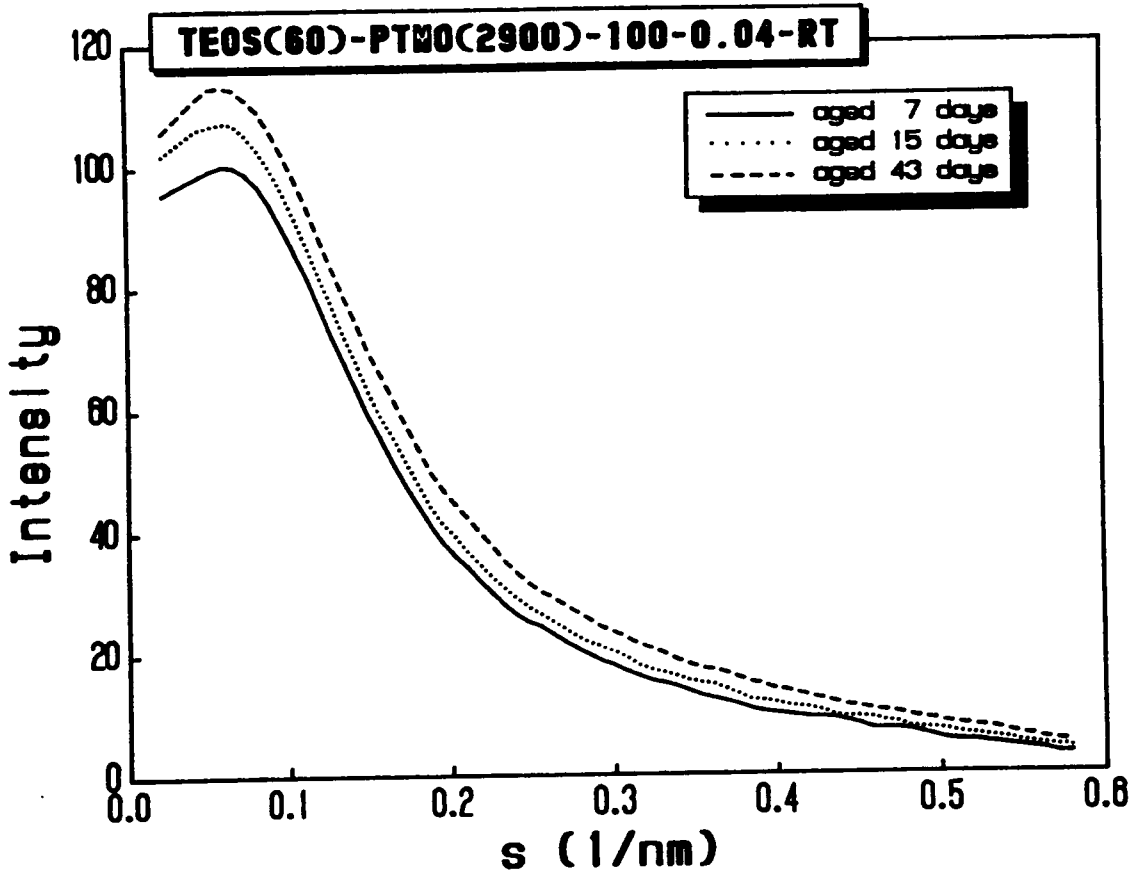
Figure 5.38 Aging effect on the SAXS behavior of a material prepared with 60 wt% TEOS and PTMO(2900).
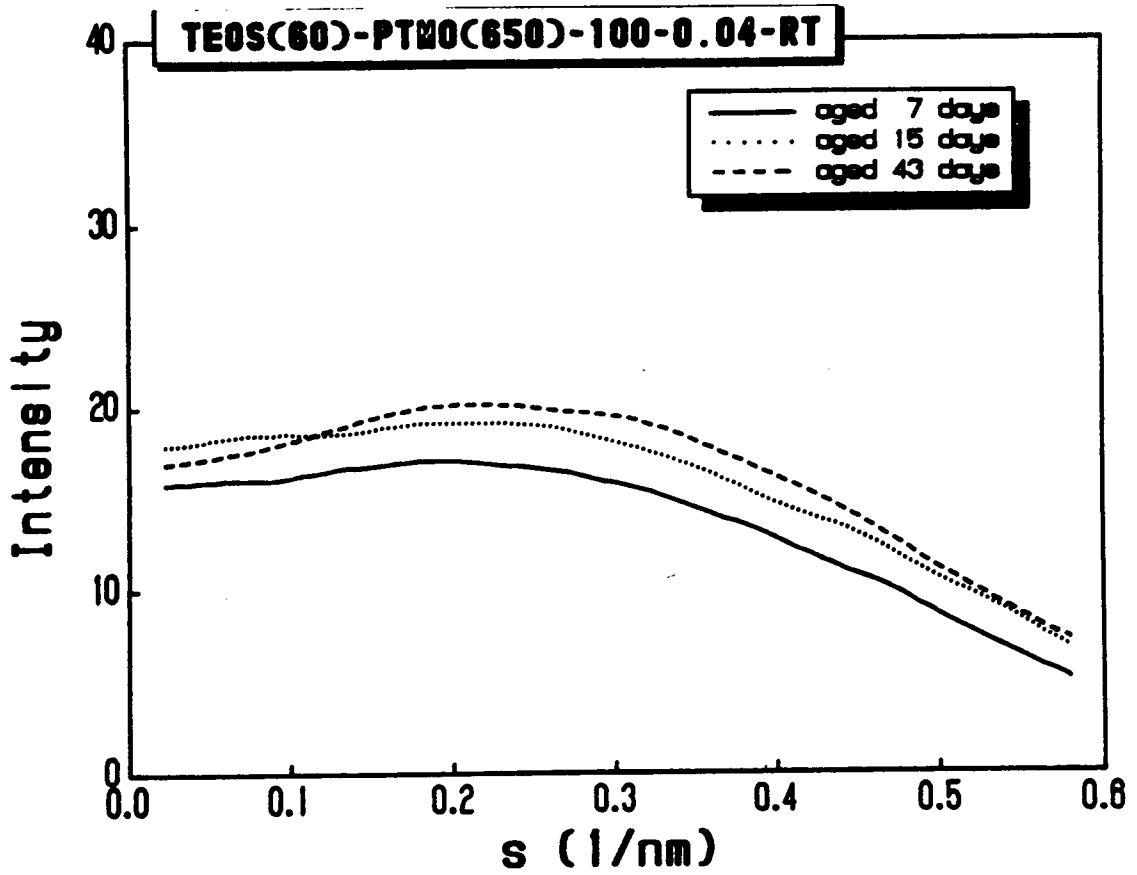
Figure 5.39 Aging effect on the SAXS behavior of a material prepared with 60 wt% TEOS and PTMO(650).
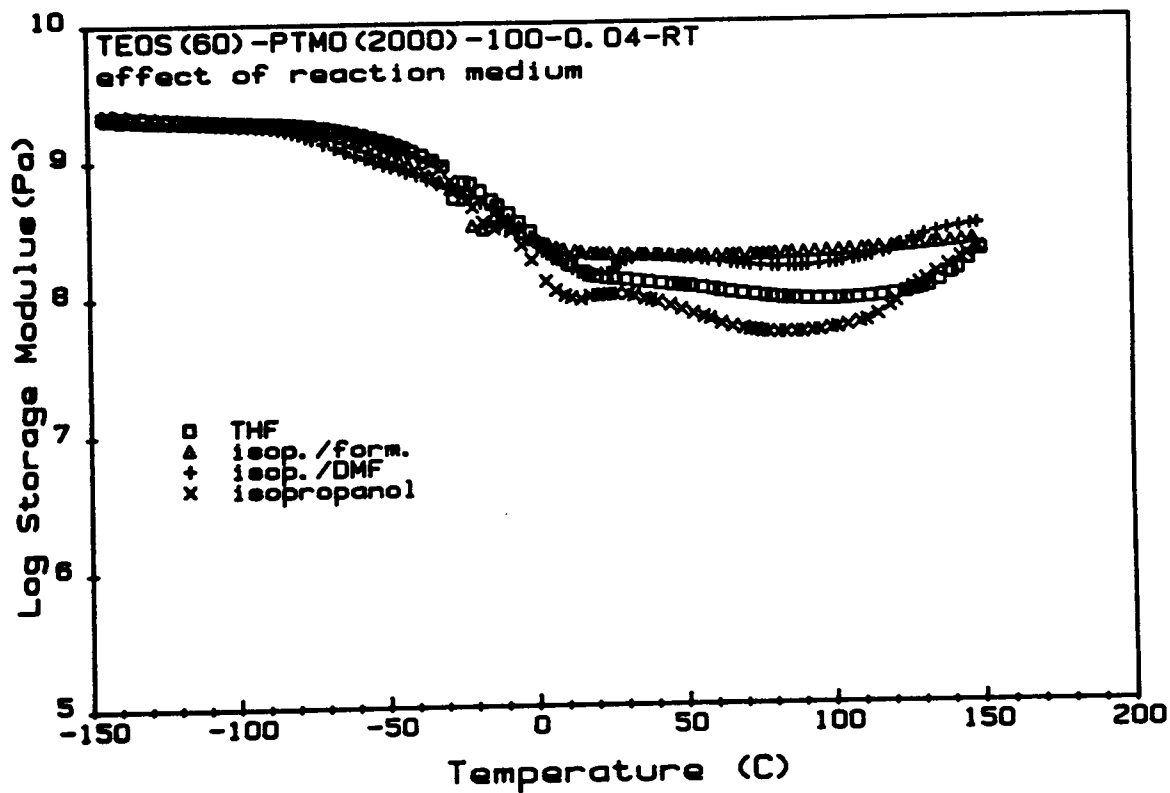
Figure 5.40 Spectra of storage modulus of materials prepared with 60 wt% TEOS, PTMO(2000), and various reaction media.
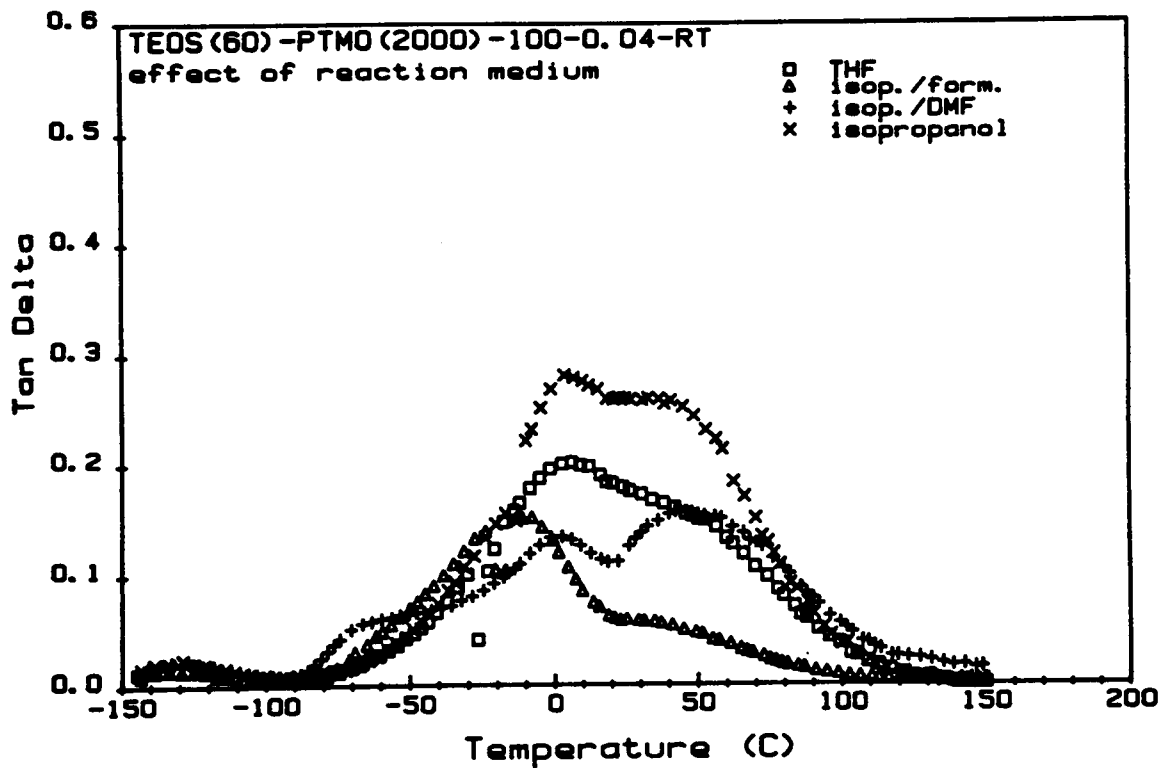
Figure 5.41 Spectra of tanδ of materials prepared with 60 wt% TEOS, PTMO(2000), and various reaction media.
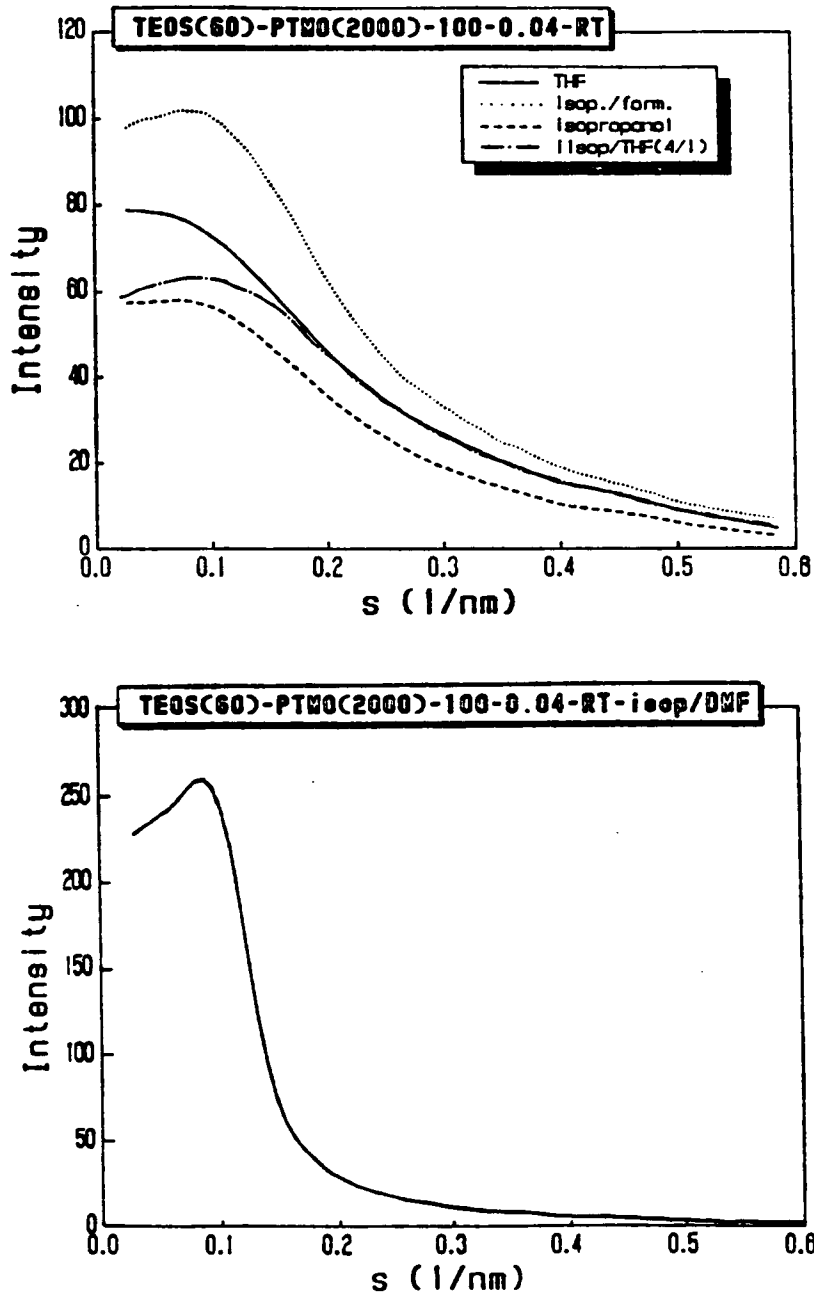
**Figure 5.42** SAXS profiles of materials prepared with 60 wt% TEOS, PTMO(2000), and various reaction media.

CHAPTER SIX

HYBRID SYSTEMS BASED ON TEOS AND PTMO

POSSESSING MULTIPLE TRIETHOXYSILANE GROUPS

In the previous chapters, low molecular weight functionalized oligomers were utilized to produce hybrid materials. It was hoped that an intimate incorporation could be achieved by using these short chains. However, this does not exclude the possibility of using organic components with higher molecular weights. In fact, for the same glass content the material prepared with PTMO(2900) showed a higher tensile strength than all the others, indicating this approach to be a good prospect for using other polymeric compounds for this modified sol-gel reaction. Nevertheless, this material also showed lower values of modulus and glass transition temperature than those made with lower oligomeric molecular weights. These results indicated that the continuity of the glassy phase decreased and, therefore, the oligomers became less restrained and the final material was less stiff. As the molecular weight of the organic component increases further, one may expect to observe an even lower stiffness.

One way to increase the stiffness and, hopefully, the strength of the final materials is to increase the continuity of the glassy phase. Although an increase in glass content is an alternative, this will usually result in a drastic drop in the extendibility and, consequently, a decrease in the tensile strength. Another way to potentially promote the continuity of the glassy phase is to increase the number of reactive sites on the organic component. In other words, besides the terminal functional groups as those in all the PTMO oligomers, some functional groups along the backbone of the chain should help achieve this purpose. The success of the incorporation of these multifunctional

compounds should not only produce materials with higher stiffness and strength, it should also provide a promising way for incorporating polymeric species into these hybrid systems.

In this part of investigation, PTMO based species with various numbers of triethoxysilane (tri-EOS) groups were utilized for the modified sol-gel reaction. The procedure of preparing these new species were given earlier in chapter three. Basically, it is a procedure that is rather similar to producing segmented polyurethanes. Hydroxyl terminated PTMO with a molecular weight of 1000 was utilized to form the main part of the backbone, and these oligomers were reacted with isophorone diisocyanate to form urethane linkages. The approach is similar to many synthesizing segmented polyurethane materials in which butanediol(BD) is used as the chain extender. In the present case, the molar ratio of BD/PTMO is approximately 2. To insure a hydroxyl termination for the final product, an NCO/OH ratio of 0.88 was used in all cases. After this hydroxyl terminated species was formed, an excess amount of isocyanato-triethoxysilane was added to the system and formed the necessary functional groups for the sol-gel reaction. This procedure would produce linear molecules with terminal tri-EOS groups. In order to obtain additional tri-EOS groups, tri-hydroxyl species would have to be used. Therefore, in the first step of the reaction, part of the butanediol was replaced by trimethylol propane to achieve this purpose. Due to the low NCO/OH ratio and steric hindrance, the third hydroxyl group on the trimethylol propane would most likely be preserved after the first step of the reaction, resulting in additional reactive groups along the backbone of the PTMO based species. These additional hydroxyl groups would then react with the isocyanato-triethoxysilane (due to the large excess amount of the latter) and establish the tri-EOS groups needed for the sol-gel reaction. According to this

reaction procedure, the number of reactive groups per molecule could be controlled by adjusting the amount of trimethylol propane in the reaction.

To illustrate the structure of these multifunctional materials, a simplified drawing is provided in Fig. 6.1. For simplification, only four tri-EOS groups are shown in this illustration. Obviously, with the increased functionality, the mobility of this molecule will be greatly reduced when connected to the final network. Furthermore, the glassy phase may even become continuous if bridging between tri-EOS groups and TEOS occurs. As the number of tri-EOS group increases, these effects should be even more significant. Experimental results that support this point will be provided in section 6.1. However, there are some general remarks about these new organic species which should be first noted:

1. As mentioned earlier, the number of tri-EOS group per molecule can be controlled by adjusting the amount of trimethylol propane for the reaction. However, this number should only be taken as an average value and a distribution is expected in the real system. Even though this average number can be controlled by the reaction stoichiometry, the positions of these tri-EOS groups are random due to the reaction procedure.

2. Although these new organic species are based on PTMO oligomers (MW = 1000), a direct comparison with those shown in the previous chapter may not be appropriate. This is mainly due to the existence of the hard segments (isophorone and butanediol), which may influence the behavior of the PTMO oligomers. Hence, instead of appending this part of work to those shown in the last chapter, it is reasonable to make these new hybrid systems stand on their own right.

3. Since these multifunctional materials were dissolved in THF (30 wt% solid), the reaction medium used for the modified sol-gel reaction was somewhat changed also. Instead of using a mixture of isopropanol and THF, only isopropanol was added to the solution and its amount was equal to that of THF from the PMTO oligomers. This change resulted in a more dilute system than those in the previous chapter.

All the materials prepared using these multifunctional oligomers were transparent, and the strength seemed to be much higher than those discussed in the previous two chapters. Due to the large amount of solvent added, these systems were relatively less viscous. The effects of two important variables -- the number of tri-EOS group per molecule and the TEOS content --were studied, and the results of properties measurements and structural characterization will now be discussed.

6.1 EFFECT OF NUMBER OF REACTIVE GROUPS

As illustrated by the schematic drawing shown in Fig. 6.1, the presence of additional tri-EOS groups along the backbone of the PTMO should enhance the incorporation of the oligomer/polymeric species, increase the restriction on the mobility of these species, and promote the continuity of the glassy phase. However, all these speculations need to be proven or disproven by the experimental results. Furthermore, as discussed earlier in this chapter, the number of tri-EOS group per molecule can be controlled by adjusting the amount of trimethylol propane for the reaction. As this number changes, the incorporation of these species into the silicate network should also be affected and, as a result, the final properties and structure also would be changed. Therefore, it should be important to understand not only the effect of the presence of additional tri-EOS groups,

but also the effect of the number of tri-EOS groups per molecule on the structure-property behaviors of the final hybrid materials.

In order to understand these effects, four PTMO oligomers with various numbers of tri-EOS groups per molecule were used to prepare hybrid materials. The overall molecular weight of these oligomers before reacting with isocyanato-triethoxysilane was 5800 g/mole; the calculated average number of tri-EOS groups per molecule ranged from 2 to 5. The water content was 100%, the acid content was 0.04, and the initial TEOS content was 50 wt%. Due to the finite molecular weight of the triethoxysilane, the actual initial silane content would be slightly higher than 50 wt%. Depending on the average numbers of tri-EOS groups, this value would also be different. However, due to the high molecular weight of these species, the difference in the initial silane content was rather insignificant (ranging from 52.5 to 56 wt%). Therefore, any variation in the final structure and properties should be attributed to the effect of the number of tri-EOS groups per molecule.

All the solutions of this series of systems were clear and free of any phase separation. Also, all the materials prepared were transparent. Although all systems still gelled within a few minutes, the gelation time was slightly longer than those observed for the PTMO containing systems. This may be attributed to the higher dilution of these systems. Warping and cracking problems became more noticeable as the average number of tri-EOS groups per molecule increased, indicating that the crosslinking density increased and the system became more densely connected. This point will be verified by other data given later in this section. Without carrying out any measurements on mechanical properties, it was apparent that the stiffness increased with the average number of tri-EOS groups. In fact, it became rather difficult to cut a dogbone sample for the

material prepared with PTMO with 5 tri-EOS groups. This again was an indication of difference in the crosslinking density. One important point should be noted that some of the materials were cast onto a glass surface to test the potential of coating application, and the results were very encouraging. No cracking was observed after long drying times, and these transparent coatings adhered to the glass surface very well. The coating possibility of using these systems for coatings could become an important feature in considering potential applications.

Stress-strain experiments were first carried out on these materials, and a set of examples for this series is shown in Fig. 6.2. The variable X in this figure represents the average number of tri-EOS groups for the oligomer. One sees that the range of elongation at break is considerably higher than those shown by the endcapped PTMO materials (see chapter 5), which is somewhat reasonable since the molecular weight is higher in this case. However, this elongation at break decreases as the average number of tri-EOS groups decreases. Secondly, the tensile strength is also much higher for these materials than those shown before. In fact, it reaches 50 MPa. for the sample with only two tri-EOS groups (i.e., tri-EOS terminated.) This relatively high strength makes these materials more attractive in terms of practical applications. Finally and most importantly, these stress-strain curves show a distinct new feature-- a yield point. For the sample with two tri-EOS groups, the stress increases sharply with the strain at the beginning. However, after the strain reaches about 10%, a "bending" of the curve is observed and the increasing trend of the stress becomes lower. As the average number of tri-EOS groups increases to 3, this bending becomes more noticeable and the stress is almost constant after the bending point for a while before increasing again. Although this bending can not yet be viewed as a yield point, the trend with increasing number of tri-EOS groups is clear. As the average number of tri-EOS groups increases to 4 and

higher, a yield point is clearly shown and it tends to be sharper for the one with higher number of tri-EOS groups (i.e., x = 5.) This observation of a yield point and its trend with increasing number of tri-EOS groups strongly imply that the glassy phase has become more continuous.

To further understand the effect of the number of reactive groups on the mechanical properties, repetitive experiments were performed and the data are shown in Table 6.1. Similar to the trend shown by the examples in Fig. 6.2, the elongation at break increases from 48% to ca. 250% as the average number of tri-EOS group decreases from 5 to 2. Furthermore, the Young's modulus increases from ca. 210 to 720 MPa. as the number of tri-EOS groups increases from 2 to 5. This range of modulus is considerably higher than most of the materials prepared using the endcapped PTMO oligomers, and the magnitude is close to that of a glassy polymer, especially the material with the highest number of tri-EOS groups. Above all, both of these trends indicate that the nature of the material becomes more glassy as the number of tri-EOS groups increases. Regarding the tensile strength, a slight increasing trend is observed as the number of tri-EOS groups decreases. Furthermore, the magnitude is always higher than 40 MPa. and is a significant improvement over the previous hybrid materials.

As shown by the stress-strain results, the modulus of these multifunctional PTMO containing materials is always close to that of a glassy polymer. This observation indicates that the T_g of the PTMO oligomers in these systems is higher than the ambient temperature, under which the stress-stain experiments were carried out. To verify this speculation, dynamic mechanical experiments were performed and the results are shown in Figs. 6.3 & 6.4. The general behavior of storage modulus is similar for all the materials. A very long plateau region with a magnitude of 10^9 Pa. is observed ranging

from -150°C to near 0°C, depending on the average number of tri-EOS groups. The temperature at which the modulus begins to decrease depends on the number of tri-EOS groups that the oligomer possesses. The more the tri-EOS group present, the higher this temperature will be. After this glassy plateau region, the modulus begins to decrease with increasing temperature until reaching a minimum with a magnitude in the order of 10^7. Pa. The more tri-EOS groups the oligomer possesses, the higher the magnitude of this minimum will be. After reaching this minimum, the modulus begins to increase with the temperature until the end of the experiment. General speaking, this behavior is similar to all the previous results. However, the glassy plateau is relatively long considering the high oligomeric molecular weight. This indicates the absence of oligomer rich region, and the T_g of the oligomers has been shifted to a much higher temperature. One more thing to mention is that the trend of modulus shown by these data is consistent with what was shown in the earlier stress-strain experiments.

To further understand the physico-chemical environment of the oligomers in these hybrid materials, the tanδ spectra that shown in Fig. 6.4 were examined. First, a low maximum is observed at -130°C for all the materials. As being reported by a previous work [80], this can be attributed to the rotation of the methylene groups of the PTMO. Secondly, a very low maximum is observed at -70°C. As shown in the previous chapter on the endcapped PTMO containing materials, this can likely be attributed to the PTMO rich phase. However, since the intensity of this maximum is so low, it is reasonable to conclude that very little PTMO rich phase exists in the present systems. Finally, a high-intensity maximum is observed at higher temperatures. This major transition temperature increases from 63°C to 102°C as the average number of tri-EOS groups increases from 2 to 5, which clearly indicates that the restrictions on the oligomers change with the number of tri-EOS groups.

As discussed in previous chapters, the restrictions being imposed on the oligomers have a direct effect on the mobility of these incorporated chains and, consequently, on the glass transition temperature of these oligomers. For the endcapped PTMO species discussed in chapter 5, restrictions are caused by both the endlinking of these oligomeric chains and the interaction between them and those partially condensed TEOS. However, in the present systems, two more factors need to be taken into account. First is the restrictions caused by linking the tri-EOS groups with the condensed TEOS. For molecules with the same molecular weight, this type of restriction should increase with the number of tri-EOS groups. This point is strongly supported by the fact that the T_g observed in the tanδ spectra increases with the average number of tri-EOS groups. Secondly, the mobility of the chain may also be reduced by the aggregation of the hard segments. As mentioned earlier, these multifunctional PTMO oligomers are basically segmented polyurethanes. The soft segments consist of the PTMO(1000) and the hard segments are formed by isophorone and butanediol. Due to the presence of these hard segments, the mobility of the PTMO chain may also be affected.

To understand the effect of these hard segments, one can compare the sample with only terminal tri-EOS groups (i.e., $x = 2$) to those made with endcapped PTMO oligomers (see chapter 5.) The general structure (in terms of tri-EOS groups) of these species are basically the same, except that the former has a higher molecular weight and some hard segments in the backbone. Therefore, difference in properties could partially be caused by the presence of these hard segments. As concluded earlier, the T_g of the oligomers decreases as the molecular weight increases. For the material made with PTMO(2000), the T_g is near 0°C. Therefore, if there were no hard segments, the T_g for a PTMO oligomer with a molecular weight of 5800 should be even lower. However, as shown in

Fig. 6.4, the T_g of this particular material ($x = 2$) is 63°C. This great difference (63 and 0°C) indicates that the hard segments may well influence the T_g.

In addition to increasing the restrictions, the presence of additional tri-EOS groups also causes the silicate species to become more continuous. As discussed in the previous chapter, the organic species will be the dominant component for a 50 wt% TEOS loading system due to the large weight loss of TEOS in the hydrolysis reaction. As a result, the organic component will most likely be the continuous phase (see the model suggested in chapter 5.) As the oligomeric molecular weight increases, it will be even more difficult for the condensed TEOS to connect together and form the continuous phase. As such systems are subjected to some deformation, the continuous phase (i.e., the rubbery oligomers) will sustain most of the stresses. The result will be that the modulus is low and the extendibility is high, as those shown in the systems prepared with endcapped PTMO oligomers. However, with the presence of some additional tri-EOS groups along the backbone of the oligomers, it is possible for the condensed TEOS to connect and become more continuous. This increase of continuity in the glassy phase will result in an increase in the stiffness and, meanwhile, a decrease in the extendibility. This trend is clearly shown by the mechanical properties shown in Table 6.1. However, some of these extra linkages resulted from the tri-EOS groups may break if the stress is high. This breaking of glassy linkages does not necessary cause the material to fracture since the rubbery phase may still able to sustain the stress. However, it should result in a drastic drop in the stress level and cause the appearing of a yield point. The more tri-EOS groups the oligomers possess, the higher the continuity is for the glassy phase. As a result, the higher the probability is for the final material to shown a yield point. This point is again strongly supported by the stress-strain curves shown in Fig. 6.2.

Another method to verify this postulation of higher continuity is the degree of swelling. As the number of tri-EOS groups increases, the oligomers are connected into the network through more sites and, therefore, the crosslinks per unit volume should increase. This increase in the crosslinking density should result in a decrease of the swelling ability of the final material. To verify this point, all the materials were swollen with THF and the results are shown in Fig. 6.5. As the average number of tri-EOS groups increase, the swelling ratio of the final material decreases, which is exactly in line with all the other experimental results.

To provide further information on the structure of these hybrid materials, SAXS experiments were performed. The resulting profiles are shown in Fig. 6.6. Similar to all the previous SAXS results of PTMO containing materials, a broad maximum is observed in all cases. As discussed in the previous chapter, the presence of a maximum indicates that a correlation distance exists in the scattering sample. Furthermore, the value of s at which the maximum is observed increases with the average number of tri-EOS groups. Since the correlation distance is inversely related to the value of s, this trend means that the distance increases as the number of tri-EOS groups decreases. Furthermore, the intensity in the tail region tends to increase as the number of tri-EOS groups increases. This indicates that not only the correlation distance changes, but a smaller periodicity in structure results with an increase in the number of tri-EOS groups.

For the hybrid systems prepared with endcapped PTMO oligomers, a schematic model was suggested in the previous chapter to explain the SAXS behavior. As suggested by the model, part of the TEOS may become highly condensed and forms the cluster structure. Due to the high functionality of the end groups, both ends of the oligomers will most likely be connected to these clusters. As a result, the SAXS correlation distance

should be equal to the average center-to-center distance of these clusters, which is close to the sum of the size of the cluster and the end-to-end distance of the oligomers. This model has proven to be consistent with all the experimental results. Although this model can still be applied for the present systems, some important points should be considered in interpreting the results:

1. Due to the presence of the hard segments, the end-to-end distance of the oligomers may not be the same as that of a pure PTMO oligomer with the same total molecular weight. Therefore, although the molecular weight is 5800, the end-to-end distance for the oligomer with 2 tri-EOS groups (i.e., tri-EOS terminated) may not be estimated by the Flory-Fox equation based on $M_n = 5800$. In fact, the SAXS correlation distance for the case of $x = 2$ in Fig. 6.6 is lower than that of the case with endcapped PTMO(2900). This means that the presence of the hard segments may cause the end-to-end distance to become lower than that calculated theoretically.

2. With additional tri-EOS groups present, they may also connected to the highly condensed TEOS clusters. In fact, from the results of the dynamic mechanical experiments, these tri-EOS groups appear to be linked to the glassy phase (i.e., the clusters). Therefore, the distance between clusters will most likely decrease, which results in a decrease in the SAXS correlation distance. As the number of tri-EOS groups increases, this distance should decrease even further. This line of argument is consistent with the trend shown by the SAXS results.

3. Since the positions of the tri-EOS groups are not controllable in the present systems, a distribution is expected. As the number of tri-EOS group increases, not only the average distance between tri-EOS groups decreases, the distribution of this distance should also shift toward smaller values. The former results in the decrease of the

SAXS correlation distance, and the latter results in the increase in the tail scattering intensity.

4. Another interesting point to note is that as the number of tri-EOS groups increases, the SAXS correlation distance approaches that of the material prepared with endcapped PTMO(1000), which is the major component of these multifunctional species. This can be understood by the following interpretations. The extreme case for the addition of tri-EOS group is that all the butanediols are replaced by trimethylol propane, and these tri-EOS groups will then be separated by, on the average, a PTMO(1000) oligomer. After the formation of the silicate network, these tri-EOS groups will most likely be connected to highly condensed TEOS clusters. Therefore, the SAXS correlation distance should approach that of the material with endcapped PTMO(1000) oligomers. This result again supports the validity of the suggested model.

Generally speaking, the SAXS results confirm that the tri-EOS groups along the backbone offer additional linkages for the oligomers to be incorporated into the silicate network. Most of these tri-EOS groups will most likely be connected to the silicate clusters suggested in the previous model, and these additional crosslinks cause the oligomeric chains to be more restrained and the stiffness of the final material to become higher. In other words, the results of structural characterization offer further support to the interpretation given before based on the mechanical properties.

To summarize, the addition of tri-EOS groups to the oligomers shows a significant effect on the incorporating process. Due to the additional connection caused by these tri-EOS groups along the backbone, the mobility of the oligomers decreases and results in a higher T_g. Furthermore, higher continuity of the glassy phase is shown by the presence

of a yield point in the stress-strain behavior. This higher continuity also causes the stiffness to increase considerably. The model suggested before can still be applied to the present systems, except that the end-to-end distance of the oligomers can no longer be estimated by the Flory-Fox equation due to the existence of the hard segments. One important improvement of these materials is the tensile strength, which reaches 50 MPa. for some cases. This high strength may become crucial when considering practical applications for these hybrid materials. Furthermore, the success of preparing these systems also provokes the possibility of utilizing high molecular weight polymers for this modified sol-gel reaction.

6.2 EFFECT OF TEOS CONTENT

From the results shown in the previous section, one can see that a change in oligomeric structure and addition of tri-EOS groups considerably improved the final strength of the material. For these new hybrid systems, the continuity of the glassy phase could be achieved without going through a phase inversion. As a result, the elongation at break was still high and, consequently, the tensile strength was relatively high. However, these results were obtained using a fixed TEOS content (50 wt%.) As the TEOS content changes, this continuity should also be affected and so should the final structure and properties. Therefore, a study on the effect of TEOS content should be necessary. Moreover, this study should also provide some information on the validity of the model suggested before.

A series of materials with various TEOS content, ranging from 0 to 70 wt%, were prepared using the PTMO oligomer with four (average) tri-EOS groups. The water content was 100% and the reaction procedure was according to that shown in section

3.3. Similar to that observed in the TEOS series using endcapped PTMO oligomers (see section 5.2), the gelation time tended to increase with TEOS content. Although quantitative comparison could not be made until the stress-strain experiments were performed, the material apparently became stiffer and stronger as the TEOS content increased. Even for the material with 70 wt% TEOS, cutting dogbone samples was still possible (unlike the case of endcapped PTMO.)

As shown in the previous section, the continuity of the glassy phase is strongly indicated by the presence of a yield point in the stress-strain curve. Therefore, the stress-strain experiments were first carried out on this TEOS series so that an understanding on the macroscopic properties could be achieved. In Fig. 6.7, examples of the resulting stress-strain curves for each TEOS content are shown. It is obvious that the general behavior is quite different among these curves. For the materials with low TEOS contents (i.e., 0 and 20 wt%), the stress increases steadily with the strain. The initial modulus is low and the elongation at break is relatively high, which implies the rubbery nature of these materials. As the TEOS content increases to 40 wt%, a bending in the curve is observed. As noted earlier, this bending can be viewed as a first indication of increasing continuity of the glassy phase. In addition, the initial modulus is now higher and the elongation at break is somewhat lower than the previous samples. As the TEOS content increases further to 50 wt%, a yield point begins to show, which implies that the continuity of the glassy phase has increased considerably. Meanwhile, the initial modulus shows a drastic increase while the elongation at break decreases to less than half of the 40 wt% TEOS material. Finally, for the case of 60 wt% TEOS, the yield point becomes even more significant. The modulus is the highest among all the materials while the elongation at break is the lowest. From this trend of changing in the general stress-strain behavior, one can see the developing of the continuity of the glassy phase

with the increasing TEOS content. Another point should be noted is that the tensile strength increases with the TEOS content up to 60 wt%.

To further verify the trends observed in the mechanical properties, repetitive experiments were performed and the results are shown in Table 6.2. The modulus increases systematically with the TEOS content and seems to reach a plateau at 60 wt%. The magnitude is ca. 10^9 Pa., which is similar to that of a glassy polymer. The values of the elongation at break for the three lower TEOS content samples are approximately in the same range. However, it decreases significantly as the TEOS content increases to 50 wt%. More importantly, this is also the point where a yield behavior begins to show. Furthermore, as the TEOS content increases to 70 wt%, the elongation at break again decreases drastically from ca. 70% to 9%. This large drop indicates that there may be a phase inversion taking place. Regarding the tensile strength, a maximum is observed for the sample with 60 wt% TEOS, which is close to the onset point of a phase inversion. This observation is in line with what shown before for the systems with endcapped PTMO oligomers.

To better understand how the TEOS content influences the environment of the oligomers, dynamic mechanical experiments were carried out. The results of the storage modulus spectra are shown in Fig. 6.8. By recalling the results shown in Fig. 5.9 on a TEOS series for endcapped PTMO(2000) oligomers, the material made with very low TEOS content shows a crystallization behavior at low temperatures. However, for the present systems, even the material made with 0 wt% TEOS shows no crystallization in the experiment. In addition, the modulus does not show a significant decrease until approximate -10°C. Both these observations indicate that the presence of both the hard segments and tri-EOS groups along the backbone has produced sufficiently high

restriction and, therefore, the oligomeric chains are not able to form any crystalline structure. As the TEOS content increases further, the modulus becomes higher and the point at which the modulus begins to decrease shifts toward high temperatures. This increasing trend in modulus is consistent with that shown by the stress-strain results.

The corresponding tanδ spectra are shown in Fig. 6.9. A trend is clearly shown for the transition temperature (taken as the point where the maximum occurs): as the TEOS content increases, the T_g shifts to higher temperatures. The overall intensity is approximately the same for the three lower TEOS content materials. However, as the TEOS increases to 50 wt%, the intensity decreases considerably. Interestingly, this is also the point where the stress-strain curve begins to show a yield point. Therefore, it is reasonable to conclude that the continuity of the glassy phase becomes significant at this composition. By recalling the tanδ spectrum the sample made with 10 wt% TEOS and endcapped PTMO(2000), the T_g was near -70°C and was close to that of the pure PTMO oligomers (see Fig. 5.10.) However, for the present systems, the T_g of the material with 0 wt% TEOS is 32°C. This high transition temperature again indicates the high restrictions caused by the presence of tri-EOS groups along the backbone and hard segments.

In the previous section of the effect of number of reactive groups, the presence of a yield point has been attributed to the continuity of the condensed TEOS species. However, one may also argue that this yield point is simply the result of the connection between the tri-EOS groups only and has nothing to do with the TEOS species. With only one composition, it is not possible to judge which one is the correct interpretation. Therefore, this series of varying TEOS content becomes very important. If the latter argument was correct, a yield point should be observed regardless the composition of the

system. On the other hand, if the first interpretation is correct, one should observe the developing of the yield point with the TEOS content. From the results of the stress-strain experiments (see Fig. 6.7), one can now better accept the first interpretation with more confidence.

From the tanδ spectrum of the 0 wt% TEOS material, one can see that the glass transition temperature has shifted considerably from that of the pure PTMO oligomers. As explained in the previous section, this has to be attributed to a combined effect of the oligomeric structure (i.e., the presence of hard segments) and tri-EOS groups. As the TEOS content increases, more mixing between the two components is expected and, therefore, the T_g will increase. This effect on the glass transition temperature has also been observed in the TEOS content series described in section 5.2. As this T_g increases well above the ambient temperature as the TEOS content increases further, most of the oligomers are basically in the glassy state and, therefore, the modulus of the material becomes very high. Although some continuity of the condensed TEOS species is present, the organic species should still be the dominant component. Therefore, as these glassy continuity is broken by deformation, the system can still sustain some stress without being fractured. However, the stress level should decrease considerably due to the rubbery nature of the oligomers. This line of argument can explain the presence of a yield point in these systems. The result of this yield behavior is that the material will show high modulus and still possess a considerable extendibility. Consequently, the tensile strength will become relatively high. As the TEOS content increases to an extent that the condensed TEOS species becomes the dominant component, the elongation will drop drastically and the sample will most likely fracture before showing any yield behavior. For the present series of materials, this phase inversion point is likely below 70 wt%. For this kind of material, the elongation at break is rather low and, as a result,

the tensile strength is lower than the material just before the phase inversion. In fact, the systems prepared with endcapped PTMO(2000) also show a maximum strength for sample made with a TEOS content just below the phase inversion point.

Up to this point, it has been assumed that the general structure of these new hybrid materials can still be represented by the schematic model suggested in the previous chapter. However, the highly condensed TEOS clusters will now be connected not only to the end groups, but also to the reactive groups along the backbone. For the systems prepared with endcapped PTMO oligomers, an increase of the TEOS content causes the cluster size to increase. As a result, the SAXS correlation distance also increases with TEOS content. For the present systems, the situation may be different. Since the average distance between tri-EOS groups is fixed by the structure of the oligomer and some of the clusters are connected with these tri-EOS groups, a change in TEOS content should not significantly change the distance between the clusters. Therefore, the SAXS correlation distance should be somewhat constant. To confirm this speculation, SAXS experiments were performed on this TEOS series and the resulting profiles are shown in Fig. 6.11. Obviously, the peak position does not show significant change with the TEOS content, which again provides strong support to the suggested model.

Although the correlation distance does not greatly change, the overall scattering intensity increases with the TEOS content. By recalling Fig. 5.11, a similar trend was also observed for the TEOS series based on the endcapped PTMO(2000) oligomer. This increasing tendency may be attributed to the formation of more highly condensed TEOS clusters, which causes the electron density to increase and, as a result, the overall intensity to increase as well. However, as the TEOS content increases to 60 wt%, the profile begins to change its shape and the scattering intensity at the tail region increases

considerably. This can be viewed as an indication of the onset for the phase inversion, which was also observed in the previous chapter.
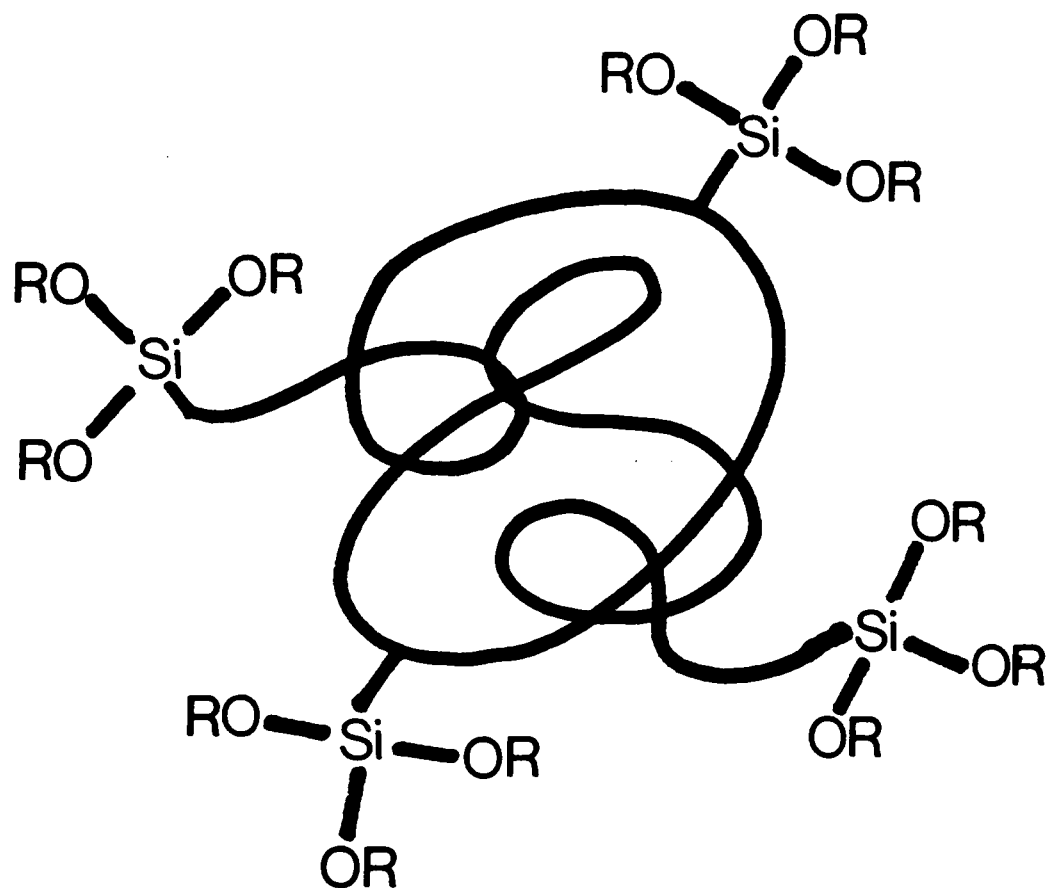
Generally speaking, the effect of TEOS content on these new hybrid systems is similar to that shown in the endcapped PTMO systems. As the TEOS content increases, the modulus increases and the elongation at break decreases. The glass transition temperature, taken as the point where a tanδ peak is observed, also increases with the TEOS content. These trends are due to the increase in the glass content and, therefore, the restrictions on the mobility of the oligomers. However, another important and unique observation in these multifunctional PTMO containing materials is the development of a yield point in the stress-strain curve. This indicates that some continuity of the condensed TEOS species has been developed. This partial continuity causes the stiffness to increase drastically while still possesses a considerable extendibility, which results in an increase in the tensile strength. However, this tensile strength will drop after the occurrence of the phase inversion. The schematic model suggested before can still be utilized to interpret the present systems, except that the highly condensed TEOS clusters may now be formed along the backbone of the oligomers. This should result in an approximately constant distance between clusters, and this point is confirmed by the SAXS results.

Table 6.1   Mechanical properties of materials prepared with 50 wt% TEOS and PTMO with various average numbers of tri-EOS groups --- a series of TEOS(50)-PTMO(58-X)-100-0.04-RT.

functional groups	elongation at break (%)	ultimate strength (MPa)	Young's modulus (MPa)
2	225	35	209
	257	52	230
3	147	45	366
	158	43	393
4	82	43	602
5	48	39	718

Table 6.2 Mechanical properties of materials prepared with various TEOS contents and PTMO with four tri-EOS groups --- a series of TEOS(X)-PTMO(58-4)-100-0.04-RT.

TEOS content	elongation at break (%)	ultimate strength (MPa)	Young's modulus (MPa)
0	255	6	3
20	244	13	12
	200	9	11
40	209	33	92
	208	29	84
50	82	43	602
60	70	50	1030
	75	50	1060
70	9	32	940

Figure 6.1   A simplified drawing of a PTMO oligomer with four tri-EOS groups.
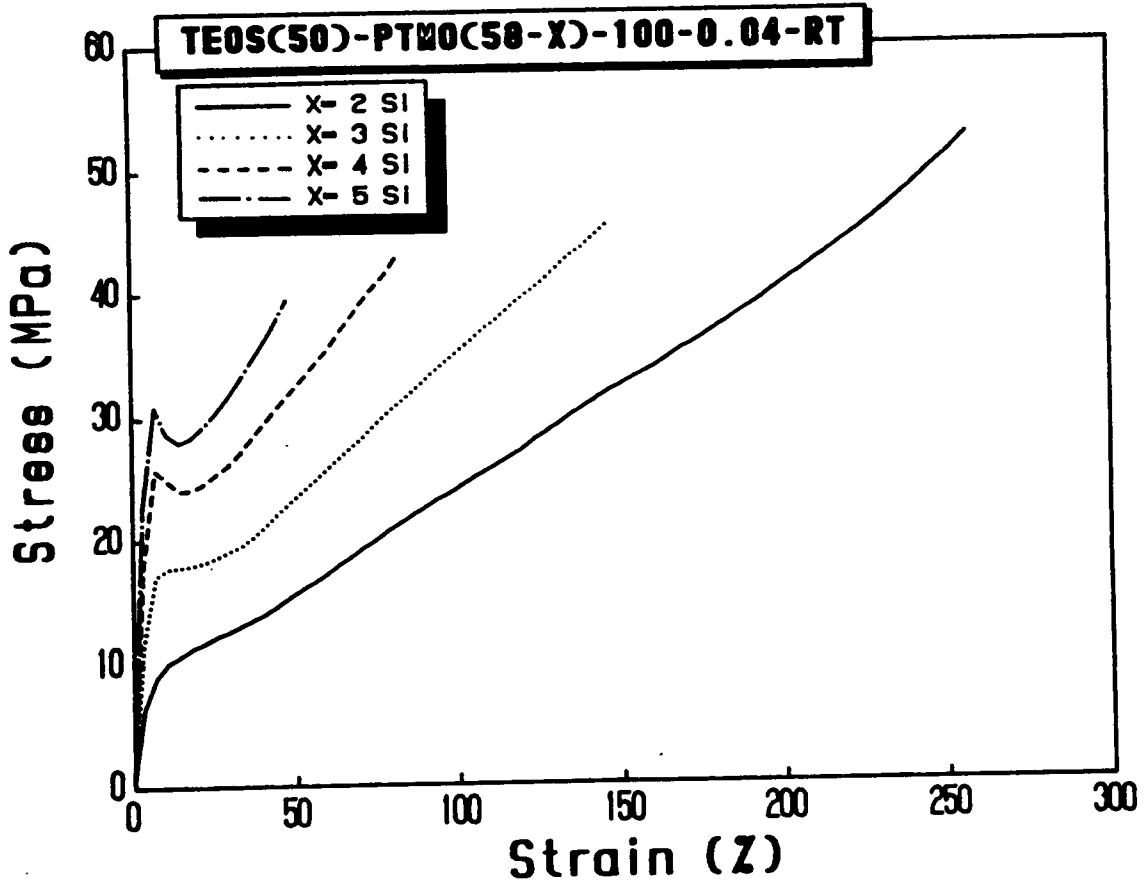
Figure 6.2 Stress-strain behaviors of materials prepared with 50 wt% TEOS and PTMO with various numbers of tri-EOS groups.

Figure 6.3 Spectra of storage modulus of materials prepared with 50 wt% TEOS and PTMO with various numbers of tri-EOS groups.
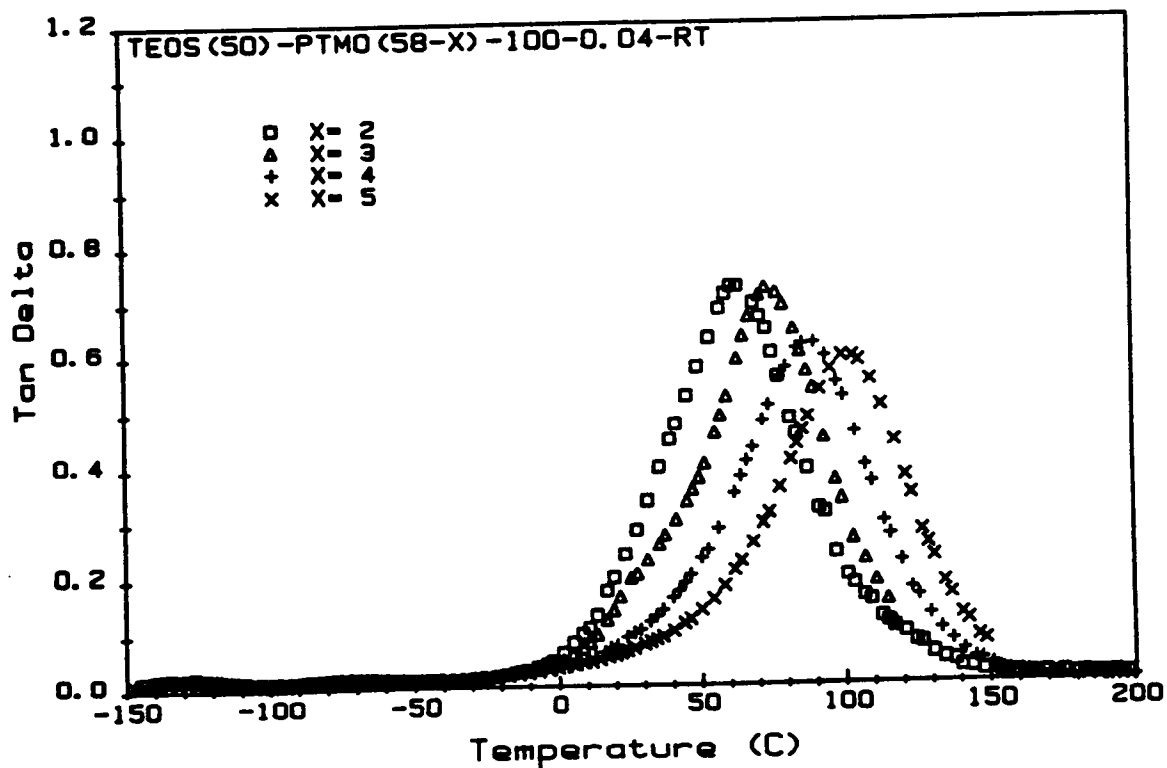
Figure 6.4 Spectra of tanδ of materials prepared with 50 wt% TEOS and PTMO with various numbers of tri-EOS groups.
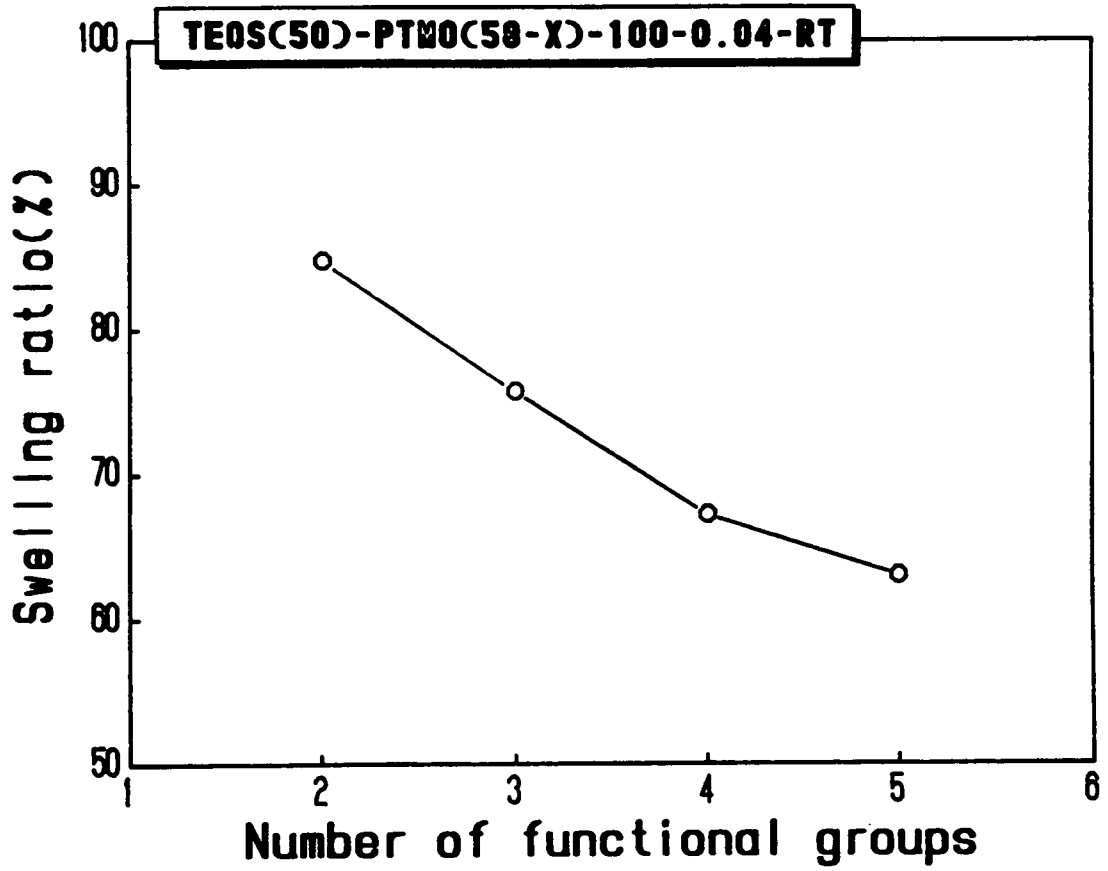
Figure 6.5 Swelling ratio of materials prepared with 50 wt% TEOS and PTMO with various numbers of tri-EOS groups.
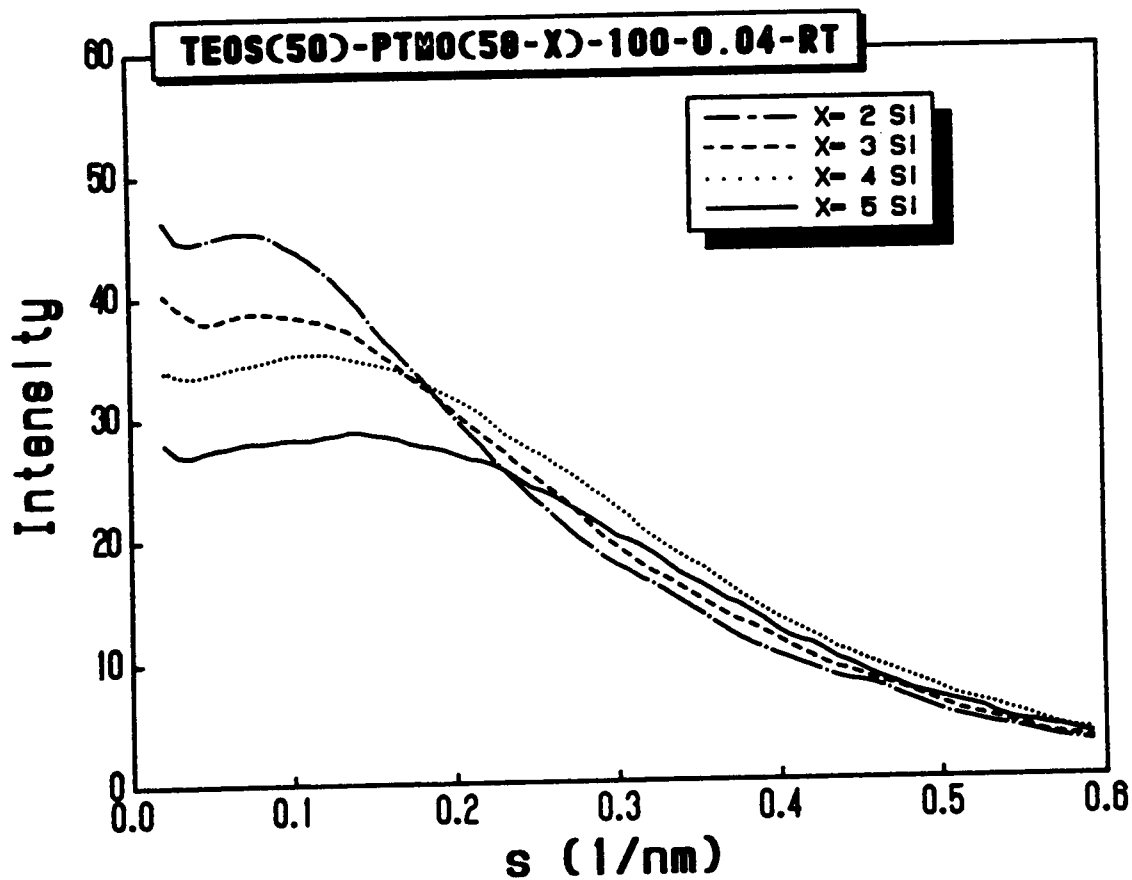
Figure 6.6 SAXS profiles of materials prepared with 50 wt% TEOS and PTMO with various numbers of tri-EOS groups.
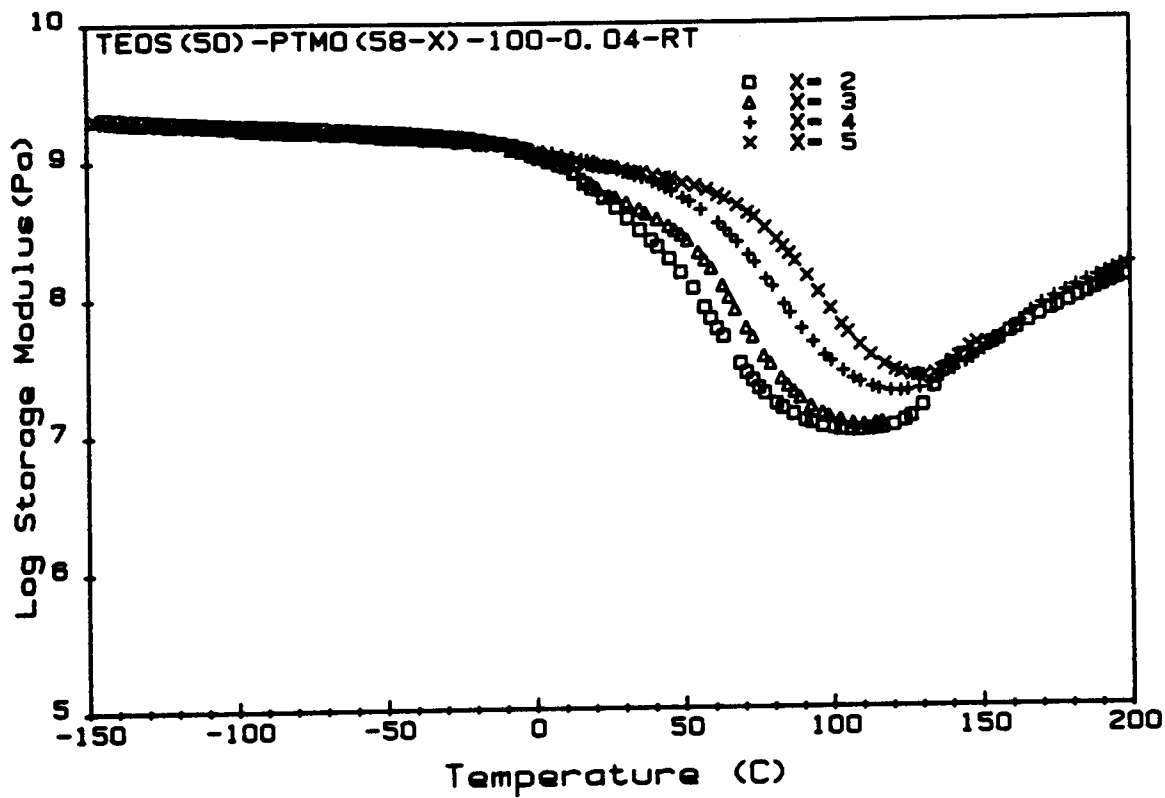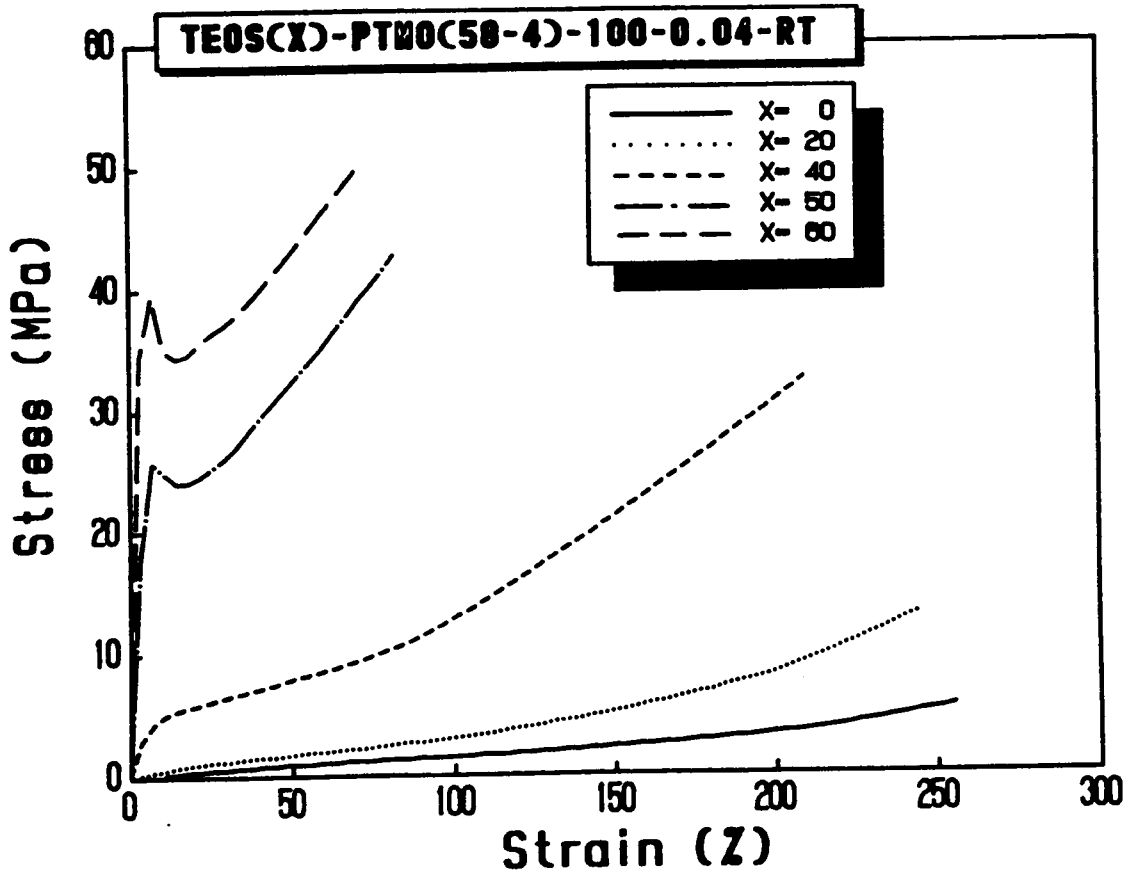
Figure 6.7 Stress-strain behaviors of materials prepared with various TEOS contents and PTMO with four tri-EOS groups.

Figure 6.8 Spectra of storage modulus of materials prepared with various TEOS contents and PTMO with four tri-EOS groups.

Figure 6.9 Spectra of tanδ of materials prepared with various TEOS contents and PTMO with four tri-EOS groups.

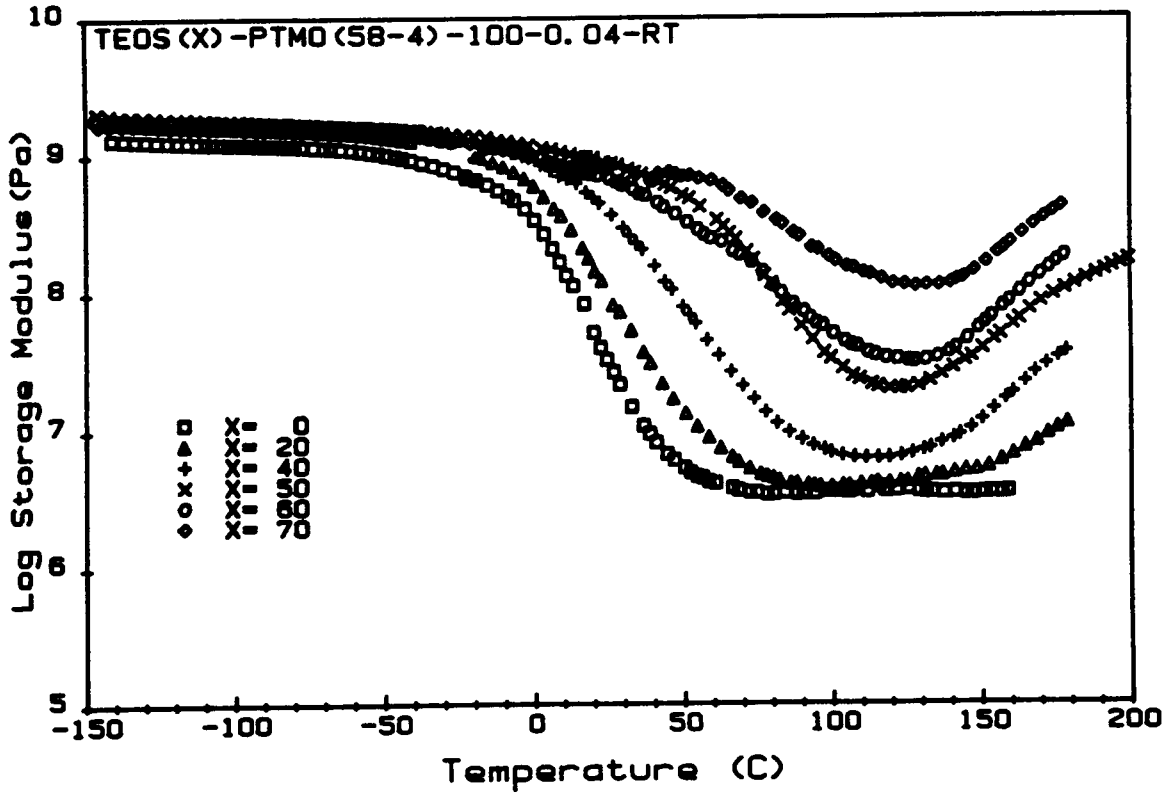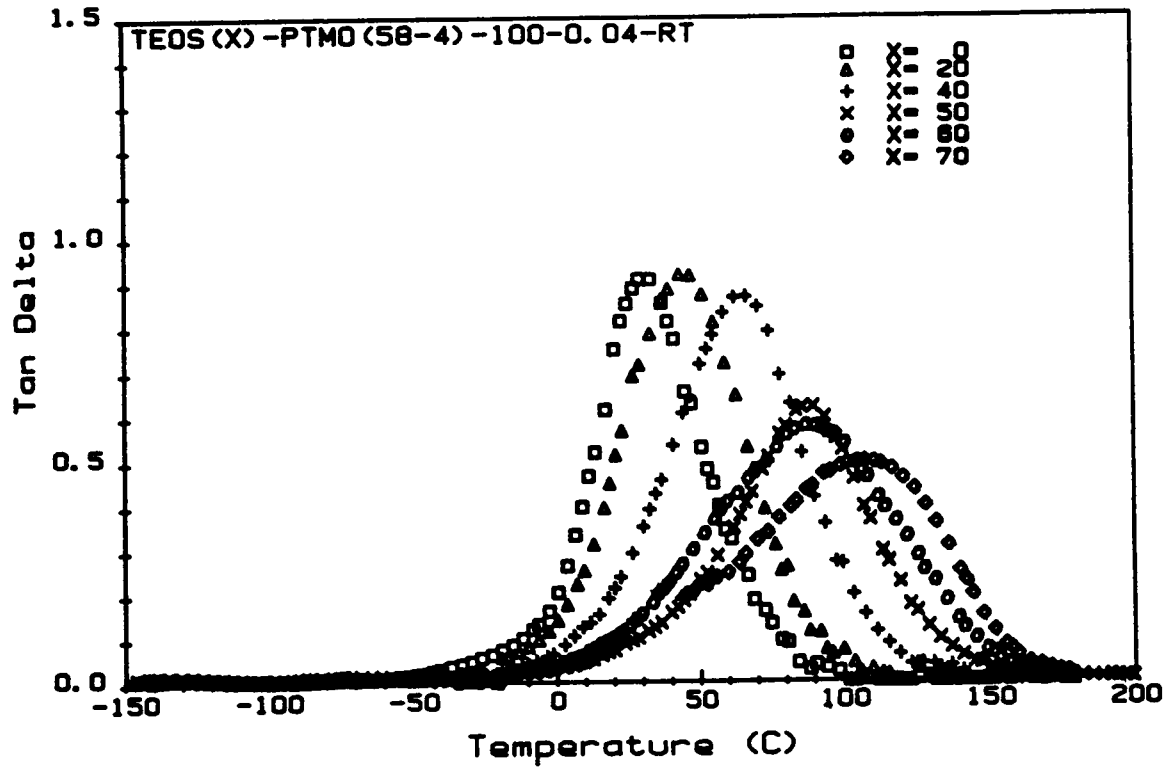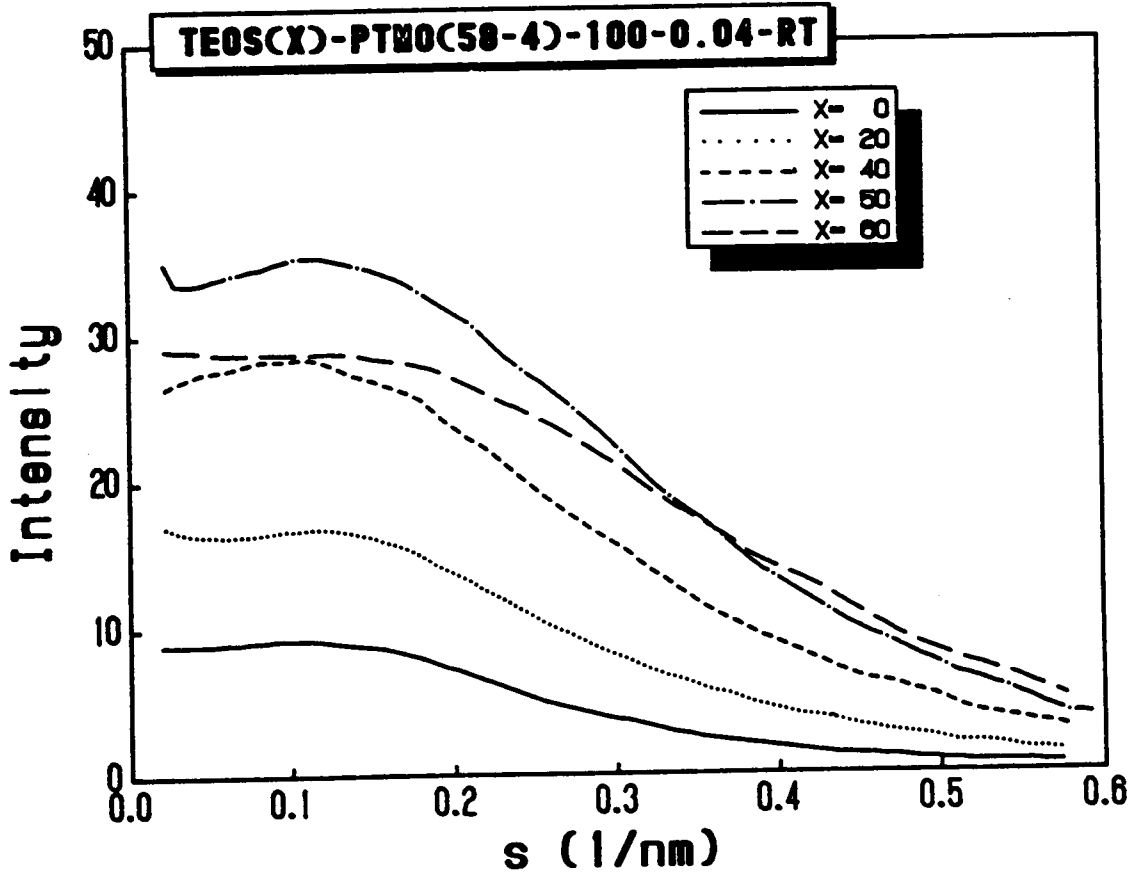**Figure 6.10** SAXS profiles of materials prepared with various TEOS contents and PTMO with four tri-EOS groups.

CHAPTER SEVEN

CONCLUSIONS AND RECOMMENDATIONS

The sol-gel process was successfully utilized to produce hybrid materials incorporating functionalized oligomers with inorganic silicates. The final products showed some characteristics of the inorganic glassy component as well as some properties of the elastomeric oligomers. Cast films with a thickness ranging from a few mils to over 30 mils were successfully produced, and the cracking problem usually found for pure sol-gel systems was considerably reduced. All of the materials prepared by this modified sol-gel process were transparent, which indicated that no large scale phase separation was observed -- at least in the range of the wavelength of light. Even though some of the pure oligomeric components were crystallizable, WAXS and dynamic mechanical experiments showed no crystallinity in most systems. These results indirectly suggested that the oligomers were well dispersed within the final network structure and, therefore, environmental restrictions on the oligomers were sufficiently high so that no crystallization occurred.

One of the oligomers employed to prepare hybrid materials was silanol terminated polydimethyl siloxane (PDMS). The thermal stability of the final product was high, and the ambient modulus was ca. 10^7 Pa. However, the elongation at break for these PDMS containing materials was always lower than 25% and the tensile strength never exceeded 5 MPa. For materials made with 48 wt% initial TEOS content, the tanδ spectra showed a bimodal type of behavior with a sharp maximum at -106°C and a broader maximum or shoulder near -10°C. The first maximum was attributed to a PDMS rich phase, which had lower environmental restrictions and thus showed a T_g close to that of the pure

PDMS (ca. -120°C). The second maximum or shoulder was attributed to those oligomeric chains that were more dispersed into the silicate network. Due to the rigid nature of the TEOS based species, the restrictions on the mobility of these dispersed PDMS oligomers should be rather high and, hence, caused the T_g to increase considerably. By increasing the acid content of the system, the intensity of the first maximum (-106°C) decreased while the second maximum or shoulder increased. From this result, it was suggested that the acid tended to promote a better dispersion of the PDMS oligomers. Due to this, the homogeneity of the final product would increase and this postulation was strongly supported by the invariant analysis on the SAXS data. In terms of mechanical properties, this increase in homogeneity caused the elongation at break to increase from 6 to 15% while the modulus decreased from 20 to 8 MPa. However, the tensile strength showed no noticeable change with acid content.

As the TEOS content increased from 48 to 60 wt%, the overall intensity of tanδ decreased considerably and the T_g dispersion became much broader -- some extended to almost 200°C. This broader transition was attributed to even greater dispersion of the PDMS oligomers, and the lower tanδ intensity was caused by higher glass content in the final materials. Also due to this higher glass content, the modulus became higher but, surprisingly, the elongation at break was in the same range as the 48 wt% TEOS samples. Also, the tensile strength increased by almost 200%. For the systems with 70 wt% TEOS, the stiffness further increased. However, the brittleness also became very high which severely limited the mechanical evaluation of these materials.

Another variable that was studied in these PDMS containing hybrid systems was the oligomeric molecular weight. Two types of PDMS -- with molecular weights of 1700 and 550 g/mole -- were used, and the tanδ behavior showed that the T_g dispersion of the

oligomer shifted toward higher temperatures as the oligomeric molecular weight decreased. In addition, SAXS results indicated that the homogeneity increased as well. A "bending" in the stress-strain behavior was observed in these materials, which was speculated to be caused by the increase of the continuity of the glassy component. Both the modulus and tenisle strength showed an increase with the decrease of the PDMS molecular weight, however, the elongation at break was in the same range. Finally, a triethoxysilane endcapped PDMS with a molecular weight of 1000 was used to study the effect of the oligomeric functionality. The material made with this particular type of high funcitonality (i.e., 6) PDMS was very stiff and brittle, therefore, dogbone samples were not obtainable. Dynamic mechanical result showed that this material possessed a very high modulus (higher than 10^8 Pa.) throughout the entire temperature range for the experiment (i.e., -150 to 200°C.) Furthermore, the tanδ behavior showed almost no loss at low temperatures which indicated the absence of the PDMS rich phase. This significant increase in stiffness and the T_g dispersion were attributed to the high functionality of the oligomers, which resulted in no dangling ends in the system and good dispersion of PDMS.

The second type of oligomer used was the triethoxysilane endcapped polytetramethyleneoxide (PTMO). In this case, the oligomeric hydrophobicity was lower than that of PDMS and the functionality was higher. Both of these factors were expected to improve the dispersion of the oligomers and, hopefully, could result in more homogeneous systems and different mechanical properties. Generally speaking, the materials prepared using these functinalized PTMO possessed higher strength and flexibility. Furthermore, these materials would not adhere to a polystyrene surface. With this higher strength and the usage of a smooth, polystyrene casting substrate, large, highly transparent films were obtained.

The tensile strengths of these PTMO containing materials were in the range of 10-35 MPa., which was a considerable improvement over the earlier TEOS-PDMS systems. Furthermore, only one broad maximum was observed in tanδ behavior and its temperature was always much higher than the T_g of pure PTMO oligomers. This was a strong indication of the absence of a pure PTMO phase. To study the effect of the oligomeric molecular weight, four different types of PTMO --- with molecular weights of 650, 1000, 2000, 2900 g/mole (before endcapping) --- were used to prepare hybrid materials. The results showed that although the modulus tended to decrease, both the elongation at break and tensile strength increased as the PTMO molecular weight increased. SAXS results showed a broad maximum in every sample, which indicated that a correlation distance existed in these materials. This is quite different from the monotonic behavior observed in the TEOS-PDMS systems. Furthermore, the correlation distance of these materials increased with PTMO molecular weight. To rationalize these results, a schematic model was suggested for these PTMO containing systems. Basically, this model suggested two different regions. One was the glassy clusters formed by the highly condensed TEOS species, whereas the other one represented a mixed region of PTMO and partially condensed TEOS. To further verify this model, a series of materials with various TEOS contents were prepared. The results showed that as the TEOS content increased, both the T_g and the SAXS correlation distance increased while the swelling ratio decreased. When extrapolating to zero TEOS content, the SAXS correlation distance was very close to the PTMO end-to-end distance calculated by the Flory-Fox equation. Since the cluster size should increase with TEOS content, this trend agreed well with the suggested model. Furthermore, drastic changes in the mechanical properties and SAXS behavior were observed as the TEOS content increased beyond 70 wt%. The stiffness and brittleness increased considerably after this point and, therefore, a phase inversion was suggested. After this inversion, the TEOS

based species might become the continuous phase and, thus, the materials would show characteristics similar to inorganic glasses -- stiff and brittle. However, the cracking problem was still much less severe than the pure TEOS system.

One important point for these PTMO containing materials was that the mechanical properties changed significantly with time. Generally, the materials became stiffer and less flexible after exposing to air for a long period of time. This phenomenon was termed the "aging" effect. This aging process was attributed to the further curing of the systems, which was caused by the hydrolysis reaction of residual ethoxy groups. Nevertheless, the SAXS correlation distance was not significantly affected by this aging process. Finally, several different reaction media were used to study the effect on the final materials. The results showed that the addition of formamide always produce highly condensed silicate network, which caused the final material to be brittle and stiff. The addition of DMF tended to induce microphase separation and change the SAXS behavior considerably. Nevertheless, all these materials still displayed high transparency.

The last type of oligomer used was PTMO with various numbers of triethoxysilane groups, ranging from 2 (triethoxysilane terminated) to 5 (2 terminal and 3 along the backbone of the chain.) The molecular weight of these oligomers was 5800 g/mole, and they were used with TEOS to prepare the hybrid systems. The resulting materials showed distinct mechanical properties. The Young's modulus was always in the order of 10^8 Pa., and the tensile strength was in the range of 30-60 MPa. Interestingly, a yield point was observed in the stress-strain behavior for some of the materials which possessed more than three triethoxysilane groups. This yield behavior indicated that the glassy phase had become more continuous as the additional reactive groups were introduced, and this continuity resulted in a high modulus without losing much

extendibility. This continuity was further confirmed by the results of a series of materials prepared with various TEOS contents and PTMO with four triethoxysilane groups, in which the development of the yield point was observed with an increase of TEOS content. Furthermore, from the nearly constant SAXS correlation distance of these materials, the model suggested before was again confirmed.

To summarize, this new route of bridging organic and inorganic species has proven to be feasible. With the addition of oligomeric/polymeric components to the silicate network, the flexibility was greatly improved and the cracking problem was considerably suppressed. Although the silanol terminated PDMS was incorporated successfully, the PTMO containing materials apparently showed high mechanical strength. In addition to the variables which were important for the pure sol-gel process, some new variables such as the oligomeric molecular weight, the silicate content, and the average number of triethoxysilane groups also showed significant effects on the final structure and properties. In particular, with the success of incorporating PTMO with multiple functional groups, the possibility of utilizing higher molecular weight species was greatly promoted.

Due to the newness of these hybrid materials, their future development seems exciting and may offer much potential for specific applications. However the author would like to highlight some of the important directions concerning the present project:

1. The structure of these hybrid materials is still far from being completely understood. Although a simplified morphological model was suggested to represent the structure of the PTMO containing materials, further understanding about the clusters, the existence of linear or lightly branched TEOS based species, and the encapsulation of PTMO chains is still needed. To accomplish this, some potential methods are

given as follows: (i) Raman spectroscopy has been used in pure sol-gel systems for studying the molecular structure and, hence, it should be useful in investigating the cluster structure, (ii) Solid state NMR may be used to study the cluster structure and the environment of the oligomers, and (iii) TEM may be used for etched or stained samples to study the structure at a scale of several hundreds of angstroms.

2. In this thesis, mechanical properties were a focal point of the investigation. However, as more potential applications become important in the future, measurements of some other properties may be necessary. For example, in order to use these hybrid materials for coatings, the adhesive and wear properties should be studied. For the application of porous support or substrate, the surface area and porosity should be studied. For the application which requires high thermal stability, the degradation behavior should be investigated. Finally, for the application of fiber drawing, the rheological properties should be first understood.

3. As was discussed in the section on the PTMO containing materials, aging effects were quite significant for these systems. Mechanical properties change considerably with time, which may limit the application of these hybrid materials. One of the potential approaches to minimize this aging effect is to increase the extend of reaction, so that less ethoxy groups will exist to undergo further curing. As shown by the preliminary results in section 5.6, the usage of different reaction media may drive the reaction further to completion. Therefore, it is worthwhile to pursue this approach further so that the stability of these PTMO containing materials can be improved.

4. As was demonstrated in chapter 6, higher molecular weight PTMO with multiple reactive groups produced materials with very high tensile strength -- ca. 55 MPa. This success provokes some other potential studies in the future. First, PTMO with even higher molecular weight and more reactive groups may be used to produce

materials with different properties. Secondly, the PDMS oligomers which showed good thermal stability but poor tensile strength can also be used as the backbone of these high molecular weight, multifunctional compounds. It will be interesting to study the mechanical properties of these new PDMS based hybrid materials. Finally, instead of urethane linkages, other types that are more thermally stable may be developed to produce these multifunctional compounds.

5. As stressed several times in the text, the versatility of this modified sol-gel route is by no means limited to organic elastomeric compounds. Glassy or highly thermally stable compounds can surely be considered in the future. Since the inorganic component(s) is usually very stable, using this approach to produce materials for high temperature applications should be feasible and attractive. However, some new chemistry or reaction procedure may have to be developed so that homogeneous systems can be prepared.

REFERENCES

1. Dislich, H. *J. Non-Cryst. Solids* 1985, *73,* 599.

2. Flory, P. J. *Principles of Polymer Chemistry* Cornell University Press, 1953.

3. Schmidt, H. *Mate. Res. Soc. Symp. Proc.* 1984, *32,* 327.

4. Philipp, G.; Schmidt, H. *J. Non-cryst. Solids* 1984, *63,* 283.

5. Schmidt, H. *J. Non-Cryst. Solids* 1985, *73,* 681.

6. Scholze, H. *J. Non-cryst. Solids* 1985, *73,* 669.

7. Schmidt, H.; Seiferling, B. *Mate. Res. Soc. Symp. Proc.* 1986, *73,* 739.

8. Dislich, H.; Hinz, P. *J. Non-Cryst. Solids* 1982, *48,* 11.

9. Yoldas, B. E. *J. Mate. Sci.* 1979, *14,* 1843.

10. Yamane, M.; Aso, S.; Okano, S.; Sakaino, T. *J. Mate. Sci.* 1979, *14,* 607.

11. Nogami, M.; Moriya, Y. *J. Non-Cryst. Solids* 1980, *37,* 191.

12. Mukherjee, S. P. *J. Non-Cryst. Solids* 1980, *42,* 477.

13. Klein, L. C.; Garvey, G. J. *J. Non-Cryst. Solids* 1982, *48,* 97.

14. MacKenzie, J. D. *J. Non-cryst. Solids* 1982, *48,* 1.

15. Dislich, H. *J. Non-cryst. Solids* 1983, *57,* 371.

16. Wenzel, J. *J. Non-cryst. Solids* 1985, *73,* 693.

17. Aelion, R.; Loebel, A.; Eirich, F. *J. Amer. Chem. Soc.* 1950, 72, 5705.

18. Keefer, K. D. *Mate. Res. Soc. Symp. Proc.* 1984, *32,* 15.

19. Brinker, C. J.; Scherer, G. W. *J. Non-Cryst. Solids* 1985, *70,* 301.

20. Kawaguchi, T.; Hishikura, H.; Iura, J.; Kokubu, Y. *J. Non-Cryst. Solids* 1984, *63,* 61.

21. Iler, R. K. *The Chemistry of Silica* John Wiley, New York, 1979.

22. Schaefer, D. W.; Wilcoxon, J. P.; Keefer, K. D.; Bunker, B. C.; Pearson, R. K.; Thomas, I. M.; Miller, D. E. *AIP Conf. Proc.* 1987, *154*, 63.

23. Pope, E. J. A.; MacKenzie, J. D. *J. Non-Cryst. Solids* 1986, *87*, 185.

24. Sakka, S.; Kamiya, K. *J. Non-Cryst. Solids* 1980, *42*, 403.

25. Sakka. S. *Mate. Res. Soc. Symp. Proc.* 1984, *32*, 91.

26. Schaefer, D. W.; Keefer, K. D. *Mate. Res. Soc. Symp. Proc.* 1984, *32*, 1.

27. Schaefer, D. W.; Keefer, K. D. *Mate. Res. Soc. Symp. Proc.* 1986, *73*, 277.

28. Klein, L. C.; Garvey, G. J. *Mate. Res. Soc. Symp. Proc.* 1984, *32*, 33.

29. Yoldas, B. E. *J. Non-Cryst. Solids* 1982, *51*, 105.

30. Strawbridge, I.; Craievich, A. F.; James, P. F. *J. Non-Cryst. Solids* 1985, *72*, 139.

31. Duran, A.; Serna, C.; Fornes, V.; Navarro, J. M. F. *J. Non-Cryst. Solids* 1986, *82*, 69.

32. Ruland, W. *J. Appl. Cryst.* 1971, *4*, 70.

33. Yoldas, B. E. *Ceramic Bull.* 1975, *54(3)*, 286.

34. Dislich, H. *J. Non-Cryst. Solids* 1983, *57*, 371.

35. Yamane, M.; Inoue, S.; Nakazawa, K. *J. Non-Cryst. Solids* 1982, *48*, 153.

36. Hench, L. L.; Prassas, M.; Phalippon, J. *J. Non-Cryst. Solids* 1982, *53*, 183.

37. Prassas, M.; Phalippou, J.; Hench, L. L. *J. Non-Cryst. Solids* 1984, *63*, 375.

38. Mukherjee, S. P. *J. Non-Cryst. Solids* 1984, *63*, 35.

39. Yoldas, B. E. *J. Mate. Sci.* 1977, *12*, 1203.

40. Dislich, H. *Angew. Chem. Int. Ed. Engl.* 1971, *10(6)*, 363.

41. Hayashi, T.; Yamada, T.; Saito, H. *J. Mate. Sci.* 1983, *18*, 3137.

42. Colby, M. W.; Osaka, A.; MacKenzie, J. D. *J. Non-Cryst. Solids* 1986, *82*, 37.

43. Brinker, C. J.; Mukherjee, S. P. *J. Mate. Sci.* 1981, *16*, 1980.

44. Prassas, M.; Phalippou, J.; Zarzycki, J. *J. Mate. Sci.* 1984, *19*, 1656.

45. Laudise, R. A.; Johnson, D. W. Jr. *J. Non-Cryst. Solids* 1986, *79*, 155.

46. Wallace, S.; Hench, L. L. *Mate. Res. Soc. Symp. Proc.* 1984, *32*, 47.

47. Orcel, G.; Hence, L. L. *J. Non-Cryst. Solids* 1986, *79*, 177.

48. Hench, L. L.; Orcel, G.; Nogues, J. L. *Mate. Res. Soc. Symp. Proc.* 1986, *73*, 35.

49. Artaki, I.; Zerda, T. W.; Jones, J. *J. Non-Cryst. Solids* 1986, *81*, 381.

50. McGrath, J. E.; Pullockaren, J. P.; Riffle, J. S.; Kilic, S.; Elsbernd, C. S. *AFOSR Conf. Proc.* San Diego, February, 1987, in press.

51. Schmidt, H.; Scholze, H.; Kaiser, A. *J. Non-Cryst. Solids* 1984, *63*, 1.

52. Ravaine, D.; Seminel, A.; Charbouilot, Y.; Vincens, M. *J. Non-Cryst. Solids* 1986, *82*, 210.

53. Parkhurst, C. S.; Doyle, L. A.; Silverman, L. A.; Singh, S.; Anderson, M. P.; McClurg, D.; Wnek, G. E.; Uhlmann, D. R. *Mate. Res. Soc. Symp. Proc.* 1986, *73*, 769.

54. Balaba, W. M.; DiFranco, G. J. *Polym. Mate. Sci. Eng.* 1987, *57*, 800.

55. Mark, J. E.; Sullivan, J. L. *J. Chem. Phys.* 1977, *66(3)*, 1006.

56. Jiang, C. Y.; Mark, J. E. *Colloid Polym. Sci.* 1984, *262*, 758.

57. Jiang, C. Y.; Mark, J. E. *Makromol. Chem.* 1984, *185*, 2609.

58. Mark. J. E.; Ning, Y. P. *Polym. Bull.* 1984, *12*, 413.

59. Ning, Y. P.; Tang, M. Y.; Jiang, C. Y.; Mark, J. E.; Roth, W. C. *J. Appl. Polym. Sci.* 1984, *29*, 3209.

60. Mark. J. E.; Ning, Y. P.; Jiang, C. Y.; Tang, M. Y.; Roth, W. C. *Polymer* 1985, *26*, 2069.

61. Mark, J. E.; Jiang, C. Y.; Tang, M. Y. *Macromolecules* 1984, *17*, 2613.

62. Tang, M. Y.; Mark, J. E. *Polym. Eng. Sci.* 1985, *25(1)*, 29.

63. Beshah, K.; Mark, J. E.; Ackerman, J. L.; Himstedt, A. *J. Polym. Sci. Polym. Phys.* 1986, *24*, 1207.

64. Hashimoto, T.; Shibayama, M.; Fujimura, M.; Kawai, H. *Memoirs of the Faculty of Engineering, Kyoto University*, 1981, 43.

65. Molau, G. E. *Block Polymers* S. L. Aggarwal ed. Plenum Press, New York, 1970.

66. Ophir, Z.; Wilkes, G. L. *J. Polym. Sci. Polym. Phys.* 1980, *18*, 1469.

67. Koberstein, J. T.; Stein, R. S. *J. Polym. Sci. Polym. Phys.* 1983, *21*, 1439.

68. Leung, L. M.; Koberstein, J. T. *J. Polym. Sci. Polym. Phys.* 1985, *23*, 1883.

69. Kakudo, M.; Kasai, N. *X-ray Diffraction by Polymers* Kodansha Ltd., Tokyo, 1972.

70. Alexander, L. E. *X-ray Diffraction Methods in Polymer Science* John Wiley & Sons, New York, 1969.

71. Glatter, O.; Kratky, O. *Small Angle X-ray Scattering* Academic Press, London, 1982.

72. Lovelace, S. undergraduate project, VPI&SU, 1984.

73. Brandrup, J.; Immergut, E. H. *Polymer Handbook* 2nd ed., John Wiley & Sons, N.Y., 1975.

74. Wetton, R. E.; Allen, G. *Polymer* 1966, *7*, 331.

75. Noll, W. *Chemistry and Technology of Silicones* Academic Press, N.Y., 1968.

76. Bonart, R.; Muller, E. H. *J. Macromol. Sci. Phys.* 1974, *B(10)*, 177.

77. Enns, J. B.; Gillham, J. K. *J. Appl. Polym. Sci.* 1983, *28(8)* 2567.

78. Faucher, J. A.; Koleske, J. V. *Polymer* 1968, *9*, 44.

79. Chen, K. C.; Tsuchiya, T.; MacKenzie, J. D. *J. Non-Cryst. Solids* 1986, *86*, 227.

80. Bradley, D. C.; Mehrotra, R. C.; Gaur, D. P. *Metal Alkoxides* Academic Press, London, 1978.

81. Evans, J. M.; Huglin, M. B. *Die Makromol. Chemie* 1969, *127*, 141.

82. Critchfield, F. E.; Koleske, J. V.; Magnus, G.; Dodd, J. L. *J. Elastoplastics* 1972, *4*, 22.